https://2025.ksum.or.kr

KOREAN SOCIETY OF ULTRASOUND IN MEDICINE

KSUM

KSUM 2025

The 56th Annual Congress of Korean Society of Ultrasound in Medicine

May 8 (Thu) – 9 (Fri), 2025 | Coex, Seoul, Korea

Scan QR Code to check KSUM 2025 Website!

https://2025.ksum.or.kr

Program & Abstract Book

Canon

Aplio™ i-series
Prism Edition

Light your day. Color your world.

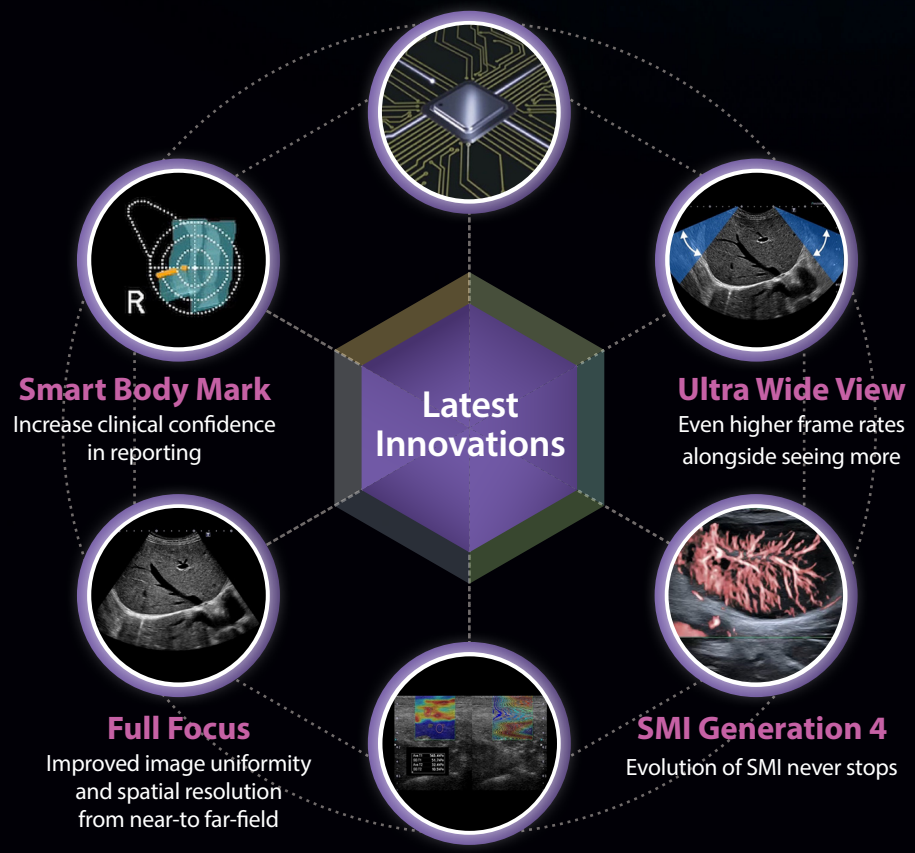

iBeam+
Improved frame rate, image quality and depth, plus high homogeneity and sensitivity

Smart Body Mark
Increase clinical confidence in reporting

Ultra Wide View
Even higher frame rates alongside seeing more

Full Focus
Improved image uniformity and spatial resolution from near-to far-field

SMI Generation 4
Evolution of SMI never stops

Expanded Range SWE
Boost your clinical confidence

CANON MEDICAL SYSTEMS KOREA CO., LTD.
https://kr.medical.canon

Made For life

Contents

4 Welcome Message
5 Organizing Committee
6 Program at a Glance
8 Scientific Program Overview
- Scientific Exhibition (E-Poster)
- Case of the Day (Quiz)
- Interactive Case Review
- Hands-on Session
- Live Demonstration
- Ultrasound, the Best (Informal Scientific Presentation)
- Luncheon Symposium

13 Should Not Miss!
- Jisan Lecture
- Young Investigator Award 2025 Session
- Interactive Case Review
- Live Demonstration
- Congress Dinner

14 Scientific Awards
15 List of Invited Guests
17 Floor Plan
19 Congress Information
- Registration Desk Operation Hours
- Registration Fee Includes
- KSUM 2025 on Mobile Device
- Internet Access
- Preview Lounge
- Coffee Station
- Morning Coffee & Bread
- E-Poster
- Certificate of Attendance
- 대회 연수평점 (For Koreans Only)

21 Sponsors
22 Exhibition Layout
23 Scientific Programs
- 24 Day 1 (May 8, Thu)
- 30 Day 2 (May 9, Fri)
- 38 Ultrasound, the Best (Informal, Scientific Presentation)
- 40 Scientific Exhibition (E-Poster)

47 Advertisement

Welcome Message

Dear Colleagues,

On behalf of the Korean Society of Ultrasound in Medicine (KSUM), it is our great pleasure to welcome you to the 56th Annual Congress of the Korean Society of Ultrasound in Medicine (KSUM 2025), which is scheduled to be held at Coex from May 8 (Thu) to 9 (Fri), 2025.

KSUM 2025 promises an outstanding program featuring high-quality scientific sessions that will provide participants with a valuable opportunity to keep up-to-date with the latest research findings in various fields of ultrasound in medicine and biology. A large number of world-renowned speakers and delegates will share their expertise, remarkable achievements, and most recent discoveries.

A wide-ranging scientific program consisting of the Jisan Lecture, Categorical Course, Special Focus, Hot Issues, Interactive Case Review, Live Demonstration, Hands-on sessions, and scientific presentations including the Young Investigator Award Session, Oral Presentations, "Ultrasound, the Best" (Informal Scientific Session), and E-Posters on the most critical issues challenging our field will be covered.

We have also arranged a string of colorful social program including the Congress Dinner, which we hope all our participants will enjoy.

Last but not least, we would like to take this opportunity to express our sincere appreciation to our Industry Partners and Supporters for their continued support of the KSUM.

We are confident that you will enjoy your stay in Seoul. With best wishes for a most enjoyable and beneficial experience, please accept once again our heartfelt welcome to all of you to KSUM 2025!

Sincerely yours,

Dal Mo Yang, M.D.
President

Jeong Yeon Cho, M.D.
Chair, Organizing Committee

Organizing Committee

Congress President
Dal Mo Yang
Kyung Hee University Hospital at Gangdong

Vice-president
Boo-Kyung Han
Samsung Medical Center

Chair, Organizing Committee
Jeong Yeon Cho
Seoul National University Hospital

Secretary General
Sung Il Jung
Konkuk University Medical Center

Treasurer
Seong Jin Park
Kyung Hee University Medical Center

Chair, Scientific Program Committee
Woo Kyoung Jeong
Samsung Medical Center

Chair, Publication Committee
Jung-Eun Cheon
Seoul National University Hospital

Chair, Sponsorship & Exhibition Committee
Jae Young Lee
Seoul National University Hospital

Chair, Scientific Exhibition Committee
Hong Eo
Samsung Medical Center

Chair, Registration Committee
Ji-Hoon Kim
Seoul National University Hospital

Chair, Information & Communication Committee
Ho-Taek Song
Severance Hospital

Chair, International Liaison Committee
Ah Young Jung
Asan Medical Center

Chair, Public Relation Committee
Jung Min Chang
Seoul National University Hospital

Chair, Education Program Committee
Bong Joo Kang
The Catholic University of Korea, Seoul St. Mary's Hospital

Chair, Social Program Committee
Min Hoan Moon
SMG-SNU Boramae Medical Center

Chair, Special Program Committee
Chang Ho Kang
Korea University Anam Hospital

Advisory Committee

*In alphabetical order by last name

Jung Hwan Back
Jae Young Byun
Bum Sang Cho
Kyoung-Sik Cho
Kil-Ho Cho
Byung Ihn Choi
Kyoo Byung Chung
Jae-Joon Chung
Chang Kok Hahm
Joon Koo Han
Sung il Hwang
Hae Jeong Jeon
Yong Yeon Jeong
So Lyung Jung
Heoung Keun Kang
Kun-Sang Kim
Ki-hwang Kim
Seung Hyup Kim
Woo Sun Kim
In-One Kim
Pyo Nyun Kim
Hyungmin Kim
Young Tae Ko
Young Ho Lee
Won Jae Lee
Jong Tae Lee
Jae Hoon Lim
Hyo-Keun Lim
Cheol Min Park
Hyunchul Rhim
Kyung Nam Ryu
Jung Suk Sim
Jin Yong Sung
Hyung Sik Yoo
Seong Kuk Yoon

KSUM 2025 Program at a Glance

Day 1 - May 8 (Thu)

Date Time/ Room	1F			2F	
	GBR 101	GBR 102	GBR 103	Room 203	Room 209
8:30	Morning Coffee & Bread				
9:00	BR Meet the Professor 1 (p 24)	GU Meet the Professor 2 (p 24)	ABD Meet the Professor 3 (p 24)	HN Meet the Professor 4 (p 24)	PHY Meet the Professor 5 (p 24)
9:30	BR Categorical Course 1 (p 25)	GU Scientific Session 1 (p 25)	ABD Categorical Course 2 (p 25)	HN Categorical Course 3 (p 26)	Young Investigator Award 2025 Session (p 26)
10:50	Coffee Break (Ultrasound, the Best 01)				
11:10			Jisan Lecture (p 26)		
12:20	Coffee Break				
12:40	Luncheon Symposium 1 (Beam Works & Monitor Corp.) (p 27)		KSUM General Assembly (Korean) (p 27)		
13:40	Coffee Break				
14:10	BR Scientific Session 2 (p 27)	GU Categorical Course 4 (p 27)	ABD Hot Issue 1 (p 28)	THY Hot Issue 2 (p 28)	[14:10-15:10] Ultrasonography Editorial Workshop (Korean) (p 28) Break Inter-section Symposium
15:30	Coffee Break (Ultrasound, the Best 02)				[15:20-16:20] Physics and Clinic (p 29)
16:00	Interactive Case Review (p 29)				PHY [16:20-17:20] Special Focus Session 1 (p 29)
17:20			Reception		
18:00			Congress Dinner		
20:00					

Day 2 - May 9 (Fri)

Date Time/ Room	1F			2F	
	GBR 101	GBR 102	GBR 103	Room 203	Room 209
8:30	Morning Coffee & Bread				
9:00		THY Meet the Professor 6 (p 30)	MSK Meet the Professor 7 (p 30)	PED Meet the Professor 8 (p 30)	CV Meet the Professor 9 (p 30)
9:30	ABD Categorical Course 5 (p 31)	THY Categorical Course 6 (p 31)	MSK [Live Demo] Categorical Course 7 (p 31)	PED Categorical Course 8 (p 32)	CV Special Focus Session 2 (p 32)
10:30	Coffee Break (Ultrasound, the Best 03)				
11:00	ABD Scientific Session 3 (p 32)	THY Scientific Session 4 (p 33)	MSK Multisession 1 (p 33)	PED Multisession 2 (p 34)	Hands-on Hands-on Session (p 34)
12:20	Coffee Break				
12:40	Luncheon Symposium 2 (PHILIPS) (p 34)	Luncheon Symposium 3 (Bracco Imaging Korea) (p 34)			
13:40	Coffee Break				
14:00	GU Special Focus Session 3 (p 35)	BR Hot issue 3 (p 35)	Live Demonstration Live Demonstration 1 (MSK) (p 35)	KSTU Categorical Course 9 (p 36)	
15:00	Coffee Break (Ultrasound, the Best 04)				
15:20	ABD Special Focus Session 4 (p 36)	BR Special Focus Session 5 (p 36)	Live Demonstration Live Demonstration 2 (THY) (p 37)	KSTU Special Focus Session 6 (p 37)	
16:20	Coffee Break				
16:40	Inter-section Symposium Inter-body part symposium: AI (p 37)		Live Demonstration Live Demonstration 3 (ABD) (p 37)		
17:50					
20:00					

Topic Abbreviation			
ABD	Abdomen	MSK	Musculoskeletal
BR	Breast	PED	Pediatric
CV	Cardiovascular	PHY	Physics
GU	Genitourinary	THY	Thyroid
HN	Head & Neck	KSTU	The Korean Society for Therapeutic Ultrasound

Scientific Program Overview

Scientific Exhibition (E–Poster)

Place	Scientific Exhibition Area, Exhibition Hall (Grand Ballroom 104+105, 1F)
Date & Time	May 8 (Thu) 09:00-17:30
	May 9 (Fri) 09:00-18:00

Case of the Day (Quiz)

Participants can answer 13 multiple-choice questions, each asking for the correct diagnosis for various cases. The participants with the most correct answers will have the opportunity to win a prize.

Place	Scientific Exhibition Area, Exhibition Hall (Grand Ballroom 104+105, 1F)
Date & Time	May 8 (Thu) 09:00-17:30
	May 9 (Fri) 09:00-13:00
Announcement of Winners	After 13:00, May 9 (Fri), the winners will be announced in the Scientific Exhibition area. * Prizes will be offered to the winners and the prize will be given after the congress.

Interactive Case Review

The Interactive Case Review(ICR) is an exciting and dynamic quiz session that all participants can join. Challenge yourself in the ICR and learn diagnoses of various cases!
All participants will be asked to choose the correct diagnosis for different cases from a series of about 28 quizzes.

Place	101+102 (1F)
Date & Time	May 8 (Thu) 16:00-17:20
Director	Seungchul Han (Samsung Medical Center, Korea)
MC	Seungchul Han (Samsung Medical Center, Korea)
	Seung-Seob Kim (Severance Hospital, Korea)

Hands-on Session

Get ready to take your skills to the next level!
The Hands-on Session will be held exclusively for pre-registered participants, with 30 registrants selected to engage in this intensive program.
Participants will go beyond theoretical knowledge and acquire practical, real-world skills under the expert guidance of renowned specialists.
Don't miss this unique opportunity to deepen your expertise and elevate your clinical capabilities to new heights.

Place	Room 209 (2F)
Date & Time	May 9 (Fri) 11:00-12:20

May 9 (Fri)	Hands-on Session (ABD/CV)
11:00-11:20	(ABD) Liver Doppler Dong Ik Cha (Samsung Medical Center, Korea)
11:20-11:40	(CV) Basics and Tips for Peripheral Artery and Vein Ultrasound: A Comprehensive Guide Ki Seok Choo (Pusan National University Yangsan Hospital, Korea)
Hands-on Training	Instructors
Instructor	(ABD) Dong Ik Cha (Samsung Medical Center, Korea)
Instructor	(ABD) Eun Sun Lee (Chung-Ang University Hospital, Korea)
Instructor	(CV) Ki Seok Choo (Pusan National University Yangsan Hospital, Korea)
Instructor	(CV) Yoonseong Lee (Seoul National University Hospital, Korea)

* Application for the Hands-on Session is closed. The Hands-on Information Desk will be open at 10:30 on May 9 (Fri) in front of Room 209.

Live Demonstration

Place	Grand Ballroom 103 (1F)
Date	May 9 (Fri)

Session	Session Time	Program
Categorical Course 7 (MSK)	09:30-10:30	• Topic: Nerve Imaging around the Upper Extremity • Speaker: Carlo Martinoli (DISSAL. University of Genova, Italy) * Live demonstration after two lectures.
Live Demonstration 1 (MSK)	14:00-15:00	• Topic: US of Elbow Joint • Speaker: Eun Hae Park (Jeonbuk National University Hospital, Korea) • Topic: US of Elbow Joint • Speaker: Chee Yeong Lim(Singapore General Hospital, Singapore)
Live Demonstration 2 (THY)	15:20-16:20	• Topic: Ultrasound Anatomy of the Neck: Introduction to Thyroid and Adjacent Anatomy • Speaker: Leehi Joo (Chung-Ang University Hospital, Korea) • Topic: Ultrasound Anatomy of the Neck: Nerves • Speaker: Min Kyoung Lee (The Catholic University of Korea, Yeouido St. Mary's Hospital, Korea)
Live Demonstration 3 (ABD)	16:40-17:50	• Topic: Liver Fat Measurement • Speaker: Dong Wook Kim (Asan Medical Center, Korea) • Topic: Liver Focal Lesion CEUS • Speaker: Woo Kyoung Jeong (Samsung Medical Center, Korea)

Ultrasound, the Best (Informal Scientific Presentation)

Oral presentations of Case Reports will be made during the break times, which will take place at the right side of the Exhibition Hall (Grand Ballroom 104+105, 1F).

Place	Ultrasound, the Best, Exhibition Hall (Grand Ballroom 104+105, 1F)
Date	May 8 (Thu)-May 9 (Fri)

Date	Presenting Time	Session	Presentation by Specialty
May 8 (Thu)	10:50-11:10	USB01	ABD (2)
	15:30-16:00	USB02	GU (6) / BR (1)
May 9 (Fri)	10:30-11:00	USB03	ABD (4) / MSK (1)
	15:00-15:20	USB04	PED (2) / THY (1) / CV (1)

Luncheon Symposium

Luncheon Symposium 1 (BeamWorks & Monitor Corporation)	*(p. 27)*
Place	Grand Ballroom 101 (1F)
Date & Time	May 8 (Thu) 12:40-13:40
Chairperson	Eun Young Ko (Samsung Medical Center, Korea)
Speakers	Jung Hyun Yoon (Severance Hospital, Korea)
	Kyung Hee Ko (Yongin Severance Hospital, Korea)

Luncheon Symposium 2 (PHILIPS)	*(p.34)*
Place	Grand Ballroom 101 (1F)
Date & Time	May 9(Fri) 12:40-13:40
Chairperson	Jeong Min Lee (Seoul National University Hospital, Korea)
Speaker	Seung-Seob Kim (Severance Hospital, Korea)

Luncheon Symposium 3 (Bracco Imaging Korea)	*(p. 34)*
Place	Grand Ballroom 102 (1F)
Date & Time	May 9(Fri) 12:40-13:40
Topic	Beyond Boundaries: Unlocking the Full Potential of Contrast-Enhanced Ultrasound
Chairperson	Sang Il Choi (Seoul National University Bundang Hospital, Korea)
Speakers	Dong Jae Shim (The Catholic University of Korea, Incheon St. Mary's Hospital, Korea)
	Seung Hyun Lee (Seoul National University Hospital, Korea)

Should Not Miss!

Jisan Lecture

- Date: May 8 (Thu), 2025
- Time: 11:10-12:20
- Place: Grand Ballroom 103 (1F), Coex

- Topic: Liver Fatty Quantification
- Speaker: Ioan Sporea (Romania)

- Topic: The Evolution of Ultrasound-Guided Liver Ablation: Past, Present, and Future
- Speaker: Hyunchul Rhim (Korea)

Young Investigator Award 2025 Session

Oral presentation session for the candidates of KSUM Young Investigator Award!

- Date: May 8 (Thu), 2025
- Time: 09:30-10:50
- Place: Room 209 (2F), Coex

Interactive Case Review

- Date: May 8 (Thu), 2025
- Time: 16:00-17:20
- Place: Grand Ballroom 101+102 (1F), Coex

Live Demonstration

- Date: May 9(Fri)
- Place: Grand Ballroom 103 (1F), Coex

[Categorical Course 7 (MSK)]

* Live demonstration after two lectures.

- Time: 09:30-10:30
- Lecture: Nerve Imaging around the Upper Extremity

[Live Demonstration 1 (MSK)]

- Time: 14:00-15:00
- Lecture 1: US of Elbow Joint
- Lecture 2: US of Knee Joint

[Live Demonstration 2 (THY)]

- Time: 15:20-16:20
- Lecture 1: Ultrasound Anatomy of the Neck: Introduction to Thyroid and Adjacent Anatomy
- Lecture 2: Ultrasound Anatomy of the Neck: Nerves

[Live Demonstration 3 (ABD)]

- Time: 16:40-17:50
- Lecture 1: Liver Fat Measurement
- Lecture 2: Liver Focal Lesion CEUS

Congress Dinner

Enjoy the wonderful evening of KSUM 2025 with an excellent dinner and a great performance.

- Date: May 8 (Thu), 2025
- Time: 18:00-20:00 (Reception 17:20-18:00)
- Place: Grand Ballroom 103 (1F), Coex
- Ticket: USD 20 / KRW 20,000

※ Only participants who have paid for the congress dinner can attend this event.

Scientific Awards

KSUM 2025 Organizing Committee is preparing various awards and prizes to encourage scientific activities.

International Grant Award

Awarded to all overseas presenters of the abstracts accepted to be presented onsite at the Scientific Session, Scientific Exhibition (E-Poster) or Informal Scientific Presentation_ Ultrasound, the Best. The award is given only once to the presenting author regardless of the number of accepted abstracts or co-authors.

International Grant Award
USD 300

Young Investigator Award

Awarded to presenters under the age of 40 whose abstracts were selected as the most outstanding among the oral presentations.

Grand Prix (1 Winner)	Gold (2 Winners)
KRW 1,000,000	KRW 500,000

Ultrasound, the Best Award

Awarded to the top 3 Informal Scientific Presentation presenters based on the peer review of the scientific content of presentations.

Ultrasound, the Best Award (3 Winners)
KRW 100,000

Best Poster Award

Awarded to presenting authors of selected scientific exhibitions based on the peer review of the scientific content of presentations.

Grand Prix (1 Winner)	Gold (2 Winners)	Silver (3 Winners)	Bronze (4 Winners)
KRW 500,000	KRW 300,000	KRW 200,000	KRW 100,000

* Please be informed that the prizes of all awards will be presented after deducting 22% tax from the original amount in the case of awardees from the following countries: Afghanistan, Argentina, Belgium, Brazil, Cameroon, Costa Rica, Denmark, Guatemala, Lebanon, Mozambique, Paraguay, Puerto Rico, Republic of Suriname, Singapore, Sudan, Switzerland, Chinese Taipei, Turkiye.

List of Invited Guests

Invited Speakers

*In alphabetical order by last name

Dongbin Ahn, Korea
Hye Shin Ahn, Korea
Kyung-Sik Ahn, Korea
Jin Kyung An, Korea
Soong June Bae, Korea
Sung Hwan Bae, Korea
Sua Bae, Korea
Jung Hwan Baek, Korea
Dong Ik Cha, Korea
Jung Min Chang, Korea
Jin Ho Chang, Korea
Won Seok Chang, Korea
Jung-Eun Cheon, Korea
Ka-Fung Peter Chiu, Hong Kong, China
Gayoung Choi, Korea
Ki Seok Choo, Korea
A Jung Chu, Korea
Stamatia Destounis, USA
Hye-Joung Eom, Korea
Yeo Eun Han, Korea
Shiro Horisawa, Japan
Jisun Hwang, Korea
Sin Hye Hwang, Korea
Sungjun Hwang, Korea
Sung Il Hwang, Korea
Weon Jang, Korea
Sun Kyung Jeon, Korea
Woo Kyoung Jeong, Korea
Ren Jie, China
Leehi Joo, Korea
Jeeun Kang, USA
Jisoo Kim, Korea
Chi Kyung Kim, Korea
Youe Ree Kim, Korea
Kyuwon Kim, Korea
Won Hwa Kim, Korea
Min Je Kim, Korea
Dong Wook Kim, Korea
Jinwook Kim, Korea
Chulhong Kim, Korea
Seung-Seob Kim, Korea
kyung Hee Ko, Korea
Supika Kritsaneepaiboon, Thailand
Jennifer Kuo, USA
Jin Young Kwak, Korea
Yong Wonn Kwon, Korea
Jeong Hyun Lee, Korea
Min Kyoung Lee, Korea
Jongmin Lee, Korea
Yoonseong Lee, Korea
Hyo Jeong Lee, Korea
Myoungseok Lee, Korea
Byung Chul Lee, Korea
Jeonghyun Lee, Korea
Seung Hyun Lee, Korea
Chee Yeong Lim, Singapore
Hunjong Lim, Korea
Rameysh Danovani Mahmood, Singapore
Carlo Martinoli, Italy
Ji Hye Min, Korea
Yasunori Minami, Japan
Sung Kyoung Moon, Korea
Dong-Guk Paeng, Korea
Sang Ik Park, Korea
Eun Hae Park, Korea
Jinhyoung Park, Korea
Mi-Yeon Park, Korea
Hyungjun Park, Korea
Hyunchul Rhim, Korea
Yun Hwa Rho, Korea
Jiwoon Seo, Korea
Dong Jae Shim, Korea
Jae Ho Shin, Korea
Sung Ui Shin, Korea
Kushaljit Singh Sodhi, India
Jung Hee Son, Korea
You Seon Song, Korea
Ioan Sporea, Romania
Pae Sun Suh, Korea
Hyun Kyung Yang, Korea
Hyun Jung Yi, Korea
Jeongin Yoo, Korea
Jung Hyun Yoon, Korea
Jaesok Yu, Korea

Chairpersons

*In alphabetical order by last name

Jung Hwan Baek, Korea
Joo Hee Cha, Korea
Eun Young Chae, Korea
Jee Won Chai, Korea
Jung Min Chang, Korea
Bum Sang Cho, Korea
Young Seo Cho, Korea
Kil-Ho Cho, Korea
Young Ah Cho, Korea
Yeon Hyeon Choe, Korea
Joon-Il Choi, Korea
Yun Sun Choi, Korea
Jung-Ah Choi, Korea
Sang Il Choi, Korea
Soo-jung Choi, Korea
Yoon Jung Choi, Korea
Yong Eun Chung, Korea
Doo Hoe Ha, Korea
Soo Yeon Hahn, Korea
Boo-Kyung Han, Korea
Byoung Hee Han, Korea
Seungchul Han, Korea
Sukhee Heo, Korea
Seok Ho Hong, Korea
Ji Young Hwang, Korea
Sung Il Hwang, Korea
Woo Kyoung Jeong, Korea
Ijin Joo, Korea
Dae Chul Jung, Korea
So Lyung Jung, Korea
Chan Kyo Kim, Korea
Ji-Hoon Kim, Korea
Hye-Won Kim, Korea
Jin-Woong Kim, Korea
Hye Jung Kim, Korea
See Hyung Kim, Korea
Kyoung Won Kim, Korea
Jihun Kim, Korea
Yong-woo Kim, Korea
Min Ju Kim, Korea
Sang Youn Kim, Korea
Sung Hun Kim, Korea
Young Sun Kim, Korea
Se Hyung Kim, Korea
Min Jung Kim, Korea
Eunkyung Kim, Korea
Eun Young Ko, Korea
Sung Min Ko, Korea
Chang Hee Lee, Korea
Young Hen Lee, Korea
Jae Young Lee, Korea
Jeong Eun Lee, Korea
Myoungseok Lee, Korea
Young-Hwan Lee, Korea
Young Hwan Lee, Korea
Hee Jung Lee, Korea
Bae Young Lee, Korea
Jeong Min Lee, Korea
Hyun Kyung Lim, Korea
Dong Gyu Na, Korea
Dong-Guk Paeng, Korea
Jinhyoung Park, Korea
Jeong Seon Park, Korea
Eun-Ah Park, Korea
Young Mi Park, Korea
Eun-Joo Park, Korea
Yongrae Roh, Korea
Bo Kyoung Seo, Korea
Su-mi Shin, Korea
Jung Hee Shin, Korea
Kyung Sook Shin, Korea
Ji Soo Song, Korea
Jin Yong Sung, Korea
Dal Mo Yang, Korea
So-Young Yoo, Korea
Seong Kuk Yoon, Korea
Hee Mang Yoon, Korea
Jung Hyun Yoon, Korea

Floor Plan

Level 2

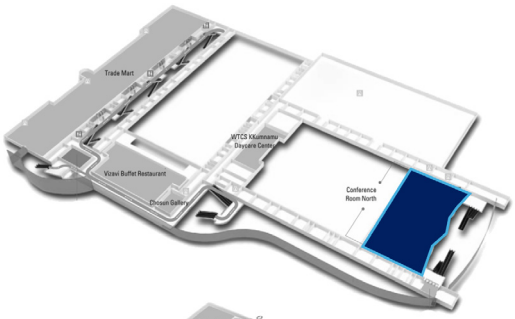

Conference Room (Room. 201~211)

- Scientific Sessions
- Hands-on Session
- Secretariat

Level 1

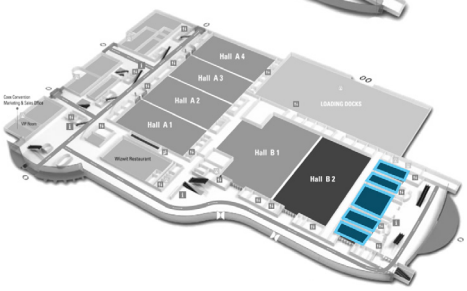

Grand Ballroom (Room. 101~105)

- Scientific Sessions
- Interactive Case Review
- Live Demonstrations
- Scientific Exhibition (E-Poster)
- Technical Exhibition
- Preview Lounge
- Ultrasound, the Best (Informal Scientific Presentation)
- Registration Desk

1F_GRAND BALLROOM & LOBBY

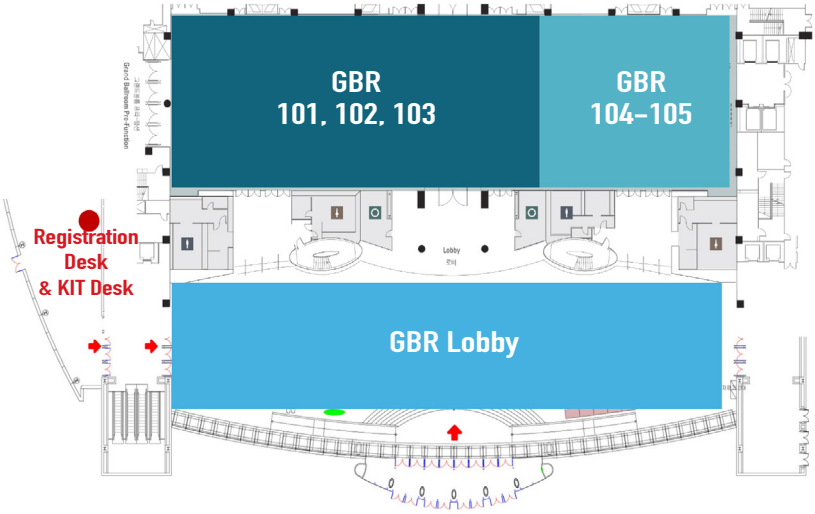

GBR 101, 102, 103

- Scientific Sessions
- Jisan Lecture
- Interactive Case Review
- KSUM General Assembly
- Luncheon Symposium
- Live Demonstrations

GBR 104-105

- Technical Exhibition
- Preview Lounge
- Ultrasound, the Best (Informal Scientific Presentation)
- Scientific Exhibition (E-Poster)
- Case of the Day
- Coffee Station & Rest Area

GBR Lobby

- Registration Desk
- Technical Exhibition
- Coffee Break

2F_CONFERENCE ROOM NORTH

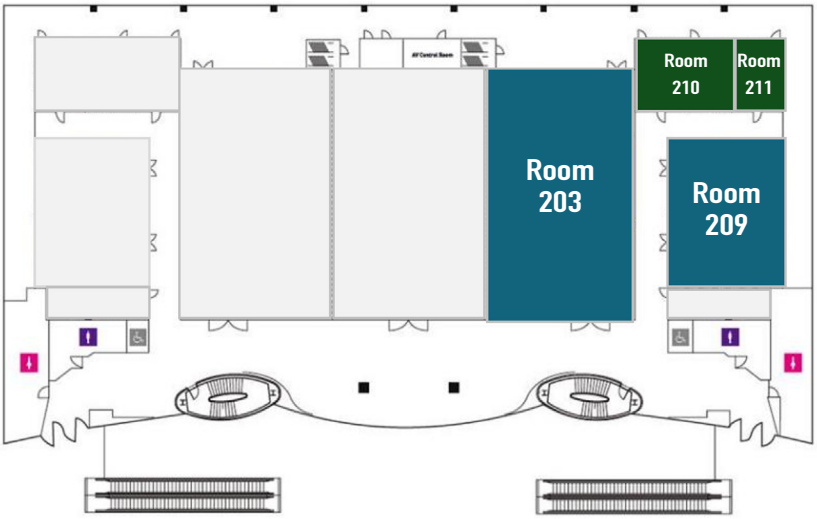

Room 203

- Scientific Sessions

Room 209

- Scientific Sessions
- Hands-on Session
- Young Investigator Award 2025 Session

Room 210

- KSUM 2025 Secretariat

Room 211

- Organizing Committee

Congress Information

Registration Desk Operation Hours

Place Grand Ballroom Left-Lobby (1F)
Time May 8 (Thu), 08:00-17:30
May 9 (Fri), 08:00-18:00

Registration Fee Includes

- Access to all sessions (except Hands-on Session)
- Access to all exhibition halls
- Congress Kit and Program Book
- Morning Coffee & Bread

KSUM 2025 Mobile Web

Scan the QR Code on the right to find various information on the congress through the mobile website.

- Congress Information
- Program
- Awards & Events
- Sponsorship & Technical Exhibition
- Travel Information

Internet Access

When setting Wi-Fi, select "COEX Free Wi-Fi Zone" or "Public Wi-Fi Free" on your mobile device.

Preview Lounge

Place Left side of the Exhibition Hall (Grand Ballroom 104+105, 1F)
Time May 8 (Thu), 08:00-17:30
May 9 (Fri), 08:00-18:00

Coffee Station

Place Exhibition Hall (Grand Ballroom 104+105, 1F, Coex)
Time May 8 (Thu), 10:00-17:00
May 9 (Fri), 10:00-17:00

Morning Coffee & Bread

Place Grand Ballroom Lobby 1F, Coex
Time May 8 (Thu)-May 9 (Fri), 08:30-09:00

E-Poster

Place Left side of the Exhibition Hall (Grand Ballroom 104+105, 1F)
Time May 8 (Thu), 09:00-17:30
May 9 (Fri), 09:00-18:00

Certificate of Attendance

All participants are able to download and print out of a certificate of attendance at MY PAGE of the KSUM 2025 website (2025.ksum.or.kr). Participants who register on-site, please contact the secretariat (reg_ksum@ultrasound.or.kr) after the congress for the certificate.

[대회 연수평점 (For Koreans Only)]

대한의사협회 연수교육 관리지침에 따라 세션에 참석한 시간에 비례하여 이수 가능한 평점이 달라집니다.
세션 시작과 종료 시 반드시 네임택의 QR 코드를 스캔 해주시기 바랍니다. (1일 2회 이상)

대한의사협회 평점 인정 기준 (실 출석 시간에 따라 부분평점 인정) 5월 8일(목) - 9일(금)	
1시간 미만	1평점 인정 불가
1시간 이상 2시간 미만	1평점 인정
2시간 이상 3시간 미만	2평점
3시간 이상 4시간 미만	3평점
4시간 이상 5시간 미만	4평점
5시간 이상 6시간 미만	5평점
6시간 이상	6평점

* 대한의사협회 지침에 따라 학회 입장과 퇴장시간의 승인은 QR 코드 스캔방식으로 진행됩니다.
* 평점 인정을 위한 QR 코드 스캔은 등록데스크를 방문하시거나 각 세션장 앞에 설치된 셀프 평점 체크기를 이용하여주시기 바랍니다.

대회 일자 별 최대 인정 평점	
일자	평점
5월 8일(목)	6평점
5월 9일(금)	6평점

* (Coffee) Break, Luncheon Symposium, KSUM General Assembly (Korean), Congress Dinner 세션은 평점이 인정되지 않는 점 참고하여 주시기 바랍니다.

Sponsors

The Organizing Committee of KSUM 2025 gratefully acknowledges the sponsorship of the following companies.

Gold

CMS Central Medical Service

Canon

SAMSUNG

GE HealthCare

Silver

Dongkook Lifescience

PHILIPS

Bronze

Guerbet

BRACCO LIFE FROM INSIDE

WiTH HEALTHCARE

JW Medical

BAYER

Supported by

SEOUL METROPOLITAN GOVERNMENT

Exhibition Layout

Grand Ballroom

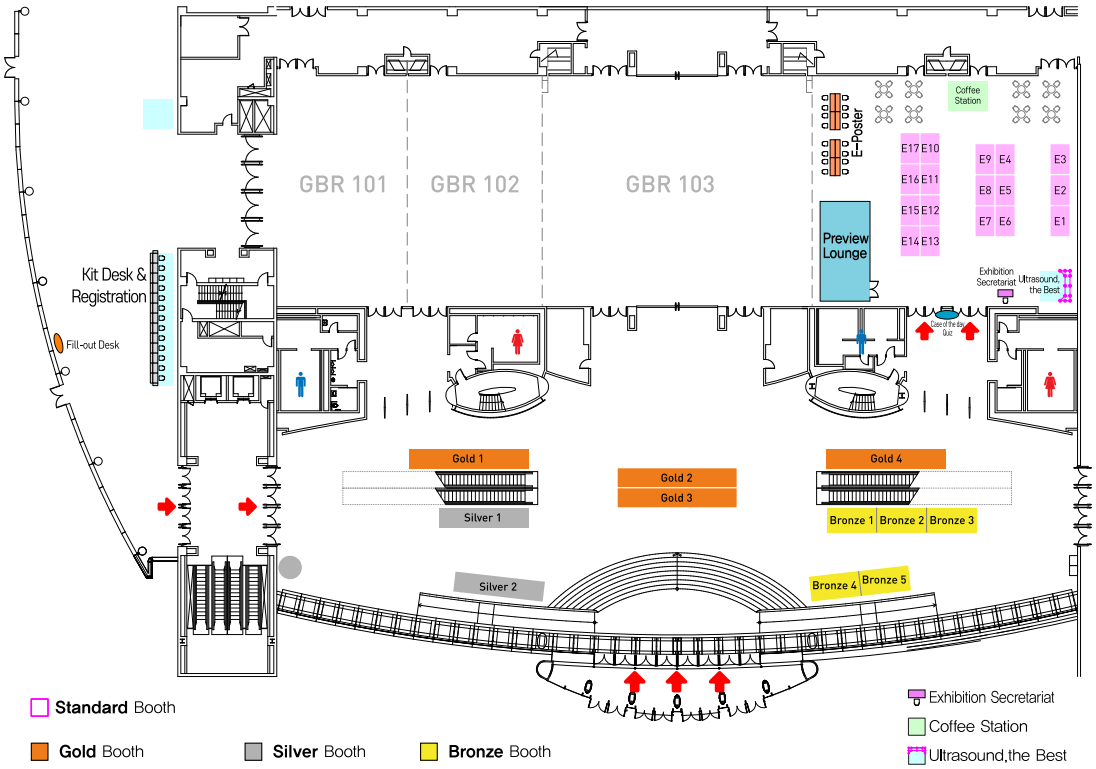

Booth No.	Sponsor	Booth No.	Sponsor
Gold 1	Canon Medical Systems Korea	Bronze 1	Guerbet Korea Ltd.
Gold 2	Central Medical Service	Bronze 2	Bayer Korea Ltd.
Gold 3	GE Healthcare Korea	Bronze 3	JW Medical
Gold 4	Samsung Medison Co., Ltd.	Bronze 4	WiTH Healthcare
Silver 1	Dongkook Lifescience	Bronze 5	Bracco Imaging Korea
Silver 2	PHILIPS		

Booth No.	Exhibitor	Booth No.	Exhibitor
E1	AFSUMB 2026	E10	Dasol Life Science
E2	KCR 2025	E11	SIEMENS Healthineers Ltd.
E3	SEJONG MEDICAL BOOKS	E12	MEDICAL IP
E4	Encormac	E13	monitor corporation
E5	Mammotome	E14	PUZZLEAI
E6	ACCUZEN	E15	BD Korea
E7	BEAMWORKS	E16	ALPINION MEDICAL SYSTEMS
E8	RF Medical Co., Ltd.	E17	STARmed
E9	Flower Medical Co.,Ltd		

KSUM 2025

Scientific Programs

Daily Scientific Program

Day 1 – May 8 (Thu)

GBR 101

09:00-09:30

Meet the Professor 1 (BR) (p 47)

Optimizing Supplemental Screening

Chairperson(s)
Jung Min Chang (Seoul National University Hospital, Korea)

09:00-09:30 (MP01-S1)
Supplemental Screening Strategies: Deciding on DBT, Ultrasound, or MRI [VOD]
Stamatia Destounis (Elizabeth Wende Breast Care, USA)

GBR 102

09:00-09:30

Meet the Professor 2 (GU) (p 48)

Chairperson(s)
Chan Kyo Kim (Samsung Medical Center, Korea)

09:00-09:30 (MP02-S1)
Various Focal Therapy for Prostate Cancer and the Role of Imaging in Focal Therapy
Ka-Fung Peter Chiu (The Chinese University of Hong Kong, Hong Kong, China)

GBR 103

09:00-09:30

Meet the Professor 3 (ABD) (p 49)

All about Liver RFA

Chairperson(s)
Chang Hee Lee (Korea University Guro Hospital, Korea)

09:00-09:30 (MP03-S1)
All about Liver RFA
Yasunori Minami (Kindai University, Japan)

Room 203

09:00-09:30

Meet the Professor 4 (HN) (p 50)

Multimodal Imaging for the Assessment of Head and Neck Tumors

Chairperson(s)
Ji-Hoon Kim (Seoul National University Hospital, Korea)

09:00-09:30 (MP04-S1)
Multimodal Imaging for the Assessment of Head and Neck Tumors: From Ultrasound to MRI
Jeong Hyun Lee (Asan Medical Center, Korea)

Room 209

09:00-09:30

Meet the Professor 5 (PHY) (p 51)

Chairperson(s)
Jinhyoung Park (Sungkyunkwan University, Korea)

09:00-09:30 (MP05-S1)
Principles of Ultrasound Doppler and Advanced Blood Flow Imaging
Dong-Guk Paeng (Jeju National University, Korea)

GBR 101

09:30-10:50

Categorical Course 1 (BR) (p 52-55)

Enhancing Breast Ultrasound

Chairperson(s)
Joo Hee Cha (Asan Medical Center, Korea)
Hye-Won Kim (Wonkwang University Hospital, Korea)

09:30-09:57 (CC01-S1)
Combining Ultrasound and Mammography: A Case-Based Review
A Jung Chu (Seoul National University Boramae Medical Center, Korea)

09:57-10:24 (CC01-S2)
Basics and Tips to MRI-Targeted Ultrasound: A Case-Based Review
Hye-Joung Eom (Asan Medical Center, Korea)

10:24-10:50 (CC01-S3)
ABUS and Hand-held US: A Case-Based Review
Sung Ui Shin (Seoul National University Bundang Hospital, Korea)

GBR 102

09:30-10:50

Scientific Session 1 (GU) (p 160-162)

Chairperson(s)
Bum Sang Cho (Chungbuk National University Hospital, Korea)
Seong Kuk Yoon (Dong-A University Hospital, Korea)

09:30-09:40 (SS01-P1)
Effect of Structured Pelvic Floor Muscle Training on Pelvic Floor Muscle Contraction and Treatment of Pelvic Organ Prolapse in Postpartum Women: Ultrasound and Clinical Evaluations
Hui Zhao (Shanghai Tenth People's Hospital, Tongji University, China)

09:40-09:50 (SS01-P2)
Ultrasound Localization Microscopy: Optimization of Renal Cortical Examination Strategies and Diagnosis of Chronic Kidney Disease [VOD]
Hong Han (Zhongshan Hospital Fudan University, China)

09:50-10:00 (SS01-P3)
Ultrasound-Guided Microwave Ablation for Symptomatic Abdominal Wall Endometriosis
Jiaxin Li (Shanghai Tenth People's Hospital, China)

10:00-10:10 (SS01-P4)
Contrast-Enhanced Ultrasound of Renal Transplant in Recipients with Acute Vascular Rejection
Natalia Vetsheva (FSBEI FPE RMACPE MON Russia, Russia)

10:10-10:20 (SS01-P5)
Clinical Value of Multi-Modal Ultrasound Data of Brain-Dead Donor Kidneys in Predicting Early Post-Transplant Graft Function Recovery
Bei Wang (The First Affiliated Hospital of Shandong First Medical University & Shandong Provincial Qianfoshan Hospital, China)

GBR 103

09:30-10:50

Categorical Course 2 (ABD) (p 56-61)

Normal Anatomy, Variation and Congenital Disease

Chairperson(s)
Joon-Il Choi (The Catholic University of Korea, Seoul St. Mary's Hospital, Korea)
Jin-Woong Kim (Chosun University Hospital, Korea)

09:30-09:50 (CC02-S1)
Liver and Perihepatic Space
Jeongin Yoo (Seoul National University Hospital, Korea)

09:50-10:10 (CC02-S2)
GB and Bile Duct
Shinhye Hwang (Yongin Severance Hospital, Korea)

10:10-10:30 (CC02-S3)
Pancreas and Spleen
Sung Hwan Bae (Soon Chun Hyang University Seoul Hospital, Korea)

10:30-10:50 (CC02-S4)
GI Tract
Yeo Eun Han (Korea University Anam Hospital, Korea)

Room 203

09:30-10:50

Categorical Course 3 (HN)

(p 62-65)

US Diagnosis and Management of Benign Neck Masses

Chairperson(s)
Young Hen Lee (Korea University Ansan Hospital, Korea)
Hyun Kyung Lim (Soon Chun Hyang University Seoul Hospital, Korea)

09:30-09:55 (CC03-S1)
US Guided Biopsy of Benign Nodal Masses
Sang Ik Park (Asan Medical Center, Korea)

09:55-10:20 (CC03-S2)
US Guided Biopsy of Neck Masses Other Than LNs
Yun Hwa Roh (Samsung Medical Center, Korea)

10:20-10:45 (CC03-S3)
Management of Benign Neck Masses: US Guided Intervention vs. Surgery
Dongbin Ahn (Kyungpook National University, Korea)

Room 209

09:30-10:50

Young Investigator Award 2025 Session

(p 163-166)

Chairperson(s)
Boo-Kyung Han (Samsung Medical Center, Korea)
Woo Kyoung Jeong (Samsung Medical Center, Korea)

09:30-09:40 (YIA-P1)
Development of a Simplified Prediction Model for Diagnosing Progressive Central Precocious Puberty Using Clinical and Pelvic Ultrasound Parameters
Yeseul Kang (Yongin Severance Hospital, Korea)

09:40-09:50 (YIA-P2)
Echocardiographic Evaluation of LV Parameters and Insulin Resistance in Non-Diabetic STEMI Patients
Javad Alizargar (National Taipei University of Nursing and Health Sciences, Chinese Taipei)

09:50-10:00 (YIA-P3)
Comparison of Integrated vs. Sequential AI-CAD in Breast US: A Prospective Pilot Study on Scan Time, Reproducibility, and Diagnostic Performance
Haejung Kim (Samsung Medical Center, Korea)

10:00-10:10 (YIA-P4)
Diagnostic Value of High-frequency Ultrasound in Unclarified Lesions at the End of Extremities
Haojie Yang (Tenth People's Hospital of Tongji University, China)

10:10-10:20 (YIA-P5)
Inconclusive Cytology Results of Fine-Needle Aspiration for Thyroid Nodules: The Gravity of Strict Guideline Implementation
Sangwoo Cho (Yonsei University College of Medicine, Korea)

10:20-10:30 (YIA-P6)
Effect of Structured Pelvic Floor Muscle Training on Pelvic Floor Muscle Contraction and Treatment of Pelvic Organ Prolapse in Postpartum Women: Ultrasound and Clinical Evaluations
Hui Zhao (Shanghai Tenth People's Hospital, Tongji University, China)

10:50-11:10

Coffee Break
Ultrasound, the Best 1 (GBR 104+105)

GBR 103

11:10-12:20

Jisan Lecture

(p 66-68)

Chairperson(s)
Dal Mo Yang (Kyung Hee University Hospital at Gangdong, Korea)

11:15-11:45 (JSL-S1)
Liver Fatty Quantification
Ioan Sporea (Victor Babes University of Medicine and Pharmacy Timisoara, Romania)

11:45-12:15 (JSL-S2)
The Evolution of Ultrasound-Guided Liver Ablation: Past, Present, and Future
Hyunchul Rhim (Samsung Changwon Hospital, Korea)

12:20-12:40

Coffee Break

GBR 101

12:40-13:40

Luncheon Symposium 1 (Beam Works & Monitor Corp.)

Chairperson(s)
Eun Young Ko (Samsung Medical Center, Korea)

12:40-13:00 (LS01-S1)
Experience Using CadAI-B on Realtime Handheld Breast US
Jung Hyun Yoon (Severance Hospital, Korea)

13:00-13:20 (LS01-S2)
Clinical Application of AI to ABUS
Kyung Hee Ko (Yongin Severance Hospital,Korea)

GBR 103

12:40-13:40

KSUM General Assembly

13:40-14:10

Coffee Break

GBR 101

14:10-15:30

Scientific Session 2 (BR) (p 168-171)

Chairperson(s)
Eun Young Chae (Asan Medical Center, Korea)
Hye Jung Kim (Kyungpook National University Chilgok Hospital, Korea)

14:10-14:20 (SS02-P1)
Comparison of Integrated vs. Sequential AI-CAD in Breast US: A Prospective Pilot Study on Scan Time, Reproducibility, and Diagnostic Performance
Haejung Kim (Samsung Medical Center, Korea)

14:20-14:30 (SS02-P2)
A Preliminary Study of Non-Invasive Prediction of Breast Cancer Molecular Markers Using Deep Learning-Based Molecular Markers Prediction Network on Automated Breast Volume Scanner Images
Lixia Yan (Zhongshan Hospital, Fudan University, China)

14:30-14:40 (SS02-P3)
Intra-Observer and Inter-Observer Agreement in Glandular Tissue Component Assessment Using Automated Breast Ultrasound
Haejung Kim (Samsung Medical Center, Korea)

14:40-14:50 (SS02-P4)
Evaluating Clinico-Pathological Characteristics of Non-Massive Breast Cancer on Ultrasound
Yanwen Luo (Zhongshan Hospital, Fudan University, China)

GBR 102

14:10-15:30

Categorical Course 4 (GU) (p 69-73)

Emergency GU Ultrasound

Chairperson(s)
Sukhee Heo (Chonnam National University Hwasun Hospital, Korea)
See Hyung Kim (Kyungpook National University Hospital, Korea)

14:10-14:30 (CC04-S1)
Acute Flank Pain
Hyo Jeong Lee (Ewha Womans University Mokdong Hospital, Korea)

14:30-14:50 (CC04-S2)
Acute Scrotal Pain
Weon Jang (Jeonbuk National University Hospital, Korea)

14:50-15:10 (CC04-S3)
Gynecologic Emergency US (Cyst Rupture, Torsion, PID)
Mi-Yeon Park (Asan Medical Center, Korea)

15:10-15:30 (CC04-S4)
Obstetric Emergency US
Min Je Kim (Samsung Medical Center, Korea)

GBR 103

14:10-15:30

Hot Issue 1 (ABD)

(p 74)

New & Cool for the Liver

Chairperson(s)
Jae Young Lee (Seoul National University Hospital, Korea)
Jeong Eun Lee (Chungnam National University Hospital, Korea)

14:10-14:30 (HI01-S1)
Continuously Evolving Elastography
Ioan Sporea (Victor Babes University of Medicine and Pharmacy Timisoara, Romania)

14:30-14:40 (HI01-P1) (p 166)
Ultrasound-Based Fat Fraction for Detection of Hepatic Steatosis and Quantification of Liver Fat Content Using Liver Biopsy as the Reference Standard: A Prospective Study
Huixiong Xu (Zhongshan Hospital Fudan University, China)

14:40-14:50 (HI01-P2) (p 167)
The Value of Ultrasound Fat Fraction as Compared to Controlled Attenuation Parameter for the Severity of Liver Steatosis Assessment
Ioan Sporea (Victor Babes University of Medicine and Pharmacy Timisoara, Romania)

14:50-15:10 (HI01-S2) (p 75)
Accurate Fat Measurement
Sun Kyung Jeon (Seoul National University Hospital, Korea)

15:10-15:20 (HI01-P3) (p 167)
Ultrasound-Guided Attenuation Parameter (UGAP) for Diagnosing Metabolic Dysfunction-Associated Steatotic Liver Disease [VOD]
Yi Dong (Xinhua Hospital Affiliated to Shanghai Jiao Tong University School of Medicine, China)

Room 203

14:10-15:30

Hot Issue 2 (THY)

(p 76-80)

Cutting-Edge Strategies in Thyroid RFA: From Experimental Studies to Patient Wellbeing

Chairperson(s)
Dong Gyu Na (GangNeung Asan Hospital, Korea)
Jin Yong Sung (Daerim St. Mary's Hospital, Korea)

14:10-14:35 (HI02-S1)
Experimental Studies to Enhance the Efficacy and Safety in Thyroid RFA
Ren Jie (The Third Affiliated Hospital of Sun Yat-sen University, China)

14:35-15:00 (HI02-S2)
Tips for Effective and Safe Thyroid RFA
Jung Hwan Baek (Asan Medical Center, Korea)

15:00-15:25 (HI02-S3)
Quality of Life in Thyroid RFA vs. Surgery
Jennifer Kuo (Columbia University, USA)

Room 209

14:10-15:10

Ultrasonography Editorial Workshop (Korean)

Chairperson(s)
Woo Kyoung Jeong (Samsung Medical Center, Korea)

14:10-14:30 (UEW-S1)
Ultrasonography 연간 보고
Jung-Eun Cheon (Seoul National University Hospital, Korea)

14:30-15:00 (UEW-S2)
Ultrasonography: Journal Performance
Hyun Jung Yi (Hanyang University Guri Hospital, Korea)

15:00-15:10
Discussion

Room 209

15:10-15:20

Coffee Break

Room 209

15:20-16:20

[Inter-section Symposium 1] Physics and Clinic

(p 81-85)

Novel Technology on Vascular Imaging

Chairperson(s)
Dong-Guk Paeng (Jeju National University, Korea)
Kyoung Won Kim (Asan Medical Center, Korea)

15:20-15:40 (IS01-S1)
Clinical Photoacoustic Imaging
Chulhong Kim (Pohang University of Science and Technology, Korea)

15:40-16:00 (IS01-S2)
Microflow Imaging Technique: Clinical Application
Pae Sun Suh (Severance Hospital, Korea)

16:00-16:20 (IS01-S3)
Ultrasound Vascular Imaging for Focused Ultrasound Blood-Brain Barrier Opening
Sua Bae (Sogang University, Korea)

15:30-16:00

Coffee Break
Ultrasound, the Best 2 (GBR 104+105)

GBR 101+102

16:00-17:20

Interactive Case Review

Room 209

16:20-17:20

Special Focus Session 1 (PHY)

(p 86-88)

Vascular Imaging Systems

Chairperson(s)
Dong-Guk Paeng (Jeju National University, Korea)
Jihun Kim (Kangnam University, Korea)

16:20-16:40 (SF01-S1)
Implantable Ultrasound Doppler Transducer for Monitoring Vascular Recovery Post-Anastomosis
Jinhyoung Park (Sungkyunkwan University, Korea)

16:40-17:00 (SF01-S2)
Ultrafast Doppler Imaging and Ultrasound Localized Microscopy for Rodent Brain Vascular Monitoring
Jaesok Yu (Daegu Gyeongbuk Institute of Science and Technology, Korea)

17:00-17:20 (SF01-S3)
Harnessing Light and Sound to Advance Critical Care Medicine
Jeeun Kang (Johns Hopkins University, USA)

Day 2 – May 9 (Fri)

GBR 102

09:00-09:30

Meet the Professor 6 (THY) (p 89)

Artificial Intelligence in Thyroid US

Chairperson(s)
Jung Hwan Baek (Asan Medical Center, Korea)

09:00-09:30 (MP06-S1)
Artificial Intelligence in Thyroid US
Jin Young Kwak (Severance Hospital, Korea)

Room 203

09:00-09:30

Meet the Professor 8 (PED) (p 91)

Ultrasound of Acute Abdomen in Children

Chairperson(s)
Yong-woo Kim (Severance Hospital, Korea)
So-Young Yoo (Samsung Medical Center, Korea)

09:00-09:30 (MP08-S1)
Ultrasound of Acute Abdomen in Children
Kushaljit Singh Sodhi (Postgraduate Institute of Medical Education and Research, India)

GBR 103

09:00-09:30

Meet the Professor 7 (MSK) (p 90)

US of Knee and Ankle

Chairperson(s)
Yun Sun Choi (Nowon Eulji Medical Center, Eulji University, Korea)
Young-Hwan Lee (Daegu Catholic University Medical Center, Korea)

09:00-09:30 (MP07-S1)
Nerve Anatomy and Pathology around Knee and Ankle
Chee Yeong Lim (Singapore General Hospital, Singapore)

Room 209

09:00-09:30

Meet the Professor 9 (CV) (p 92)

Chairperson(s)
Yeon Hyeon Choe (Samsung Medical Center, Korea)
Sung Min Ko (Wonju Severance Christian Hospital, Korea)

09:00-09:30 (MP09-S1)
Comprehensive Guide to Doppler Ultrasound for Optimal Vascular Assessment
Jongmin Lee (Kyungpook National University Hospital, Korea)

GBR 101

09:30-10:30

Categorical Course 5 (ABD) (p 93-98)

Who Are You, the Mysterious Stranger?

Chairperson(s)
Young Hwan Lee (Wonkwang University Hospital, Korea)
Yong Eun Chung (Severance Hospital, Korea)

09:30-09:45 (CC05-S1)
Incidentally Found Hepatic Focal Lesions
Sungjun Hwang (Inje University Ilsan Paik Hospital, Korea)

09:45-10:00 (CC05-S2)
Incidentally Found Pancreas Focal Lesions
Ji Hye Min (Samsung Medical Center, Korea)

10:00-10:15 (CC05-S3)
Incidental Focal Splenic Lesions
Hyun Kyung Yang (Severance Hospital, Korea)

10:15-10:30 (CC05-S4)
Incidentally Found Peritoneal/Retroperitoneal Focal Lesions
Youe Ree Kim (Wonkwang University Hospital, Korea)

GBR 102

09:30-10:30

Categorical Course 6 (THY) (p 99-102)

US Based Management of Thyroid Nodules

Chairperson(s)
Jeong Seon Park (Hanyang University Medical Center, Korea)
Soo Yeon Hahn (Samsung Medical Center, Korea)

09:30-09:50 (CC06-S1)
US Assessment of Thyroid Nodules: K-TIRADS
Hunjong Lim (Seoul National University Bundang Hospital, Korea)

09:50-10:10 (CC06-S2)
Management of Thyroid Nodules after Biopsy and Nodules not Meeting Biopsy Criteria
Hye Shin Ahn (Chung-Ang University Hospital, Korea)

10:10-10:30 (CC06-S3)
CNB Techniques for FNA Challenging Thyroid Nodules
Jae Ho Shin (Korea University Anam Hospital, Korea)

GBR 103

09:30-10:30

Categorical Course 7 (MSK) (p 103-105)

US of Nerve Imaging (Lecture & Live Demo)

Chairperson(s)
Kil-Ho Cho (Kumi Hyundai Hospital, Korea)
Jee Won Chai (Seoul National University Boramae Medical Center, Korea)

09:30-09:50 (CC07-S1)
Nerve Imaging around the Shoulder (Lecture)
Carlo Martinoli (DISSAL. University of Genova, Italy)

09:50-10:10 (CC07-S2)
Nerve Imaging around the Elbow and Forearm (Lecture)
Carlo Martinoli (DISSAL. University of Genova, Italy)

10:10-10:30 (CC07-S3)
Nerve Imaging around the Upper Extremity (Live Demo)
Carlo Martinoli (DISSAL. University of Genova, Italy)

Room 203

09:30-10:30

Categorical Course 8 (PED) (p 106-111)

Bowel US in Pediatric Patients

Chairperson(s)
Hee Jung Lee (Keimyung University Dongsan Medical Center, Korea)
Su-mi Shin (Seoul National University Boramae Medical Center, Korea)

09:30-09:50 (CC08-S1)
Bowel US in Neonates/Infants
Gayoung Choi (Korea University Ansan Hospital, Korea)

09:50-10:10 (CC08-S2)
Bowel US in Children
Jisun Hwang (Seoul National University Bundang Hospital, Korea)

10:10-10:30 (CC08-S3)
Bowel US in IBD Patients
Jisoo Kim (Gangnam Severance Hospital, Korea)

Room 209

09:30-10:30

Special Focus Session 2 (CV)

(p112-115)

Advancements in Vascular Ultrasound: From Early Detection to Post-Treatment Surveillance

Chairperson(s)
Eun-Ah Park (Seoul National University Hospital, Korea)
Bae Young Lee (The Catholic University of Korea, Eunpyeong St. Mary's Hospital, Korea)

09:30-09:50 (SF02-S1)
The Role of Ultrasound in Abdominal Aortic Aneurysm Surveillance and Management
Yoonseong Lee (Seoul National University Hospital, Korea)

09:50-10:10 (SF02-S2)
Learning Vascular Ultrasound in Private Clinics: Key Insights and Practical Tips for Radiologists
Yong Wonn Kwon (Cheil Orthopedic Hospital, Korea)

10:10-10:30 (SF02-S3)
Advanced Techniques in Carotid Ultrasound Imaging for Stroke Patients
Chi Kyung Kim (Korea University Guro Hospital, Korea)

10:30-11:00

Coffee Break
Ultrasound, the Best 3 (GBR 104+105)

GBR 101

11:00-12:20

Scientific Session 3 (ABD) (p 171-175)

Chairperson(s)
Min Ju Kim (Korea University Anam Hospital, Korea)
Ijin Joo (Seoul National University Hospital, Korea)

11:00-11:10 (SS03-P1)
Utilization of High-Resolution Kupffer Phase Imaging and Contrast-Enhanced Superb Microvascular Imaging for Focal Liver Lesion Characterization
Jeongin Yoo (Seoul National University Hospital, Korea)

11:10-11:20 (SS03-P2)
Combining Heuristic Knowledge and Multi-Model Machine Learning for Sonazoid-Enhanced Ultrasound in Liver Tumor Differentiation
Naohisa Kamiyama (GE HealthCare Japan, Japan)

11:20-11:30 (SS03-P3)
Super Resolution Ultrasound Microvascular Imaging Revealing Hidden Vascular Patterns for Enhancing Hepatocellular Carcinoma Diagnosis
Qi Zhang (Zhongshan Hospital Fudan University, China)

11:30-11:40 (SS03-P4)
Impact of Histologic Subtype on Survival Outcomes in Patients with Recurrent Hepatocellular Carcinoma Treated with Radiofrequency Ablation
Kyowon Gu (Samsung Medical Center, Korea)

11:40-11:50 (SS03-P5)
Noninvasive Subharmonic Aided Pressure Estimation (SHAPE) in the Assessment of Portal Hypertension in Patients with Decompensated Cirrhosis [VOD]
Yunlin Huang (Xinhua Hospital Affiliated to Shanghai Jiao Tong University School of Medicine, China)

11:50-12:00 (SS03-P6)
Perfusion Patterns of Contrast Enhanced Ultrasound Correlated with Histopathological Response of Neoadjuvant Chemotherapy for Borderline Resectable or Locally Advanced Pancreatic Cancer [VOD]
Xiaoyi Yan (Peking Union Medical College Hospital, Peking Union Medical College, China)

12:00-12:10 (SS03-P7)
A Study of Contrast-Enhanced Ultrasound in the Differentiation of Mass-Forming Pancreatitis From Pancreatic Ductal Adenocarcinoma [VOD]
Ke Lyu (Peking Union Medical College Hospital, China)

11:40-11:50 (SS04-P5)
Thyroid Nodules with Spoke-Wheel Blood Flow on US: Novel Indicators to Enhance Diagnostic Accuracy
Li Xu (The first Medical Centre, Chinese PLA General Hospital, China)

11:50-12:00 (SS04-P6)
Radiofrequency Ablation of Low-Risk Papillary Thyroid Microcarcinoma: A Retrospective Cohort Study Including Patients with More Than 10 Years of Follow-Up
So Yeong Jeong (Seoul National University Bundang Hospital, Korea)

GBR 102

11:00-12:20

Scientific Session 4 (THY)

(p 175-179)

Chairperson(s)
Jung Hee Shin (Samsung Medical Center, Korea)
Jung Hyun Yoon (Severance Hospital, Korea)

11:00-11:10 (SS04-P1)
Inconclusive Cytology Results of Fine-Needle Aspiration for Thyroid Nodules: The Gravity of Strict Guideline Implementation
Sangwoo Cho (Yonsei University College of Medicine, Korea)

11:10-11:20 (SS04-P2)
Differences in Diagnostic Trends When Using K-TIRADS and the ACR TI-RADS: A Reader Study
Seohyun Ryu (Yonsei University College of Medicine, Korea)

11:20-11:30 (SS04-P3)
Risk Stratification of Thyroid Follicular Neoplasm Diagnosed on Core Needle Biopsy by Histology Subcategory and Ultrasound
Dong Gyu Na (GangNeung Asan Hospital, Korea)

11:30-11:40 (SS04-P4)
Application of Follicular Thyroid Imaging Reporting and Data System to 116 Cases of Follicular Thyroid Carcinoma Diagnosed Over 28 Years at a Single Institution: Associated with TERT Promoter Mutation
Myoung Kyoung Kim (Samsung Medical Center, Korea)

GBR 103

11:00-12:20

Multisession 1 (MSK)

(p 116-119)

US of Various MSK Diseases

Chairperson(s)
Jung-Ah Choi (Hallym University Dongtan Sacred Heart Hospital, Korea)
Ji Young Hwang (Ewha Womans University Seoul Hospital, Korea)

11:00-11:20 (MS01-S1)
US of MSK Soft Tissue Tumorous Lesions
Kyung-Sik Ahn (Korea University Anam Hospital, Korea)

11:20-11:40 (MS01-S2)
US of MSK Soft Tissue Nontumorous Lesions
You Seon Song (Pusan National University Hospital, Korea)

11:40-12:00 (MS01-S3)
US Diagnosis of Finger Flexion Dysfunction
Jiwoon Seo (Seoul National University Boramae Medical Center, Korea)

12:00-12:10 (MS01-P1) (p 179)
Usefulness of Ultrasound Elastography in Differential Diagnosis of Epidermal Cysts and Ruptured Epidermal Cysts
Hee Jin Park (Kangbuk Samsung Hospital, Korea)

12:10-12:20 (MS01-P2) (p 180)
Atelocollagen Injection with Polydeoxyribonucleotide in Supraspinatus Tendon Tear
Gi-young Park (Daegu Catholic University Medical Center, Korea)

Room 203

11:00-12:20

Multisession 2 (PED)

(p 120-121)

Chairperson(s)
Byoung Hee Han (GangNeung Asan Hospital, Korea)
Young Ah Cho (Asan Medical Center, Korea)

11:00-11:20 (MS02-S1)
Ultrasound in Pediatric Cystic Kidney Diseases
Supika Kritsaneephaiboon (Prince of Songkla University, Thailand)

11:20-11:30 (MS02-P1) (p 180)
Accuracy of Large Language Models in Detecting Cases Requiring Prompt Radiology Reporting in a Pediatric Emergency Setting: A Feasibility Study Using Publicly Available Clinical Vignettes
Pyeong Hwa Kim (Asan Medical Center, Korea)

11:30-11:40 (MS02-P2) (p 181)
Neonatal Brain Perivascular Space Volume Measurement Using Cranial Ultrasound: Association with Germinal Matrix Hemorrhage
Hyun Gi Kim (The Catholic University of Korea, Eunpyeong St. Mary's Hospital, Korea)

11:40-11:50 (MS02-P3) (p 182)
Correlation Between Ultrasound Derived Fat Fraction and Proton Density Fat Fraction for Evaluating Pediatric Hepatic Steatosis with Consideration of the Breathing Effect
Jisoo Kim (Gangnam Severance Hospital, Korea)

11:50-12:00 (MS02-P4) (p 182)
Optimum Minimal Number for Proper Acquisition of Ultrasound-Derived Fat Fraction in Pediatric Patients with Suspicious Fatty Liver Disease in Consideration with the Effect of Breathing
Haesung Yoon (Severance Hospital, Korea)

12:00-12:10 (MS02-P5) (p 183)
Optimal Minimal Number for the Proper Aquisition of Multisample Ultrasound Point Shear Wave Elastography for Evaluating Pediatric Liver in Consideration with the Effect of Breathing
Yonghan Kwon (Severance Hospital, Korea)

12:10-12:20 (MS02-P6) (p 183)
Development of a Simplified Prediction Model for Diagnosing Progressive Central Precocious Puberty Using Clinical and Pelvic Ultrasound Parameters
Yeseul Kang (Yongin Severance Hospital, Korea)

Room 209

11:00-12:20

Hands-on Session (ABD/CV)

(p 122-124)

11:00-11:20 (HS01-S1)
(ABD) Liver Doppler
Dong Ik Cha (Samsung Medical Center, Korea)

11:20-11:40 (HS01-S2)
(CV) Basics and Tips for Peripheral Artery and Vein Ultrasound: A Comprehensive Guide
Ki Seok Choo (Pusan National University Yangsan Hospital, Korea)

12:20-12:40

Coffee Break

GBR 101

12:40-13:40

Luncheon Symposium 2 (PHILIPS)

Chairperson(s)
Jeong Min Lee (Seoul National University Hospital, Korea)

12:40-13:40 (LS02-S1)
Philips Auto ElastQ: Easier, Faster and More Reliable 2D Shear Wave Elastography
Seung-Seob Kim (Severance Hospital, Korea)

GBR 102

12:40-13:40

Luncheon Symposium 3 (Bracco Imaging Korea)

Chairperson(s)
Sang Il Choi (Seoul National University Bundang Hospital, Korea)

12:40-13:00 (LS03-S1)
The Clinical Value of CEUS: Ablation and Endoleak Management
Dong Jae Shim (The Catholic University of Korea, Incheon St. Mary's Hospital, Korea)

13:00-13:20 (LS03-S2)
A Radiation-free Solution: The Growing Impact of CEUS in Pediatric VUR
Seung Hyun Lee (Seoul National University Hospital, Korea)

13:20-13:40
Q&A

13:40-14:00

Coffee Break

GBR 101

14:00-15:00

Special Focus Session 3 (GU)

(p 125-127)

Ultrasound in the Diagnosis and Treatment of Prostate Cancer

Chairperson(s)
Dae Chul Jung (Severance Hospital, Korea)
Sang Youn Kim (Seoul National University Hospital, Korea)

14:00-14:20 (SF03-S1)
Transperineal MR-US Fusion Biopsy
Ka-Fung Peter Chiu (The Chinese University of Hong Kong, Hong Kong, China)

14:20-14:40 (SF03-S2)
Microultrasound and Microvascular Imaging for Prostate Cancer
Myoungseok Lee (Seoul National University Boramae Medical Center, Korea)

14:40-15:00 (SF03-S3)
HIFU as a Treatment Option of Prostate Cancer
Sung Il Hwang (Seoul National University Bundang Hospital, Korea)

GBR 102

14:00-15:00

Hot Issue 3 (BR)

(p 128-131)

AI and Breast US

Chairperson(s)
Sung Hun Kim (The Catholic University of Korea, Seoul St. Mary's Hospital, Korea)
Young Mi Park (Inje University Busan Paik Hospital, Korea)

14:00-14:20 (HI03-S1)
Supplemental Screening Ultrasound in Dense Breast: Comparison with Mammography with AI
Jung Min Chang (Seoul National University Hospital, Korea)

14:20-14:40 (HI03-S2)
AI in Screening Ultrasound
Won Hwa Kim (Kyungpook National University Chilgok Hospital, Korea)

14:40-15:00 (HI03-S3)
AI Use in US: Beyond Detection and Diagnosis
Jin Kyung An (Nowon Eulji Medical Center, Eulji University, Korea)

GBR 103

14:00-15:00

Live Demonstration 1 (MSK)

(p 132-133)

Chairperson(s)
Doo Hoe Ha (CHA University Bundang Medical Center, Korea)
Soo-jung Choi (GangNeung Asan Hospital, Korea)

14:00-14:30 (LD01-S1)
US of Elbow Joint (Live Demo)
Eun Hae Park (Jeonbuk National University Hospital, Korea)

14:30-15:00 (LD01-S2)
US of Knee Joint (Live Demo)
Chee Yeong Lim (Singapore General Hospital, Singapore)

Room 203

14:00-15:00

Categorical Course 9 (KSTU)

(p 134-136)

Advancing Therapeutic Ultrasound: Insights into Fundamentals and Innovations

Chairperson(s)
Yongrae Roh (Kyungpook National University, Korea)
Young Sun Kim (MINT Hospital, Korea)

14:00-14:20 (CC09-S1)
Customized Ultrasonic Devices and Techniques for Cavitation-Assisted Sonothrombolysis
Jinwook Kim (Kyungpook National University, Korea)

14:20-14:40 (CC09-S2)
Disposable Wearable Ultrasound: An Emerging Device for Clinical Translation
Byung Chul Lee (Korea Institute of Science and Technology, Korea)

14:40-15:00 (CC09-S3)
Ultrasound-Induced Optical Clearing for Deep Optical Imaging and Photothermal Therapy
Jin Ho Chang (Daegu Gyeongbuk Institute of Science and Technology, Korea)

15:00-15:20

Coffee Break
Ultrasound, the Best 4 (GBR 104+105)

GBR 101

15:20-16:20

Special Focus Session 4 (ABD)

(p 137-140)

Intestinal US is Coming Back!

Chairperson(s)
Se Hyung Kim (Seoul National University Hospital, Korea)
Ji Soo Song (Chonbuk National University Hospital, Korea)

15:20-15:40 (SF04-S1)
Recent Changes in Diagnosis & Management of IBD
Kyuwon Kim (Chung-Ang University Hospital, Korea)

15:40-16:00 (SF04-S2)
Role of Imaging for IBD (CT & MR)
Jung Hee Son (Inje University Haeundae Paik Hospital, Korea)

16:00-16:20 (SF04-S3)
Assessment and Monitoring of IBD with US
Sung Kyoung Moon (Kyung Hee University Medical Center, Korea)

GBR 102

15:20-16:20

Special Focus Session 5 (BR)

(p 141-143)

High Risk Lesions of Breast

Chairperson(s)
Bo Kyoung Seo (Korea University Ansan Hospital, Korea)
Min Jung Kim (Severance Hospital, Korea)

15:20-15:50 (SF05-S1)
Management of High Risk Lesions-Singapore Experience
Rameysh Danovani Mahmood (Changi General Hospital, Singapore)

15:50-16:20 (SF05-S2)
Managing High-Risk Lesions: Key Considerations
Soong June Bae (Gangnam Severance Hospital, Korea)

GBR 103

15:20-16:20

Live Demonstration 2 (THY)

(p 144-147)

Ultrasound Anatomy of the Thyroid and Neck

Chairperson(s)
So Lyung Jung (The Catholic University of Korea, St. Vincent's Hospital, Korea)
Yoon Jung Choi (Kangbuk Samsung Hospital, Korea)

15:20-15:50 (LD02-S1)
Ultrasound Anatomy of the Neck: Introduction to Thyroid and Adjacent Anatomy
Leehi Joo (Chung-Ang University Hospital, Korea)

15:50-16:20 (LD02-S2)
Ultrasound Anatomy of the Neck: Nerves
Min Kyoung Lee (The Catholic University of Korea, Yeouido St. Mary's Hospital, Korea)

Room 203

15:20-16:20

Special Focus Session 6 (KSTU)

(p 148-149)

Therapeutic Ultrasound in Brain Application

Chairperson(s)
Seok Ho Hong (Asan Medical Center, Korea)
Eun-Joo Park (Seoul National University Hospital, Korea)

15:20-15:50 (SF06-S1)
Focused Ultrasound Surgery for Dystonia
Shiro Horisawa (Tokyo Women's Medical University, Japan)

15:50-16:20 (SF06-S2)
FUS Medicated BBBO to Enhance Delivery Lazertinib Delivery for Metastatic Brain Tumor from NSCLC
Won Seok Chang (Severance Hospital, Korea)

16:20-16:40

Coffee Break

GBR 101

16:40-17:50

[Inter-section Symposium 2] Inter-body part symposium: AI

(p 150-155)

Chairperson(s)
Eunkyung Kim (Yongin Severance Hospital, Korea)
Sung Il Hwang (Seoul National University Bundang Hospital, Korea)

16:40-17:00 (IS02-S1)
The Present and Future of Medical Imaging AI
Hyungjun Park (Shihwa Medical Center, Korea)

17:00-17:20 (IS02-S2)
Using Mammographic AI to care for Patients with Breast Diseases: Applications in Breast US Exam
Jung Hyun Yoon (Severance Hospital, Korea)

17:20-17:40 (IS02-S3)
Generating Radiology Reports of Ultrasound Exams Using LLMs
Jeonghyun Lee (Samsung Medical Center, Korea)

GBR 103

16:40-17:50

Live Demonstration 3 (ABD)

(p 156-159)

Chairperson(s)
Kyung Sook Shin (Chungnam National University Hospital, Korea)

16:40-17:15 (LD03-S1)
Liver Fat Measurement
Dong Wook Kim (Asan Medical Center, Korea)

17:15-17:50 (LD03-S2)
Liver Focal Lesion CEUS
Woo Kyoung Jeong (Samsung Medical Center, Korea)

Ultrasound, the Best

(Informal Scientific Presentation)

Day 1 – May 8 (Thu)

GBR 104+105

10:50-11:10

Ultrasound, the Best 1

(p 184-185)

Chairperson(s)
Young Seo Cho (Hanyang University Guri Hospital, Korea)

10:50-10:53 (USB01-P1)
Diffuse Hepatic Hemangiomatosis in a Young Mongolian Female
Ariunbold Gankhuyag (Asralt Med Hospital, Mongolia)

10:53-10:56 (USB01-P2)
Transient Type Ischemic Enterocolitis Diagnosed by Contrast Enhanced Ultrasonography
Misato Maeyama (Osaka Ekisaikai Hospital, Japan)

15:30-16:00

Ultrasound, the Best 2

(p 185-189)

Chairperson(s)
Myoungseok Lee (Seoul National University Boramae Medical Center, Korea)

15:30-15:33 (USB02-P1)
Tracing the Tardus Parvus: Unmasking Common Iliac Artery Stenosis as a Cause of Renal Allograft-Mediated Hypertension
Ahnee Mae Ahyong (National Kidney and Transplant Institute, Philippines)

15:33-15:36 (USB02-P2)
The Value of Color Doppler Ultrasound in the Diagnosis and Management of Symptomatic Enhanced Myometrial Vascularity (EMV)
Inshirah Momin (Bhatia General Hospital, India)

15:36-15:39 (USB02-P3)
The Role of Ultrasound in the Detection of Urothelial Carcinoma in Low-Resource Settings
Karen Tehani San Pedro (National Kidney and Transplant Institute, Philippines)

15:39-15:42 (USB02-P4)
The Great Escape with Good Steal: A Case Report of an Arteriovenous Fistula of the Arm with Thrombi, Collaterals and Steal Phenomenon in a Chronic Kidney Disease Patient
Ma Katrina Villanueva (National Kidney and Transplant Institute, Philippines)

15:42-15:45 (USB02-P5)
A Case Report of Ductal Carcinoma of the Breast Metastasizing to the Ipsilateral Axillary Lymph Node
Khishgee Tsolmon (Mongolian National University of Medical Sciences, Mongolia)

15:45-15:48 (USB02-P6)
Cesarean Scar Endometriosis: A Case Report with Ultrasound and CT Imaging Features
Munkh-Uyanga Boldbaatar (Rehamed Hospital, Mongolia)

15:48-15:51 (USB02-P7)
The Role of Ultrasound in First Episode of Urinary Tract Infection in Females - A Case Report
Xanicia Long (National Healthcare Group, Singapore)

Day 2 – May 9 (Fri)

GBR 104+105

10:30-11:00

Ultrasound, the Best 3 (p 189-191)

Chairperson(s)
Seungchul Han (Samsung Medical Center, Korea)

10:30-10:33 (USB03-P1)
Ultrasound and Computed Tomography in the Diagnosis of Hepatocellular Carcinoma Complicated by Hepatogastric Fistula [VOD]
Bat-Erdene Battseren (Third State Central Hospital of Mongolia, Mongolia)

10:33-10:36 (USB03-P2)
Decreasing Mortality Risk in Hepatic Abscesses – The Value of Ultrasound in Early Recognition and Percutaneous Drainage
Karen Tehani San Pedro (National Kidney and Transplant Institute, Philippines)

10:36-10:39 (USB03-P3)
Peroneal Brevis Tendon Passes Under the Peroneal Trochlea at the Lateral Hindfoot: A Case Report
Kwang Jae Lee (Presbyterian Medical Center (Jesus Hospital), Korea)

10:39-10:42 (USB03-P4)
Acute Acalculous Cholecystitis
Saindelger Batbaatar (Allergy Med Hospital, Mongolia)

10:42-10:45 (USB03-P5)
From Start to Finish: The Role of Ultrasound in the Diagnosis and Management of Portal Vein Thrombosis
Tanya Katherine Cinco (NKTI, Philippines)

15:00-15:20

Ultrasound, the Best 4 (p 192-194)

Chairperson(s)
Hee Mang Yoon (Asan Medical Center, Korea)

15:00-15:03 (USB04-P1)
Postoperative Recurrence of a Yolk Sac Tumor in a Pediatric Patient with Immature Testicular Teratoma [VOD]
Huiyong Hu (Shanghai Children's Hospital, Shanghai Jiao Tong University, China)

15:03-15:06 (USB04-P2)
Microvascular Imaging (Advanced Dynamic Flow) for Detection, RFA Planning, Post-RFA Evaluation of Recurrent Thyroid Cancer
Jae Ho Shin (Korea University Anam Hospital, Korea)

15:06-15:09 (USB04-P3)
Ultrasound Detection and Aspiration of Milk of Calcium in Juvenile Dermatomyositis: A Case Report
Jae-Yeon Hwang (Seoul National University Hospital, Korea)

15:09-15:12 (USB04-P4)
Common Carotid Artery–Internal Jugular Vein Fistula – A Rare Complication of Central Venous Catheterization
Karen Tehani San Pedro (National Kidney and Transplant Institute, Philippines)

Scientific Exhibition

[Abdomen]

(p 194-201)

SE-001
A Case of Diaphragmatic Lipoma Initially Misdiagnosed as a Hepatic Tumor
Yasushi Seki
Department of Radiology, IKEDA City Hospital, Japan

SE-002
A Rare Case of Liposarcoma in Retroperitoneal Space
Dorjkhand Ichinkhorloo
Department of Radiology, Mongolian National University of Medical Sciences, Mongolia

SE-003
Acute Cholangitis Caused by Choledocholithiasis and Common Bile Duct Ascariasis: A Case Report
Saranchimeg Boldbaatar, Erdenesuren Dashzeveg, Munkh-Orgil Rentsensambuu, Erdenebulgan Batmunkh
Department of Radiology, The Second State Central Hospital, Mongolia

SE-004
AI-Guided Ultrasound and Epigenetic Analysis of Hepatic Fibrosis: A Multi-Omics Deep Learning Model for Predicting Fibroblast Plasticity and Cirrhotic Progression in Non-Alcoholic Steatohepatitis
Sahnaz Vivinda Putri[1], Rini Winarti[2], Prihantini Prihantini[3], Rifaldy Fajar[3]
[1]Health Management Laboratory, International University Semen Indonesia, Indonesia, [2]Department of Biology, Yogyakarta State University, Indonesia, [3]Mathematical and Computational BioMedicine Research Group, The Integrated Mathematical, Computational, and Data Science for BioMedicine Research Community Foundation, Indonesia

SE-005
Bibliometric Analysis of Machine Learning-Driven Ultrasound in Liver Cancer Diagnosis: Trends and Insights (2020-2025)
Rian Ka Praja, Reny Rosalina
Universitas Palangka Raya, Indonesia

SE-007
Cystic Echinococcosis of the Liver
Saindelger Batbaatar
Department of Radiology, Allergy Med Hospital, Mongolia

SE-009
Endoscopic Ultrasonography (EUS) Compared with Magnetic Resonance Cholangiopancreatography (MRCP) in Diagnosing Patients with Malignancy Causing Obstructive Jaundice: A Systematic Review and Meta-analysis
Divo Helmizar[1], Roland H[2]
[1]STAN, Indonesia, [2]Department of Internal Medicine, Siti Rahmah Islamic Hospital, Indonesia

SE-011
Machine Learning-Driven Ultrasound Multi-Omics Profiling for Real-Time Prediction of Hepatic Stellate Cell Activation and Fibrotic Progression
Elfiany Syafruddin[1], Sahnaz Vivinda Putri[2], Rini Winarti[3], Prihantini Prihantini[4], Rifaldy Fajar[4]
[1]Computational Science Research Laboratory, Bulukumba Muhammadiyah University, Indonesia, [2]Health Management Laboratory, International University Semen Indonesia, Indonesia, [3]Department of Biology, Yogyakarta State University, Indonesia, [4]Mathematical and Computational BioMedicine Research Group, The Integrated Mathematical, Computational, and Data Science for BioMedicine Research Community Foundation, Indonesia

SE-012
The Impact of Ultrasound Quality Control on Liver Cancer Screening Outcomes: The Importance of Intercostal Scan Quality
Woo Kyoung Jeong, Yeun-Yoon Kim
Department of Radiology, Samsung Medical Center, Korea

SE-013
Ultrasound Liver Imaging Reporting and Data System Version 2017: A Systematic Review and Meta-Analysis
Sunyoung Lee[1], Ja Kyung Yoon[1], Jaeseung Shin[2], Anum Aslam[3], Aya Kamaya[4], Shuchi K Rodgers[5], Claude B. Sirlin[6], Victoria Chernyak[7]
[1]Department of Radiology, Severance Hospital, Korea, [2]Department of Radiology, Samsung Medical Center, Korea, [3]Department of Radiology, University of Michigan Medicine, United States, [4]Department of Radiology, Stanford University, United States, [5]Department of Radiology, Thomas Jefferson University, United States, [6]Department of Radiology, University of California San Diego, United States, [7]Department of Radiology, Columbia University Irving Medical Center, United States

SE-014
Utilizing Machine Learning-Integrated Endoscopic Ultrasound for Optimized Prediction of Biliary Drainage Success in Patients with Malignant Biliary Obstruction: Insights from a Retrospective Analysis
Aryofri Afan[1], Divo H[2]
[1]Institut Asia Malang, Indonesia, [2]STAN, Indonesia

[Breast] (p 201-202)

SE-015

Comparative Diagnostic Accuracy of Ultrasound, Mammography, and Magnetic Resonance Imaging in Detecting Breast Cancer Lesions in Patients with Breast Implants: A Comprehensive Systematic Review

Roland Helmizar[1], Vina Tri Septiana[2], Nana Liana[3]
[1]Department of Internal Medicine, Baiturrahmah University, Indonesia, [2]Department of Radiology, Baiturrahmah University, Indonesia, [3]Department of Pathology, Baiturrahmah University, Indonesia

SE-016

Initial Experience of Ultrasound-Guided Intralesional Steroid Injection in Treating Idiopathic Granulomatous Mastitis – Still an Uphill Task or There Is Light at the End of the Tunnel?

Asif Momin[1], Shenaz Momin[2], Manthan Parikh[1]
[1]Department of Radiology, Head & Neck Cancer Institute of India, India, [2]Department of Radiology, BYL NAIR HOSPITAL and TN Medical College Mumbai, India

SE-017

The Correlation Between Ultrasound Features and Histologic Findings of BI-RADS 3 Breast Nodular Lesions

Tsendsaikhan Batkhuu
Department of Radiology, Radiologist, Mongolia

[Cardiovascular] (p 203-205)

SE-018

Deep Learning-Driven Nanobubble Ultrasound Imaging for Subcellular Endothelial Dysfunction Assessment in Atherosclerosis: A Multi-Scale Computational Approach

Rini Winarti[1], Sahnaz Vivinda Putri[2], Elfiany Syafruddin[3], Prihantini Prihantini[4], Andi Nursanti[5], Rifaldy Fajar[4]
[1]Department of Biology, Yogyakarta State University, Indonesia, [2]Health Management Laboratory, International University Semen Indonesia, Indonesia, [3]Computational Science Research Laboratory, Bulukumba Muhammadiyah University, Indonesia, [4]Mathematical and Computational BioMedicine Research Group, The Integrated Mathematical, Computational, and Data Science for BioMedicine Research Community Foundation, Indonesia, [5]Department of Pharmacology, Wallacea University, Indonesia

SE-019

Evaluation of Access Routes Using Ultrasound Before Cardiac Catheterization

Masayuki Fujioka[1], Koichi Yabunaka[3], Tomohiro Nakashouji[2]
[1]Department of Laboratory Medicine, Katsuragi Hospital, Japan, [2]Department of Internal Medicine-Cardiology, Katsuragi Hospital, Japan, [3]Department of Radiology, Ono Memorial Hospital, Japan

SE-020

Implementing Vascular Scientist-Led Contrast-Enhanced Ultrasound (CEUS) Endovascular Aneurysm Repair (EVAR) Scans to Enhance the Patient Pathway in the United Kingdom

Ming Yeung
Department of Surgery, Manchester University NHS Foundation Trust, United Kingdom

SE-021

Molecular Imaging Agents in Cardiovascular Ultrasound: Bridging Diagnostics and Targeted Therapy

Reny Rosalina[1], Rian Ka Praja[2]
[1]Department of Biochemistry & Molecular Biology, Universitas Palangka Raya, Indonesia, [2]Department of Microbiology, Universitas Palangka Raya, Indonesia

[Genitourinary] (p 205-209)

SE-022

Bilateral Duplex Collecting Systems With Bilateral Ectopic Vaginal Implantation Causing Recurrent Urinary Tract Infection and Incontinence in a Pediatric Patient

Raenald Julian, Maria Regina Cruz-Tuble, June Danica Dumago
Department of Radiology, National Kidney and Transplant Institute, Philippines

SE-024

Interdisciplinary Expansion of Ultrasound in Ovarian Cancer: Insights from a Bibliometric Analysis of Screening, Biomarkers, and Computational Advancements

Reny Rosalina[1], Rian Ka Praja[2]
[1]Department of Biochemistry & Molecular Biology, Universitas Palangka Raya, Indonesia, [2]Department of Microbiology, Universitas Palangka Raya, Indonesia

SE-025

Modifying Sleeping Posture May Be an Effective Management Plan in Patients with Nutcracker Syndrome

Seung Hyup Kim[1], Joongyub Lee[1], Eungtaek Kang[2], Suhnggwon Kim[2], Hyo Jeong Lee[3], Myung Kim[4], Dong Hyun Lee[4], Sang Eun Lee[4]
[1]Department of Radiology, Seoul National University Hospital, Korea, [2]Department of Internal Medicine-Nephrology, Seoul K Clinic, Korea, [3]Department of Radiology, Ewha Womans University Mokdong Hospital, Korea, [4]Department of Urology, SNU Healthy Prostate Clinic, Korea

SE-026

Study on Changes in Blood Flow Through Uterine Arteries, Umbilical Artery and Cerebral Media Artery During Preeclampsia by Doppler Ultrasound

Zambaga Ganzorigt
Department of Radiology, Khuree Maternity Hospital, Mongolia

SE-027

The Role of Ultrasound in Diagnosis of Renal Lymphangiectasia, an Uncommon Cause of Perirenal Collections

Xanicia Long[1], Kok Kit Ng[2]
[1]Department of Family Medicine, National Healthcare Group, Singapore, [2]Department of Urology, Changi General Hospital, Singapore

SE-028

Young Female Perivascular Epithelioid Cell Tumor of Uterus: A Case Report

Garamjav Khishigdavaa[1], Uyan-Egshig Dorjnamjim[1], Nergui Olzvoi[2]
[1]Department of Radiology, DCDR Hospital of Mongolia, Mongolia, [2]Department of Radiology, Grandmed Hospital, Mongolia

[Head & Neck]

(p 209)

SE-029

Small but Significant Carotid Space – Pictorial Essay of Common and Rare Pathologies

Shenaz Momin[1], Asif Momin[2], Inshirah Momin[3]
[1]Department of Radiology, BYL NAIR HOSPITAL and TN Medical College Mumbai, India, [2]Department of Radiology, Head and Neck Cancer Institute of India and Bhatia Hospital, India, [3]Department of Radiology, Bhatia General Hospital, India

[Musculoskeletal]

(p 210-212)

SE-030

A Case of Extensor Carpi Radialis Brevis Tear Following Internal Fixation of Distal Radius Fracture

Dong Hwee Kim, Ki Hoon Kim, Hong Bum Park
Department of Rehabilitation Medicine, Korea University Ansan Hospital, Korea

SE-033

Diagnostic Shoulder Ultrasound: A Case-Based Review of Its Clinical Impact

Jee Won Chai, Dong Hyun Kim, Hyo Jin Kim, Jiwoon Seo
Department of Radiology, Seoul National University Boramae Medical Center, Korea

SE-035

High Resolution Ultrasound Finding of Big Toe Lesion: MR Correlation

Dalsu Park
Department of Radiology, OSBONE HOSPITAL, Korea

SE-036

Median Neuropathy as a Complication of Radial Forearm Free Flap Surgery: A Case Report

Nackhwan Kim
Department of Rehabilitation Medicine, Incheon Sejong Hospital, Korea

SE-037

Phlegmasia Alba Dolens in May-Thurner Syndrome: A Rare Syndrome of Acute Deep Vein Thrombosis and Literature Review

Seul Ki Lee
Department of Radiology, The Catholic University of Korea, St. Vincent's Hospital, Korea

SE-038

Reproducibility of Shear Wave and Strain Elastography Depending on the Size of the Region of Interest: A Study Using Epidermal Cysts

Hee Jin Park, Sungchul Wee
Department of Radiology, Kangbuk Samsung Hospital, Korea

SE-040

Sonographic Mulder Sign: Does It Always Indicate Morton's Neuroma?

Hyejung Choo
Department of Radiology, Inje University Busan Paik Hospital, Korea

SE-041

State of Musculoskeletal Ultrasound in Kazakhstan: Teaching Resources and Literature Availability

Yerlan Yemeshev
Department of Radiology, TMC Qonrad, Kazakhstan

[Pediatric] (p 213-218)

SE-042
A Systematic Review and Meta-Analysis of Diagnostic Performance of Ultrasound for Differentiating Malignant From Benign Cervical Lymphadenopathy in Children
Jayoung Moon[1], Jisun Hwang[2], Pyeong Hwa Kim[3]
[1]Department of Radiology, Ajou University Hospital, Korea, [2]Department of Radiology, Seoul National University Bundang Hospital, Korea, [3]Department of Radiology, Asan Medical Center, Korea

SE-043
Challenging Pilomatricoma in Children: Sonographic Clues and Seiral Change
So-Young Yoo, Ji Hye Kim, Tae Yeon Jeon, Ji Eun Park
Department of Radiology, Samsung Medical Center, Korea

SE-044
Pediatric Hernias Reviews
Ji Eun Park, Ji Hye Kim, So-Young Yoo, Tae Yeon Jeon
Department of Radiology, Samsung Medical Center, Korea

SE-045
Sonographic Findings of Renal Cystic Lesions in Pediatric Patients: Key Features and Differential Diagnoses
Minjee Cho[1], Haesung Yoon[1], Jisoo Kim[2], Yong-woo Kim[1], Mi-Jung Lee[1]
[1]Department of Radiology, Severance Hospital, Korea, [2]Department of Radiology, Gangnam Severance Hospital, Korea

SE-046
Ultrasonographic Measurement of Anterior Fontanelle Size in Infants with Deformational Plagiocephaly: Correlation with Severity and Developmental Delay
Dong Rak Kwon
Department of Rehabilitation Medicine, Daegu Catholic University Medical Center, Korea

SE-047
Ultrasound Diagnosis of Inflammatory Processes in Soft Tissues of the Gluteal Region: A Case of a Benign Neoplasm with Calcification Signs
Zhanar Kozhakhmetova, Inabat Sary, Yurana Albaeva
Department of Radiology, University Medical Centre, Kazakhstan

SE-048
Ultrasound Diagnosis of Patau Syndrome
Baigalmaa Ulaankhuu
Department of Radiology, Gurvan Gal General Hospital, Mongolia

SE-049
Ultrasound Diagnosis of Soft Tissue Lesions of the Anterior Chest Wall: A Clinical Case of Tuberculosis
Zhanar Kozhakhmetova, Nurgul Orynbassar, Yurana Albaeva
Department of Radiology, University Medical Centre, Kazakhstan

SE-050
Ultrasound Imaging of Inguinal Lesions in Infancy: Differential Diagnoses and Key Features
Jeongil Son, Haesung Yoon, Jisoo Kim, Yongwoo Kim, Mijung Lee
Department of Radiology, Severance Hospital, Korea

[Physics] (p 218-221)

SE-051
A High-Frequency Real-Time Doppler System for Monitoring Hemodynamics of the Microcirculation in Small Animal Brains
Wontae Son, Seoyun Chang, Changyang Lee, Jinhyoung Park
Sungkyunkwan University, Korea

SE-052
AI-Driven Ultrasound Chromatin Profiling for Non-Invasive, Real-Time Detection of 3D Genome Architecture Disruptions in Early Cancer and Aging
Rifaldy Fajar[1], Prihantini Prihantini[1], Sahnaz Vivinda Putri[2], Rini Winarti[3], Andi Nursanti[4]
[1]Mathematical and Computational BioMedicine Research Group, The Integrated Mathematical, Computational, and Data Science for BioMedicine Research Community Foundation, Indonesia, [2]Health Management Laboratory, International University Semen Indonesia, Indonesia, [3]Department of Biology, Yogyakarta State University, Indonesia, [4]Department of Pharmacology, Wallacea University, Indonesia

SE-053
AI-Driven Ultrasound-Based Intracellular Trafficking Profiling for Real-Time, Non-Invasive Detection of Organelle Transport Dysregulation in Neurodegeneration and Cancer Metastasis
Prihantini Prihantini[1], Sahnaz Vivinda Putri[2], Rini Winarti[3], Andi Nursanti[4], Rifaldy Fajar[1]
[1]Mathematical and Computational BioMedicine Research Group, The Integrated Mathematical, Computational, and Data Science for BioMedicine Research Community Foundation, Indonesia, [2]Health Management Laboratory, International University Semen Indonesia, Indonesia, [3]Department of Biology, Yogyakarta State University, Indonesia, [4]Department of Pharmacology, Wallacea University, Indonesia

SE-054
Developing a Dual-Frequency Needle Ultrasonic Transducer for Cortical Network Study in Small Animal Brains with Low-Frequency
Daegan Kee, Taewon Choi, Seunghoo Kim, Yeji Seo, Jinhyoung Park
Sungkyunkwan University, Korea

SE-055
Dual-Frequency Implantable Transparent Ultrasonic Transducers for Integrated Brain Stimulation and Monitoring
Minseok Koo, Changyang Lee, Jinhyoung Park
Sungkyunkwan University, Korea

[Therapeutic Ultrasound]

(p 221-223)

SE-056
Cryo-Shocked Tumor-Reprogrammed Sonosensitive Antigen-Presenting Cells Improving Sonoimmunotherapy via T Cells and NK Cells Immunity
Xindi Qian
Department of Medical Ultrasound and Center of Minimally Invasive Treatment for Tumor, Shanghai Tenth People's Hospital, Tongji University, China

SE-057
Dual Receptor Targeting, Treatment, and Imaging With a Chitosan Nanoplatform That Simultaneous Administration of Gallic Acid and Ultra-Small Magneses Nanoaggregates
D Singh
MPGI, India

SE-058
RCP vs. EUS-FNA in the Diagnosis of Presumed Malignant Biliary Obstruction: A Systematic Review and Meta-analysis
Derizal Derizal[1], Roland Helmizar[2]
[1]IP Trisakti, Indonesia, [2]Department of Internal Medicine, Baiturrahmah University, Indonesia

[Thyroid]

(p 223-230)

SE-060
A Study Compared the Thyroid Ultrasound Measurements of Citizens and Those of Workers Who Were Exposed to X-Rays
Amgalanbayar Tumendelger
Department of Otorhinolaryngology, ENT DOCTORS SOCIETY IN MONGOLIA, Mongolia

SE-061
Efficacy and Determinants of Single-Session Ethanol Ablation in Thyroid Cysts 10 mL and Larger
Kai-Lun Cheng
Department of Radiology, Chung Shan Medical University Hospital, Chinese Taipei

SE-062
Efficacy and Safety of Thermal Ablation for Indeterminate Thyroid Nodules: A Systematic Review and Meta-Analysis
Hunjong Lim[1], Se Jin Cho[1], Younbeom Jeong[1], So Yeong Jeong[1], Jung Hwan Baek[2]
[1]Department of Radiology, Seoul National University Bundang Hospital, Korea, [2]Department of Radiology, Asan Medical Center, Korea

SE-063
Efficacy of Radiofrequency Ablation for Solid Thyroid Nodules
Javzmaa Divaa[1], Otgonbayar Setevdorj[2]
[1]Department of Radiology, The Mongolian Society of Radiology, [2]Department of Surgery, First Central Hospital of Mongolia, Mongolia

SE-064
Longterm Clinical Outcomes of Thermal Ablation for Benign Thyroid Nodules and Unresolved Issues: A Comprehensive Systematic Review
So Yeong Jeong[1], Jung Hwan Baek[2]
[1]Department of Radiology, Seoul National University Bundang Hospital, Korea, [2]Department of Radiology, Asan Medical Center, Korea

SE-065
Prognostic Significance of Clinicopathological and Ultrasonographic Features in Anaplastic Thyroid Carcinoma Beyond TERT Promoter Mutation
Haejung Kim[1], Goeun Park[2], Myoung Kyoung Kim[1], Jae Ho Lee[1], Young Lyun Oh[3], Tae Hyuk Kim[4], Jung Hee Shin[1], Soo Yeon Hahn[1]
[1]Department of Radiology, Samsung Medical Center, Korea, [2]Samsung Medical Center, Korea, [3]Department of Pathology, Samsung Medical Center, Korea, [4]Department of Internal Medicine-Endocrine, Samsung Medical Center, Korea

SE-066

Radiofrequency Ablation for Patients with Primary Hyperparathyroidism: A Multicenter, Non-Randomized, Open-Label, Single-Arm Prospective Clinical Trial

Eun Ju Ha[1], Jihoon Kim[2], Jung Hwan Baek[3]
[1]Department of Radiology, Ajou University Hospital, Korea, [2]Department of Radiology, Seoul National University Hospital, Korea, [3]Department of Radiology, Asan Medical Center, Korea

SE-067

Reevaluating the Malignancy Risk of K-TIRADS 2 Benign Thyroid Nodules: An Intracystic Small Echogenic Focus With a Comet-Tail Artifact Is Not Highly Specific for Benignity

Jaeyong Min[1], Dong Gyu Na[1], Byeong-Joo Noh[2]
[1]Department of Radiology, GangNeung Asan Hospital, Korea, [2]Department of Pathology, GangNeung Asan Hospital, Korea

SE-068

Role of Radiofrequency Ablation in the Treatment of Symptomatic Distant Metastasis of Thyroid Cancer

Jae Ho Lee[1], Sae Rom Chung[1], Jung Hwan Baek[1], Dong Eun Song[2], Won Gu Kim[3], Tae Yong Kim[3], Tae Yon Sung[4], Jeong Hyun Lee[1]
[1]Department of Radiology, Asan Medical Center, Korea, [2]Department of Pathology, Asan Medical Center, Korea, [3]Department of Internal Medicine, Asan Medical Center, Korea, [4]Department of Surgery, Asan Medical Center, Korea

SE-069

Temporal Involutional Change on Ultrasonography After RFA for PTMC

Taehyuk Ham, Ji-hoon Kim, Ji Ye Lee, Meesun Lee
Department of Radiology, Seoul National University Hospital, Korea

SE-070

The Intersection of Machine Learning and Ultrasound in Thyroid Cancer Diagnosis: A Bibliometric Study

Rian Ka Praja, Reny Rosalina
Universitas Palangka Raya, Indonesia

SE-071

Thyroid Volume and Morphologic Change After Radiofrequency Ablation for Papillary Thyroid Microcarcinoma: CT-Based Analysis

Meesun Lee, Taehyuk Ham, Inpyeong Hwang, Ji Ye Lee, Ji-hoon Kim
Department of Radiology, Seoul National University Hospital, Korea

SE-072

Ultrasound Characteristics of High-Grade Follicular-derived Carcinomas: Insights into Poorly Differentiated and Differentiated High-Grade Thyroid Carcinoma

Myoung Kyoung Kim, Jaeho Lee, Haejung Kim, Soo Yeon Hahn, Jung Hee Shin
Department of Radiology, Samsung Medical Center, Korea

KSUM 2025

Abstract Book

MP01-S1 **Optimizing Supplemental Screening**

09:00-09:30 **GBR 101**

Chairperson(s): Jung Min Chang *(Seoul National University Hospital, Korea)*

Supplemental Screening Strategies: Deciding on DBT, Ultrasound, or MRI

Stamatia Destounis
Elizabeth Wende Breast Care, USA

This presentation reviews the American College of Radiology (ACR) recommendations for supplemental breast cancer screening, focusing on selecting the most appropriate modality based on individual risk factors. It outlines criteria for high-risk patients and discusses the effectiveness of different imaging techniques.

Key topics covered include:

- Digital Breast Tomosynthesis (DBT): Research findings on its benefits in reducing recall rates and improving cancer detection compared to standard mammography.
- Screening Breast Ultrasound: Evidence supporting its use, particularly for women with dense breast tissue, despite concerns about false positives.
- Screening Breast MRI: The gold standard for high-risk patients, offering superior sensitivity but with higher costs and logistical considerations.

Additionally, the presentation briefly explores emerging technologies like contrast-enhanced mammography (CEM) and molecular breast imaging (MBI) as potential supplemental screening tools.

Ultimately, the selection of a supplemental screening strategy depends on individual patient risk factors, access, and the strengths and limitations of each modality.

MP02-S1

09:00-09:30 GBR 102

Chairperson(s): Chan Kyo Kim *(Samsung Medical Center, Korea)*

Various Focal Therapy for Prostate Cancer and the Role of Imaging in Focal Therapy

Ka-Fung Peter Chiu

Department of Surgery, The Chinese University of Hong Kong, Hong Kong, China

Treatments for localized prostate cancer recommended by major guidelines include radical prostatectomy and radiotherapy. They can both achieve excellent cancer control, but long term side effects including stress urinary incontinence (10-15%), erectile dysfunction (up to 50-80%), and irradiation cystitis and proctitis (5-15%) can be debilitating to the patients. Focal therapy involves ablation of prostate cancer cells with various energies, and serves as a middleground between active surveillance and radical treatments for prostate cancer. Conventional ablation of prostate cancer were usually whole-gland ablation or hemi-gland ablation. With the advancement of MRI-guided prostate cancer diagnosis and precision biopsy in recent years, cancer locations can be precisely mapped on 3D biopsy models. Therefore, focal therapy can be accurately performed using MRI-guidance. In this talk, various prostate cancer focal therapy modalities (HIFU, Cryotherapy, IRE, Microwave, etc) will be discussed and compared, followed by MRI-Ultrasound fusion guided ablation of the prostate.

MP03-S1 **All about Liver RFA**

09:00-09:30 **GBR 103**

Chairperson(s): Chang Hee Lee *(Korea University Guro Hospital, Korea)*

All about Liver RFA

Yasunori Minami
Department of Gastroenterology and Hepatology, Kindai University, Japan

Percutaneous thermal ablation including radiofrequency ablation (RFA) is a minimally invasive treatment that is being increasingly performed because it achieves good clinical outcomes with a lower risk of complications. However, an image-guided RFA may be challenging in hepatocellular carcinoma (HCC) cases. Tumor/patient conditions and imaging/technical factors may have an impact on whether RFA is the appropriate treatment choice. Therefore, a basic understanding of the advantages and limitations of RFA and imaging guidance techniques, respectively, is quite important. I would like to provide an overview of the pre and intra ablation management for liver cancer. Especially, the ultrasound (US) imaging technology, including contrast-enhanced US (CEUS) and fusion imaging is useful to overcome the problem of poor conspicuous HCC. We will discuss associated challenges and how they may be overcome using optimized techniques.

MP04-S1 Multimodal Imaging for the Assessment of Head and Neck Tumors

09:00-09:30 Room 203

Chairperson(s): Ji-Hoon Kim *(Seoul National University Hospital, Korea)*

Multimodal Imaging for the Assessment of Head and Neck Tumors: From Ultrasound to MRI

Jeong Hyun Lee

Department of Radiology, Asan Medical Center, Korea

In the radiologic evaluation of head and neck tumors, cross-sectional imaging modalities such as CT and MRI are the main tools. Especially for malignant masses, their role is significant in staging and establishing pre-treatment strategies. Although the role of ultrasound has diminished compared to the past, it still remains important in the radiologic assessment of head and neck tumors. Compared to CT or MRI, ultrasound is more accessible and allows for the rapid evaluation of palpable abnormalities. It also helps characterize lesions, and in some cases, enables diagnosis without the need for additional tests.

Most palpable neck masses in adults originate from lymph nodes, and many of these are malignant. Malignant lymph nodes typically show low echogenicity on ultrasound; however, metastases from thyroid cancer or certain adenocarcinomas may appear hyperechoic, which requires caution. Among hypoechoic tumors that need to be differentiated from malignant lymph nodes, depending on location, are salivary gland tumors, parathyroid adenomas, and soft tissue tumors.

One of the most common benign soft tissue mass is lipoma. Although benign lipomas appear similar to many malignant tumors on ultrasound as hypoechoic masses comparable to surrounding subcutaneous fat, they characteristically have soft consistency and contain internal echogenic strands running parallel to the skin regardless of scanning angle. Some lipoma variants may show atypical ultrasound findings, and well-differentiated or myxoid liposarcomas may resemble benign lipomas. However, liposarcomas tend to be larger than 10 cm, located in deeper spaces, and show hyperechogenicity or vascular signals—features that distinguish them from simple lipomas. Therefore, if a lesion suspected to be a lipoma shows hyperechogenicity or vascularity on ultrasound, CT, MRI, or biopsy should be performed to confirm the diagnosis. Among hyperechoic lesions with an infiltrative nature, lymphoma should be considered. Particularly, in cases such as peripheral T-cell lymphoma, which may show vascular predilection, the appearance can mimic panniculitis, requiring careful evaluation.

Today, one of the most important roles of ultrasound is guiding minimally invasive procedures such as fine-needle aspiration for cytologic diagnosis, radiofrequency ablation, or sclerotherapy. In cancer patients scheduled for surgery, biopsy plays a critical role in staging. However, if CT or MRI is planned, one should consider that biopsy-induced tissue changes may affect imaging findings, so the sequence and timing of tests should be adjusted accordingly to ensure accurate staging. After procedures like radiofrequency ablation or radiation therapy, various tissue changes may occur, so awareness of post-treatment changes is crucial for accurate ultrasound evaluation.

Ultrasound has increasingly become not just a diagnostic imaging tool but also a guide for obtaining tissue and performing minimally invasive treatments. Despite advances in other imaging modalities, ultrasound still holds a critical role due to its high accessibility, absence of radiation, and no need for contrast agents. For effective use, it is essential to understand the diseases diagnosable by ultrasound, their atypical features, and the limitations of ultrasound-based diagnosis.

MP05-S1

09:00-09:30 **Room 209**

Chairperson(s): Jinhyoung Park *(Sungkyunkwan University, Korea)*

Principles of Ultrasound Doppler and Advanced Blood Flow Imaging

Dong-Guk Paeng
Department of Ocean System Engineering, Jeju National University, Korea

Ultrasound Doppler techniques are real-time and non-invasive blood flow measurement and visualization. This lecture explores the principles and advancements in ultrasound Doppler technology, seeking to deepen the understanding and applications of these techniques.

The lecture will begin with a foundational overview of continuous and pulsed Doppler methodologies, highlighting their roles in the Doppler spectrograms and spectral broadening for assessing blood flow dynamics. We will include color Doppler imaging, emphasizing the correlation techniques to improve spatial and temporal resolution. Additionally, the session will cover power Doppler imaging, highlighting its effectiveness in detecting blood flow in small vessels.

This lecture will also address the uncertainties in Doppler flow measurement, providing insights into the factors influencing measurement accuracy and reliability. A practical emphasis will be placed on addressing measurement errors arising from differences between longitudinal and cross-sectional imaging planes. Additionally, we will present techniques for 3-dimensional blood vessel visualization and blood flow measurements with conventional and advanced 2-dimensional ultrasound transducers.

The lecture will introduce advanced concepts such as vector flow imaging, which offers a more comprehensive visualization of complex flow patterns, and high frame rate imaging, which significantly enhances the temporal and spatial resolution of blood flow measurements, particularly in microvessels. Further, the session will introduce photoacoustic blood flow measurement and visualization, a technique that combines laser-induced photoacoustic effects and ultrasound to provide high-contrast and high-resolution images of blood flow.

This comprehensive lecture is designed to equip ultrasound professionals with cutting-edge knowledge and skills that may be helpful for improved clinical practice and patient outcomes.

CC01-S1 Enhancing Breast Ultrasound

09:30-09:57 GBR 101

Chairperson(s): **Joo Hee Cha** *(Asan Medical Center, Korea)*
Hye-Won Kim *(Wonkwang University Hospital, Korea)*

Combining Ultrasound and Mammography: A Case-Based Review

A Jung Chu
Department of Radiology, Seoul National University Boramae Medical Center, Korea

Integrating ultrasound with mammography enhances diagnostic accuracy, particularly in challenging cases such as dense breast tissue or asymmetry. In the Japan Strategic Anti-cancer Randomized Trial (J-START), the sensitivity was significantly higher in the intervention group (mammography and ultrasonography, 91.1%) than in the control group (mammography alone77.0%), whereas specificity was significantly lower. Also, the interval cancer rate was significantly lower in the intervention group (0.05% vs. 0.10%). Especially, this study revealed supplementary ultrasonography improved the detection rate of small (less than 1 cm), early-stage (stage 0 and stage 1) and invasive cancers. In the secondary analysis study, ultrasonography also increased the rate of early invasive cancers in both dense breasts and non-dense breasts.

Breast Ultrasound is a safe and cost-effective imaging modality that can be performed without additional radiation risk or pain. In this lecture, I will demonstrate real-life scenarios through case examples where breast ultrasound proves beneficial and share key imaging features for differential diagnosis in each clinical context.

CC01-S2 Enhancing Breast Ultrasound

09:57-10:24 GBR 101

Chairperson(s): Joo Hee Cha *(Asan Medical Center, Korea)*
Hye-Won Kim *(Wonkwang University Hospital, Korea)*

Basics and Tips to MRI-Targeted Ultrasound: A Case-Based Review

Hye-Joung Eom
Department of Radiology, Asan Medical Center, Korea

Introduction

Second-look US is a targeted examination of MRI-detected lesions, primarily used to facilitate lesion localization and allow for US-guided biopsy, which is generally preferred over MRI-guided biopsy due to its greater accessibility, lower cost, and improved patient comfort. Lesion identification during second-look US relies on factors such as lesion morphology and anatomical landmarks, including glandular patterns, Cooper's ligaments, fat distribution, and vascular structures. However, prior research has shown that 9% of MRI findings were inaccurately correlated on second-look US. A systematic review of 17 studies reported wide variability in second-look US detection rates, ranging from 22.6% to 82.1%. Detection was significantly higher for mass and malignant lesions compared to nonmass and benign lesions. Pooled positive and negative predictive values for US correlation with MRI-detected lesions were 30.7% and 87.8%, respectively. Lesions with a US correlate are more likely to be malignant than those without. US correlation was present in 75% of malignant and 52% of benign lesions. Also, among 253 lesions with a US correlate, 34% were confirmed as malignant, compared to 20% of 169 lesions lacking a US correlate. Larger lesions, masses on MRI, and invasive ductal carcinomas are more likely to be detected on US than smaller lesions, nonmass enhancement, invasive lobular carcinoma, or ductal carcinoma in situ.

MRI and US correlation

When correlating US findings with MRI to accurately localize and identify breast masses, several factors should be taken into account: lesion location, depth, size, shape, and surrounding anatomical structures. Begin by estimating the lesion's position using a quadrant-based or clock-face approach and measuring its distance from the nipple. It's important to note that this distance can vary depending on the amount of fatty tissue within the breast. Understanding the lesion's relationship to surrounding tissues and its position within breast anatomy—whether in the subcutaneous fat, parenchyma, or retromammary fat—is also key. If the lesion is within the mammary zone, it can be further categorized as anterior, middle, or posterior. However, in patients with minimal breast tissue or when lesions are located peripherally, compression and stretching of the breast during US may significantly alter the perceived depth compared to MRI. Also, it is important to recognize the differences in patient positioning during US and MRI examinations. Evaluating lesion size and shape across modalities is critical, though discrepancies are common, particularly for nonmass lesions. Due to vertical compression from the US probe, lesions often appear smaller or oval on US, where they may look larger or round on MRI. Identifying nearby structures such as cysts, fibroadenomas, surgical scars, implants, prominent blood vessels, or an index tumor can serve as helpful reference points for localization. To improve detection, supplementary US techniques such as Doppler

imaging, tissue harmonic imaging, and elastography can be employed to improve lesion conspicuity and diagnostic accuracy. A previous study evaluating subcentimeter enhancing lesions incidentally found on preoperative breast MRI found that most malignant lesions showed benign US features, making MRI enhancement patterns, particularly washout, a more reliable indicator of malignancy. This study suggested maintaining a low threshold for biopsy based on MRI characteristics.

References

1. H. Abe, R.A. Schmidt, R.N. Shah, A. Shimauchi, K. Kulkarni, C.A. Sennett, G.M. Newstead, MR-directed ("Second-Look") ultrasound examination for breast lesions detected initially on MRI: MR and sonographic findings, AJR Am J Roentgenol 194(2) (2010) 370-7.
2. L.R. LaTrenta, J.H. Menell, E.A. Morris, A.F. Abramson, D.D. Dershaw, L. Liberman, Breast lesions detected with MR imaging: utility and histopathologic importance of identification with US, Radiology 227(3) (2003) 856-61.
3. M. Meissnitzer, D.D. Dershaw, C.H. Lee, E.A. Morris, Targeted ultrasound of the breast in women with abnormal MRI findings for whom biopsy has been recommended, AJR Am J Roentgenol 193(4) (2009) 1025-9.
4. S.J. Nam, E.K. Kim, M.J. Kim, H.J. Moon, J.H. Yoon, Significance of incidentally detected subcentimeter enhancing lesions on preoperative breast MRI: role of second-look ultrasound in lesion detection and management, AJR Am J Roentgenol 204(3) (2015) W357-62.
5. V.Y. Park, M.J. Kim, E.K. Kim, H.J. Moon, Second-look US: how to find breast lesions with a suspicious MR imaging appearance, Radiographics 33(5) (2013) 1361-75.
6. C. Spick, P.A. Baltzer, Diagnostic utility of second-look US for breast lesions identified at MR imaging: systematic review and meta-analysis, Radiology 273(2) (2014) 401-9.
7. L.A. Carbonaro, P. Tannaphai, R.M. Trimboli, N. Verardi, M.P. Fedeli, F. Sardanelli, Contrast enhanced breast MRI: spatial displacement from prone to supine patient's position. Preliminary results, Eur J Radiol 81(6) (2012) e771-4.
8. J.H. Shin, B.K. Han, Y.H. Choe, K. Ko, N. Choi, Targeted ultrasound for MR-detected lesions in breast cancer patients, Korean J Radiol 8(6) (2007) 475-83.
9. W.B. Demartini, P.R. Eby, S. Peacock, C.D. Lehman, Utility of targeted sonography for breast lesions that were suspicious on MRI, AJR Am J Roentgenol 192(4) (2009) 1128-34.

CC01-S3 **Enhancing Breast Ultrasound**

10:24-10:50 **GBR 101**

Chairperson(s): **Joo Hee Cha** *(Asan Medical Center, Korea)*
Hye-Won Kim *(Wonkwang University Hospital, Korea)*

ABUS and Hand-held US: A Case-Based Review

Sung Ui Shin
Department of Radiology, Seoul National University Bundang Hospital, Korea

1. Technical differences
2. Pros and Cons of ABUS and Hand-held US
3. Case with Artifacts
4. Case of Multimodality correlation
5. Case of Preoperative state
6. Case of Postoperative state

CC02-S1 Normal Anatomy, Variation and Congenital Disease

09:30-09:50 GBR 103

Chairperson(s): **Joon-Il Choi** *(The Catholic University of Korea, Seoul St. Mary's Hospital, Korea)*
Jin-Woong Kim *(Chosun University Hospital, Korea)*

Liver and Perihepatic Space

Jeongin Yoo
Department of Radiology, Seoul National University Hospital, Korea

Ultrasound has the significant advantage of non-invasiveness and real-time images, making it easily applicable to patients. With recent technological advancements, its use has greatly increased, contributing to the early detection and differential diagnosis of upper abdominal diseases. Unlike CT or MRI, the quality of ultrasound examinations is highly dependent on the operator's experience and technique. Therefore, unlike objective tests like CT or MRI, ultrasound can be considered a subjective test. Due to its subjective nature and the ability to obtain real-time images, the accurate interpretation of ultrasound requires the operator to perform the examination and simultaneously make a diagnosis. To achieve this, a thorough understanding of the operation of ultrasound equipment, the range of tests that can be performed, preparation of the patient, as well as knowledge and experience in anatomy, physiology, pathology, and ultrasound findings are essential.

The standard examination method for upper abdominal ultrasound is as follows: First, perform a transverse scan of the main portal vein bifurcation to observe the right and left portal veins. During this scan, also check for any dilation of the intrahepatic bile ducts and examine the caudate lobe and ligamentum venosum. Next, scan the main portal vein along its long axis and observe the common bile duct running alongside it. If possible, also assess the hepatic artery. Measure the diameter of the main portal vein and the common bile duct at this stage. If the images are unclear while the patient's position is supine, reposition the patient to left lateral decubitus and recheck. Scan the gallbladder in both long and short axes. If the gallbladder is poorly visible or if stones are present, change the patient's position for additional imaging, measure the thickness of the gallbladder wall, and check for tenderness by applying pressure with the probe. Scan the lower part of the liver in a transverse plane to observe the right, middle, and left hepatic veins and their confluence, as well as the intrahepatic inferior vena cava. Transverse scan the left lobe of the liver to view the left portal vein and use both transverse and longitudinal scans to examine the hepatic parenchyma of the left lobe. At the right bifurcation point of the main portal vein, perform a transverse scan of the right lobe of the liver. Use an intercostal scan to observe the hepatic parenchyma of the right lobe and examine the right hepatic vein and right portal vein. Finally, scan the liver dome using either an intercostal or subcostal scan at the posterior axillary line. Additionally, perform a longitudinal scan to include both the lower part of the liver and the right kidney, comparing the liver's echogenicity with that of the kidney cortex.

CC02-S2 **Normal Anatomy, Variation and Congenital Disease**

09:50-10:10 **GBR 103**

Chairperson(s): **Joon-Il Choi** *(The Catholic University of Korea, Seoul St. Mary's Hospital, Korea)*
Jin-Woong Kim *(Chosun University Hospital, Korea)*

GB and Bile Duct

Shinhye Hwang
Department of Radiology, Yongin Severance Hospital, Korea

The right and left hepatic ducts converge at the liver hilum to form the common hepatic duct, which is joined by the cystic duct and continues as the common bile duct. This common bile duct merges with the pancreatic duct and drains into the duodenum through the major duodenal papilla. The junction of the right and left hepatic ducts and the cystic duct exhibits various anatomical variations. The gallbladder is a sac-like structure with a capacity of 30-50 ml. The gallbladder can also show various anatomical variations such as Phrygian cap, multiseptation, and duplication.

Congenital diseases of the biliary tract include biliary atresia and choledochal cyst. These diseases present with symptoms such as jaundice, cholelithiasis, and cholangitis, and also carry risks for cirrhosis, liver failure, and malignant neoplasms. Ultrasound is widely used as the first-line imaging modality.

In this lecture, we will discuss the normal anatomical structure and variations of the biliary tract and gallbladder, as well as congenital diseases associated with these organs.

CC02-S3 **Normal Anatomy, Variation and Congenital Disease**

10:10-10:30 **GBR 103**

Chairperson(s): **Joon-Il Choi** *(The Catholic University of Korea, Seoul St. Mary's Hospital, Korea)*
Jin-Woong Kim *(Chosun University Hospital, Korea)*

Pancreas and Spleen

Sung Hwan Bae
Department of Radiology, Soon Chun Hyang University Seoul Hospital, Korea

Pancreas

1. Anatomy

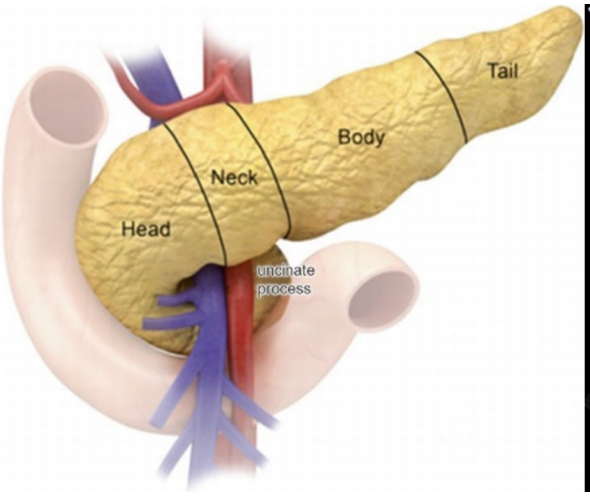

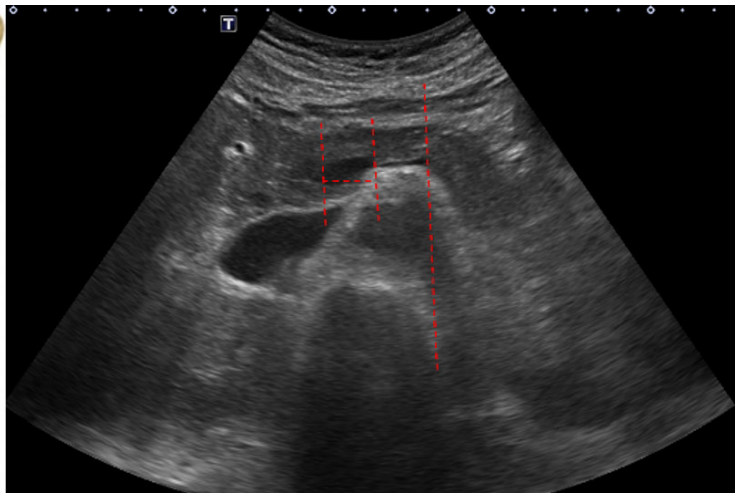

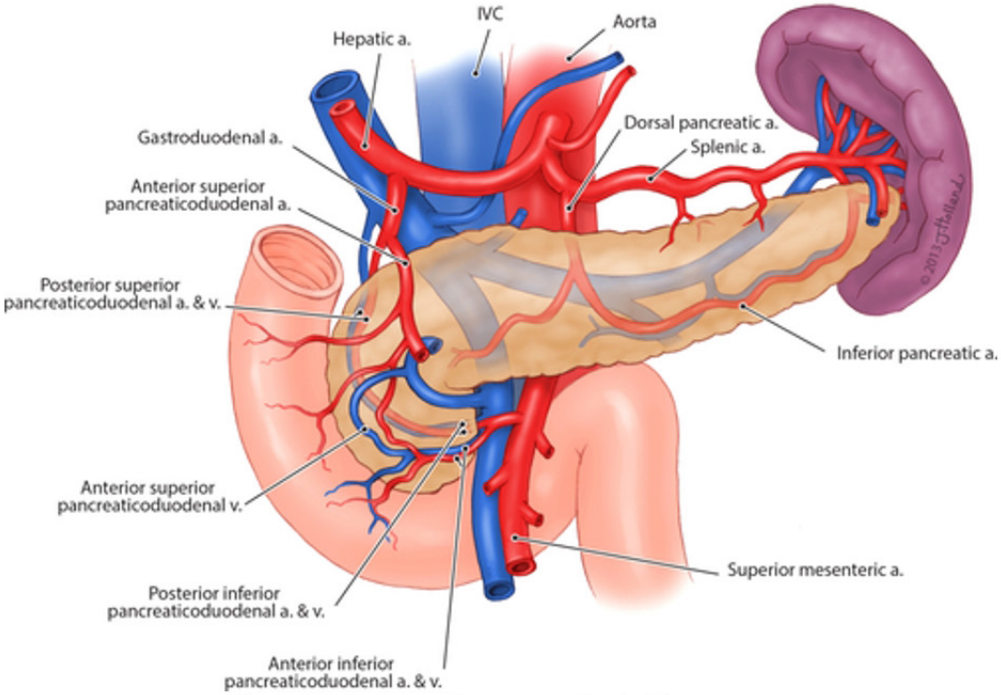

2. Normal variation and congenital disease

- Congenital variation of pancreatic duct
  - Pancreatic divisum
- Pancreatic agenesis/hypoplasia
- Annular pancreas
- Ectopic pancreas

Spleen

1. Anatomy

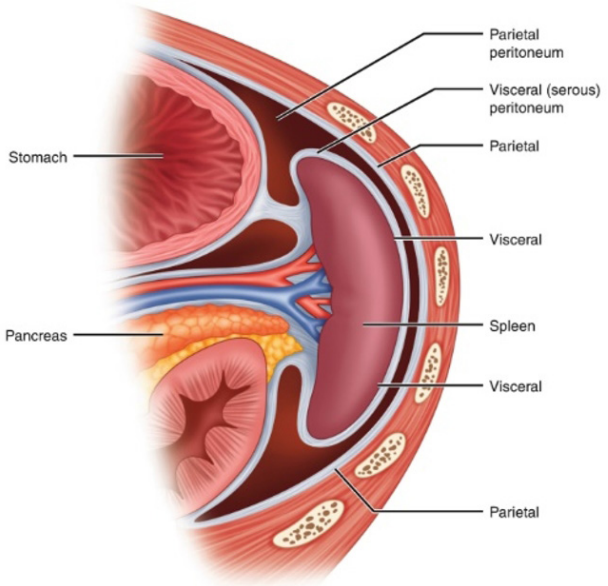

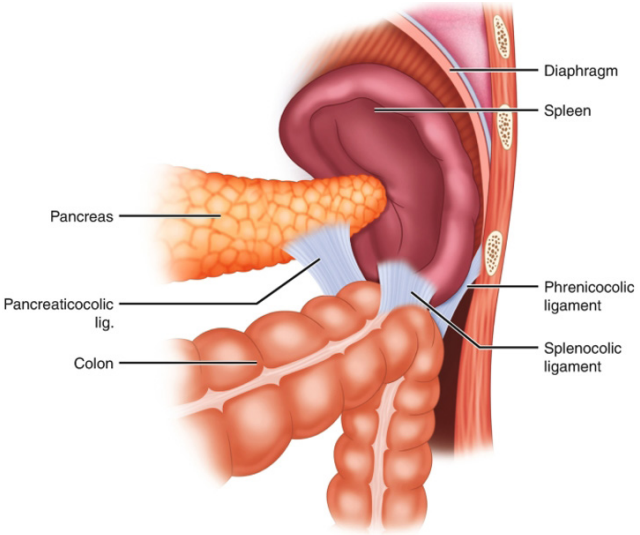

2. US of normal spleen

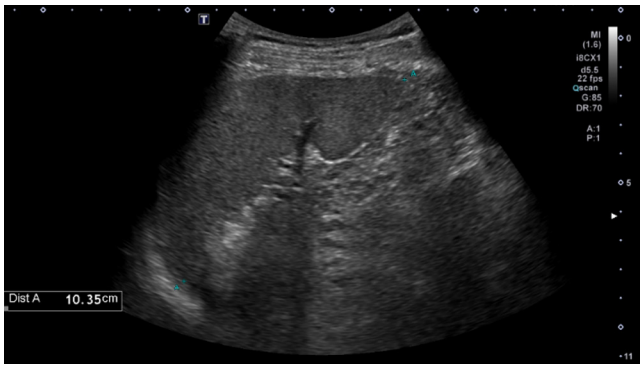

- Homogenous echogenicity
  - Spleen>Liver, kidney
- Splenomegaly>12 cm, longitudinal coronal oblique plane

3. Normal variation and congenital disease of spleen

- Accessory spleen
- Polysplenia syndrome
- Asplenia
- Wandering spleen

This lecture will provide an overview of anatomy and congenital disease of pancreas and spleen and basic knowledge.

CC02-S4 Normal Anatomy, Variation and Congenital Disease

10:30-10:50 GBR 103

Chairperson(s): **Joon-Il Choi** *(The Catholic University of Korea, Seoul St. Mary's Hospital, Korea)*
Jin-Woong Kim *(Chosun University Hospital, Korea)*

GI Tract

Yeo Eun Han
Department of Radiology, Korea University Anam Hospital, Korea

Ultrasound examination of the bowel provides valuable diagnostic information with the advantages of accessibility, patient comfort, and detailed assessment of bowel wall layers and motility. This lecture presents a comprehensive overview of bowel ultrasound techniques, normal bowel anatomy, and the recognition of congenital abnormalities in adult patients.

Examination Techniques

Patient preparation with 4-6 hours of fasting is essential to reduce luminal air and decrease peristalsis for optimal visualization. The systematic approach begins with a convex probe (3-5MHz) for overall assessment, followed by a high-frequency linear probe (5-15MHz) for detailed evaluation of bowel wall structures. The examination sequence starts at the cecum in the right iliac fossa, following the colon segments continuously to the sigmoid, then returning to assess the terminal ileum and other small bowel loops.

Graded compression technique is crucial in bowel ultrasound, allowing reduction of the distance between the transducer and target area while displacing intestinal gas. This technique improves the acoustic window and enables assessment of wall compressibility, rigidity, and pain response. When encountering acoustic shadowing, changing patient position can help optimize visualization. Color or power Doppler assessment requires careful parameter adjustment to detect low-velocity flow in bowel wall vascularity.

Normal Bowel Wall

A normal bowel wall typically measures less than 2 mm when distended, though this varies by location. The collapsed small intestine may measure up to 3 mm and the colon up to 4 mm. Notable exceptions include rectum (up to 7 mm) and sigmoid colon (up to 5 mm). High-frequency probes can identify five distinct sonographic layers corresponding to the mucosa, submucosa, muscularis propria, and serosa with their interfaces.

Accurate measurement of the bowel wall thickness requires perpendicular probe positioning to avoid tangential measurements. Normal bowel shows minimal or no blood flow on Doppler examination. Peri-intestinal features include the mesentery, appearing as mildly hypoechoic parallel layers alternated with hyperechoic strips, and normal lymph nodes that appear as oval or elongated hypoechoic nodules with shorter diameter <4 mm.

Normal Bowel Anatomy

The small bowel is centrally located with the jejunum in the left upper abdomen and ileum in the right lower abdomen. Valvulae conniventes are a key distinguishing feature, being most prominent in jejunum. The small bowel shows peristalsis (3-5 contractions per minute in jejunum). Normal small bowel diameter is less than 3 cm.

The large bowel is located peripherally with distinct segments: the retroperitoneal ascending and descending colon along the right and left abdomen, respectively; the transverse colon crossing the mid-abdomen; the pelvic sigmoid colon; and the

extraperitoneal rectum. Haustra appear as curved sacculations at 3-5 cm intervals. The colon diameter normally measures up to 5 cm, with the cecum potentially wider. Unlike the small bowel, the colon displays minimal observable peristalsis.

The normal appendix (visualized in about 50% of healthy subjects) originates from the posterior medial aspect of the cecum, measures ≤6 mm in diameter, appears compressible, and shows minimal or no Doppler flow. Common positions include retrocecal (65%), pelvic (30%), and pre- or post-ileal (5%).

Congenital Diseases in Adults

Intestinal malrotation (1:500 live births) results from abnormal midgut rotation during embryonic development. In adults, it is mostly asymptomatic and discovered incidentally, appearing as altered positions of small and large intestines.

Meckel's diverticulum (2% of population) represents the most common congenital anomaly of the gastrointestinal tract. This true diverticulum arises from the antimesenteric border of the distal ileum and contains all intestinal wall layers. On ultrasound, it appears as a tubular blind-ending structure with normal bowel wall layers.

Enteric duplication cysts (1:4,500, primarily diagnosed in children, very rare in adults) can occur anywhere along the digestive tract but most commonly in the ileum. The diagnostic "double wall sign" (gut signature sign) shows inner hyperechoic mucosa-submucosa and outer hypoechoic muscularis propria layers.

Adult Hirschsprung's disease (1:5,000 live births, rarely diagnosed in adulthood) presents with chronic constipation and appears on ultrasound as proximal colon dilation (>6-8 cm) with a narrowed transition zone, most commonly at the rectosigmoid junction.

Understanding these examination techniques and recognizing normal anatomy and congenital diseaseenables accurate diagnosis and appropriate management of bowel pathologies using ultrasound imaging.

CC03-S1 US Diagnosis and Management of Benign Neck Masses

09:30-09:55 Room 203

Chairperson(s): **Young Hen Lee** *(Korea University Ansan Hospital, Korea)*
Hyun Kyung Lim *(Soon Chun Hyang University Seoul Hospital, Korea)*

US Guided Biopsy of Benign Nodal Masses

Sang Ik Park
Department of Radiology, Asan Medical Center, Korea

US-guided fine-needle aspiration biopsy (FNAB) and core needle biopsy (CNB) are important tools in the evaluation of cervical lymphadenopathy. Indications are persistent or unexplained lymph node enlargement, particularly when imaging findings are indeterminate; suspicion of granulomatous diseases such as tuberculosis or sarcoidosis; and the need to confirm or exclude rare benign conditions. US-guided FNAB and CNB help establish diagnosis and guide appropriate medical management.

FNAB is performed using a thin needle (usually 21–23G) under US, with to-and-fro passes to obtain cytologic material. CNB is done with a spring-loaded 18G device to obtain core tissue, preserving architectural details essential for diagnosing diseases like lymphoma or Castleman disease. Both techniques are considered safe. Minor complications such as bleeding or pain are usually self-limited. Infection is rare, and injury to surrounding structures can be minimized through US evaluation.

Reactive hyperplasia is the most common benign cause of lymphadenopathy. On US, reactive nodes are oval-shaped, with a preserved echogenic hilum, thin uniform cortex, and hilar vascularity. They are usually symmetric and homogeneous. Pathologically, they show polyclonal lymphoid proliferation with preserved nodal architecture. No specific treatment is needed, but biopsy is often performed to rule out malignancy in persistent cases.

Suppurative lymphadenitis results from bacterial infection, leading to intranodal abscess formation. US shows enlarged lymph nodes with central hypoechoic/anechoic areas suggesting necrosis, poorly defined margins, and surrounding infiltration. FNAB yields pus. Culture confirms the pathogen, and aspiration can serve as both diagnostic and therapeutic modalities.

Tuberculous lymphadenitis often presents as multiple matted nodes with central necrosis. On US, affected nodes are hypoechoic, round, and can show internal heterogeneity, necrosis, or calcifications. CT may demonstrate rim enhancement or surrounding soft tissue infiltration. FNAB or CNB reveals caseating granulomas, and microbiologic confirmation is needed via AFB stain, PCR, or culture.

Sarcoidosis is a multisystem granulomatous disease that may manifest as cervical lymphadenopathy. On US, affected nodes are usually well-defined, hypoechoic, and homogeneous, without necrosis. Imaging may mimic reactive or lymphoma nodes. CNB demonstrates non-caseating granulomas, and diagnosis requires exclusion of infection.

Castleman disease, particularly the unicentric hyaline-vascular subtype, appears as a solitary, well-defined, round or oval lymph node that is homogeneously hypoechoic and often markedly hypervascular on Doppler US. CT typically shows strong, homogeneous enhancement. CNB may reveal abnormal lymphoid follicles with vascular proliferation, but excisional biopsy is often needed for confirmation.

Kikuchi disease often affects young Asian females and presents with fever and multiple enlarged and tender lymph nodes. On US, nodes are hypoechoic, mildly enlarged, and may show perinodal fat stranding. The diagnostic rate of FNA cytology for Kikuchi disease is estimated to be 45–56% and that of CNB is 82–96%. The disease is self-limited.

Kimura disease presents with painless subcutaneous

masses and enlarged lymph nodes, typically in the parotid or submandibular region of young Asian males. US shows large, well-defined, homogeneously hypoechoic masses. Associated soft tissue swelling or salivary gland involvement may be present. FNAB is often non-diagnostic. CNB or excisional biopsy reveals lymphoid follicular hyperplasia with dense eosinophilic infiltrates and vascular proliferation. Elevated serum IgE and eosinophilia support the diagnosis.

IgG4-related lymphadenopathy may present with multiple, non-tender, symmetrically enlarged nodes. On US, the nodes are well-defined, hypoechoic, and homogeneous, typically without necrosis. CT may show associated organ involvement (salivary glands, lacrimal glands). CNB reveals dense lymphoplasmacytic infiltrates with numerous IgG4-positive plasma cells. Diagnosis requires clinical and laboratory (serum IgG4 levels) correlation.

In conclusion, US-guided FNAB and CNB are important tools in diagnosing benign neck nodal diseases. Radiologists should be aware of the imaging findings and clinical presentation to make accurate diagnoses and guide optimal management.

References

1. Moon WK, Han MH, Chang KH, Im JG, Kim HJ, Sung KJ, et al. CT and MR imaging of head and neck tuberculosis. Radiographics 1997;17:391-402.
2. Song JY, Cheong HJ, Kee SY, Lee J, Sohn JW, Kim MJ, et al. Disease spectrum of cervical lymphadenitis: analysis based on ultrasound-guided core-needle gun biopsy. J Infect 2007;55:310-316.
3. Hegde AN, Mohan S, Pandya A, Shah GV. Imaging in infections of the head and neck. Neuroimaging Clin N Am 2012;22:727-754.
4. Sato Y, Yoshino T. IgG4-Related Lymphadenopathy. Int J Rheumatol 2012;2012:572539.
5. Jiang XH, Song HM, Liu QY, Cao Y, Li GH, Zhang WD. Castleman disease of the neck: CT and MR imaging findings. Eur J Radiol 2014;83:2041-2050.
6. Al Kadah B, Popov HH, Schick B, Knöbber D. Cervical lymphadenopathy: study of 251 patients. Eur Arch Otorhinolaryngol 2015;272:745-752.
7. Eisenmenger LB, Wiggins RH, 3rd. Imaging of head and neck lymph nodes. Radiol Clin North Am 2015;53:115-132.
8. Aiken AH. Image-Guided Biopsies in the Head and Neck: Practical Value and Approach. AJNR Am J Neuroradiol 2020;41:2123-2125.
9. Park SG, Koo HR, Jang K, Myung JK, Song CM, Ji YB, et al. Efficacy of Ultrasound-Guided Needle Biopsy in the Diagnosis of Kikuchi-Fujimoto Disease. Laryngoscope 2021;131:E1519-e1523.
10. Lee CC, Yu KH, Chan TM. Kimura's disease: A clinicopathological study of 23 cases. Front Med (Lausanne) 2022;9:1069102.

CC03-S2 US Diagnosis and Management of Benign Neck Masses

09:55-10:20 Room 203

Chairperson(s): Young Hen Lee *(Korea University Ansan Hospital, Korea)*
Hyun Kyung Lim *(Soon Chun Hyang University Seoul Hospital, Korea)*

US Guided Biopsy of Neck Masses Other Than LNs

Yun Hwa Roh
Department of Radiology, Samsung Medical Center, Korea

1. Introduction

Ultrasound is widely utilized in the head and neck region owing to its real-time capability, accessibility, and excellent spatial resolution. When histologic confirmation is required, ultrasound-guided biopsy serves as a safe and effective diagnostic tool for evaluating various neck masses.

2. Benign Salivary Gland Masses

Pleomorphic adenoma is the most common benign salivary gland tumor. On ultrasound, it typically presents as a well-defined, solid, hypoechoic mass with homogeneous internal echogenicity and posterior acoustic enhancement. Larger lesions may demonstrate heterogeneous internal echoes due to internal hemorrhage or necrosis. Color Doppler may reveal peripheral venous vessels.

Warthin tumor is the second most common benign salivary gland neoplasm. Smaller lesions usually appear as well-circumscribed, oval, hypoechoic masses with prominent central (hilar) vascularity. As the lesion enlarges, it may show a heterogeneous echotexture with both cystic and solid components, sometimes appearing as a multiseptated cystic mass. Because Warthin tumors are frequently bilateral or multifocal, it is essential to evaluate both glands carefully.

3. Benign Cystic Neck Masses

Thyroglossal duct cysts (TGDCs) typically appear as midline cystic neck masses embedded within the infrahyoid strap muscles. Their relationship to the hyoid bone and their location along the expected embryologic course from the foramen cecum to the thyroid bed are key diagnostic clues. Although they are congenital lesions, rare cases of thyroid carcinoma may arise within TGDCs, requiring close evaluation.

Second branchial cleft cysts are typically located posterolateral to the submandibular gland, lateral to the carotid space, and anteromedial to the sternocleidomastoid muscle. They appear as unilocular, anechoic cysts with thin walls, posterior acoustic enhancement, and occasional faint internal debris. When uninfected, there is usually no internal vascularity.

4. Benign Solid Neck Masses

Neurogenic tumors appear as solid, hypoechoic, and often heterogeneous masses with fusiform or oval shapes. A key diagnostic feature is continuity with an adjacent nerve or thickening of the involved nerve. Biopsy of these lesions should be performed with caution, as it may provoke pain and carries a risk of nerve injury.

Lipomas most commonly occur in the posterior cervical and submandibular spaces. On ultrasound, they appear as well-circumscribed, compressible, homogeneous masses with internal echogenic lines oriented parallel to the transducer surface. These lesions typically show no significant vascularity on color Doppler imaging.

CC03-S3 **US Diagnosis and Management of Benign Neck Masses**

10:20-10:45 **Room 203**

Chairperson(s): **Young Hen Lee** *(Korea University Ansan Hospital, Korea)*
Hyun Kyung Lim *(Soon Chun Hyang University Seoul Hospital, Korea)*

Management of Benign Neck Masses: US Guided Intervention vs. Surgery

Dongbin Ahn
Department of Otorhinolaryngology, Kyungpook National University, Korea

Benign neck masses encompass a heterogeneous group of lesions arising from various anatomical and embryological origins. Common entities include thyroglossal duct cysts (TGDCs), second branchial cleft cysts (2nd BCCs), parathyroid cysts, parotid cysts, and ranulas. While traditionally managed through surgical excision, recent advances in imaging and minimally invasive techniques have led to the emergence of ultrasound (US)-guided interventions, particularly ethanol ablation (EA), as viable alternatives for selected cases.

Rationale for Minimally Invasive Alternatives

Surgery, while definitive in most cases, is associated with potential morbidity such as scarring, nerve injury, anesthesia-related risks, and prolonged recovery. In contrast, US-guided interventions offer a non-surgical, outpatient-based treatment modality with fewer complications, minimal recovery time, and preserved tissue integrity. However, the long-term efficacy, recurrence risk, and lesion-specific indications of these approaches remain subjects of ongoing debate.

Emerging Role of US-Guided Ethanol Ablation

Ethanol ablation, under real-time ultrasound guidance, has demonstrated promising outcomes in managing simple cystic or predominantly cystic lesions of the neck. Its expanding application in head and neck pathology parallels the successful use of EA in thyroid cysts and nodules, supported by a growing body of evidence. Yet, its role in treating non-thyroidal neck cysts such as TGDCs, BCCs, and ranulas demands further clarification through comparative studies and long-term follow-up data.

Purpose of the Presentation

This presentation aims to provide a comprehensive review and comparative analysis of US-guided ethanol ablation versus surgical excision in the management of benign neck masses. By focusing on lesion-specific characteristics, procedural techniques, clinical outcomes, and recurrence rates, we seek to offer evidence-based guidance for optimizing patient-specific treatment strategies.

JSL-S1

11:15-11:45 GBR 103

Chairperson(s): Dal Mo Yang *(Kyung Hee University Hospital at Gangdong, Korea)*

Liver Fatty Quantification

Ioan Sporea

Department of Gastroenterology and Hepatology, Victor Babes University of Medicine and Pharmacy Timisoara, Romania

Fatty liver disease, particularly Metabolic dysfunction-Associated Steatotic Liver Disease (MASLD), is now recognized as the most prevalent chronic liver condition worldwide, closely linked to obesity, dyslipidemia, type 2 diabetes mellitus, and metabolic syndrome. Given its silent progression and potential to evolve into Metabolic dysfunction-Associated Steatohepatitis (MASH), advanced fibrosis or cirrhosis, and hepatocellular carcinoma, early detection and accurate quantification of hepatic steatosis are of paramount importance. As liver biopsy—once the gold standard—is invasive, costly, and associated with procedural risks, the demand for reliable, non-invasive imaging methods has increased, with ultrasound emerging at the forefront.

Conventional B-mode ultrasonography remains the first-line imaging tool in routine clinical assessments due to its widespread availability, safety, and low cost. Increased hepatic echogenicity, vascular blurring, and posterior beam attenuation are characteristic sonographic features of fatty infiltration. However, despite its clinical utility, traditional grayscale ultrasound is limited by operator dependence and reduced sensitivity, particularly for detecting mild steatosis (<20%) and in patients with high BMI.

To address these limitations, several quantitative ultrasound (QUS) techniques have been developed and validated for hepatic fat quantification. One of the most widely adopted advancements is the Controlled Attenuation Parameter (CAP), integrated into transient elastography platforms (e.g., FibroScan). CAP measures the attenuation of ultrasound waves as they pass through liver tissue, providing a numerical estimate of fat content. It offers rapid, reproducible, point-of-care results and is less operator-dependent than B-mode ultrasound. However, its diagnostic accuracy may be diminished in patients with obesity, narrow intercostal spaces, and is not possible in patients with ascites.

In response, newer QUS-based approaches have emerged and are increasingly incorporated into advanced ultrasound systems. These techniques generate color-coded maps and quantitative values that reflect hepatic attenuation, backscatter, or speed of sound—or a combination of these parameters—allowing for more objective and reproducible assessments. Clinical studies have demonstrated strong correlations between QUS metrics and liver fat content assessed by MRI-PDFF or histology, supporting their use in both clinical and research settings.

Despite these promising developments, several challenges remain. Variability among ultrasound vendors, lack of standardized cut-off values, and technical limitations in obese patients continue to hinder widespread adoption. Ongoing research and large-scale validation studies are essential to establish universal protocols and reference ranges. The integration of machine learning algorithms into ultrasound systems may further enhance diagnostic accuracy and reduce inter-operator variability in the near future. The new WFUMB Guideline on Fatty Liver Quantification, published in 2024, aims to provide practical recommendations for clinicians using ultrasound in routine practice.

In conclusion, ultrasound is undergoing a significant transformation in its role in fatty liver quantification—from a qualitative screening tool to a sophisticated platform capable of delivering

quantitative, reproducible measurements. As MASLD becomes an increasingly prominent public health issue, quantitative ultrasound is poised to play a central role in early detection, disease monitoring, and therapeutic evaluation, offering a safe, accessible, and cost-effective solution across both primary care and specialized hepatology settings.

JSL-S2

11:45-12:15 **GBR 103**

Chairperson(s): Dal Mo Yang *(Kyung Hee University Hospital at Gangdong, Korea)*

The Evolution of Ultrasound-Guided Liver Ablation: Past, Present, and Future

Hyunchul Rhim

Department of Radiology, Samsung Changwon Hospital, Korea

Liver ablation has significantly advanced from invasive surgical methods to safer, minimally invasive techniques, largely due to ultrasound guidance. Previously performed through open surgeries with extensive recovery times, the introduction of percutaneous approaches revolutionized the field, enhancing precision and reducing complications.

Over the past 30 years, clinical research has established local ablation as a primary treatment for early-stage hepatocellular carcinoma (HCC) in major guidelines, offering outcomes comparable to surgery with lower risk and cost. Innovations such as ultrasound fusion imaging, contrast-enhanced ultrasound, and artificial ascites have improved the safety and precision of tumor targeting. Additionally, newer energy sources like microwave ablation, cryoablation, and irreversible electroporation (IRE) have allowed for more tailored treatment strategies.

Future advancements include AI-driven electrode positioning, robotic-assisted techniques, and enhanced post-treatment evaluation. Research is also exploring the synergy between ablation and immunotherapy to identify patient groups that may benefit most from combination treatments.

With continuous technological improvements, US-guided liver ablation is evolving into a more advanced, precise, and effective therapeutic option, shaping the future of liver cancer treatment.

CC04-S1 **Emergency GU Ultrasound**

14:10-14:30 **GBR 102**

Chairperson(s): **Sukhee Heo** *(Chonnam National University Hwasun Hospital, Korea)*
See Hyung Kim *(Kyungpook National University Hospital, Korea)*

Acute Flank Pain

Hyo Jeong Lee
Department of Radiology, Ewha Womans University Mokdong Hospital, Korea

Acute flank pain is one of the most common complaints encountered in emergency departments worldwide, with urolithiasis accounting for approximately 60-70% of cases. A significant proportion of patients present with non-stone etiologies, including acute pyelonephritis, non-calculous ureteral obstruction, and various non-urological causes such as biliary disease, musculoskeletal disorders, and gynecological conditions.

This lecture focuses on the systematic ultrasonographic evaluation of patients with acute flank pain, highlighting the diagnostic protocol and key sonographic findings for urological etiologies. Ultrasound offers significant advantages in an emergency setting, including its non-invasive nature, absence of radiation, cost-effectiveness, and real-time assessment capability. We will review standardized scanning techniques, characteristic imaging findings of common pathologies, and potential pitfalls in interpretation.

CC04-S2 Emergency GU Ultrasound

14:30-14:50 GBR 102

Chairperson(s): **Sukhee Heo** *(Chonnam National University Hwasun Hospital, Korea)*
See Hyung Kim *(Kyungpook National University Hospital, Korea)*

Acute Scrotal Pain

Weon Jang
Department of Radiology, Jeonbuk National University Hospital, Korea

Acute scrotal pain is a common clinical presentation in pediatric and young adult populations, with potentially emergent etiologies that require timely diagnosis to ensure appropriate management and preservation of testicular viability. High-frequency linear transducers (7.5–12 MHz) are typically used for ultrasonographic evaluation, in conjunction with color and power Doppler imaging to assess testicular perfusion and extratesticular vascular structures. In cases where vascular findings are equivocal, contrast-enhanced ultrasound (CEUS) may provide additional diagnostic information. The examination should begin on the asymptomatic side for comparison, followed by focused assessment of the area of maximal tenderness.

Etiologies of acute scrotal pain are broadly categorized into vascular (e.g., testicular torsion, torsion of testicular appendages), infectious/inflammatory (e.g., epididymitis, epididymo-orchitis, Fournier's gangrene), traumatic (e.g., testicular contusion, rupture), and other causes (e.g., acute idiopathic scrotal edema, scrotal hernia). Classic sonographic findings are critical for accurate diagnosis, including absent intratesticular blood flow in testicular torsion, hypervascularity of the epididymis in infection, disruption of the tunica albuginea in testicular rupture, and echogenic foci with posterior acoustic shadowing in Fournier's gangrene.

CC04-S3 Emergency GU Ultrasound

14:50-15:10 GBR 102

Chairperson(s): **Sukhee Heo** *(Chonnam National University Hwasun Hospital, Korea)*
See Hyung Kim *(Kyungpook National University Hospital, Korea)*

Gynecologic Emergency US (Cyst Rupture, Torsion, PID)

Mi-Yeon Park
Department of Radiology, Asan Medical Center, Korea

Gynecologic Emergency US (cyst rupture, torsion, PID)

When patients with gynecologic issues present to the emergency department, they often report symptoms like abdominal pain or vaginal bleeding. In cases where gynecologic causes of pain are suspected, ultrasound is a valuable initial modality because it is easily accessible and non-invasive. Ultrasound is an important tool for making fast and accurate diagnoses, which can help guide appropriate treatment.

Hemorrhagic Cyst & Cyst Rupture

Transvaginal ultrasound can be used to assess whether hemorrhage is present within a cyst. If hemorrhage is occurring, it may appear differently depending on the stage. In the acute phase, the hemorrhage may show an echo pattern similar to ovarian stroma. As time passes, blood clots may form, leading to findings such as fluid-debris levels, septations, thickened walls, and internal echoes. If a hemorrhagic cyst ruptures into the peritoneal cavity, the ruptured cyst may have an irregular border, and peritoneal fluid due to hemoperitoneum can be observed on ultrasound.

Ovarian Torsion

Ovarian torsion occurs when the ovary and adnexa rotate abnormally around the tubo-ovarian ligament, leading to a loss of blood flow. Patients often present with lower abdominal pain, and torsion is more likely to occur in the presence of an ovarian tumor. Quick diagnosis and treatment are crucial to prevent ovarian necrosis. On ultrasound, the ovary may appear displaced toward the midline, and swelling due to reduced blood flow can lead to ovarian enlargement. Doppler ultrasound may show absent blood flow to the ovary, and a characteristic "whirlpool sign" can appear around the ovary and fallopian tube, indicating twisting of the adnexal structures.

Pelvic Inflammatory Disease (PID)

PID encompasses a range of conditions including endometritis, salpingitis, and tubo-ovarian abscesses. On ultrasound, signs of PID can include uterine enlargement, thickened or irregular endometrial lines, and dilated fallopian tubes. In cases of pyosalpinx, dilated fallopian tubes may contain heterogeneous fluid with echogenic debris. If a tubo-ovarian abscess develops, the ovary may show cystic lesions with echogenic debris.

CC04-S4 Emergency GU Ultrasound

15:10-15:30 GBR 102

Chairperson(s): **Sukhee Heo** *(Chonnam National University Hwasun Hospital, Korea)*
See Hyung Kim *(Kyungpook National University Hospital, Korea)*

Obstetric Emergency US

Min Je Kim
Department of Radiology, Samsung Medical Center, Korea

Introduction

Obstetric emergencies—such as ectopic pregnancy, cervical incompetence, and placental abruption—require prompt diagnosis to prevent severe maternal and fetal complications. Ultrasound is the imaging modality of choice in these situations due to its real-time capabilities, safety, and diagnostic accuracy. This lecture provides a focused review of common obstetric emergencies and their characteristic sonographic findings to guide timely and effective clinical management.

1. Ectopic Pregnancy

Ectopic pregnancy is a potentially life-threatening condition in which a fertilized egg implants outside the uterine cavity, most commonly in the fallopian tube. It typically presents with pelvic pain and vaginal bleeding, along with a positive pregnancy test showing low or plateauing hCG levels.

Ultrasound is essential for early diagnosis. The absence of an intrauterine gestational sac raises suspicion. Instead, a complex adnexal mass—often with a "tubal ring" appearance—may be visualized, representing a thick-walled fallopian tube. Color Doppler imaging can reveal a “ring of fire” sign, indicating trophoblastic flow. The presence of free fluid, particularly echogenic fluid, suggests hemoperitoneum and possible tubal rupture. A definitive diagnosis is made by identifying a yolk sac or embryo outside the uterus. Additional signs such as the intradecidual or double-decidual sac sign may help differentiate a true intrauterine pregnancy from a pseudogestational sac.

2. Cervical Incompetence

Cervical incompetence refers to painless cervical dilation, typically occurring in the second trimester, and can result in miscarriage or preterm delivery. Patients may present with bulging fetal membranes or premature rupture. Transvaginal ultrasound is the modality of choice. A shortened cervical length (< 3 cm) and funneling of the internal os are key findings. The use of provocative maneuvers, such as fundal pressure or Valsalva, may demonstrate dynamic shortening or progressive funneling, supporting the diagnosis.

3. Placental Abruption and Retroplacental Hematoma

Placental abruption involves the premature separation of the placenta from the uterine wall, leading to compromised fetal oxygenation and maternal bleeding. Risk factors include trauma, hypertension, and smoking. On ultrasound, a retroplacental hematoma may appear as a hypoechoic or heterogeneous area between the placenta and uterine wall. In some cases, it may mimic a thickened placenta due to its isoechoic appearance. A hypoechoic crescent or visible separation supports the diagnosis. However, small abruptions may not be visualized, and a negative ultrasound does not exclude the condition.

4. Uterine Rupture and Dehiscence

Uterine rupture is a critical complication, particularly in patients with prior cesarean section or uterine surgery. Dehiscence represents partial separation with an intact serosal layer. Ultrasound findings may include a discontinuity in the myometrium, an extrauterine hematoma or fluid collection, or fetal parts outside the uterine contour. A myometrial defect near a previous scar may also be seen. When sonographic findings are equivocal, MRI may assist in evaluating the uterine wall and surrounding tissues.

5. Puerperal Ovarian Vein Thrombosis

Ovarian vein thrombosis is a rare but potentially life-threatening postpartum condition that typically presents with fever, lower abdominal pain, and a palpable mass. Ultrasound may show a dilated, noncompressible ovarian vein extending into the inferior vena cava, with or without echogenic thrombus. Differentiation from adjacent structures such as the ureter or fallopian tube is essential. Doppler may reveal absent or diminished venous flow.

6. Retained Products of Conception (RPOC)

RPOC involves the persistence of placental or fetal tissue after delivery, abortion, or miscarriage, often leading to delayed postpartum bleeding or infection. Sonographically, the endometrium appears thickened and heterogeneous, often containing echogenic material or calcifications. Color Doppler may show increased vascularity with low-resistance arterial flow, distinguishing RPOC from endometritis, which typically has little or no flow.

Conclusion

Ultrasound remains the cornerstone of rapid and accurate diagnosis in obstetric emergencies. Familiarity with the characteristic sonographic features of conditions such as ectopic pregnancy, cervical incompetence, placental abruption, uterine rupture, ovarian vein thrombosis, and RPOC enables effective clinical decision-making and improves maternal and fetal outcomes.

References

1. Kaakaji Y, Nghiem HV, Nodell C, Winter TC. Sonography of obstetric and gynecologic emergencies: Part I, Obstetric emergencies. AJR Am J Roentgenol. 2000 Mar;174(3):641–649.
2. Frates MC, Laing FC. Sonographic evaluation of ectopic pregnancy: update. AJR Am J Roentgenol. 1995;165:251–259.
3. Taylor KW, Ramos IM, Feycock AL, et al. Ectopic pregnancy: duplex Doppler evaluation. Radiology. 1989;173:93–97.
4. Ackerman T, Levi C, Dashefsky S, et al. Interstitial line: sonographic findings in interstitiall (cornual) ectopic pregnancy. Radiology. 1993;189:83–87.
5. Iams JD, Goldenberg RL, Meis PJ, et al. The length of the cervix and the risk of spontaneous premature delivery. N Engl J Med. 1996;334:567–572.

HI01-S1 New & Cool for the Liver

14:10-14:30 GBR 103

Chairperson(s): **Jae Young Lee** *(Seoul National University Hospital, Korea)*
Jeong Eun Lee *(Chungnam National University Hospital, Korea)*

Continuously Evolving Elastography

Ioan Sporea
Department of Gastroenterology and Hepatology, Victor Babes University of Medicine and Pharmacy Timisoara, Romania

Liver elastography has become a cornerstone in the non-invasive evaluation of hepatic fibrosis, offering clinicians a reliable alternative to liver biopsy. Over the past decade, this technique has undergone continuous evolution, driven by technological advancements and the growing clinical demand for safer, faster, and more accurate diagnostic tools. This transformation reflects a broader paradigm shift in hepatology—toward earlier detection, dynamic monitoring, and personalized patient care.

Initially developed as qualitative strain imaging, liver elastography has progressed to highly quantitative modalities such as point shear wave elastography (pSWE), two-dimensional shear wave elastography (2D-SWE)(both called ARFI), and the widely adopted vibration-controlled transient elastography (VCTE). These methods provide reproducible liver stiffness measurements that correlate with histological fibrosis stages, allowing real-time monitoring of disease progression, regression under therapy, and risk stratification for complications such as portal hypertension and hepatocellular carcinoma.

Recent advancements include the integration of high-frequency transducers, enhanced penetration capabilities, and higher frame rates, significantly improving measurement reliability in challenging patient populations, including those with obesity or ascites. Moreover, automated acquisition and AI-assisted interpretation are reducing inter-operator variability and facilitating broader adoption in routine clinical workflows. While each ultrasound manufacturer previously proposed its own cutoff values for different degrees of fibrosis, the more recent "rule of 5" for VCTE and the "rule of 4" for ARFI-based methods (pSWE and 2D-SWE) have simplified interpretation for clinicians.

Beyond fibrosis staging, the clinical applications of liver elastography are expanding to include the assessment of steatosis (via the controlled attenuation parameter or attenuation imaging) and hepatic inflammation (via viscosity measurements). These capabilities are particularly valuable in managing complex conditions such as MASLD/MASH and in evaluating treatment responses.

Multiple liver elastography guidelines have been developed over time, including the EFSUMB Guideline (2013), Romanian Guideline (2014), WFUMB Guidelines (2015, 2018), again EFSUMB Guideline 2017 and more recently, the 2024 WFUMB Guidelines (fibrosis and steatosis assessment). Today, elastography enables the use of Multiparametric Ultrasound (MPUS) in MASLD patients, allowing for the evaluation of fatty liver infiltration, fibrosis (stiffness), and inflammation (viscosity).

The future of liver elastography lies in its continued integration into multiparametric imaging platforms, its role in screening algorithms, and the development of portable, point-of-care devices. As technology advances, liver elastography is not only evolving—it is reshaping the approach to chronic liver disease management across healthcare systems worldwide.

This presentation will review the key milestones in the evolution of liver elastography, highlight recent technological innovations, and explore future directions aimed at improving diagnostic accuracy, patient access, and clinical impact.

HI01-S2 **New & Cool for the Liver**

14:50-15:10 **GBR 103**

Chairperson(s): **Jae Young Lee** *(Seoul National University Hospital, Korea)*
Jeong Eun Lee *(Chungnam National University Hospital, Korea)*

Accurate Fat Measurement

Sun Kyung Jeon
Department of Radiology, Seoul National University Hospital, Korea

Hepatic steatosis is an increasingly prevalent global health concern. Early detection and management are critical, as they can halt or even reverse disease progression. Moreover, identifying hepatic steatosis and quantifying liver fat content can help predict the future development of metabolic diseases such as cardiovascular disease and diabetes.

Although several noninvasive screening tools—such as ultrasound (US), liver function tests, and composite indices like the FIB-4 score—are available, a reliable and widely accepted modality for screening or surveillance remains a clinically unmet need.

Recently, quantitative ultrasound (QUS) techniques based on radiofrequency (RF) data analysis have emerged as promising, noninvasive, and objective methods for detecting and grading hepatic steatosis. Various QUS parameters—including speed of sound, ultrasound attenuation, backscatter coefficient, and shear-wave dispersion—have been proposed and have shown strong correlations with hepatic fat content.

In this talk, I will highlight the potential and clinical applicability of QUS techniques for the accurate assessment of hepatic steatosis.

HI02-S1 Cutting-Edge Strategies in Thyroid RFA: From Experimental Studies to Patient Wellbeing

14:10-14:35 Room 203

Chairperson(s): Dong Gyu Na *(GangNeung Asan Hospital, Korea)*
Jin Yong Sung *(Daerim St. Mary's Hospital, Korea)*

Experimental Studies to Enhance the Efficacy and Safety in Thyroid RFA

Ren Jie
Department of Medical Ultrasonic, The Third Affiliated Hospital of Sun Yat-sen University, China

1. Background:

(1) Definition of hydrodissection and clinical applications in various thermal ablation procedures.
(2) Role of hydrodissection in thermal ablation for thyroid tumors.
(3) Current challenges of hydrodissection in thermal ablation for thyroid tumors (Issues 1–4).

2. Issue 1: Selection of the fluid for hydrodissection

(1) The consensus: 5% dextrose for radiofrequency ablation and 5% dextrose or 0.9% saline for microwave ablation.
(2) In vitro study: comparison of the heat insulation efficacy of 5% dextrose and 0.9% saline during radiofrequency ablation.
(3) Conclusion: The heat insulation efficacy of 5% dextrose is better than 0.9% saline at identical distances and in a common thermal environment during radiofrequency ablation.

3. Issue 2: Safety and efficacy of large-volume hydrodissection during thermal ablation for thyroid tumors

(1) Retrospective clinical study: Continuous large-volume hydrodissection during thermal ablation for thyroid tumors didn't cause severe complications.
(2) Animal experiment: Distribution patterns of large-volume fluid when injected around the thyroid during thermal ablation.
(3) Conclusion: Continuous large-volume hydrodissection during thermal ablation for thyroid tumors is safe.

4. Issue 3: Optimization of injection of continuous large-volume hydrodissection

(1) Case reports: the current needle-stay for continuous hydrodissection caused unintended hemorrhage during ablation.
(2) Optimization of injection of continuous large-volume hydrodissection: a proposal of a new three-step method.
(3) Retrospective clinical study: the three-step method reduced the perithyroidal hemorrhage during thermal ablation for thyroid tumors.
(4) Conclusion: The new three-step method for continuous large-volume hydrodissection is superior to the current needle-stay method.

5. Issue 4: Optimization of hydrodissection material.

(1) Previous researches of the optimization of hydrodissection materials and possible disadvantages.
(2) Development of a self-engineered hydrogel as a new hydrodissection material.
(3) In vitro and in vivo studies of this new hydrogel using as hydrodissection material during thermal ablation for thyroid tumors.

(4) Conclusion: The self-developed hydrogel could achieve excellent thermal-protection with a minimal volume, showing promising clinical potential.

HI02-S2 Cutting-Edge Strategies in Thyroid RFA: From Experimental Studies to Patient Wellbeing

14:35-15:00 **Room 203**

Chairperson(s): **Dong Gyu Na** *(GangNeung Asan Hospital, Korea)*
Jin Yong Sung *(Daerim St. Mary's Hospital, Korea)*

Tips for Effective and Safe Thyroid RFA

Jung Hwan Baek
Department of Radiology, Asan Medical Center, Korea

Thermal ablations, especially radiofrequency ablation (RFA), are promising treatment modalities not only for benign thyroid nodules but also for thyroid cancers. In thyroid various tumors, RFA effectively improves tumor-related symptoms and cosmetic problems by reducing the tumor volume. RFA is recently adopted to primary thyroid cancers. However, in terms of complication of RFA, major complication rate was reported as 1.4% - 8% according to the locations and size of the thyroid tumors.

Therefore, proper techniques and experience of operators are key factors to achieve effective and safe RFA. To maximize efficacy and to minimize complications, the Korean Society of Thyroid Radiology Guideline recommends the use of several standard techniques for thyroid RFA; the perithyroidal lidocaine injection technique to control pain, trans-isthmic approach, moving-shot technique and hydrodissection (HD) technique. Furthermore, various advanced techniques, such as vascular ablation or tracheal stent assisted RFA, were developed and recommended.

In this lecture, I will introduce various basic and advanced techniques to minimize injury of critical structures and to maximize the ablation zone. Furthermore I will briefly touch "how to combine proper device and techniques.

HI02-S3 Cutting-Edge Strategies in Thyroid RFA: From Experimental Studies to Patient Wellbeing

15:00-15:25 **Room 203**

Chairperson(s): Dong Gyu Na *(GangNeung Asan Hospital, Korea)*
Jin Yong Sung *(Daerim St. Mary's Hospital, Korea)*

Quality of Life in Thyroid RFA vs. Surgery

Jennifer Kuo
Department of Surgery, Columbia University, USA

Introduction

Health-related quality of life (HRQOL) is an individual's or a group's perceived physical and mental health over time. It has become an important measure of overall health, especially in patients with chronic diseases that may have minimal impact on the duration of their life, but have significant impact on the quality of their life. Thyroid diseases are a prime example of these common diseases, rising in incidence, have no impact on mortality, but can have a negative impact on HRQOL encompassing physical, social, and psychological aspects, and present with persistent symptoms that can lead to reduced well-being.

Developed in 2007, The Thyroid Patient Related Outcomes Questionnaire (ThyPro) aimed to measure quality of life in patients across all benign thyroid diseases(1). Since that time, it, and its abbreviated version ThyPro39(2), have been validated and proven to be a reliable measurement of QOL across many different cultures and has been translated into 21 different languages(3).

This presentation will highlight the effect of interventional treatment of benign thyroid nodules on patients' QOL, with a specific focus on thyroidectomy and thermal ablative techniques.

Results

Using ThyPro, Cramon et al (4) were able to demonstrate that Danish patients with non-toxic multinodular goiter had disease-specific symptoms across all 9 domains that negatively impacted their QOL compared to the general population, with the strongest impairments seen in goiter symptoms and anxiety. Six months after treatment with either radioactive iodine or thyroidectomy, patients had improvement in disease-specific and non-disease specific QOL measures, the greatest in goiter symptoms and anxiety, but still demonstrated persistent impairment in 8 of 9 domains compared to the general population.

Similarly, a systematic review and meta-analysis of ThyPRO studies of patients with benign goiter who underdo surgical treatment found the greatest improvement in the goiter symptoms, tiredness, and overall QOL domains(5).

In the United States, our group was the first to evaluate QOL in patients with benign thyroid nodules after treatment with RFA. In our pilot study of 38 patients, we found that patients reported improvement in goiter symptoms, anxiety, appearance and overall QOL at 3 months post-RFA. (6)

Summary

Health related quality of life (HRQOL) or patient reported outcomes (PRO) are important measures of overall health especially in thyroid diseases. ThyPRO and ThyPRO39 are the most reliable measures of thyroid specific QOL for benign thyroid disease. Patients with benign thyroid nodules do have significant impairment to QOL compared to the general population. Both thyroidectomy and RFA can improve QOL in patients with benign thyroid nodules, especially within the domains of goiter symptoms and anxiety, leading to better QOL.

References

1. Watt T, Cramon P, Hegedüs L, Bjorner JB, Bonnema SJ, Rasmussen ÅK, et al. The thyroid-related quality of life measure ThyPRO has good responsiveness and ability to detect relevant treatment effects. Journal of Clinical Endocrinology and Metabolism [Internet]. 2014 Oct 1 [cited 2021 Jun 2];99(10):3708–17. Available from: https://academic.oup.com/jcem/article/99/10/3708/2836423
2. Törring O, Watt T, Sjölin G, Byström K, Abraham-Nordling M, Calissendorff J, et al. Impaired Quality of Life after Radioiodine Therapy Compared to Antithyroid Drugs or Surgical Treatment for Graves' Hyperthyroidism: A Long-Term Follow-Up with the Thyroid-Related Patient-Reported Outcome Questionnaire and 36-Item Short Form Health Status . Thyroid [Internet]. 2019 Mar 1 [cited 2021 Dec 17];29(3):322–31. Available from: https://www.liebertpub.com/doi/abs/10.1089/thy.2018.0315
3. Watt T, Barbesino G, Bjorner JB, Bonnema SJ, Bukvic B, Drummond R, et al. Cross-cultural validity of the thyroid-specific quality-of-life patient-reported outcome measure, ThyPRO. Quality of Life Research [Internet]. 2015 Mar [cited 2020 Mar 25];24(3):769–80. Available from: http://www.ncbi.nlm.nih.gov/pubmed/25194574
4. Cramon P, Bonnema SJ, Bjorner JB, Ekholm O, Feldt-Rasmussen U, Frendl DM, et al. Quality of life in patients with benign nontoxic goiter: Impact of disease and treatment response, and comparison with the general population. Thyroid [Internet]. 2015 Mar 1 [cited 2021 Dec 19];25(3):284–91. Available from: www.liebertpub.com
5. Chaves N, Rodriguez MJ, Broekhuis JM, Chen HW, Bain PA, James BC. Quality of Life in Patients with Benign Non-Toxic Goiter After Surgical Intervention: A Systematic Review and Meta-Analysis. World J Surg [Internet]. 2022 May 1 [cited 2025 Mar 26];46(5):1093–104. Available from: https://onlinelibrary.wiley.com/doi/full/10.1007/s00268-022-06452-w
6. Collins RA, McManus C, Kuo EJ, Liou R, Lee JA, Kuo JH. Improvement in thyroid-specific quality of life following radiofrequency ablation of benign thyroid nodules: A USA study. Surgery [Internet]. 2025 Jan 1 [cited 2025 Mar 26];177. Available from: https://pubmed.ncbi.nlm.nih.gov/39384472/

IS01-S1 **Novel Technology on Vascular Imaging**

15:20-15:40 **Room 209**

Chairperson(s): **Dong-Guk Paeng** *(Jeju National University, Korea)*
Kyoung Won Kim *(Asan Medical Center, Korea)*

Clinical Photoacoustic Imaging

Chulhong Kim
Department of Mechanical Engineering, Pohang University of Science and Technology, Korea

Trans-energy imaging modalities have been significantly explored to overcome existing problems in conventional imaging modalities with respect to spatial/temporal resolutions, penetration depth, signal-to-noise ratio, contrast, and so on. Among them, photoacoustic imaging, an emerging hybrid modality that can provide strong endogenous and exogenous optical absorption contrasts with high ultrasonic spatial resolution, has overcome the fundamental depth limitation while keeping the spatial resolution. The image resolution, as well as the maximum imaging depth, is scalable with ultrasonic frequency within the reach of diffuse photons. In this presentation, the following topics will be discussed; (1) multiscale and multiparametric trans-energy imaging systems, (2) novel deep-learning powered image processing, (3) recent clinical study results in pathology, endocrinology, oncology, cardiology, dermatology, and radiology, (4) label-free ultrafast ultrasound Doppler imaging, and (5) efforts to commercialization.

IS01-S2 Novel Technology on Vascular Imaging

15:40-16:00 Room 209

Chairperson(s): Dong-Guk Paeng *(Jeju National University, Korea)*
Kyoung Won Kim *(Asan Medical Center, Korea)*

Microflow Imaging Technique: Clinical Application

Pae Sun Suh
Department of Radiology, Severance Hospital, Korea

Microvascular flow imaging (MVFI)

- Advanced Doppler imaging techniques using advanced filters to detect slow or small vessel signals
- Selectively removes the tissue component while preserving the microvascular blood flow signal
- Sensitively detects vascular flows
- Commercially available on many US systems: Superb Microvascular Imaging SMI (Canon Medical), Slow Flow (Siemens Healthineers), Microvascular Imaging MVI (GE Healthcare), MicroFlow Imaging (Philips), and MV-flow (Samsung)

Application of MVFI to thyroid diseases

1. Differentiation of benign and malignant thyroid nodules

I. MVFI has advantages in detecting low-velocity blood flow signals from neovascularization in malignant tumors
II. Emerging as an effective non-invasive diagnostic tool for distinguishing between benign and malignant thyroid nodules
III. Usefulness of MVFI
- Vascularity patterns of malignant nodules: intramodular vascularity, penetrating vessel
- Vascularity index (VI)
  i. VI (%): the ratio between pixels for Doppler signal and total lesion
  ii. Significantly higher in malignant thyroid nodules compared to benign ones
- Meta-analysis showed pooled sensitivity of 0.80–0.84 and specificity of 0.79–0.86.
- Diagnostic performance is higher than color Doppler flow imaging
- SMI in combination with TIRADS can improve diagnostic performance (not SMI alone)

IV. Diagnostic criteria for malignant nodules varied among the studies (no consensus)

2. Differentiation of benign and metastatic cervical lymph nodes

I. Central/peripheral vascular signals
- Benign cervical lymph nodes: central hilar distribution of vascularity
- Malignant cervical lymph nodes: Peripheral or mixed vascularity

II. Effectively stratify indeterminate lymph nodes by visualizing additional vascular signals

3. Application to procedure

I. Radiofrequency ablation (RFA) in recurrent thyroid cancer
- MVFI is superior to power Doppler US imaging (PDUS) for assessing intra-tumoral vascularity
- Higher sensitivity and accuracy without sacrificing specificity
- Before RFA: vascular mapping of the lesion

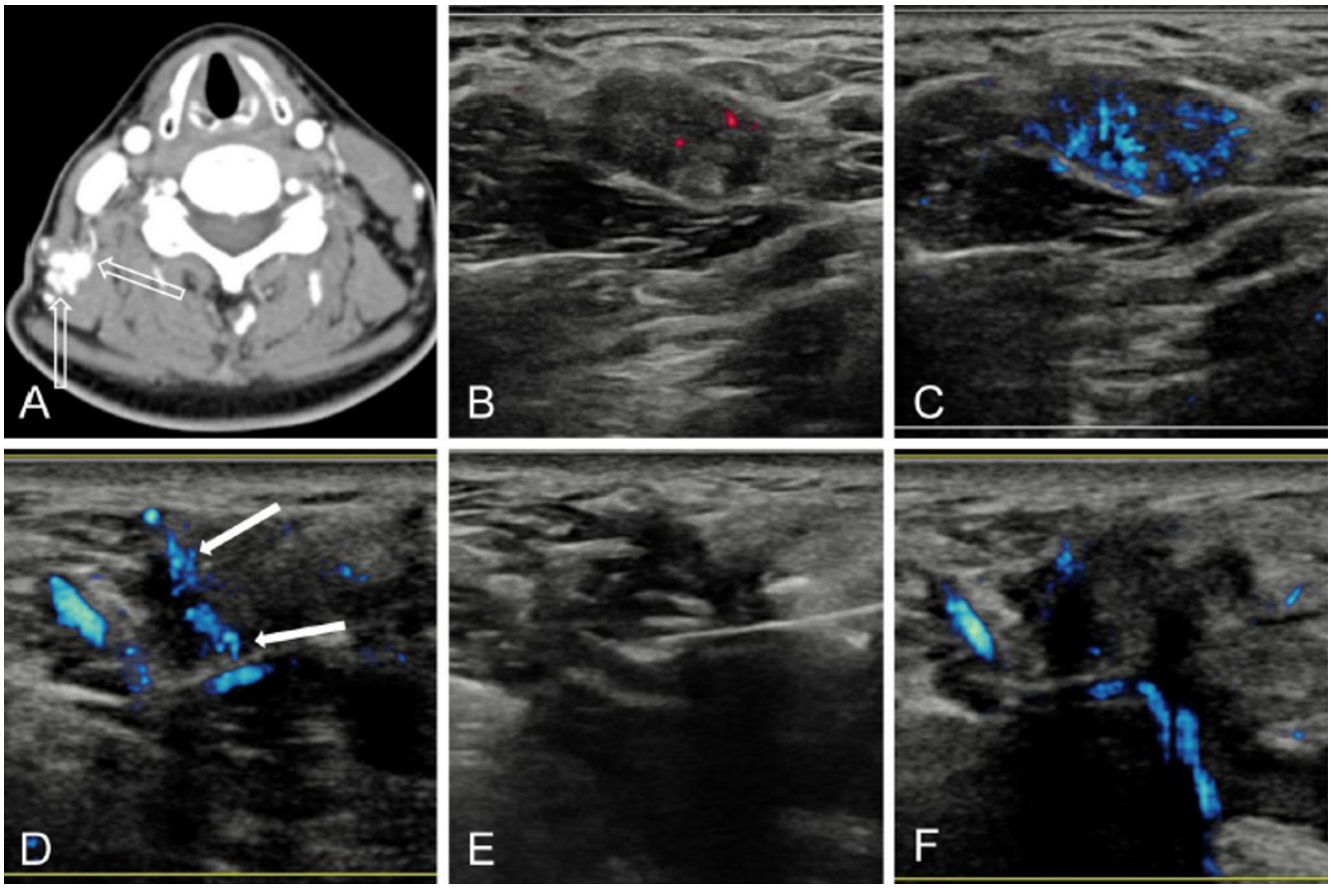

Fig. 1. Usefulness of MVFI in detecting feeding artery during RFA.

II. After RFA: identifying viable tumor

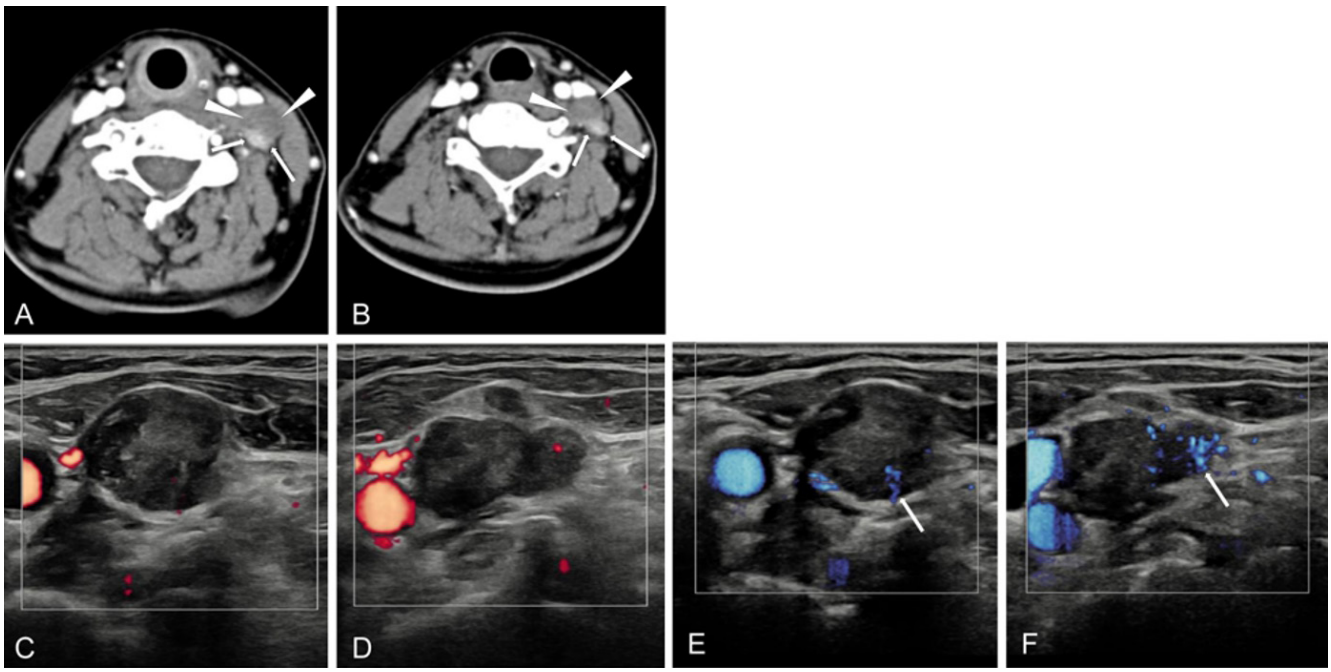

Fig. 2. Usefulness of MVFI in identifying viable tumor after RFA.

III. Thermal ablation of thyroid nodules
- Assessing volume measurement of the ablated zone
  i. Shows high consistency and correlation with contrast-enhanced ultrasound (CEUS)
- Artery-first ablation in microwave ablation of benign thyroid nodules
  i. Facilitates identification of the feeding artery prior to ablation
  ii. Significantly higher 3 months and 6 months volume reduction rates

IV. Biopsy
- Distinguishing the necrotic area from the viable area
- Biopsy at the viable area can improve the success rate of sampling and positivity of pathological diagnosis

V. MVFI is expected to replace CEUS

4. Evaluation of thyroiditis

I. Graves' disease (GD) vs. Hashimoto thyroiditis (HT)
- Patients with GD exhibit significantly higher mean thyroid volume, peak systolic velocity, lower resistive index, higher median VI compared to patients with Hashimoto thyroiditis
- A significant strong positive correlation between VI and thyrotropin receptor autoantibody levels

II. Median vascular index in HT is also higher than healthy controls, and VI is significantly positively correlated with the level of antithyroglobulin

Application of MVFI to other head & neck regions

1. Differentiation of pleomorphic adenoma and Warthin tumors of salivary glands

I. Most pleomorphic adenomas showed avascular pattern, whereas most Warthin tumors showed central or mixed vascularity

II. Analysis of vascular pattern and degree of internal vascularity is more helpful using SMI than PDUS

IS01-S3 **Novel Technology on Vascular Imaging**

16:00-16:20 **Room 209**

Chairperson(s): Dong-Guk Paeng *(Jeju National University, Korea)*
Kyoung Won Kim *(Asan Medical Center, Korea)*

Ultrasound Vascular Imaging for Focused Ultrasound Blood-Brain Barrier Opening

Sua Bae
Department of Electronic Engineering, Sogang University, Korea

Microbubble-mediated focused ultrasound (Mb-FUS) offers a non-invasive method for the blood-brain barrier opening (BBBO), enhancing drug delivery or immunomodulation for treating brain diseases. In Mb-FUS, microbubble cavitation exerts mechanical stress on the walls of blood vessels. While microbubble cavitation is commonly utilized for monitoring, leveraging the vascular response to predict treatment outcomes remains unexplored. This study employs super-resolution flow imaging for the first time to quantify bubble dynamic changes that represent cerebrovascular changes resulting from BBBO.

We established a method utilizing contrast-enhanced power Doppler (CEPD) and ultrasound localization microscopy (ULM) to quantify cerebrovascular changes in mice following FUS. This method involves intravenous microbubble injection, with their concentration in the brain monitored in real-time through CEPD intensity level. Ultrasound flow imaging data were collected before and after Mb-FUS, ensuring consistency in CEPD intensity levels. Blood volume and flow were measured by ULM based on the number of detected microbubbles and their speed, respectively. Wild-type male mice (6–10 wks) were used (n=4 without skull, n=10 with skull). We used short pulse sequence for Mb-FUS without skull (15 MHz, 60 bursts, 100 pulses per burst, 1-kHz PRF, 0.5-Hz burst repetition frequency) and the traditional FUS sequence for transcranial Mb-FUS (1.5 MHz, 10-ms pulse, 2-Hz PRF). Left hippocampus/thalamus was sonicated for 2 min for BBBO. A linear array transducer (L22-14vXLF) with an ultrasound system (Vantage 256, Verasonics) was used for imaging and FUS.

In both open-skull and transcranial studies, ULM revealed blood flow and volume reductions following Mb-FUS BBBO. The microbubble speed map shows vessels with reduced flow post-FUS. A leftward shift in the histogram after FUS indicates an overall flow decrease. The mean flow speed in the sonicated region decreased or increased less than in the contralateral region in all mice. The ULM intensity also decreased suggesting blood volume reduction. We also demonstrated the transcranial feasibility of detecting the same cerebrovascular changes. Flow speed maps showed a flow reduction post-FUS, and time-lapse snapshots demonstrated a microbubble moving slower through a vessel post-FUS than pre-FUS. The mean flow reduction in the sonicated region significantly correlated with the size of BBBO, while no correlation was found in the contralateral region. A significant correlation was also found between the reduction in blood volume and BBBO size. Pressure-group-wise analysis indicated greater reductions in blood flow and volume, as pressure increased. These results suggest that ultrasound super-resolution imaging could be a valuable tool for assessing the safety and effectiveness of FUS-induced BBBO with micrometer precision. Additionally, this technique could be readily integrated into ultrasound-guided FUS systems, enhancing the portability and cost-effectiveness of BBBO treatments.

SF01-S1 Vascular Imaging Systems

16:20-16:40 Room 209

Chairperson(s): **Dong-Guk Paeng** *(Jeju National University, Korea)*
Jihun Kim *(Kangnam University, Korea)*

Implantable Ultrasound Doppler Transducer for Monitoring Vascular Recovery Post-Anastomosis

Jinhyoung Park
Department of Medical Engineering, Sungkyunkwan University, Korea

Vascular anastomosis in free-flap transfer requires continuous postoperative monitoring of blood flow to ensure the long-term patency of the sutured blood vessels, typically for more than two weeks. Although external ultrasound imaging devices are commonly used to intermittently assess the surgical site, this approach is limited by difficulties in consistently locating the vessels and the inability to provide continuous monitoring. To address this, a previously developed 1 mm-sized implantable ultrasonic transducer was placed on the vascular pedicle for continuous monitoring and later removed by extracting the device once the vessel had healed. However, the device remained relatively bulky and often became lodged in the polymer sheath used to secure the transducer around the vessel. Additionally, the conventional system only provided Doppler audio signals, which lacked sufficient information to detect vascular compromise—particularly in venous flow. In this study, we developed a sub-millimeter-sized high-frequency (>20 MHz) ultrasonic transducer designed to minimize removal burden and improve diagnostic capability. Instead of reducing the transducer width to 800 μm, we extended its length to 2 mm to generate a geometric focus at 13.30 mm, forming less attenuation for a larger blood vessel at the operating frequency of 20 MHz. A slab of PZT (lead zirconate titanate) with a width and height of 8.66 mm and 2 mm, respectively, was mounted on a flexible printed circuit board and diced into 10 elements using a micro-dicer. The digitizer operated at a 50 MHz sampling rate, and Doppler signal processing was implemented using a field-programmable gate array (FPGA). The performance of the high-frequency implantable Doppler system was validated by measuring the velocity of a moving wire in a custom-designed string phantom. Additionally, the catheter tip was positioned over an exposed artery in the thigh of a mouse, where arterial pulsatile Doppler signals were successfully detected. This system is intended for continuous blood flow monitoring in anastomosed vessels during free-flap transfer procedures, offering improved sensitivity to vascular compromise and reduced invasiveness for long-term monitoring.

SF01-S2 **Vascular Imaging Systems**

16:40-17:00 **Room 209**

Chairperson(s): **Dong-Guk Paeng** *(Jeju National University, Korea)*
Jihun Kim *(Kangnam University, Korea)*

Ultrafast Doppler Imaging and Ultrasound Localized Microscopy for Rodent Brain Vascular Monitoring

Jaesok Yu
Department of Robotics and Mechatronics Engineering, Daegu Gyeongbuk Institute of Science and Technology, Korea

Ultrasound localization microscopy (ULM) is a groundbreaking, non-invasive imaging technique that enables high-resolution monitoring of vascular hemodynamics and neuronal activity in rodent models. However, the large data volume required by conventional ULM systems limits their broader applicability.

To address this challenge, we propose a sub-Nyquist sampling approach for band-limited radio-frequency (RF) signals, aiming to reduce data size while maintaining image quality. We experimentally demonstrate the in vivo feasibility of this method. Our results show that 67% of the band-limited signal images maintain high signal-to-noise ratio (SNR) and contrast-to-noise ratio (CNR), comparable to those obtained with conventional 200% bandwidth signals.

Even under aggressive data reduction, the proposed method achieves approximately one-third data size reduction without degrading image quality. These findings underscore the potential of our approach to improve the efficiency and scalability of ULM, facilitating resource-efficient, non-invasive imaging of deep neuronal activity.

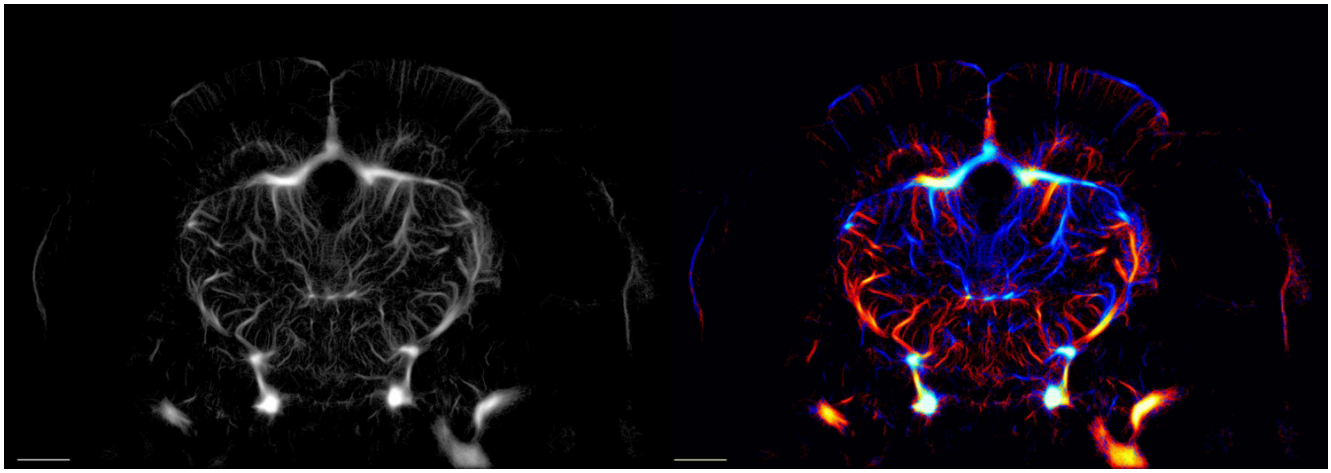

SF01-S3 Vascular Imaging Systems

17:00-17:20 Room 209

Chairperson(s): **Dong-Guk Paeng** *(Jeju National University, Korea)*
Jihun Kim *(Kangnam University, Korea)*

Harnessing Light and Sound to Advance Critical Care Medicine

Jeeun Kang
Department of Anesthesiology and Critical Care Medicine, Johns Hopkins University, USA

Medical imaging holds a pivotal position in critical care medicine, enabling real-time, noninvasive assessment of dynamic pathophysiological states. Our research at Johns Hopkins University endeavors to bridge the gap between episodic diagnostics and continuous physiological surveillance. Ultimately, our goal is to empower clinicians with actionable insights at the bedside, facilitating timely interventions and enhancing outcomes for vulnerable patient populations.

In this presentation, I will outline the evolution of our research. We commenced with foundational investigations into noninvasive detection of hypoxic-ischemic encephalopathy (HIE) and perinatal stroke. We pioneered transcranial photoacoustic imaging methods to assess cerebral oxygen saturation and neurovascular coupling in neonatal piglet models, complemented by functional imaging of neural activity using voltage-sensitive dyes (VSDs). These early studies established a physiologically grounded, multi-parametric imaging platform for identifying early brain injury with high sensitivity and specificity.

Building upon these discoveries, our efforts have progressed toward translational applications. We have developed wearable and miniaturized ultrasound/photoacoustic imaging systems for continuous fetal and neonatal brain monitoring. These devices are designed to meet the unique temporal, spatial, and physiological requirements of critical care environments, including labor and delivery, the neonatal intensive care unit (NICU), and pediatric critical care settings.

MP06-S1 **Artificial Intelligence in Thyroid US**

09:00-09:30 **GBR 102**

Chairperson(s): Jung Hwan Baek *(Asan Medical Center, Korea)*

Artificial Intelligence in Thyroid US

Jin Young Kwak
Department of Radiology, Severance Hospital, Korea

Artificial intelligence can assist doctors in the interpretation of medical images. CAD is an interdisciplinary technology that combines elements of artificial intelligence and computer vision to process radiological images. We use this system to detect, quantify, and classify tumors. In other words, CAD systems provide diagnostic aid to physicians so they can make better decisions.

In my talk, I will be doing a simple review of the artificial intelligence and its role and limitations in the ultrasound classification of thyroid nodules. I also will show the diagnostic performance of AI according to the user of the CAD system.

MP07-S1 US of Knee and Ankle

09:00-09:30 GBR 103

Chairperson(s): **Yun Sun Choi** *(Nowon Eulji Medical Center, Eulji University, Korea)*
Young-Hwan Lee *(Daegu Catholic University Medical Center, Korea)*

Nerve Anatomy and Pathology around Knee and Ankle

Chee Yeong Lim
Department of Diagnostic Radiology, Singapore General Hospital, Singapore

Peripheral nerves around the knee and ankle are frequently involved in entrapment, trauma, or post-surgical syndromes. Ultrasound offers an excellent modality to evaluate these structures, with high spatial resolution, dynamic assessment capabilities, and the advantage of real-time correlation with symptoms. However accurate diagnosis and interpretation require understanding of nerve anatomy, sonographic appearances, common sites of pathology and appreciation of clinical context.

This lecture reviews the anatomy of key nerves around the knee and ankle, with emphasis of understanding sonographic features and landmarks though MRI and illustrative correlations. At the knee, attention will be given to the common peroneal nerve, tibial and saphenous nerves. Around the ankle, the focus shifts to the tibial nerve, the sural nerve, superficial and deep peroneal and interdigital nerves. Technical aspects of sonographic nerve optimisation such as equipment selection, positioning and artefect reduction will be briefly described.

Common pathological conditions will be elaborated with case-based examples, including compressive / entrapment neuropathies such as tarsal tunnel syndrome, traumatic injuries, iatrogenic issues, neoplasm and inflammatory neuritis. These cases will showcase clinical scenarios, classic sonographic appearance cross referenced with MRI features and imaging guided interventions when appropriate.

MP08-S1 **Ultrasound of Acute Abdomen in Children**

09:00-09:30 **Room 203**

Chairperson(s): **Yong-woo Kim** *(Severance Hospital, Korea)*
So-Young Yoo *(Samsung Medical Center, Korea)*

Ultrasound of Acute Abdomen in Children

Kushaljit Singh Sodhi
Department of Radiodiagnosis, Postgraduate Institute of Medical Education and Research, India

Ultrasound is an invaluable tool in the assessment of children with acute abdominal pain. It plays a vital role in diagnosing common causes like appendicitis, intussusception, and mesenteric lymphadenitis, while also helping to rule out most other non-gastrointestinal causes. Its non-invasive nature, portability, ability to provide real-time imaging, and lack of radiation make it especially suitable for pediatric patients. Ultrasound can assist in guiding both diagnosis and treatment, specifically in children with Intussusception and Drainage of abscesses. While it has some limitations, its role in managing acute abdomen in children remains indispensable.

MP09-S1

09:00-09:30 Room 209

Chairperson(s): **Yeon Hyeon Choe** *(Samsung Medical Center, Korea)*
Sung Min Ko *(Wonju Severance Christian Hospital, Korea)*

Comprehensive Guide to Doppler Ultrasound for Optimal Vascular Assessment

Jongmin Lee
Department of Radiology, Kyungpook National University Hospital, Korea

Doppler ultrasonography is one of the primary scanning modes in ultrasonography. It utilizes the Doppler equation to measure the frequency shift of ultrasound waves reflected by moving objects. This frequency shift is influenced by several factors, including the input ultrasound frequency, the velocity of ultrasound in soft tissue, the insonation angle, and the velocity of the reflector. By applying the Doppler equation, the velocity of moving reflectors within the body—primarily blood cells—can be assessed, providing critical insightsinto blood flow velocity. This technique is referred to as Doppler ultrasonography.

Since Doppler signals provide numerical data related to the position and velocity of reflectors, they are typically overlaid onto B-mode ultrasonography to offer spatial context. This combination is known as duplex ultrasonography. In duplex imaging, velocity data can be color-mapped onto the grayscale anatomical image, with or without a time-velocity spectrum. When displayed dynamically in cine mode, the mapped velocitiesreveal qualitative blood flow patterns over time.

The time-velocity spectrum represents a plot of all velocity signals detected within a specific sample volume. The peak and mean velocity curves throughout the cardiac cycle are derived from this spectrum, offering crucial hemodynamic insights.

Beyond measuring velocity, Doppler ultrasonography allows for the estimation of secondary hemodynamic parameters, including:

- Unit flow volume (mL/min)
- Blood flow patterns
- Flow resistance and impedance
- Pressure gradients along blood vessels

These parameters can be derived despite the inherent limitations of ultrasound imaging.

In this lecture, we will explore the fundamental concepts, physics, practical techniques, data interpretation, and clinical applications of Doppler ultrasonography.

CC05-S1 **Who Are You, the Mysterious Stranger?**

09:30-09:45 **GBR 101**

Chairperson(s): **Young Hwan Lee** *(Wonkwang University Hospital, Korea)*
Yong Eun Chung *(Severance Hospital, Korea)*

Incidentally Found Hepatic Focal Lesions

Sungjun Hwang
Department of Radiology, Inje University Ilsan Paik Hospital, Korea

1. Benign Liver Masses

A. Benign Solid Liver Masses

1. Hemangioma
- Typical hemangioma: Well-defined margins, homogenous hyperechoic, posterior acoustic enhancement
- Atypical hemangioma: Heterogeneous internal echogenicity, hyperechoic rim

2. Focal Nodular Hyperplasia (FNH)
- Well-circumscribed, unencapsulated, central hypoechoic scar (in some cases)
- "Spoke-wheel" pattern of blood vessels on color Doppler imaging

3. Hepatic Adenoma
- Nonspecific, variable appearance (hyper- or hypoechoic)
- More common in females with oral contraceptive

B. Benign Cystic Liver Masses

1. Simple Hepatic Cyst
- Well-defined anechoic structure with thin walls
- Posterior acoustic enhancement

2. Liver Abscess
- Variable appearance depending on stage of development
- Mature stage: Mixed echogenicity with irregular wall thickening

3. Mucinous Cystic Neoplasm
- Previously termed biliary cystadenoma
- Multilocular cystic tumor with internal septations
- More common in females > 30 years

2. Malignant Liver Masses

A. Malignant Solid Liver Masses

1. Hepatocellular Carcinoma (HCC)
- Hypoechoic halo: 25~70%
- Posterior acoustic shadowing: 44~88%
- Mosaicism or "Nodule-in-nodule" appearance: characteristic finding
- Lateral shadow
- Hepatic vessel invasion: 30~60%
- Color Doppler findings:
  1. Basket pattern (network of peripheral vessels surrounding tumor nodule)
  2. Intratumoral vascular pattern (blood flow running into and branching within tumor)

2. Intrahepatic Cholangiocarcinoma
- Lobulated contour with potential satellite lesions
- Often hypoechoic

3. Metastasis
- Multiple masses with hypoechoic halo (target sign or "Bull's eye")
- Hyperechoic: Colorectal, renal cell carcinoma, neuroendocrine tumors
- Hypoechoic: Lymphoma, lung, breast, pancreatic, gastric cancers
- Diffuse infiltrative pattern (in some cases): Breast, lung cancer, melanoma

B. Malignant Cystic Liver Masses

1. Mucinous Cystic Neoplasm (biliary cystadenocarcinoma)

- Key features suggesting malignancy: Papillary proliferation, solid components, multilocular septa

2. Hepatic Angiosarcoma

- Rare malignant vascular tumor
- Cystic changes due to intratumoral hemorrhage and necrosis: Multiple hyperechoic masses with anechoic components

3. Key Differential Features on Ultrasonography

- Hyperechoic rim: Hemangioma
- Hypoechoic halo (surrounding tumor): Malignancy
- Multiple masses with target sign: Metastases

References

1. Abdominal Ultrasonography Diagnosis, Edited by Byung Ihn Choi, Iljogak.
2. SW Jeong, "Diagnosis of Focal Liver Masses on Ultrasonography," Clinical Ultrasound 2017;2:9-20. https://doi.org/10.18525/cu.2017.2.1.9
3. Abdominal Ultrasonography Course Materials, 2023, 2024, Department of Radiology, Seoul National University.

CC05-S2 **Who Are You, the Mysterious Stranger?**

09:45-10:00 **GBR 101**

Chairperson(s): **Young Hwan Lee** *(Wonkwang University Hospital, Korea)*
Yong Eun Chung *(Severance Hospital, Korea)*

Incidentally Found Pancreas Focal Lesions

Ji Hye Min
Department of Radiology, Samsung Medical Center, Korea

This lecture introduces a case-based approach to incidentally detected pancreatic lesions on abdominal ultrasound, emphasizing real-world imaging patterns and diagnostic strategies. A variety of cases will be discussed, ranging from common pancreatic tumors to less typical or unexpected findings. Correlation with CT and MRI will be used to highlight key diagnostic clues and support clinical decision-making.

1. Pancreatic Lesions: From Common to Unusual

The lecture will begin with a review of focal pancreatic lesions frequently encountered in clinical practice. These include both solid and cystic masses, with a focus on distinguishing typical imaging appearances from more atypical or challenging presentations.

The discussion will cover a broad range of diagnostic considerations—from malignant tumors and cystic neoplasms to benign entities—highlighting how ultrasound findings can guide initial interpretation and further evaluation.

2. When It's Not a Tumor: Inflammatory, Benign, or Congenital

The second part of the lecture will address pancreatic lesions that mimic tumors but are non-neoplastic in origin. These include inflammatory processes, benign cystic or fatty lesions, and congenital anomalies. Recognizing their characteristic sonographic features and clinical context is important to avoid unnecessary diagnostic or therapeutic procedures.

3. Peripancreatic Mimickers

Finally, the lecture will discuss lesions adjacent to the pancreas that can mimic pancreatic masses. These include lymph nodes, cystic or vascular lesions, and tumors arising from surrounding organs. Understanding their imaging characteristics is crucial for accurate localization and diagnosis.

Conclusion

Incidental found pancreatic lesions can be diagnostically challenging, particularly on ultrasound. This lecture introduces a case-based approach to help radiologists recognize key imaging features, consider the clinical context, and determine appropriate next steps. The aim is to support practical decision-making and improve confidence in everyday clinical practice.

CC05-S3 Who Are You, the Mysterious Stranger?

10:00-10:15 GBR 101

Chairperson(s): Young Hwan Lee *(Wonkwang University Hospital, Korea)*
Yong Eun Chung *(Severance Hospital, Korea)*

Incidental Focal Splenic Lesions

Hyun Kyung Yang
Department of Radiology, Severance Hospital, Korea

Incidental focal splenic lesions (FSLs) are uncommon. In one unpublished series regarding ultrasound, FSLs were identified in 0.27% (550/200,000) of ultrasound examinations; approximately 25% of the 550 lesions were observed incidentally (1). In the retrospective studies, incidental splenic findings were detected in 1–3% of abdominal CT scans in the setting of trauma or suspected appendicitis (2-4).

The likelihood of malignancy in an incidental asymptomatic indeterminate splenic mass is small (5). In one study, without a history of malignancy, only 1% (2/205) of FSLs incidentally detected on CT were malignant (6).

Splenic cysts

Splenic cysts can be broadly categorized as congenital, pseudocysts or cystic masses secondary to infection/inflammation or neoplasia. The majority of splenic cysts are pseudocysts secondary to trauma. Thick peripheral calcification in an otherwise simple cyst is a feature of some benign post-traumatic pseudocysts. Color Doppler ultrasound should be employed to exclude intrasplenic pseudoaneurysm. Splenic lymphangioma is benign and has a well-defined multi-locular appearance. Splenic abscesses can be asymptomatic if the patient is immunocompromised. Multiple incidental complex splenic nodules in an immunocompromised patient should raise the possibility of fungal (candida) infection. Parasitic infection with *Echinococcus granulosus* (hydatid disease) is also usually asymptomatic. Other splenic pathologies which may result in complex splenic masses with a cystic component include hematoma, infarction, metastasis, and primary splenic malignancy.

Solid FSLs

Benign solid FSLs include hemangioma, hamartoma, littoral cell angioma, extramedullary hematopoiesis, myolipoma, sclerosing angiomatoid nodular transformation of the spleen, and inflammatory pseudotumor (IPT).

Malignant FSLs include lymphoma, non-lymphomatous metastasis, angiosarcoma, littoral cell angiosarcoma, leiomyomsarcoma, Kaposi's sarcoma, hemangiosarcoma, and fibrosarcoma.

Hemangiopericytoma can be either benign or malignant (7). Hemangioendothelioma is considered to be of intermediate malignant potential (8). IPT-like follicular dendritic cell tumor is considered a low-grade malignant lesion (9).

According to a recent meta-analysis, findings associated with malignancy were portal phase hypoenhancement, hypovascular enhancement pattern, diffusion restriction and late phase hypoenhancement, solid morphology, lymphadenopathy, presence of perisplenic fluid, arterial hypoenhancement, hypoechogenicity on ultrasound, splenomegaly, and presence of multiple lesions (10). In contrast, cystic morphology, hypervascular-washout and hypervascular-persistent pattern of enhancement, late phase hyperenhancement, anechogenicity on ultrasound, portal phase hyperenhancement, well-defined borders, and calcification are in favor of benignity (10).

Splenic calcifications

In homozygous sickle cell anemia, the spleen can be visualized as a calcified sickle-shaped organ. Rarely, this pattern can also be observed in autoimmune diseases. Focal calcifications may be seen as the residua of infectious (granulomatous) diseases or after cyst treatment with sclerotherapy.

Management of incidental FSLs

A few guidelines were published regarding management of incidental FSLs. The American College of Radiology White Paper states that most incidental splenic masses are benign; imaging findings are nonspecific in most cases and definitive imaging diagnosis is possible only in exceptional cases; and application of specific imaging criteria can help determine if the lesion is more likely to be malignant and should undergo further evaluation with PET or biopsy (5). According to the World Federation for Ultrasound in Medicine and Biology, incidental indeterminate FSLs are often best managed by an interval follow-up examination (initially after 3 months) unless there are clearly malignant clinical or sonographic features (1). The European Federation of Societies for Ultrasound in Medicine and Biology Guidelines state that contrast-enhanced ultrasound can be used to diagnose splenic infarction (11). It can also identify benign FSLs by showing persistent enhancement in the late phase (11).

References

1. Trenker C, Gorg C, Freeman S, et al. WFUMB Position Paper-Incidental Findings, How to Manage: Spleen. Ultrasound Med Biol. 2021;47(8):2017-32.
2. Paluska TR, Sise MJ, Sack DI, Sise CB, Egan MC, Biondi M. Incidental CT findings in trauma patients: incidence and implications for care of the injured. J Trauma. 2007;62(1):157-61.
3. Ekeh AP, Walusimbi M, Brigham E, Woods RJ, McCarthy MC. The prevalence of incidental findings on abdominal computed tomography scans of trauma patients. J Emerg Med. 2010;38(4):484-9.
4. Ozao-Choy J, Kim U, Vieux U, Menes TS. Incidental findings on computed tomography scans for acute appendicitis: prevalence, costs, and outcome. Am Surg. 2011;77(11):1502-9.
5. Heller MT, Harisinghani M, Neitlich JD, Yeghiayan P, Berland LL. Managing incidental findings on abdominal and pelvic CT and MRI, part 3: white paper of the ACR Incidental Findings Committee II on splenic and nodal findings. J Am Coll Radiol. 2013;10(11):833-9.
6. Siewert B, Millo NZ, Sahi K, et al. The Incidental Splenic Mass at CT: Does It Need Further Work-up? An Observational Study. Radiology. 2018;287(1):156-66.
7. Illuminati G, Pizzardi G, Calio F, et al. Hemangiopericytoma of the spleen. Int J Surg. 2015;15:6-10.
8. Li WW, Liang P, Zhao HP, Zhang YX, Liu YY, Gao JB. Composite hemangioendothelioma of the spleen with multiple metastases: CT findings and review of the literature. Medicine (Baltimore). 2021;100(21):e25846.
9. Kim N, Auerbach A, Manning MA. Algorithmic Approach to the Splenic Lesion Based on Radiologic-Pathologic Correlation. Radiographics. 2022;42(3):683-701.
10. Valizadeh P, Jannatdoust P, Tahamtan M, et al. Differentiating malignant from benign splenic lesions: a meta-analysis and pictorial review of imaging features. Abdom Radiol (NY). 2024;49(8):2833-57.
11. Sidhu PS, Cantisani V, Dietrich CF, et al. The EFSUMB Guidelines and Recommendations for the Clinical Practice of Contrast-Enhanced Ultrasound (CEUS) in Non-Hepatic Applications: Update 2017 (Long Version). Ultraschall Med. 2018;39(2):e2-e44.

CC05-S4 Who Are You, the Mysterious Stranger?

10:15-10:30 GBR 101

Chairperson(s): **Young Hwan Lee** *(Wonkwang University Hospital, Korea)*
Yong Eun Chung *(Severance Hospital, Korea)*

Incidentally Found Peritoneal/Retroperitoneal Focal Lesions

Youe Ree Kim
Department of Radiology, Wonkwang University Hospital, Korea

Incidentally detected peritoneal and retroperitoneal focal lesions are increasingly encountered with the widespread use of ultrasound and cross-sectional imaging. These asymptomatic findings, often discovered during evaluations for unrelated conditions, can present significant diagnostic challenges.

Peritoneal and retroperitoneal lesions comprise a broad spectrum of benign and malignant entities, as well as infectious, inflammatory, and other miscellaneous conditions. Ultrasound features such as echogenicity, vascularity, and relationship to adjacent structures offer essential clues for differential diagnosis. Recognition of clinical context—such as prior malignancy, recent surgery, or systemic illness—is key to accurate interpretation. This lecture will also include representative cases to demonstrate diagnostic pitfalls and guide appropriate management strategies.

This lecture aims to provide a practical and systematic approach to the sonographic evaluation of these "mysterious" lesions of the peritoneum and retroperitoneum, helping radiologists approach incidental findings with confidence and clinical insight.

CC06-S1 **US Based Management of Thyroid Nodules**

09:30-09:50 **GBR 102**

Chairperson(s): **Jeong Seon Park** *(Hanyang University Medical Center, Korea)*
Soo Yeon Hahn *(Samsung Medical Center, Korea)*

US Assessment of Thyroid Nodules: K-TIRADS

Hunjong Lim
Department of Radiology, Seoul National University Bundang Hospital, Korea

Ultrasound is the primary imaging modality for the evaluation of thyroid nodules due to its accessibility, safety, and high-resolution capability in characterizing nodule features. To enhance consistency and reproducibility in ultrasound-based risk stratification and biopsy decisions, the Korean Society of Thyroid Radiology (KSThR) released a revised version of the Korean Thyroid Imaging Reporting and Data System (K-TIRADS) in 2021, based on the latest clinical evidence and expert consensus.

The 2021 K-TIRADS adopts a pattern-based classification system that assigns thyroid nodules to one of five categories (K-TIRADS 1 to 5) according to their ultrasound features. These include composition, echogenicity, orientation, margins, and echogenic foci. It emphasizes the importance of interpreting key suspicious findings like punctate echogenic foci, a taller-than-wide shape, and irregular margins in the context of each nodule's overall ultrasound characteristics. This approach allows for a more accurate and clinically meaningful assessment of malignancy risk.

By clearly defining ultrasound descriptors and applying a consistent risk stratification algorithm, the revised K-TIRADS supports more reliable diagnostic decision-making. Rather than relying on a single sonographic feature, the system encourages integrative assessment using multiple characteristics to guide risk classification. This approach not only improves diagnostic accuracy but also promotes clarity and efficiency in daily clinical practice.

This lecture will provide a focused overview of the 2021 K-TIRADS, highlighting its core structure, terminology, and clinical utility. Attendees will gain practical insight into how to interpret thyroid ultrasound findings using the updated lexicon and classification criteria, ultimately improving patient care through standardized, evidence-based imaging evaluation.

CC06-S2 US Based Management of Thyroid Nodules

09:50-10:10 GBR 102

Chairperson(s): **Jeong Seon Park** *(Hanyang University Medical Center, Korea)*
Soo Yeon Hahn *(Samsung Medical Center, Korea)*

Management of Thyroid Nodules after Biopsy and Nodules not Meeting Biopsy Criteria

Hye Shin Ahn
Department of Radiology, Chung-Ang University Hospital, Korea

Thyroid Imaging Reporting and Data System (TIRADS) can be used to assess the malignancy risk in nodules, identify poor prognostic factors in cancer, select patients for biopsy, and determine the optimal management plan for patients with thyroid nodules. The Korean Society of Thyroid Radiology (KSThR) published consensus recommendations for US-based management of thyroid nodules in 2011 and revised them in 2016. However, recent advances in the diagnosis and management of thyroid nodules have necessitated a revision of the previous recommendations. For the revision, KSThR organized a taskforce in January 2021 and this taskforce recommended major revisions including recommendations for US follow-up before and after biopsy of thyroid nodules. In this lecture, I'd like to present revised management of thyroid nodules that meet the biopsy criteria or do not meet the biopsy criteria.

1. Management of thyroid nodules after biopsy

The follow-up and post-FNA management strategies should be determined on the basis of the US and clinical features, as well as the FNA results. The combined use of the US-based risk stratification and the Bethesda system could make possible a more timely detection of thyroid cancer, and might be useful for arriving at an optimal management decision after FNA in thyroid nodules (1-3). The revised K-TIRADS recommended management strategies as Table 1.

FNA Diagnosis	US Patterns (K-TIRADS)	Management
Nondiagnostic	High suspicion	Repeat FNA or CNB within 6 months
	Intermediate or low suspicion	Repeat FNA or CNB within 12 months
Benign	High suspicion	Repeat FNA within 12 months
	Intermediate or low suspicion	US follow-up at 24 months
AUS/FLUS	High suspicion	Repeat FNA or CNB within 6 months
	Intermediate or low suspicion	Repeat FNA or CNB within 12 months US surveillance or Molecular test
FN/SFN	All nodules	Diagnostic surgery (lobectomy) US surveillance or Molecular test
Suspicious malignancy	High or intermediate suspicion	Surgery
	Low suspicion	Repeat FNA or Surgery Active surveillance
Malignant	All nodules	Surgery Active surveillance

2. Management of thyroid nodules not indicated for biopsy

The optimal US follow-up strategy for nodules that do not meet biopsy criteria has not been established in the previous guideline and the K-TIRADS obtain this content in the revised recommendations. The committee believes that the US follow-up of these nodules should be based upon the nodules' K-TIRADS category, with the interval for nodules with higher K-TIRADS category

should be shorter than that for nodules with lower K-TIRADS category (4-7). Regardless of K-TIRADS category of thyroid nodules, nodules that enlarge significantly during follow-up but remain below the biopsy size threshold for their K-TRIADS category continued US follow-up is probably warranted. If a nodule's K-TIRADS category changed on follow-up, the next follow-up or biopsy should be performed according to the new K-TIRADS category except nodules with significantly decreased size. If the size of a nodule decreases significantly during follow-up, US follow-up interval can be increased or further US follow-up can be stopped. In the event of compressive symptom or progression of neck bulging due to enlarged nodule, US should be performed and biopsy can be considered regardless of the initial K-TIRADS category of a nodule to determine the treatment.

Reference

1. Cibas ES, Ali SZ. The 2017 bethesda system for reporting thyroid cytopathology. Thyroid : official journal of the American Thyroid Association 2017;27:1341-1346
2. Haugen BR, Alexander EK, Bible KC et al. 2015 american thyroid association management guidelines for adult patients with thyroid nodules and differentiated thyroid cancer: The american thyroid association guidelines task force on thyroid nodules and differentiated thyroid cancer. Thyroid 2016;26:1-133
3. Gharib H, Papini E, Garber JR et al. American association of clinical endocrinologists, american college of endocrinology, and associazione medici endocrinologi medical guidelines for clinical practice for the diagnosis and management of thyroid nodules--2016 update. Endocrine practice : official journal of the American College of Endocrinology and the American Association of Clinical Endocrinologists 2016;22:622-639
4. Sugitani I, Ito Y, Takeuchi D, Nakayama H et al. Indications and Strategy for Active Surveillance of Adult Low-Risk Papillary Thyroid Microcarcinoma: Consensus Statements from the Japan Association of Endocrine Surgery Task Force on Management for Papillary Thyroid Microcarcinoma. Thyroid 2021;31:183-192.
5. Medici M, Liu X, Kwong N et al. Long- versus short-interval follow-up of cytologically benign thyroid nodules: a prospective cohort study. BMC Medicine 2016;14:11.
6. Durante C, Costante G, Lucisano G et al. The natural history of benign thyroid nodules. Jama 2015;313:926-935.
7. Mohammadi M, Betel C, Burton KR et al. Follow-up of Benign Thyroid Nodules—Can We Do Less? Canadian Association of Radiologists Journal 2019;70:62-67.

Go to the first page

CC06-S3 US Based Management of Thyroid Nodules

10:10-10:30 GBR 102

Chairperson(s): **Jeong Seon Park** *(Hanyang University Medical Center, Korea)*
Soo Yeon Hahn *(Samsung Medical Center, Korea)*

CNB Techniques for FNA Challenging Thyroid Nodules

Jae Ho Shin
Department of Radiology, Korea University Anam Hospital, Korea

In clinical practice, thyroid nodules and abnormal lymph nodes are commonly detected due to the development of high-resolution ultrasound. Since fine needle aspiration biopsy (FNAB) is simple and cost-effective, FNAB has been the first biopsy modality to sample the thyroid nodule. However, there are some challenging cases in which FNAB results in unsatisfactory specimen and equivocal FNAB results, eventually requiring repeat FNAB or subsequent core needle biopsy (CNB). In this presentation, representative challenging cases for FNAB and appropriate CNB techniques to overcome those situations are discussed.

The first challenging case is the scattered punctate echogenic foci (PEF) with or without discrete nodules. FNAB is indeed difficult in sampling the PEF and its surrounding parenchyma for accurate assessment, resulting in false negative or unsatisfactory specimen. On the other hand, CNB has an excellent diagnostic performance in those situations. For instance, a study by Yim et al., demonstrated that CNB has sensitivity of 96.9% and negative predictive value of 90.0% as compared to FNAB's sensitivity of 81.4% and negative predictive value of 57.9%. The second challenging case is entirely calcified nodule. Likewise, FNAB is notorious for poor specimen sampling due to limited needle manipulation and poor penetration through the target lesion. However, CNB has much better diagnostic performance than FNAB in sampling the entirely calcified nodule. A study by Na et al., demonstrated that non-diagnostic results were as follows: CNB (7.7%) vs. FNAB (53.8%), $p = 0.002$. The third challenging case is a small nodule in proximity to important anatomical structures such as common carotid artery. FNAB with to-and-fro motion at this target can be limited, thereby resulting in unsatisfactory specimen. Alternatively, hydrodissection-assisted CNB can provide a better and safer solution in terms of diagnostic performance. Lastly, infiltrative lesion with poor demarcation and fibrosis can be challenging for FNAB. Because CNB harvests sufficient amount of specimen, CNB can be a better alternative to FNAB when it comes to diagnosing the infiltrative lesion.

CC07-S1 **US of Nerve Imaging (Lecture & Live Demo)**

09:30-09:50 **GBR 103**

Chairperson(s): **Kil-Ho Cho** *(Kumi Hyundai Hospital, Korea)*
Jee Won Chai *(Seoul National University Boramae Medical Center, Korea)*

Nerve Imaging around the Shoulder (Lecture)

Carlo Martinoli
Department of Health Sciences, DISSAL. University of Genova, Italy

Recent advances in high-frequency ultrasound (US) technology have enabled detailed assessment of shoulder girdle nerves. Accurate US evaluation of shoulder nerves requires comprehensive anatomical knowledge and meticulous scanning technique. This lecture will explore the ultrasound anatomy, scanning approaches, and pathological conditions affecting key nerves of the shoulder, including the suprascapular, axillary, long thoracic, spinal accessory, medial and lateral pectoral, musculocutaneous, and dorsal scapular nerves. US offers unique advantages over MR imaging, such as superior spatial resolution, dynamic real-time evaluation, broader availability, and the ability to interrogate extensive nerve segments in a single examination. As an adjunct to clinical assessment and nerve conduction studies, US proves especially valuable for localizing sites of compression, detecting associated muscular changes, and identifying extrinsic causes of neuropathy. The lecture will emphasize practical scanning tips and describe a spectrum of pathological conditions affecting these nerves.

CC07-S2 US of Nerve Imaging (Lecture & Live Demo)

09:50-10:10 GBR 103

Chairperson(s): **Kil-Ho Cho** *(Kumi Hyundai Hospital, Korea)*
Jee Won Chai *(Seoul National University Boramae Medical Center, Korea)*

Nerve Imaging around the Elbow and Forearm (Lecture)

Carlo Martinoli
Department of Health Sciences, DISSAL. University of Genova, Italy

The progressive refinement of high-frequency broadband transducers has significantly enhanced the ability of ultrasound (US) to interrogate the complex anatomy of nerves around the elbow and forearm, key regions where entrapment neuropathies frequently occur. US offers the capability to explore critical anatomical sites, including the epitrochlear groove and cubital tunnel for the ulnar nerve, the pronator teres and proximal forearm for the median nerve and its anterior interosseous branch, and the supinator tunnel for the posterior interosseous branch of the radial nerve. In this lectures, special attention will also be given to the evaluation of the superficial sensory nerves of the forearm, such as the sensory branch of the radial nerve, the dorsal cutaneous branch of the ulnar nerve, and the lateral, medial, and posterior antebrachial cutaneous nerves, which may be variably involved in traumatic injuries or iatrogenic conditions. As a complement to clinical examination and nerve conduction studies, US proves particularly valuable when symptoms are atypical and electrodiagnostic findings are inconclusive. US allows high-resolution imaging of the nerve fascicular structure, evaluation of secondary muscle denervation changes, and identification of dynamic or positional compressions that often elude static imaging modalities, such as MR imaging. A precise understanding of the relationships among nerves, fascial planes, and surrounding structures is essential to optimize the diagnostic performance of US in this anatomically intricate field.

CC07-S3 **US of Nerve Imaging (Lecture & Live Demo)**

10:10-10:30 **GBR 103**

Chairperson(s): **Kil-Ho Cho** *(Kumi Hyundai Hospital, Korea)*
Jee Won Chai *(Seoul National University Boramae Medical Center, Korea)*

Nerve Imaging around the Upper Extremity (Live Demo)

Carlo Martinoli
Department of Health Sciences, DISSAL. University of Genova, Italy

Using last-generation broadband transducers, ultrasound (US) has emerged as an essential tool for evaluating peripheral nerves throughout the upper extremity, offering real-time assessment with detailed anatomical visualization of nerve bundles and their individual fascicles. This live demonstration will systematically explore the scanning techniques and anatomical landmarks for imaging major nerves from the shoulder, through the arm and elbow, down to the wrist and hand. Key nerves will include the suprascapular, axillary, long thoracic, spinal accessory, lateral and medial pectoral, musculocutaneous, median (including the anterior interosseous branch), ulnar, radial (including the posterior interosseous and superficial sensory branches), and the cutaneous sensory nerves of the arm and forearm. For each nerve, relevant anatomy, optimal scanning strategies, transducer positioning, and dynamic examination techniques will be illustrated. Special attention will be given to clinically significant fascial passageways and osteofibrous tunnels, along with practical tips and tricks for identifying small or deeply located secondary branches, recognizing anatomical variations, and avoiding common pitfalls. Overall, this session is designed to provide participants with a practical, structured approach to nerve ultrasound across the entire upper extremity, enhancing confidence in both routine assessment and the evaluation of challenging structures.

CC08-S1 Bowel US in Pediatric Patients

09:30-09:50 Room 203

Chairperson(s): **Hee Jung Lee** *(Keimyung University Dongsan Medical Center, Korea)*
Su-mi Shin *(Seoul National University Boramae Medical Center, Korea)*

Bowel US in Neonates/Infants

Gayoung Choi
Department of Radiology, Korea University Ansan Hospital, Korea

Bowel ultrasound is a non-invasive, safe, and effective imaging technique used to evaluate various gastrointestinal conditions in neonates and infants. It plays a pivotal role in diagnosing a range of disorders such as hypertrophic pyloric stenosis, intussusception, necrotizing enterocolitis (NEC), and other bowel-related pathologies. This lecture aims to provide an overview of bowel ultrasound in neonates and infants, its clinical applications, techniques, and key findings.

I. Normal Sonographic Appearance of Neonatal Bowel
II. Pathological Conditions and Ultrasound Findings
III. Advantages and Limitations of Bowel Ultrasound in Neonates and Infant

CC08-S2 **Bowel US in Pediatric Patients**

09:50-10:10 **Room 203**

Chairperson(s): **Hee Jung Lee** *(Keimyung University Dongsan Medical Center, Korea)*
Su-mi Shin *(Seoul National University Boramae Medical Center, Korea)*

Bowel US in Children

Jisun Hwang
Department of Radiology, Seoul National University Bundang Hospital, Korea

- General techniques of bowel ultrasound
  - Transducer selection
    - Choosing a proper transducer is an important factor in pediatric US
    - A high-frequency (7.5-12.0MHz) linear-array transducer is generally preferred for detecting GI problems
    - For general screening of the entire abdomen, a smaller convex-array transducer (5-8 MHz) is recommended for small children and a large convex-array transducer is used (1-5 MHz) for large patients
    - Thus, a complete examination should usually include both probe types.
  - Graded compression technique
    - Bowel gas can obscure the abdominal organs on US, especially in patients with abdominal distension and/or guarding
    - The graded compression technique is a simple, highly effective method by eliminating bowel gas and decreasing the distance between the transducer and target organ
  - Systematic approach in examining the whole intestine
    - Colon: start with the depiction of the psoas muscle and iliac vessels in the RLQ => identify terminal ileum => cecum and base of appendix => ascending colon is followed up toward the hepatic flexure => rest of the colon via the transverse segment distally towards the rectum
    - Small bowel: "Lawn Mowing" strategy is used, sweeping up and down the abdomen to provide an overview of the small bowel
  - Bowel wall thickness
    - Many GI diseases appear as bowel wall thickening
    - A bowel wall thickness of ≥3 mm in the small bowel and ≥4 mm in the colon could be considered as thickened bowel loop
  - Gut signature in normal small bowel and colon
    - Echogenic superficial mucosa, hypoechoic deep mucosa, echogenic submucosa, hypoechoic muscularis propria, echogenic serosal surface
    - Best seen when the bowel lumen is fluid-filled. When the bowel is air filled, only one or two layers may be identified
  - Color Doppler
    - Bowel wall and mesentery do not normally demonstrate significant color signals
    - Average number of visible vessels in normal bowel wall is 1 to 2 per cm^2
    - Inflamed bowel loop or mesentery can have increased color signals
  - Abnormally echogenic fat in mesentery or omentum may be the most conspicuous finding in bowel disease
  - Diminished bowel peristalsis is a nonspecific indicator of unhealthy small bowel
- Case Diagnosis: intussusception
  - m/c most common cause of small bowel obstruction in infants
  - Typical ultrasound findings of intussusception include the target sign (transverse view) or pseudokidney sign (longitudinal view), corresponding to the intussusceptum and surrounding hyperechoic mesenteric fat within the intussuscipiens
  - Imaging predictors of unsuccessful enema reduction

Go to the first page

- ◆ Small bowel obstruction
- ◆ Trapped fluid between intussusceptum and intussuscipien
- ◆ Ascites
- ◆ Absence of flow in the intussusception
- ◆ Location of the intussusception (left-sided colon)
- ◆ Pathologic lead points
- ⇨ related to possible bowel ischemia but do not necessarily indicate contraindications for non-operative enema reduction. avoid high-pressure enema

- Approximately 4% of children have pathological lead points for intussusception, and Meckel's diverticulum is the most common cause
- Older children (>5 years of age) and children with multiple episodes of recurrent intussusception are at increased risk of pathological lead points
- Other pathological lead points included duplication cyst, polyp, lymphoma
- Although US does not detect all pathologic lead points, with US it is possible to identify 66% of pathologic lead points
- When associated with intussusception, Meckel's diverticulum is more difficult to diagnose by US because of the changed shape
- A multilayer structure inside the intussusception can be observed (concentric circle sign) due to reversed Meckel's diverticulum folded into the distal ileum points

- Case Diagnosis: Foreign body ingestion
  - Ingestion of foreign bodies by children is a common and important medical condition
  - For establishing a plan for the removal of a foreign body, it is beneficial to know its precise location
  - However, not all foreign bodies are visible on radiography, with radiographic detectability depending on multiple factors, including the composition and the location of the foreign body
  - Additionally, it is often challenging to detect whether the metallic foreign body is located within the bowel lumen or extraintestinal structure because of significant beam hardening and streak CT artifacts
  - US can also localize objects that are not visible on radiography, like plastic toys or wooden items.
  - Simultaneous evaluation of bowel motility and movement of the foreign body during position change is advantageous for assessing the foreign body status
  - Furthermore, US can reveal foreign body-related complications, such as surrounding inflammation and abscess formation
  - Most foreign bodies are detected as fixed echogenic structures that often show posterior acoustic shadowing
  - Gastric bezoar: hyperechoic arc with posterior acoustic shadowing secondary to the sum of many impedances between air and tightly packed hair
- Case Diagnosis: Henoch-Schonlein purpura
  - m/c vasculitis in children, 2-6 years
  - Systemic vasculitis affecting multiple organs (small vessels in the skin, joint, GI tract and kidney)
  - Typically presents with purpuric rash and abdominal pain
  - Ultrasound
    - ◆ Multifocal circumferential bowel wall thickening due to intramural hemorrhage
    - ◆ Predominance on duodenum and proximal jejunum
    - ◆ Small bowel wall thickening (mean a maximal thickness of 9 mm), reflecting intramural hemorrhage, inflammation, or ischemia
    - ◆ Intramural hematoma can be a lead point of intussusception
  - Abdominal pain can precede skin manifestations, so consider HSP as a Ddx in chlidren with severe bowel wall thickening in the duodenum and proximal small bowel, even if skin lesions are not yet present.
- Case Diagnosis: Gastrointestinal polyp
  - Gastrointestinal polyps typically appear in early childhood, between 2 and 5 years old, often presenting with painless rectal bleeding.
  - Most are benign, confined to the colon, and classified as juvenile polyps histologically.
  - In children over 10, simple juvenile polyps are

less common, with adenomatous polyps or those linked to polyposis syndromes becoming more likely, especially if polyps are numerous, located outside the colon, or if there is a family history of polyps or early-onset colon cancer.

- Juvenile polyp
  - Symptoms: painless bloody stools, present as intussusception with the polyp as the pathologic lead point
  - Rectosigmoid colon (m/c), may be single or multiple (<5)
  - Intraluminal isolated nodular protrusion with pedicle (mushroom sign)
  - Abundant branch shaped blood flow signals within polyps, which is why these polyps frequently present with rectal bleeding
  - Mesh-like fluid areas are a characteristic feature, which are histopathologically attributed to mucus-filled glands

- Case Diagnosis: Meckel diverticulum
  - US findings:
    - Limited use in the diagnosis of an "uncomplicated" Meckel diverticulum
    - Seen as a tubular blind-ending structure arising from the ileal loops with a thick wall and the typical "gut signature" sign, as its wall consists of all the layers of a normal bowel wall
    - Diverticulitis: + surrounding mesenteric echogenic inflammatory change, hypervascularity
      + non-compressible, cystic lesion with clear or turbid content
      ("pseudo G-sac sign") (ddx. Duplication cyst)
  - Inverted diverticulum: double target appearance (mesenteric fat dragged in along with the diverticulum during invagination surrounded by inverted diverticulum and the surrounding small bowel walls)

- Acute appendicitis
  - m/c condition that requires abdominal surgery in children
  - High-frequency linear-array transducer using the graded compression technique
  - Slow compression at the site of maximum tenderness to optimize patient tolerance
  - Posterior compression technique is helpful
  - The ileocecal valve is a key landmark for identifying the appendix.
  - The base of the appendix is usually located at the medial portion of the cecum, just caudal to the ileocecal valve.
  - US findings:
    - loss of compressibility and a maximum outer diameter >6 mm (most reliable)
    - ancillary findings are a target-like appearance in the short axis view, thickening of the echogenic submucosa, a fluid-filled lumen, the presence of appendicoliths, increased periappendiceal echogenicity, periappendiceal fluid, hyperemia, inflammatory phlegmon seen as a mass with mixed echogenicity (perforation +)

Go to the first page

CC08-S3 Bowel US in Pediatric Patients

10:10-10:30 Room 203

Chairperson(s): **Hee Jung Lee** *(Keimyung University Dongsan Medical Center, Korea)*
Su-mi Shin *(Seoul National University Boramae Medical Center, Korea)*

Bowel US in IBD Patients

Jisoo Kim
Department of Radiology, Gangnam Severance Hospital, Korea

Intestinal Ultrasound (IUS) is increasingly recognized as a valuable, non-invasive diagnostic and monitoring modality in Inflammatory Bowel Disease (IBD), which includes Crohn's disease (CD) and ulcerative colitis (UC). Unlike traditional imaging methods such as endoscopy, IUS requires no bowel preparation, avoids radiation exposure, is cost-effective, and is highly acceptable to patients due to its simplicity, comfort, and safety.

In the context of IBD, IUS provides detailed visualization of the bowel wall and surrounding structures. The most frequently evaluated parameters include bowel wall thickness (BWT), bowel wall stratification (BWS), and bowel wall hyperemia using color Doppler flow imaging. Typical ultrasound findings indicative of active inflammation include increased BWT (>3–4 mm), loss of the normal layered bowel wall appearance, and enhanced vascularity. Extramural manifestations, such as proliferation of mesenteric fat and enlarged lymph nodes, are additional supportive signs. In Crohn's disease specifically, IUS is particularly advantageous due to its capacity to detect and assess complications like strictures, fistulas, and abscesses. For ulcerative colitis, continuous and symmetrical thickening of the bowel wall extending proximally from the rectum and associated hyperemia correlates strongly with disease severity.

Recent advances in IUS techniques have further enhanced its diagnostic precision. Elastography, particularly Shear Wave Elastography (SWE), is gaining attention for its capability to differentiate between inflammatory and fibrotic strictures by quantitatively measuring tissue stiffness, thus guiding clinical decision-making and treatment planning. Additionally, Contrast-Enhanced Ultrasound (CEUS), specifically using quantitative analysis such as the Time-Intensity Curve (TIC), has been shown to precisely quantify microvascular changes, thereby facilitating early assessment of treatment response.

Several scoring systems incorporating these ultrasound features have been proposed, though further standardization and validation are ongoing. A significant benefit of IUS is its capability to rapidly detect response to treatment, often observable within four weeks of initiating therapy. Conversely, lack of improvement in IUS parameters can predict the necessity for treatment intensification or surgical intervention.

Despite its numerous advantages, IUS does have limitations, notably its operator-dependent nature, emphasizing the importance of consistent training and the development of standardized imaging protocols. Nevertheless, growing clinical evidence supports broader integration of IUS into routine clinical practice, positioning it as a first-line imaging modality in both the initial diagnosis and the continuous management of IBD.

References

1. Thimm, Matthew A., et al. "Contrast-enhanced ultrasound and shear wave elastography evaluation of Crohn's disease activity in three adolescent patients." Pediatric Gastroenterology, Hepatology & Nutrition 22.3 (2019): 282.
2. Yoon, Haesung, et al. "Contrast-Enhanced Ultrasonography for the Evaluation of Crohn's Disease in Pediatric Patients." Journal of Korean medical science 38.29 (2023): e219.
3. Dal Buono, Arianna, et al. "Ultrasound elastography in

inflammatory bowel diseases: a systematic review of accuracy compared with histopathological assessment." Journal of Crohn's and Colitis 16.10 (2022): 1637-1646.

4. Hata, Jiro, and Hiroshi Imamura. "The use of transabdominal ultrasound in inflammatory bowel disease." Korean journal of radiology 23.3 (2022): 308.
5. Frias-Gomes, Catarina, Joana Torres, and Carolina Palmela. "Intestinal ultrasound in inflammatory bowel disease: a valuable and increasingly important tool." GE-Portuguese Journal of Gastroenterology 29.4 (2022): 223-239.
6. Chavannes, Mallory, et al. "AGA Clinical Practice Update on the Role of Intestinal Ultrasound in Inflammatory Bowel Disease: Commentary." Clinical Gastroenterology and Hepatology 22.9 (2024): 1790-1795.
7. Ripollés, T., et al. "Usefulness of intestinal ultrasound in inflammatory bowel disease." Radiología (English Edition) 63.1 (2021): 89-102.

SF02-S1 Advancements in Vascular Ultrasound: From Early Detection to Post-Treatment Surveillance

09:30-09:50 Room 209

Chairperson(s): **Eun-Ah Park** *(Seoul National University Hospital, Korea)*
Bae Young Lee *(The Catholic University of Korea, Eunpyeong St. Mary's Hospital, Korea)*

The Role of Ultrasound in Abdominal Aortic Aneurysm Surveillance and Management

Yoonseong Lee
Department of Radiology, Seoul National University Hospital, Korea

Abdominal aortic aneurysm (AAA) is a potentially fatal condition if left undiagnosed or untreated. Ultrasound is the primary imaging modality for AAA, offering high sensitivity and specificity without radiation exposure.

This presentation will review the role of ultrasound in the initial detection of AAA, emphasizing its effectiveness as a screening tool and summarizing current recommendations from major guidelines including those of the USPSTF and SVS.

The application of ultrasound in longitudinal surveillance will be discussed, including interval recommendations based on aneurysm size, monitoring for aneurysm growth, and recognizing the modality's strengths and limitations.

The role of ultrasound in postoperative surveillance following endovascular aneurysm repair (EVAR) will also be addressed, with particular focus on its utility in detecting complications such as endoleaks.

SF02-S2 Advancements in Vascular Ultrasound: From Early Detection to Post-Treatment Surveillance

09:50-10:10 **Room 209**

Chairperson(s): Eun-Ah Park *(Seoul National University Hospital, Korea)*
Bae Young Lee *(The Catholic University of Korea, Eunpyeong St. Mary's Hospital, Korea)*

Learning Vascular Ultrasound in Private Clinics: Key Insights and Practical Tips for Radiologists

Yong Wonn Kwon
Department of Radiology, Cheil Orthopedic Hospital, Korea

Lecture Overview

This lecture is designed to provide radiologists with a comprehensive introduction to performing and interpreting vascular ultrasound examinations in a private clinic setting. With a focus on practical applications and real-world challenges, the session will cover common vascular studies, emphasizing hands-on techniques, diagnostic criteria, and workflow optimization. Key topics will include varicose vein assessment, carotid Doppler ultrasound, and lower extremity arterial Doppler studies. The lecture will also highlight common pitfalls, image optimization strategies, and tips for effective communication with referring physicians.

Session Outline

1. Introduction: The Role of Vascular Ultrasound in Private Clinics / Non-tertiary Hospitals
- Common indications
- Patient demographics and expectations

2. Varicose Vein Ultrasound
- Anatomy of the superficial venous system
- Protocol for venous reflux testing
- Identifying saphenous vein insufficiency
- Treatment modalities

3. Carotid Doppler Ultrasound
- Scanning technique and patient positioning
- Diagnostic criteria for stenosis
- Interpretation of spectral waveforms

4. Lower Extremity Arterial Doppler Ultrasound
- Clinical presentation / Interpretation of ABI (ankle-brachial index)
- Segmental approach and protocol
- Identifying stenosis and occlusions
- Case examples and waveform analysis

5. Practical Tips for Private Practice
- Equipment and probe selection
- Dealing with suboptimal images
- Patient communication and comfort

6. Q&A and Case Review
- Interactive discussion with real-world examples
- Troubleshooting challenging cases

SF02-S3 Advancements in Vascular Ultrasound: From Early Detection to Post-Treatment Surveillance

10:10-10:30 Room 209

Chairperson(s): **Eun-Ah Park** *(Seoul National University Hospital, Korea)*
Bae Young Lee *(The Catholic University of Korea, Eunpyeong St. Mary's Hospital, Korea)*

Advanced Techniques in Carotid Ultrasound Imaging for Stroke Patients

Chi Kyung Kim
Department of Neurology, Korea University Guro Hospital, Korea

Introduction: Carotid ultrasound imaging has long been utilized as a non-invasive diagnostic tool for assessing patients at risk of cerebrovascular events such as strokes. Recent advances in ultrasonographic technology, including higher-resolution imaging, Doppler techniques, and enhanced software algorithms, have improved the diagnostic accuracy and predictive value of carotid ultrasound in stroke prevention and management. This paper explores the advanced techniques in carotid ultrasound imaging that have significantly improved patient outcomes, focusing on their application in stroke patients.

Advanced Techniques: High-Resolution B-mode Imaging: Traditional B-mode ultrasound, while effective, is limited by resolution constraints, often failing to detect subtle plaque formations or small vessel pathologies. High-resolution B-mode ultrasound has enhanced the ability to visualize the carotid intima-media thickness (IMT) and identify atherosclerotic plaques at an early stage. This technique allows clinicians to detect early vascular changes that may predispose patients to ischemic events.

Color Doppler and Power Doppler Imaging: Color Doppler imaging has significantly improved the evaluation of blood flow within the carotid arteries, offering valuable information about flow velocity, direction, and turbulence. Power Doppler imaging further enhances this capability by improving sensitivity to low-flow states and detecting small, clinically relevant flow changes in patients with subclinical carotid disease, such as those with early carotid stenosis. These technologies help in assessing the degree of stenosis and the risk of thromboembolism.

Contrast-Enhanced Ultrasound (CEUS): Contrast-enhanced ultrasound involves the use of microbubbles as a contrast agent, significantly improving the ability to visualize blood flow in carotid plaques. CEUS is particularly useful in identifying vulnerable plaques, which are more likely to rupture and lead to stroke. It allows for better characterization of plaque composition, including identifying areas with poor perfusion, which may indicate higher risk for embolic events. This is crucial for tailoring treatment strategies, particularly for patients at risk of ischemic strokes.

Elastography: Elastography, a novel ultrasound technique, measures tissue stiffness and elasticity. In carotid artery imaging, elastography is used to assess the mechanical properties of atherosclerotic plaques. Stiffer plaques are more likely to rupture and cause embolic events. Elastography provides additional insights into plaque vulnerability, complementing traditional imaging methods and allowing for more precise risk stratification in stroke patients.

3D Ultrasound Imaging and Volumetric Analysis: Three-dimensional ultrasound imaging has emerged as a powerful tool for evaluating carotid artery anatomy in a more comprehensive and detailed manner. By providing volumetric data, it enables a more accurate assessment of plaque size, distribution, and its relationship to the surrounding arterial wall. This advanced technique can aid in the early identification of potentially unstable plaques that could lead to a stroke.

Clinical Applications: The integration of these advanced techniques into routine clinical practice has significantly improved the management of stroke patients. Carotid ultrasound plays a critical role

in identifying patients with asymptomatic carotid stenosis, a condition often underdiagnosed but highly correlated with stroke risk. These advanced techniques also facilitate the monitoring of patients post-carotid interventions, such as stenting or endarterectomy, ensuring optimal post-procedural outcomes.

In addition, by combining these imaging techniques with other biomarkers and clinical information, healthcare providers can better predict stroke recurrence, assess treatment efficacy, and implement personalized preventive strategies. For example, patients with vulnerable plaques detected via CEUS or elastography can be prioritized for aggressive medical management, including antiplatelet therapy and lifestyle modifications.

Conclusion: Advanced carotid ultrasound imaging techniques have revolutionized the diagnostic and prognostic capabilities in stroke management. The combination of high-resolution imaging, Doppler flow analysis, contrast-enhanced ultrasound, elastography, and 3D volumetric analysis provides a more comprehensive understanding of carotid artery pathology. These technologies allow clinicians to better assess stroke risk, monitor disease progression, and optimize treatment strategies for stroke patients, ultimately improving clinical outcomes. Future research and development in this area promise even greater advancements in the prevention and management of cerebrovascular diseases.

MS01-S1 US of Various MSK Diseases

11:00-11:20 GBR 103

Chairperson(s): **Jung-Ah Choi** *(Hallym University Dongtan Sacred Heart Hospital, Korea)*
Ji Young Hwang *(Ewha Womans University Seoul Hospital, Korea)*

US of MSK Soft Tissue Tumorous Lesions

Kyung-Sik Ahn
Department of Radiology, Korea University Anam Hospital, Korea

Ultrasound (US) serves as a valuable diagnostic tool in the assessment of musculoskeletal (MSK) soft tissue tumorous lesions due to its accessibility, real-time imaging capabilities, and ability to perform dynamic and Doppler evaluations. This presentation outlines the advantages and limitations of US in MSK imaging, emphasizing the importance of systematic examination techniques and clinical history for accurate diagnosis. A variety of benign soft tissue masses such as lipomas, epidermal inclusion cysts, fat necrosis, peripheral nerve sheath tumors, and vascular malformations demonstrate characteristic US findings that facilitate confident diagnosis. Furthermore, lesions with specific anatomical locations, including glomus tumors and fibromatoses, tenosynovial giant cell tumors are discussed. Distinct US features that may raise suspicion for malignancy—such as deep location, disorganized hyperemia, rapid growth, and occurrence in older patients—should be addressed with caution.

MS01-S2 **US of Various MSK Diseases**

11:20-11:40 **GBR 103**

Chairperson(s): **Jung-Ah Choi** *(Hallym University Dongtan Sacred Heart Hospital, Korea)*
Ji Young Hwang *(Ewha Womans University Seoul Hospital, Korea)*

US of MSK Soft Tissue Nontumorous Lesions

You Seon Song
Department of Radiology, Pusan National University Hospital, Korea

Non-tumorous musculoskeletal soft tissue lesions encompass a wide range of conditions that mimic tumorous masses but are non-neoplastic in nature. These lesions can be diagnostic challenges due to their overlapping imaging characteristics with true tumors. This lecture aims to provide a comprehensive overview of the pathophysiology, clinical presentation, and ultrasonographic evaluation of these lesions. Key topics include inflammatory conditions such as cellulitis and abscesses, traumatic lesions like hematomas, muscle tear and myositis ossificans, and vascular abnormalities including vascular malformation, pseudoaneurysms and thrombophlebitis. Special focus will be placed on the role of ultrasonography in differentiating these conditions from neoplastic processes through features such as echotexture, vascularity, compressibility, and anatomical location. Case studies will illustrate common pitfalls and strategies for accurate diagnosis. By the end of this lecture, participants will gain enhanced proficiency in identifying and managing non-tumorous MSK soft tissue lesions using ultrasonography as a primary diagnostic tool.

MS01-S3 US of Various MSK Diseases

11:40-12:00 GBR 103

Chairperson(s): Jung-Ah Choi *(Hallym University Dongtan Sacred Heart Hospital, Korea)*
Ji Young Hwang *(Ewha Womans University Seoul Hospital, Korea)*

US Diagnosis of Finger Flexion Dysfunction

Jiwoon Seo
Department of Radiology, Seoul National University Boramae Medical Center, Korea

Finger Flexion Dysfunction: Sonographic Evaluation and Diagnostic Strategies

Ultrasound plays a pivotal role in evaluating finger flexion dysfunction by offering high-resolution and dynamic visualization of tendons, pulleys, and surrounding soft tissues. This lecture outlines a focused sonographic strategy for assessing flexor tendon disorders, emphasizing key anatomy, scanning techniques, and representative clinical pathologies.

1. Sonographic Anatomy of the Finger

- Flexor tendons and intrinsic muscles
- Pulley system
- Digital and peripheral nerves
- Volar plate and joint capsules

2. Pathology

1) Flexor Tendon Injury

- **Etiology:** Laceration, avulsion, degeneration
- **US findings**: hypoechoic gap or discontinuity in tendon, dynamic scan to assess tendon retraction and mobility

2) Trigger Finger (Stenosing Tenosynovitis)

- **Pathophysiology:** A1 pulley thickening, flexor tendon entrapment
- **US findings:** diffuse hypoechoic A1 pulley thickening, dynamic snapping of the tendon during flexion-extension

3) Pulley Injury

- **Common in:** Rock climbers and athletes
- **US findings:** bowstringing of flexor tendons, loss of pulley continuity on dynamic flexion

4) Lumbrical Muscle Injury

- **Mechanism:** Shear injury at bipennate lumbrical origins during differential finger motion
- **Clinical sign:** Palm pain with passive extension during attempted fist closure
- **US findings:** focal hypoechoic area or disruption in muscle belly, dynamic impingement or painful contraction between tendons

5) Flexor Tenosynovitis

- **Etiology:** Overuse, trauma, infection, or inflammatory arthritis
- **US findings:** tendon sheath fluid and synovial thickening, increased Doppler vascularity, restricted tendon gliding

6) Nerve Entrapment and Injury

- **Etiology:** Local trauma, entrapment, or post-surgical scarring
- **US findings:** swollen or hypoechoic nerves, fascicular pattern loss, muscle atrophy in innervated territory (e.g., FDS, FDP), clinical correlation with surgical history or paresthesia

7) Volar Plate Injury

- **Mechanism:** Hyperextension trauma to PIP or MCP joints
- **Clinical features:** Pain and instability
- **US findings:** swollen or thickened volar plate, hypoechoic cleft or avulsion at the phalangeal base

8) Sagittal Band Injury

- **Mechanism:** Direct trauma or forced MCP motion
- **Clinical impact:** Pain over dorsal MCP joint during flexion; limits active flexion
- **US findings:** irregular or thickened sagittal band, partial tear or subluxation/dislocation of the extensor tendon (dynamic exam)

9) Anatomical Variations

- **Examples:** Bifid tendons, accessory slips, anomalous lumbrical origins, variant vincula
- **Clinical relevance:** may mimic pathology or alter biomechanics, importance of side-to-side comparison and anatomical knowledge

Summary

This session provides a systematic and practical ultrasound framework for diagnosing finger flexion dysfunction, integrating anatomical landmarks, real-time dynamic assessment, and pathology-specific sonographic patterns to support accurate clinical evaluation and management.

MS02-S1

11:00-11:20 Room 203

Chairperson(s): **Byoung Hee Han** *(GangNeung Asan Hospital, Korea)*
Young Ah Cho *(Asan Medical Center, Korea)*

Ultrasound in Pediatric Cystic Kidney Diseases

Supika Kritsaneephaiboon
Department of Radiology, Prince of Songkla University, Thailand

There are 3 stages in evolution of kidney development: pronephros, mesonephros and metanephros. Regions of functional kidney derived from the metanephric mesoderm and ureteric bud. The metanephric blastema will develop Bowman's capsule, proximal convoluted tubule, Loop of Henle and distal convoluted tubule while the ureteric bud will develop the calyx, collecting tubules, collecting ducts and ureter. To understand renal embryo is helpful to classify and locate pathology of renal cystic kidney diseases. Renal cystic diseases could be classified by: hereditary/ non-hereditary, bilateral/ unilateral, or Potter classifications or by location at cortex/ medulla/ cortex & medulla.

Ultrasound is primary diagnostic tool and more superior to CT to demonstrate complex internal architectures such as internal fluid content, septation, tiny nodules, wall abnormalities including soft tissue masses. MRI provides high resolution of tissue contrast and cystic characterization but sedation is needed in children.

Normal sonographic renal findings in newborn up to 6 months of age are renal cortical echogenicity more than liver and spleen, relatively hypoechoic renal medullary pyramid, and scant or absent renal sinus fat.

The definition of simple renal cyst is single, round, thin-walled, anechoic, non-septate, separated from collecting system, and no color Doppler flow. Clinical work-up and at least one follow- up ultrasound to rule out developed other cystic kidney diseases are suggested. No further contrast enhanced US or MRI/ CT is required.

The lecture will cover common cystic kidney diseases, both hereditary and non-hereditary. The hereditary group includes autosomal dominant polycystic kidney disease (ADPKD), autosomal recessive polycystic kidney disease (ARPKD), nephronophthisis, glomerulocystic kidney disease, and malformation syndromes. The non-hereditary group includes multicystic dysplastic kidney (MCDK), obstructive renal dysplasia (ORD), and renal cystic tumors.

ADPKD: the most common hereditary renal disorder, affected nephrons and collecting ducts, rare extra-renal manifestations in children. The diagnosis in children under 15 years old requires the presence of more than one cyst and a positive family history. In children over 15 years old, the diagnosis is based on the presence of more than three cysts, either unilateral or bilateral.

ARPKD: fusiform dilatation of collecting tubules in medulla and cortex, the earlier onset, the more severe renal findings and less pronounced periportal fibrosis. An additional routine abdominal ultrasound is performed to assess for congenital hepatic fibrosis, signs of portal hypertension, and/or Caroli syndrome.

Renal medullary cysts: shared same pathology and clinical features of nephronophthisis (NPH) and medullary cystic disease. Syndromes associated with NPHP gene mutations include Senior-Loken syndrome, Joubert syndrome type B, Jeune syndrome, Meckel-Gruber syndrome, and others.

Glomerulocystic kidney disease: refers to distended Bowman spaces. The cysts are small, round, and in a subcapsular location.

Tuberous sclerosis: bilateral multiple simple cysts variable in size and numbers located in cortex and medulla. The number of cysts increases with

age. An annual renal ultrasound is recommended for children under 12 years old without AML.

Renal cystic dysplasia: failure of ureteric bud to induce metanephric blastema and varying size and shape of non - communicating cysts in MCDK-pelvoinfundibular type. Fatal urinary obstruction or reflux in obstructive renal dysplasia - ORD. Thirty percent of cases of MCDK have a contralateral renal abnormality. Ultrasound follow-up is recommended to ensure adequate compensatory hypertrophy of the contralateral kidney.

Multilocular cystic renal tumor: same imaging features between cystic nephroma (CN) and cystic partially differentiated nephroblastoma (CPDN), affected M>F less than 2 years and presence of septal blastema in CPDN. Cystic renal tumors can occur in tumor-predisposing syndromes or due to genetic mutations, such as Beckwith-Wiedemann syndrome, von Hippel-Lindau syndrome, or germline DICER1 mutations, and require regular monitoring.

HS01-S1 Liver Doppler
11:00-11:20 Room 209

Liver Doppler

Dong Ik Cha
Department of Radiology, Samsung Medical Center, Korea

Doppler ultrasound (US) is a non-invasive imaging technique that detects blood flow dynamics using the Doppler effect, where frequency shifts (Δf) reflect the velocity of moving red blood cells. The formula Δf = (2·f0·v_RBC)/C (f0: transducer frequency; v_RBC: RBC velocity; C: speed of sound) underpins this technology. Two primary modes are used:

1. Color Doppler: Visualizes flow direction (red/blue encoding) and velocity, superimposed on grayscale anatomical images.
2. Spectral Doppler: Quantifies hemodynamics via waveforms, measuring parameters like peak systolic velocity (PSV) and resistive index (RI).

Key Parameters for Optimal Liver Doppler Imaging

- Angle Correction: Ideal angles (30°–60°) ensure accurate velocity measurement; angles >60° cause significant error.
- PRF (Velocity Scale): Adjusts pulse repetition frequency to avoid aliasing (Nyquist limit: PRF > 2× max frequency shift).
- Gate Size: A sample volume covering 2/3 vessel width balances signal strength and specificity.
- Gain/Priority Settings: Balancing grayscale and color gain minimizes artifacts (e.g., flash from motion, twinkling near calcifications).

Clinical Application in Liver Transplantation

Doppler US is critical for evaluating vascular complications:

- Hepatic Artery Stenosis/Thrombosis: Diagnosed by tardus-parvus waveform (RI <0.5, systolic acceleration time >0.08s).
- Portal Vein Stenosis: Suspected if velocity at the stenosis is >3× baseline.
- Hepatic Vein Stenosis: Monophasic flow suggests obstruction but requires correlation with B-mode findings (e.g., biloma, hematoma).

Takeaway

Successful liver Doppler relies on mastering parameters (angle, PRF, gain) and recognizing artifacts. In transplants, combining waveform analysis (RI, PSV) with clinical history ensures accurate diagnosis of vascular complications.

HS01-S2 Basics and Tips for Peripheral Artery and Vein Ultrasound: A Comprehensive Guide

11:20-11:40 Room 209

Basics and Tips for Peripheral Artery and Vein Ultrasound: A Comprehensive Guide

Ki Seok Choo
Department of Radiology, Pusan National University Yangsan Hospital, Korea

Peripheral Artery

1. Patient Position

Common iliac, external iliac a.
- supine position with adequate pressure
- 3-5 MHz convex probe

Common femoral, proximal deep femoral, superficial femoral a.
- supine position with hip abduction, slightly knee flexion
- 9-15 MHz linear probe

Popliteal, post. tibial, peroneal a.
- prone position
- 9-15 MHz linear probe

Ant. tibial, dorsalis pedis
- supine position
- 9-15 MHz linear probe

2. Normal Arterial Waveforms (triphasic patterns)

(1) forward flow during systole
(2) a short period of flow reversal in early diastole
(3) low velocity flow during the remainder of diastole

3. Abnormal Wave form in Stenosis

1) Proximal to significant stenosis (possible nearly normal thiphasic wave form)
   - High resistance
   - Low volume flow
   - Low peak velocity
   - Shoulder in systolic downstroke
2) Distal to significant stenosis
   - Low resistance
   - Loss of pulsatility
   - Low peak velocity
   - Damped monophasic waveform
   - Increased systotic rise time

4. Grading of arterial stenosis
   - Peak velocity ratio(PSV at the narrowest/PSV at proximal) in diameter stenosis
     - <2 : stenosis less than 50%
     - 2-4 : stenosis more than 50-74%
     - >4 : stenosis more than 75%

Peripheral Vein

1. Anatomy of Lower Extremity Veins

The veins of the lower extremities are classified into deep veins, superficial veins, perforating veins, and communicating veins.

1) Deep veins: Located beneath the deep fascia, these include axial veins and intramuscular veins. The axial veins share the same names as the corresponding arteries and include the common iliac vein, external iliac vein, common femoral vein, superficial femoral vein, deep femoral vein, popliteal vein, and calf veins. The calf veins always exist in pairs.
2) Superficial veins: These are located above the superficial fascia and are divided into epifascial veins and saphenous veins (which lie in the saphenous space between the superficial and deep fascia).

A. The greater saphenous vein (GSV) typically

runs anterior to the medial malleolus and courses along the anteromedial aspect of the leg before joining the common femoral vein at the sapheno-femoral junction. Just before merging, it receives multiple venous branches, which are difficult to visualize on ultrasound.

B. The small saphenous vein (SSV) usually runs posterior to the lateral malleolus, ascends along the midline of the calf, and drains into the popliteal vein. However, anatomical variations exist, and it may connect to the greater saphenous vein, superficial femoral vein, or deep femoral vein.

C. Perforating veins: These connect the superficial and deep veins, with over 100 perforating veins present in the lower extremities.

D. Communicating veins: These connect superficial veins to each other.

2. Diagnosis of Deep Vein Thrombosis (DVT) via Ultrasound

1) Patient Positioning:

- Femoral vein, Anterior tibial vein (ATV): Supine position
- Popliteal vein, Posterior tibial vein (PTV), Peroneal vein, Soleus vein:
- Hip abduction with slight knee flexion
- Prone position with the ankle resting on the contralateral ankle

2) 2D Gray Scale Ultrasound Examination:

- Transverse scan to check compressibility
- Identification of non-compressible segments
- Use of color and spectral Doppler to assess blood flow

3) Ultrasound Diagnostic Criteria for DVT:

A. Direct Signs:

- Presence of an intramural thrombus
- Non-compressibility of the vein
- Non-occlusive thrombus causing partial vein collapse
- Increased vein diameter
- Absence of flow on color and spectral Doppler

B. Indirect Signs:

- Loss of phasicity → Suggests proximal thrombosis
- Loss of augmentation → Suggests distal thrombosis

3. Diagnosis of Varicose Veins via Ultrasound

1) Patient Positioning:

Erect or semi-erect position, with weight shifted to the contralateral leg

2) Evaluation Sites:

Sapheno-femoral junction:

- Assess for the presence of DVT
- Transverse and longitudinal scans
- Color and spectral Doppler to evaluate reflux
- Valsalva maneuver to induce reflux (reflux time > 1 second is considered abnormal)
- Trace the GSV in transverse view → Identify reflux in branches, relation to varicose veins, and reflux in perforators

Sapheno-popliteal junction:

- Assess anatomical variations
- The most common pattern involves the LSV draining into the popliteal vein at the popliteal fossa
- Evaluate reflux using calf augmentation or a BP cuff (Valsalva maneuver is not used)
- Trace the LSV → Identify its relation to varicose veins and reflux into perforators (gastrocnemius, soleus, lateral calf perforators)

Other Evaluation Sites:

- Perforators, Deep veins, Superficial veins
- Assessment of anatomical variations

4. Diagnosis of Venous Insufficiency via Ultrasound

- Reflux Time Criteria:
  - ✓ 1 second: Femoral and popliteal veins
  - ✓ 0.5 seconds: GSV, LSV, calf deep veins
  - ✓ 0.35 seconds: Perforators
- Perforator Diameter Criteria:
  - ✓ 4 mm: Most perforators exhibit reflux
- 2–3 mm: Reflux may be present → Confirm with Doppler
- Superficial Vein Diameter Criteria:
  - ✓ 5 mm: Most cases exhibit reflux

Ultrasound plays a crucial role in evaluating the anatomy and function of lower extremity veins and is widely used for diagnosing DVT, varicose veins, and venous insufficiency.

SF03-S1 **Ultrasound in the Diagnosis and Treatment of Prostate Cancer**

14:00-14:20 **GBR 101**

Chairperson(s): **Dae Chul Jung** *(Severance Hospital, Korea)*
Sang Youn Kim *(Seoul National University Hospital, Korea)*

Transperineal MR-US Fusion Biopsy

Ka-Fung Peter Chiu
Department of Surgery, The Chinese University of Hong Kong, Hong Kong, China

MRI-guided prostate cancer diagnosis with PI-RADS reporting is strongly recommended. In men with a suspicious MRI lesion, prostate biopsy is indicated. In order to achieve accurate targeting of MRI lesions, a reliable biopsy technique is needed. This talk will focus on:

- the advantages of transperineal approach over transrectal prostate biopsy,
- the pros and cons of MRI-Ultrasound fusion biopsy, Cognitive guided biopsy and MRI in-bore biopsy,
- the various principles and machines supporting transperineal MRI-Ultrasound fusion prostate biopsy, and
- the tips and tricks of fusion biopsy, and
- the feasibility of transperineal fusion biopsy under local anaesthesia.

SF03-S2 Ultrasound in the Diagnosis and Treatment of Prostate Cancer

14:20-14:40 GBR 101

Chairperson(s): Dae Chul Jung *(Severance Hospital, Korea)*
Sang Youn Kim *(Seoul National University Hospital, Korea)*

Microultrasound and Microvascular Imaging for Prostate Cancer

Myoungseok Lee
Department of Radiology, Seoul National University Boramae Medical Center, Korea

In the diagnosis of prostate cancer, a recent trend involves performing pre-biopsy multiparametric MRI (mpMRI) in patients with suspected malignancy, followed by real-time fusion of MRI and ultrasound imaging to guide targeted biopsies. Consequently, MRI now plays a central role in prostate cancer imaging, while ultrasound primarily serves as a biopsy-guidance tool based on the MRI findings. The limited spatial resolution of conventional ultrasound and its lack of functional imaging capability compared to mpMRI are major factors that constrain the diagnostic role of ultrasound.

Since the early 2010s, advances in computing technology have enabled the processing of large data volumes using smaller and more integrated circuits, leading to the clinical adoption of ultrafast ultrasound, which was previously confined to research applications. In parallel, hardware developments such as the use of single-crystal piezoelectric elements have contributed to significant improvements in ultrasound image quality. In B-mode imaging, micro-ultrasound, utilizing high-frequency transducers with enhanced resolution and minimized artifacts, has been introduced. In Doppler imaging, the application of advanced clutter filters has enabled microvascular imaging, allowing visualization of fine vascular structures.

This session will review how these emerging technologies are being implemented in the imaging of prostate cancer, based on a summary of key publications. In particular, micro-ultrasound, which has not yet been introduced in Korea, will be discussed in detail. The session aims to provide attendees with a foundational understanding of this technology through analysis of published data from international users, and to encourage consideration of how it could potentially contribute to the management of prostate cancer patients in the current Korean medical setting.

SF03-S3 **Ultrasound in the Diagnosis and Treatment of Prostate Cancer**

14:40-15:00 **GBR 101**

Chairperson(s): **Dae Chul Jung** *(Severance Hospital, Korea)*
Sang Youn Kim *(Seoul National University Hospital, Korea)*

HIFU as a Treatment Option of Prostate Cancer

Sung Il Hwang
Department of Radiology, Seoul National University Bundang Hospital, Korea

High-intensity focused ultrasound (HIFU) has emerged as a promising focal therapy option for localized prostate cancer, providing a minimally invasive alternative to traditional treatments such as surgery and radiation therapy. This lecture explores the current role, effectiveness, and diagnostic considerations of HIFU in the management of prostate cancer.

HIFU utilizes focused ultrasound waves to induce precise thermal ablation of targeted prostate tissues, preserving surrounding structures and minimizing side effects, including urinary incontinence and erectile dysfunction. Although HIFU demonstrates favorable functional outcomes and quality-of-life preservation, challenges persist, including the accurate identification of residual or recurrent cancer.

Magnetic resonance imaging (MRI) has become essential in post-HIFU surveillance, providing critical diagnostic information on potential recurrence. Recent systematic reviews and meta-analyses have highlighted MRI's promising diagnostic performance, with pooled sensitivity and specificity of approximately 81% and 91%, respectively. However, considerable heterogeneity exists among studies, with variability influenced by factors such as nadir prostate-specific antigen (PSA) levels, MRI interpretation criteria, and study size. Furthermore, standardized imaging guidelines tailored specifically for post-HIFU evaluation remain lacking, underscoring the need for refinement in imaging protocols.

This presentation will discuss practical considerations for patient selection, common pitfalls in MRI interpretation following HIFU, and potential avenues for enhancing diagnostic accuracy. Additionally, current limitations, including the management of MRI-negative recurrence and anterior prostate tumors, will be addressed. Understanding these challenges and opportunities is critical for optimizing patient outcomes and integrating HIFU effectively into clinical practice for prostate cancer treatment.

HI03-S1 AI and Breast US

14:00-14:20 GBR 102

Chairperson(s): **Sung Hun Kim** *(The Catholic University of Korea, Seoul St. Mary's Hospital, Korea)*
Young Mi Park *(Inje University Busan Paik Hospital, Korea)*

Supplemental Screening Ultrasound in Dense Breast: Comparison with Mammography with AI

Jung Min Chang
Department of Radiology, Seoul National University Hospital, Korea

Screening mammography enables earlier detection of breast cancer, contributing to improved prognosis and reduced mortality. However, it relies on the visual interpretation of radiologists, which can lead to missed cancers due to factors such as dense breast tissue, perceptual oversights, and interpretation errors. The sensitivity of mammography is as low as 30%–48% in women with dense breasts, prompting ongoing discussions about the need for supplemental screening methods to improve detection in this population.

There is increasing optimism about integrating AI into mammography to overcome its limitations. The incorporation of AI could significantly enhance mammography's performance by improving detection accuracy. Notable improvements in diagnostic performance have been observed in both women with dense and nondense breasts. AI has the potential to identify cancers that would typically require supplemental screening methods, such as ultrasound (US) or MRI. The comparative evaluation of AI versus breast ultrasound as a supplementary modality for women with dense breasts undergoing screening mammography is of significant interest.

Another potential application of Mammography AI is the development of AI algorithms to identify patients who would benefit from supplemental imaging including US or MRI. The identification of individual women who would benefit most from supplemental imaging, as well as those at the highest risk of potential harms from unnecessary recalls, is of great interest.

In this lecture, the potential role of mammography AI in the era of supplemental breast cancer US screening will be discussed.

HI03-S2 **AI and Breast US**

14:20-14:40 **GBR 102**

Chairperson(s): Sung Hun Kim *(The Catholic University of Korea, Seoul St. Mary's Hospital, Korea)*
Young Mi Park *(Inje University Busan Paik Hospital, Korea)*

AI in Screening Ultrasound

Won Hwa Kim
Department of Radiology, Kyungpook National University Chilgok Hospital, Korea

Breast cancer is the most common cancer in women worldwide, and its early detection is critical for improving survival outcomes. As a diagnostic and screening tool, mammography can be less effective owing to the masking effect of fibroglandular tissue, but breast US has good sensitivity even in dense breasts. However, breast US is highly operator dependent, highlighting the need for artificial intelligence (AI)-driven solutions. Unlike other modalities, US is performed using a handheld device that produces a continuous real-time video stream, yielding 12000–48000 frames per examination. This can be significantly challenging for AI development and requires real-time AI inference capabilities. In this review, we classified AI solutions as computer-aided diagnosis and computer-aided detection to facilitate a functional understanding and review commercial software supported by clinical evidence. In addition, to bridge healthcare gaps and enhance patient outcomes in geographically under resourced areas, we propose a novel framework by reviewing the existing AI-based triage workflows including mobile ultrasound.

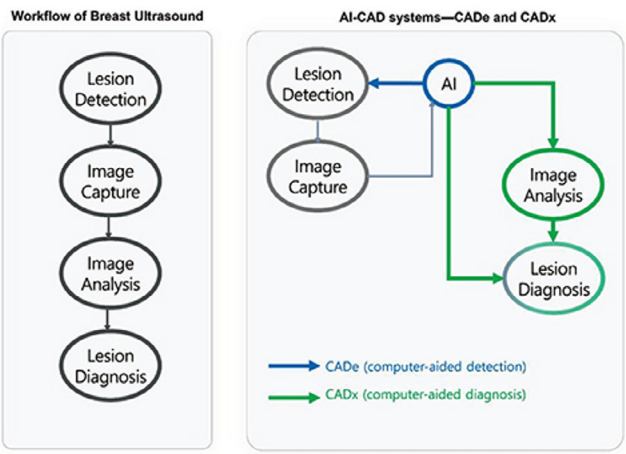

AI-CAD systems are generally divided into two categories—CADe and CADx based on the primary function. CADe focuses on identifying potential lesions or abnormalities within medical images, and CADx makes a differential diagnosis for the detected lesions (benign vs. malignant).

HI03-S3 AI and Breast US

14:40-15:00 GBR 102

Chairperson(s): Sung Hun Kim *(The Catholic University of Korea, Seoul St. Mary's Hospital, Korea)*
Young Mi Park *(Inje University Busan Paik Hospital, Korea)*

AI Use in US: Beyond Detection and Diagnosis

Jin Kyung An
Department of Radiology, Nowon Eulji Medical Center, Eulji University, Korea

Breast ultrasound (US) has long been the cornerstone of breast cancer screening and diagnosis. Breast ultrasound offers advantages, such as wide availability, low cost, and safety without radiation. It is also used for supplemental screening and diagnostic purposes. However, its utility is limited by operator dependence, a high recall rate, low positive predictive value, and low specificity.

The development of artificial intelligence (AI) has had a profound impact on medical imaging, including ultrasound. AI tools aim to improve US specificity and value as screening and diagnostic modalities. AI can assist radiologists and address the limitations of ultrasound by acting as a decision-support tool, improving diagnostic performance, decreasing interpretation times, and enhancing consistency in management.

AI used in ultrasound is being applied not only for detection and diagnosis, but also for prediction and prognosis, and has shown good results. For example, it is applied to predict molecular subtypes, preoperative prediction of axillary lymph node metastasis, and preoperative prediction of neoadjuvant chemotherapy response. AI applications can improve consistency in breast care by reducing intra- and inter-observer variabilities. AI can enable faster and more accurate interpretation, which can have a significant clinical impact. AI can play a significant role in breast ultrasound in low-income and middle-income countries.

Various studies and attempts have been conducted using AI, but there are also many challenges that need to be considered. Challenges in developing and deploying AI algorithms for breast ultrasound include a lack of curated training datasets, variability in image acquisition, and the need for diverse datasets. AI performance can be improved by training with challenging lesions, considering concurrent lesions and prior examinations. Ethical considerations for AI integration include data handling, privacy, bias, safety, and trust. Informed consent and the ability to address health disparities are crucial. Choosing the right AI system for breast imaging requires consideration of factors such as intended use, deployment possibilities, and performance for specific populations and equipment. Periodic evaluations and transparency of AI developers are important. Cost, reimbursement, and post-implementation evaluation of AI algorithms in clinical practice are important factors to consider for successful integration of AI in breast imaging. Prospective clinical trials are required to evaluate the impact of AI in real-life screening settings.

Successfully integrating AI into medical imaging, including breast ultrasound, requires not only AI research and development but also social and ethical regulations that can support it, as well as collaboration between developers, clinicians, and policymakers.

References

1. Fruchtman Brot H, Mango VL. Artificial intelligence in breast ultrasound: application in clinical practice. Ultrasonography. 2024;43:3-14.
2. Bahl M, Chang JM, Mullen LA, Berg WA. Artificial Intelligence for Breast Ultrasound: AJR Expert Panel Narrative Review. AJR Am J Roentgenol. 2024;223:e2330645.
3. Shen YT, Chen L, Yue WW, Xu HX. Artificial intelligence in

ultrasound. Eur J Radiol. 2021;139:109717.
4. Trepanier C, Huang A, Liu M, Ha R. Emerging uses of artificial intelligence in breast and axillary ultrasound. Clin Imaging. 2023;100:64-68.
5. Díaz O, Rodríguez-Ruíz A, Sechopoulos I. Artificial Intelligence for breast cancer detection: Technology, challenges, and prospects. Eur J Radiol. 2024;175:111457.
6. Ahn JS, Shin S, Yang SA, Park EK, Kim KH, Cho SI, Ock CY, Kim S. Artificial Intelligence in Breast Cancer Diagnosis and Personalized Medicine. J Breast Cancer. 2023;26:405-435.

LD01-S1

14:00-14:30 GBR 103

Chairperson(s): **Doo Hoe Ha** *(CHA University Bundang Medical Center, Korea)*
Soo-jung Choi *(GangNeung Asan Hospital, Korea)*

US of Elbow Joint (Live Demo)

Eun Hae Park
Department of Radiology, Jeonbuk National University Hospital, Korea

Ultrasound plays a vital role in the evaluation of elbow joint disorders due to its dynamic, real-time, and high-resolution capabilities — especially for superficial soft tissues

1. Anterior Aspect

- Structures:
  - Biceps tendon
  - Brachialis muscle
  - Anterior joint recess
- Look for: Effusion, synovial thickening, partial tears, bicipitoradial bursitis

2. Medial Aspect

- Structures:
  - Common flexor tendon
  - Medial epicondyle
  - Ulnar collateral ligament (UCL)
  - Ulnar nerve (in cubital tunnel)
- Pathologies:
  - Medial epicondylitis (hypoechoic tendon, calcifications)
  - UCL injury (thickening, hypoechoic gap)
  - Ulnar nerve subluxation/entrapment (dynamic scan while flexing)

3. Lateral Aspect

- Structures:
  - Common extensor tendon
  - Lateral epicondyle
  - Radial collateral ligament
  - Radial head (assess with pronation/supination)
- Pathologies:
  - Lateral epicondylitis (heterogeneous, thickened tendon)
  - Joint effusion, synovitis
  - Osteochondral lesions of radial head/capitellum

4. Posterior Aspect

- Structures:
  - Triceps tendon
  - Olecranon bursa
  - Posterior joint recess
- Pathologies:
  - Triceps tendinopathy or tears
  - Olecranon bursitis (fluid collection)
  - Posterior impingement

5. Dynamic Maneuvers

- Ulnar nerve subluxation: Flex elbow and observe movement
- Snapping triceps: Elbow flexion-extension under probe

Joint instability (valgus stress test): Check UCL integrity dynamically

LD01-S2

14:30-15:00 **GBR 103**

Chairperson(s): **Doo Hoe Ha** *(CHA University Bundang Medical Center, Korea)*
Soo-jung Choi *(GangNeung Asan Hospital, Korea)*

US of Knee Joint (Live Demo)

Chee Yeong Lim
Department of Diagnostic Radiology, Singapore General Hospital, Singapore

Demonstration in ultrasound of:

- Anterior knee (Quadriceps, patella tendon, suprapatellar recess, femoral trochlea)
- Medial knee (Medial collateral ligament, pes aserinus complex)
- Lateral knee (Iliotibial band, lateral collateral ligament)
- Posterior knee (Tendons, neurovascular structures)

CC09-S1 **Advancing Therapeutic Ultrasound: Insights into Fundamentals and Innovations**

14:00-14:20 **Room 203**

Chairperson(s): **Yongrae Roh** *(Kyungpook National University, Korea)*
Young Sun Kim *(MINT Hospital, Korea)*

Customized Ultrasonic Devices and Techniques for Cavitation-Assisted Sonothrombolysis

Jinwook Kim
School of Mechanical Engineering, Kyungpook National University, Korea

Venous thromboembolism (VTE) remains a major global health concern, contributing significantly to morbidity and mortality, particularly in aging populations. Current standard treatments, including thrombolytic drugs and mechanical thrombectomy, often suffer from limited efficacy and carry the risk of adverse effects. Ultrasound-enhanced thrombolysis (UET) has been explored for decades as a promising adjunctive therapy. More recently, biocompatible micro- and nano-scale cavitation agents have gained attention for their potential to enhance sonothrombolysis through mechanisms such as shock waves, microjets, and cavitation-induced microstreaming. However, conventional therapeutic ultrasound systems—typically large, transcutaneous devices using high-power, long-duration pulses—are not optimized to fully exploit these cavitation effects. This represents a key technological gap in UET. My research addresses this challenge by developing customized ultrasound devices and tailored pulsing protocols specifically designed for cavitation-enhanced thrombolysis. In this talk, I will introduce two innovative UET strategies for VTE treatment: 1) A forward-viewing intravascular ultrasound catheter for microbubble-mediated sonothrombolysis, and 2) A nanodroplet-mediated pulsed ultrasound system targeting chronic venous clots. Efficacy was validated in vitro through clot mass reduction, video microscopy, passive cavitation detection, and active cavitation imaging. Notably, nanodroplets demonstrated significantly enhanced clot lysis—without the use of tPA—compared to microbubbles. In a porcine deep vein thrombosis (DVT) model, our customized system restored blood flow using nanodroplet cavitation and a low dose of tPA (0.1 mg/mL, total 0.3 mg) within 40 minutes of treatment. The presentation will conclude with a discussion on future directions and design considerations for ultrasound devices for safe, efficient, and clinically translatable sonothrombolysis.

CC09-S2 **Advancing Therapeutic Ultrasound: Insights into Fundamentals and Innovations**

14:20-14:40 **Room 203**

Chairperson(s): **Yongrae Roh** *(Kyungpook National University, Korea)*
Young Sun Kim *(MINT Hospital, Korea)*

Disposable Wearable Ultrasound: An Emerging Device for Clinical Translation

Byung Chul Lee
Bionics Research Center, Korea Institute of Science and Technology, Korea

Ultrasound technology is a cornerstone of medical practice, widely employed in diagnostics and increasingly recognized for its therapeutic capabilities. However, traditional ultrasound probes suffer from rigidity, bulkiness, and substantial weight, limiting their application in prolonged imaging sessions and continuous therapeutic interventions. Recent advancements in soft electronics have led to the development of flexible, thin, and stretchable wearable ultrasound devices, overcoming these limitations and significantly expanding their clinical potential.

In particular, wearable capacitive micromachined ultrasonic transducer (CMUT)-based devices leverage advancements in soft electronics combined with semiconductor fabrication processes, enabling disposability, cost-effectiveness, and the elimination of lead contaminants commonly associated with traditional transducers. Their compact and flexible design allows precise targeting and continuous administration of ultrasound for uninterrupted imaging and various therapeutic applications, including drug delivery and neuromodulation.

This abstract introduces the fundamental principles and unique structural advantages of wearable CMUT probes, highlighting their contributions to both diagnostic and therapeutic advancements. Critical considerations for clinical translation, such as device dimensions, transmission efficiency, and disposable design, are discussed. Finally, we emphasize emerging therapeutic applications enabled by disposable wearable ultrasound devices, underscoring their transformative potential in enhancing patient care through integrated diagnostic and therapeutic systems.

CC09-S3 Advancing Therapeutic Ultrasound: Insights into Fundamentals and Innovations

14:40-15:00 Room 203

Chairperson(s): Yongrae Roh *(Kyungpook National University, Korea)*
Young Sun Kim *(MINT Hospital, Korea)*

Ultrasound-Induced Optical Clearing for Deep Optical Imaging and Photothermal Therapy

Jin Ho Chang
Department of Electrical Engineering and Computer Science,
Daegu Gyeongbuk Institute of Science and Technology, Korea

Hybrid imaging techniques have garnered significant attention, as each medical imaging modality has inherent strengths and limitations. Combining modalities allows the simultaneous acquisition of complementary information, enhancing diagnostic capabilities. Among various imaging modalities, ultrasound and optical imaging are notably compatible, each complementing the other's advantages and mitigating respective limitations. Consequently, numerous studies have explored ultrasound-optical hybrid systems to generate novel clinical value. Additionally, ultrasound has facilitated advanced optical imaging methods designed to overcome the inherent limitations of light penetration in biological tissues, notably through techniques like ultrasound-generated guidestars for wavefront shaping. In a distinctly different approach, our research team recently introduced ultrasound-induced optical clearing (US-OC), a groundbreaking method that leverages transient gas bubbles generated by ultrasound along the optical path to significantly reduce tissue optical scattering. We successfully applied US-OC to laser scanning microscopy (US-OCM), demonstrating over a six-fold increase in imaging depth compared to conventional methods, while preserving imaging resolution (Nature Photonics, vol. 16, 762-769, 2022). We have also applied US-OC to photothermal therapy (PTT), recently published in Advanced Optical Materials (2400332, 2024). PTT selectively delivers laser energy to chromophores within targeted lesions, minimizing side effects. However, its clinical applicability has been restricted by limited therapeutic depth due to optical scattering. To overcome this barrier, we developed ultrasound-induced optical clearing-assisted PTT (ULTRA-PTT). In this presentation, I will discuss the foundational principles and potential clinical applications of US-OC, US-OCM, and ULTRA-PTT.

SF04-S1 **Intestinal US is Coming Back!**

15:20-15:40 **GBR 101**

Chairperson(s): **Se Hyung Kim** *(Seoul National University Hospital, Korea)*
Ji Soo Song *(Chonbuk National University Hospital, Korea)*

Recent Changes in Diagnosis & Management of IBD

Kyuwon Kim
Department of Gastroenterology, Chung-Ang University Hospital, Korea

1. Background

Inflammatory bowel disease (IBD), encompassing Crohn's disease (CD) and ulcerative colitis (UC), is a chronic, idiopathic condition characterized by recurrent intestinal inflammation. Although previously rare in East Asia, the incidence and prevalence of IBD in Korea have increased rapidly in recent decades. According to the Songpa-Kangdong cohort study, the prevalence in 2015 was estimated at 31.59 per 100,000 for CD and 76.66 per 100,000 for UC in Korea. CD commonly presents in younger individuals, with a median age of diagnosis at 22 years, while UC has a median age of 36 years. National data indicate that CD peaks in adolescents and young adults, whereas UC is more evenly distributed across the 20s to 40s.

2. Diagnosis

Diagnosis is based on a combination of clinical assessment and findings from endoscopic, histologic, radiologic, and biochemical investigations. While serologic and genetic testing are no longer routinely recommended, comprehensive history-taking and evaluation of gastrointestinal and extraintestinal symptoms remain critical. Laboratory markers such as C-reactive protein, ESR, and fecal calprotectin are useful in assessing disease activity and distinguishing IBD from functional disorders. The first-line diagnostic procedure is ileocolonoscopy with multiple biopsies, especially useful in identifying characteristic features of CD such as patchy inflammation and skip lesions. Cross-sectional imaging (CT enterography, MR enterography) and emerging tools such as intestinal ultrasound (IUS) are increasingly utilized for initial disease extent evaluation and monitoring. IUS, in particular, is gaining attention due to its non-invasive, radiation-free, and point-of-care applicability, with good concordance to colonoscopy findings. Small bowel capsule endoscopy may be considered in patients who are highly suspicious of CD despite negative findings on standard imaging.

3. Management

A wide spectrum of medications is now available, including 5-aminosalicylic acid (5-ASA) agents, corticosteroids, immunomodulators (azathioprine, 6-mercaptopurine, methotrexate), biologic agents (intravenous or subcutaneous), and oral small molecules. However, several unmet needs remain, including the ability to predict individual therapeutic response, lack of head-to-head comparative trials, loss of treatment response over time, and significant cost burdens. Intestinal ultrasound is emerging as a valuable tool for real-time monitoring of treatment response, in addition to conventional CT and MRI. Long-term care also requires vigilance for opportunistic infections and IBD-related malignancies. In the absence of effective anti-fibrotic therapies, fibro-stenotic complications often necessitate surgical intervention.

4. Future directions

Although Korea's prevalence of IBD remains lower than in the West, it is among the highest in Asia and

continues to rise. As a chronic, incurable condition, accurate diagnosis and appropriate therapeutic strategies are essential for preventing complications. Ongoing monitoring of disease activity and complications through CT, MRI, and IUS will be critical in achieving optimal therapeutic goals and improving patient outcomes.

SF04-S2 **Intestinal US is Coming Back!**

15:40-16:00 **GBR 101**

Chairperson(s): **Se Hyung Kim** *(Seoul National University Hospital, Korea)*
Ji Soo Song *(Chonbuk National University Hospital, Korea)*

Role of Imaging for IBD (CT & MR)

Jung Hee Son
Department of Radiology, Inje University Haeundae Paik Hospital, Korea

Inflammatory bowel disease (IBD), such as Crohn's disease, is a lifelong condition, and patients often undergo multiple imaging tests throughout their lifetime. A variety of well-established, non-invasive methods are available to image the small bowel. MR enterography (MRE) is the primary imaging modality, while CT enterography (CTE) plays a lesser role due to its use of ionizing radiation.

Cross-sectional imaging techniques—including MRE, CTE, and intestinal US—are playing an increasingly important role in diagnosing IBD, staging disease extent and complications, assessing disease activity, and evaluating treatment response. Their significance is further highlighted by the growing emphasis on transmural healing as a potentially superior treatment target compared to mucosal healing alone, which can only be assessed with cross-sectional imaging.

Emerging technologies now allow for the non-invasive quantification of bowel motility, offering a potential biomarker for disease activity and therapeutic response. Novel imaging applications, such as quantifying stricture fibrosis and fat wrapping, may further contribute to disease activity assessment and prognostication.

In this lecture, we will:

- Explore the roles of CTE and MRE in the evaluation of inflammatory bowel disease.
- Discuss how to choose between imaging modalities.
- Focus on assessing Crohn's disease activity and treatment response using cross-sectional imaging.
- Review novel CT and MRI techniques for evaluating inflammatory bowel disease.

SF04-S3 **Intestinal US is Coming Back!**

16:00-16:20 **GBR 101**

Chairperson(s): **Se Hyung Kim** *(Seoul National University Hospital, Korea)*
Ji Soo Song *(Chonbuk National University Hospital, Korea)*

Assessment and Monitoring of IBD with US

Sung Kyoung Moon
Department of Radiology, Kyung Hee University Medical Center, Korea

Inflammatory bowel disease (IBD), encompassing Crohn's disease and ulcerative colitis, presents a significant clinical challenge due to its chronic, relapsing nature. The assessment of disease activity is crucial for effective management and monitoring. Among various imaging modalities, ultrasound (US) has emerged as a valuable tool due to its non-invasive nature, absence of radiation, and ability to provide real-time evaluation. This lecture contains the role of ultrasound in assessing IBD, focusing on its efficacy in determining inflammatory activity, scanning techniques, and integration with other imaging modalities.

SF05-S1 **High Risk Lesions of Breast**

15:20-15:50 **GBR 102**

Chairperson(s): **Bo Kyoung Seo** *(Korea University Ansan Hospital, Korea)*
Min Jung Kim *(Severance Hospital, Korea)*

Management of High Risk Lesions-Singapore Experience

Rameysh Danovani Mahmood
Department of Radiology, Changi General Hospital, Singapore

High risk lesions of the breasts, also known as lesions of uncertain malignant potential or pathological category B3 lesions, are commonly encountered lesions usually arising following percutaneous biopsies of an abnormal imaging finding. According to the literature, its incidence following breast biopsies is approximately 3-12%, and it is frequently discovered as screening-detected abnormalities, thought to be increasingly common in the era of routine breast screening. These lesions encompass a wide range of histopathological diagnoses, which include atypical ductal hyperplasia (ADH), lobular neoplasia, papilloma and radial scar, amongst others. Following their initial discovery, the patients are conventionally indicated for surgical excision at the site of the initial biopsy for the purpose of obtaining additional tissue samples in order to achieve completion of diagnostic process. However, there are increasing interests in the use of non-surgical approach, specifically percutaneous imaging-guided vacuum excision, for additional tissue sampling. Management guidelines have been published in the UK and the EU, outlining specific indications for vacuum assisted excision based on specific histopathological B3 diagnosis and the method of initial biopsy used. This lecture aims to review the guidelines, other literature evidences, clinical benefits, as well as sharing of our experience in Changi General Hospital in the adoption of this technique.

SF05-S2 High Risk Lesions of Breast

15:50-16:20 GBR 102

Chairperson(s): **Bo Kyoung Seo** *(Korea University Ansan Hospital, Korea)*
Min Jung Kim *(Severance Hospital, Korea)*

Managing High-Risk Lesions: Key Considerations

Soong June Bae
Department of Radiology, Gangnam Severance Hospital, Korea

In the era of precision medicine, the role of radiologic evaluation has become crucial in managing breast cancer.

In this session, I would like to introduce several real-world clinical cases where treatment strategies—including surgical and systemic therapies—are determined based on radiologic findings.

In particular, we will focus on how these evaluations guide decisions around treatment de-escalation.

1. Omission of Sentinel Lymph Node Biopsy in Patients with Early Breast Cancer

In recent years, several clinical trials have explored the omission of sentinel lymph node biopsy (SLNB) in patients with early-stage breast cancer, specifically those with cT1-2 and cN0 disease. In these studies, patients were classified as cN0 based on the absence of suspicious lymph nodes on ultrasound. However, despite this radiologic assessment, approximately 10% of patients in the SLNB group were found to have lymph node metastasis. Notably, the majority of patients enrolled in these trials had hormone receptor (HR)-positive, HER2-negative breast cancer. As a result, there is ongoing concern about whether these findings can be applied to patients with HER2-positive or triple-negative breast cancer (TNBC), which typically have more aggressive biology. In this context, I will discuss whether SLNB omission could also be feasible in HER2+ and TNBC patients by integrating more advanced radiologic evaluation.

2. Radiologic Axillary Evaluation and NAC Decision

Determining the extent of axillary lymph node involvement on imaging plays a pivotal role in deciding between upfront surgery and neoadjuvant chemotherapy (NAC). In patients with HR-positive, HER2-negative breast cancer, it is often challenging for physicians to choose the optimal initial treatment—whether to proceed with upfront surgery or start with NAC—especially when imaging shows only one or two suspicious lymph nodes, particularly if they are categorized as low suspicious. These findings highlight the importance of precise and detailed radiologic descriptions of axillary lymph node characteristics to support clinical decision-making.

3. Preservation of the Nipple-Areolar Complex Post-NAC

Advances in NAC regimens have improved tumor downstaging, making nipple-sparing mastectomy (NSM) a feasible option for more patients. Traditionally, tumor (or non-mass enhancement)-nipple distance (TND) ≤ 1.0-2.0 cm or presence at the nipple base on preoperative MRI were considered contraindications for NSM. However, recent studies demonstrate that NME extension to the nipple frequently resolves after NAC. In such cases, pathologic nipple invasion was rare, especially when a complete radiologic response was observed on post-NAC MRI. This supports NSM even in patients with initial nipple involvement if post-NAC imaging shows resolution is pathologically clear.

4. Management of Residual Microcalcifications

Residual microcalcifications on post-NAC mammography often pose a challenge for surgical planning. Although a weak to moderate correlation exists between residual microcalcification extent and residual tumor size, many patients who achieve complete MRI response—particularly those with HER2-positive or triple-negative breast cancer—show minimal or no residual carcinoma despite the presence of calcifications. Therefore, extensive surgery based solely on persistent calcifications may be unnecessary in selected cases with favorable radiologic and molecular profiles.

5. Radiologic Evaluation-based Treatment de-escalation in the Neoadjuvant Setting

In patients receiving neoadjuvant chemotherapy (NAC) for breast cancer, ongoing studies are exploring how radiologic response can guide treatment de-escalation. Notably, the TRAIN-3 trial demonstrated that in HER2-positive breast cancer, MRI-based assessment of treatment response could help identify good responders, allowing for the de-escalation of neoadjuvant chemotherapy. In addition, clinical trials such as Optimist and ASLAN are investigating the potential for surgical treatment de-escalation in patients who show favorable radiologic responses.

These cases highlight the critical role of radiologic evaluation in determining treatment strategies. With future research—including the application of AI models to improve diagnostic accuracy—we expect that radiologic evaluation will become even more precise, ultimately enabling more refined and personalized precision medicine for breast cancer patients.

LD02-S1 Ultrasound Anatomy of the Thyroid and Neck

15:20-15:50 GBR 103

Chairperson(s): **So Lyung Jung** *(The Catholic University of Korea, St. Vincent's Hospital, Korea)*
Yoon Jung Choi *(Kangbuk Samsung Hospital, Korea)*

Ultrasound Anatomy of the Neck: Introduction to Thyroid and Adjacent Anatomy

Leehi Joo
Department of Radiology, Chung-Ang University Hospital, Korea

Understanding the anatomy of the thyroid and its surrounding structures is essential for making accurate diagnoses, performing safe biopsies, and minimizing unnecessary complications. By becoming familiar with this anatomy, we can ensure better clinical outcomes. We will begin by reviewing the anatomy of the thyroid and adjacent structures, followed by a live demonstration using a simulated patient.

LD02-S2 Ultrasound Anatomy of the Thyroid and Neck

15:50-16:20 GBR 103

Chairperson(s): **So Lyung Jung** *(The Catholic University of Korea, St. Vincent's Hospital, Korea)*
Yoon Jung Choi *(Kangbuk Samsung Hospital, Korea)*

Ultrasound Anatomy of the Neck: Nerves

Min Kyoung Lee
Department of Radiology, The Catholic University of Korea, Yeouido St. Mary's Hospital, Korea

1. Nervous system

Nervous structures are the most commonly injured critical structure during procedure. Careful evaluation of nervous structures can prevent the serious complications during procedure. The nerve shows the round shaped lesion with hypoechogenicity on US. The understanding the location and variations of nerves may be helpful to differentiate between the metastatic lymph node and neurogenic tumor and prevent nerve injuries.

Vagus nerve

The vagus nerve is the longest cranial nerve. It is typically located within the carotid space, and is usually posterolateral aspect to the common carotid artery (CCA) and posteromedial aspect to the internal jugular vein (IJV). There are various variations of vagus nerve course according to the relation between the CCA and vagus nerve. Anterior variation is relatively common variation with 21.1% prevalence in previous report, but other variations, as medial and posterior variations, have a relatively lower prevalence.

The symptoms of vagus nerve injury are arrhythmia, dysphagia, dyspnea, nausea, and hiccups, and the injury of vagus nerve may also induce the dysfunction of inferior recurrent laryngeal nerve (eg. cough, dysphonia). Large thyroid mass may change the location of the vagus nerve. Therefore, physician carefully evaluates the correlation between vagus nerve and CCA.

Superior and inferior laryngeal nerves

The recurrence inferior laryngeal nerve (RLN) is a branch of the vagus nerve, and innervates the intrinsic muscles of the larynx. Due to small size, the RLN could not easily detect on US. Although the course of both RLNs are not symmetrical, it is usually located in the tracheoesophageal groove at the neck level. The non-RLN is common variation of RLN, which arises from the vagus nerve and directly enters the larynx from vagus nerve instead of making loop. The right non-RLN has association with the aberrant right subclavian artery, and the left non-RLN is associated with situs inversus. If there is the absence of the brachiocephalic trunk on US, it can predict the presence of non-RLN. The injury of RLN caused the symptoms of cough and voice change. Although the identification of RLN on US is difficult, the understanding course of RLN may reduce the complication during procedure.

The superior laryngeal nerve (SLN) is another branch of the vagus nerve, and it passes the pharynx and divides into the two branches (internal and external branches). Finally, the SLN enters the vocal cord. As the RLN, the SLN also does not easily detect on US, but external branch of the SLN could be located near the superior thyroidal artery (STA) and veins at the superior portion of the thyroid gland. Therefore, if physician performs the procedure near the superior portion of the thyroid gland, it is necessary to evaluate the patient symptom (voice change) related with the nerve injury.

Middle cervical sympathetic ganglion

Middle cervical sympathetic ganglion (MCSG) is the smallest one among the cervical sympathetic ganglion, and it is located anterior portion of the longus coli muscles (C5-7 vertebra level). On US images, the MCSG can be detected in 41%, and shows a spindle-shaped hypoechoic structure with nerve branches. Because it is usually located near the interior thyroid artery (ITA), ITA is used as the land mark of the MCSG. The injury of MCSG may occur during thyroid procedure due to located at the lower portion of the thyroid gland. Horner syndrome is the typical complication of MCSG injury. The conjunctival injection is the initial finding of MCSG injury, and other symptoms (ptosis, miosis, and anhidrosis of the face) may be combined.

Other nervous structures

Cervical plexus arises from the plexus of the ventral rami of the upper 4 cervical spinal nerves, and the brachial plexus arises from the plexus of the ventral rami of the lower 4 cervical and first thoracic spinal nerves. They are located between the anterior and posterior tubercles, and can easily detect as the cordlike hypoechoic structure on US.

The spinal accessory nerve (SAN) is a motor branch of the sternocleidomastoid (SCM) and trapezius muscles. It is located between the posterolateral border of the SCM muscles and anterior border of the trapezius muscle. The SAN may easily detect within the fat layer between the muscles. Because the SAN is far from the thyroid gland, the injury of SAN is uncommon during thyroid procedure. However, recurrent thyroid cancer can be located near the SAN. If the SAN is injured during the ablation of recurrent thyroid cancer, patients complain limitation of abduction of the shoulder and shoulder dropping.

The phrenic nerve arises from the C3-5 spinal nerves, and it passes anteriorly to the anterior scalene muscle and posteriorly to the SCM muscle. The transverse cervical artery is the land mark of the phrenic nerve, due to crossing course between two structures near the anterior scalene muscle.

References

1. Chiou H-J, Chou Y-H, Chiou S-Y, Liu J-B, Chang C-Y. Peripheral nerve lesions: role of high-resolution US. Radiographics 2003;23:e15-e.
2. Giovagnorio F, Martinoli C. Sonography of the cervical vagus nerve: normal appearance and abnormal findings. American Journal of Roentgenology 2001;176:745-9.
3. Ha EJ, Baek JH, Lee JH, Kim JK, Shong YK. Clinical significance of vagus nerve variation in radiofrequency ablation of thyroid nodules. European radiology 2011;21:2151-7.
4. Park J, Jeong S, Lee J-H, Lim G, Chang J. Variations in the course of the cervical vagus nerve on thyroid ultrasonography. American journal of neuroradiology 2011;32:1178-81.
5. Ha EJ, Baek JH, Lee JH. Ultrasonography-based thyroidal and perithyroidal anatomy and its clinical significance. Korean journal of radiology 2015;16:749-66.
6. Gong R-x, Luo S-h, Gong Y-p, Wei T, Li Z-h, Huang J-b, et al. Prediction of nonrecurrent laryngeal nerve before thyroid surgery—experience with 1825 cases. Journal of Surgical Research 2014;189:75-80.
7. Huang SM, Wu TJ. Neck ultrasound for prediction of right nonrecurrent laryngeal nerve. Head & neck 2010;32:844-9.
8. Saylam CY, Ozgiray E, Orhan M, Cagli S, Zileli M. Neuroanatomy of cervical sympathetic trunk: a cadaveric study. Clinical Anatomy: The Official Journal of the American Association of Clinical Anatomists and the British Association of Clinical Anatomists 2009;22:324-30.
9. Shin JE, Baek JH, Ha EJ, Choi YJ, Choi WJ, Lee JH. Ultrasound features of middle cervical sympathetic ganglion. The Clinical Journal of Pain 2015;31:909-13.
10. Samer Narouze M. Sonoanatomy of the Cervical Spinal Nerve Roots Implications for Brachial Plexus Block. Regional Anesthesia and Pain Medicine 2009;34:616.
11. Canella C, Demondion X, Delebarre A, Moraux A, Cotten H, Cotten A. Anatomical study of phrenic nerve using ultrasound. European radiology 2010;20:659-65.
12. Standring S. Gray's anatomy e-book: the anatomical basis of clinical practice: Elsevier Health Sciences; 2021.
13. Gervasio A, Mujahed I, Biasio A, Alessi S. Ultrasound anatomy of the neck: The infrahyoid region. Journal of ultrasound 2010;13:85-9.
14. Canella C, Demondion X, Abreu E, Marchiori E, Cotten H, Cotten A. Anatomical study of spinal accessory nerve using ultrasonography. European journal of radiology 2013;82:56-61.
15. Na DG, Baek JH, Jung SL, Kim J-h, Sung JY, Kim KS, et al. Core needle biopsy of the thyroid: 2016 consensus

statement and recommendations from Korean Society of Thyroid Radiology. Korean journal of radiology 2017;18:217-37.

16. Brand-Saberi BE, Schäfer T. Trachea: anatomy and physiology. Thoracic surgery clinics 2014;24:1-5.

SF06-S1 Therapeutic Ultrasound in Brain Application

15:20-15:50 Room 203

Chairperson(s): **Seok Ho Hong** *(Asan Medical Center, Korea)*
Eun-Joo Park *(Seoul National University Hospital, Korea)*

Focused Ultrasound Surgery for Dystonia

Shiro Horisawa
Department of Neurosurgery, Tokyo Women's Medical University, Japan

In this lecture, I will present the clinical application of magnetic resonance-guided focused ultrasound (MRgFUS) for treating dystonia, with a focus on focal hand dystonia (FHD) and cervical dystonia (CD).

For focal hand dystonia, we performed Vothalamotomy using MRgFUS in 10 patients. At 12 months after treatment, we observed significant improvements in dystonia severity and disability, including an average 71.4% improvement in the Writer's Cramp Rating Scale and a 22.9% increase in the Arm Dystonia Disability Scale. Most patients experienced meaningful functional recovery.

For cervical dystonia, we conducted the world's first clinical trial of MRgFUS targeting the pallidothalamic tract (PTT) at Forel's field. In this pilot study of 10 patients, we achieved a 43.4% reduction in the Toronto Western Spasmodic Torticollis Rating Scale at 6 months. Improvements were also observed in mood and anxiety scales. However, mild hand dexterity impairment occurred in several patients, highlighting the need for careful target planning and patient selection.

In both conditions, MRgFUS provided clinical benefits comparable to radiofrequency ablation and deep brain stimulation (DBS), while avoiding the need for implanted hardware. I will discuss optimal targeting strategies, outcome data, and future directions for FUS in functional neurosurgery.

SF06-S2 Therapeutic Ultrasound in Brain Application

15:50-16:20 Room 203

Chairperson(s): **Seok Ho Hong** *(Asan Medical Center, Korea)*
Eun-Joo Park *(Seoul National University Hospital, Korea)*

FUS Medicated BBBO to Enhance Delivery Lazertinib Delivery for Metastatic Brain Tumor from NSCLC

Won Seok Chang
Department of Neurosurgery, Severance Hospital, Korea

Background

EGFR tyrosine kinase inhibitors (TKIs) are effective for EGFR-mutant non-small cell lung cancer (NSCLC) but have limited efficacy in brain metastases due to poor blood-brain barrier (BBB) penetration, leading to recurrence. Additional interventions, such as surgery or radiotherapy, increase the risk of complications and neurocognitive decline. While third-generation TKIs like lazertinib improve CNS penetration, their effectiveness remains suboptimal. Focused ultrasound (FUS) transiently disrupts the BBB to enhance drug delivery. This aim of this study is to evaluate whether FUS improves lazertinib efficacy in an EGFR-mutant NSCLC brain metastasis model.

Methods

H-1975 cells were implanted into the rat frontal cortex to establish brain metastases. Rats were assigned to control, Lazertinib-only, or lazertinib + FUS groups. FUS and lazertinib were administered weekly, with MRI monitoring tumor progression. Drug concentrations in brain tissues were quantified via liquid chromatography-tandem mass spectrometry. Transcriptomic changes were assessed using bulk RNA sequencing and gene set enrichment.

Results

FUS significantly enhanced lazertinib drug delivery, increasing brain tumor concentrations by 2.19-fold compared to lazertinib alone. MRI revealed substantial tumor regression, with near-complete disappearance in most animals after three weeks. RNA sequencing showed increased neuronal activity and BBB transport, with decreased tumor burden and immunogenicity in the FUS group.

Conclusions

FUS-mediated BBB opening improves the delivery and efficacy of lazertinib, leading to better treatment outcomes for EGFR-mutant NSCLC brain metastases. These findings support FUS as a non-invasive strategy to overcome BBB-related drug delivery limitations

IS02-S1

16:40-17:00 GBR 101

Chairperson(s): **Eunkyung Kim** *(Yongin Severance Hospital, Korea)*
Sung Il Hwang *(Seoul National University Bundang Hospital, Korea)*

The Present and Future of Medical Imaging AI

Hyungjun Park
Internal Medicine-Pulomary, Shihwa Medical Center, Korea

Artificial intelligence in medical imaging has rapidly evolved, transitioning from basic detection of specific conditions to advanced interpretation across diverse medical scenarios. These advancements are primarily driven by developments in foundation models, which allow AI systems to perform tasks previously thought impossible. In this document, we examine the current state and evolution of AI in medical imaging, highlighting advancements from single-task detection models to sophisticated multimodal foundation models, and analyze how future developments could transform healthcare practices.

1. Current Status of Medical Image AI: Disease Detection and Classification

Historically, the primary role of medical image AI was to detect and classify a predefined, limited set of diseases, such as specific tumors identified in modalities like ultrasound, X-ray, and CT. These models helped improve diagnostic consistency and addressed some variations in physician expertise, providing modest assistance to clinical workflows. Companies like Lunit and Vuno have translated these technological capabilities into commercial applications that are now being integrated into clinical practice, though still operating within the constraints of highly specialized detection tasks rather than comprehensive diagnostic interpretation.

2. Technological Advancements in Medical Image AI

Emergence of Foundation Models

Recent AI development trends suggest a gradual shift from training empty models on basic data toward increasing utilization of pre-trained foundation models or adaptation of comprehensive models like GPT-4. Foundation models trained on massive general datasets are beginning to show potential adaptability through fine-tuning, potentially enabling more efficient deployment across various medical imaging modalities—including ultrasound, pathology slides, laparoscopic video, and radiologic imaging (CT, MRI, X-rays).

Foundation Model Evaluation: Assessing GPT-4V's Capabilities in Medical Image Interpretation

The emergence of GPT-4 has led to its evaluation in medical contexts, owing to its user-friendly interface, subscription-based accessibility, and impressive performance across various medical literature [1,2].

Assessment of GPT-4 has yielded varying results across different studies. While some research demonstrates good performance, others show limitations [3,4]. Upon closer examination, there appears to be a pattern: GPT-4 performs well when presented with rich clinical context but struggles when evaluating images in isolation without accompanying clinical history [5].

This pattern suggests that current foundation models can analyze medical images with some

degree of accuracy, but their performance is inconsistent and still contains significant errors. Notably, studies showing more favorable results often included substantial clinical context alongside the images, which appears to significantly enhance the model's interpretative abilities. When limited to image analysis alone, the performance typically declines, though not to the point of complete failure. Korean medical examinations, characterized by short prompts, illustrate this challenge clearly, as these concise questions provide minimal contextual information, resulting in suboptimal performance. However, given the rapid advancement of LLMs, current limitations may not persist in future iterations. The potential for improvement in this area warrants continued observation and research.

3. Promising Future: From Single-Modal to Multimodal Interaction

3.1 Multimodal Foundation Models and Explainable AI

Multimodal foundation models are emerging, integrating text, images, and annotations to provide richer, more explainable diagnostic outputs. Models like MAIRA-2, an open-source AI for chest X-ray interpretation developed by Microsoft, exemplify this evolution. Google's Gemini further demonstrates this multimodal advancement with abilities to process video with voice inputs, provide voice responses, and maintain contextual awareness of objects within video sequences. Unlike current foundation models providing only textual interpretations, these advanced multimodal models visually highlight lesions, track objects across time, and process multiple information streams simultaneously, significantly enhancing clinicians' understanding and facilitating better patient communication. Such developments suggest future medical AI systems may similarly evolve to maintain contextual awareness throughout patient encounters while providing more intuitive, multimodal interactions and outputs.

3.2 Leveraging Foundation Models for Rare Diseases

Foundation models show promise for addressing challenges in rare disease detection, where data scarcity has historically limited AI development. Through techniques like fine-tuning and knowledge distillation from larger models, along with human-in-the-loop annotation approaches, these models offer pathways to create effective diagnostic tools even with limited clinical data. This suggests significant potential for advancement as foundation models continue to evolve and improve.

4. Conclusion

Medical imaging AI is evolving beyond limited predictive tasks toward systems that provide clinicians with richer, more diverse information, enhancing diagnostic accuracy while streamlining workflows to allow greater focus on patient care.

Reference

1. Yan Z, Zhang K, Zhou R, et al. Multimodal ChatGPT for Medical Applications: an Experimental Study of GPT-4V. arXiv preprint arXiv:2310.19061, 2023.
2. Suh PS, Shim WH, Suh CH, et al. Comparing Diagnostic Accuracy of Radiologists versus GPT-4V and Gemini Pro Vision Using Image Inputs from Diagnosis Please Cases. Radiology 2024;312(1)
3. Kim H, Kim P, Joo I, et al. ChatGPT Vision for Radiological Interpretation: An Investigation Using Medical School Radiology Examinations. Korean J Radiol 2024;25(4):403-406.
4. Zhou Y, Ong H, Kennedy P, et al. Evaluating GPT-4V (GPT-4 with Vision) on Detection of Radiologic Findings on Chest Radiographs. Radiology 2024;311(2).
5. Nori H, Usuyama N, King N, et al. From Medprompt to o1: Exploration of Run-Time Strategies for Medical Challenge Problems and Beyond. arXiv preprint arXiv:2411.03590, 2024.

IS02-S2

17:00-17:20 GBR 101

Chairperson(s): **Eunkyung Kim** *(Yongin Severance Hospital, Korea)*
Sung Il Hwang *(Seoul National University Bundang Hospital, Korea)*

Using Mammographic AI to care for Patients with Breast Diseases: Applications in Breast US Exam

Jung Hyun Yoon
Department of Radiology, Severance Hospital, Korea

Artificial Intelligence (AI) is nowadays widely applied for mammography interpretation. With the advances in data processing and technology, the standalone performances of AI systems for mammography interpretation is currently at the level of radiologists. Studies are showing promising results for using AI in mammography interpretation in various clinical scenarios. Although there are many positive aspects in using AI for mammography, there are several aspects to consider for real world clinical application. Along with mammography, the role of breast ultrasonography (US) has expanded from diagnostic setting to supplemental screening, and how to combine mammography, US and AI for more cost-effective workflow is currently of debate. During this session, we will review the current status of AI for mammography, discuss factors to consider when using AI for practice, and how breast US exams should be integrated in this workflow.

IS02-S3

17:20-17:40 GBR 101

Chairperson(s): Eunkyung Kim *(Yongin Severance Hospital, Korea)*
Sung Il Hwang *(Seoul National University Bundang Hospital, Korea)*

Generating Radiology Reports of Ultrasound Exams Using LLMs

Jeonghyun Lee
Department of Radiology, Samsung Medical Center, Korea

1. Overview of Large Language Models (LLMs) and Vision-Language Models (VLMs)

Large Language Models (LLMs): LLMs are advanced artificial intelligence models trained on extensive text corpora to generate human-like language. In radiology, these models are being explored for various applications, including:

- Clinical Documentation: Automating radiology report generation and extracting specific data from reports [1, 2]
- Report Summarization: Condensing clinical histories or imaging findings [1]
- Decision Support: Assisting in diagnostic reasoning by providing context and suggested differential diagnoses [2]

Vision-Language Models (VLMs): VLMs are multimodal models that combine image processing with natural language understanding and generation. By integrating visual and textual data, VLMs can interpret images and produce descriptive text. In medicine, these models are being investigated for:

- Medical Image Interpretation: Providing preliminary descriptions of imaging findings
- Integrated Reporting: Generating comprehensive reports by linking visual observations with textual explanations

While promising, current general-purpose VLMs have been primarily trained on natural images and may not yet possess the domain-specific expertise required for detailed ultrasound interpretation [3].

Current Applications in Medicine: The integration of LLMs and VLMs in medical applications continues to evolve. Current research demonstrates that LLMs effectively generate well-structured, coherent text, making them valuable for drafting and refining radiology reports [1, 2]. Simultaneously, VLMs show potential for assisting in the preliminary interpretation of medical images, though their performance in specialized domains like ultrasound imaging remains an area of active investigation.

2. Ultrasound Image Interpretation Capabilities of Vision-Language Models

Existing Studies and Research: The application of VLMs to ultrasound image interpretation is a nascent field. Preliminary studies indicate that general-purpose VLMs (original CLIP, GPT-4 Vision) perform poorly in medical tasks [4, 5, 6].

Domain-Specific Adaptations: Efforts have been made to develop ultrasonography-specialized models, such as FetalCLIP for fetal ultrasound [7] and EchoCLIP for echocardiography [8]. These models, trained on extensive datasets of annotated ultrasound images, have shown improved performance on narrow tasks like standard view classification or specific pathology identification. However, they remain limited in scope and require substantial domain-specific data to approach the diagnostic accuracy of expert radiologists.

3. Report Generation Streamlining with LLMs

LLMs can expand structured inputs—such as keywords or abbreviated findings—into fully formed radiology reports [1, 9]. Radiologists frequently rely on templates and checklists during report generation, and information can be conveniently extracted to populate required data fields; for example, LI-RADS features may be extracted from liver MRI reports [10].

In ultrasound practice, these capabilities may streamline report generation by allowing radiologists to freely dictate results while the LLM structures and formats the report appropriately. This approach maintains the radiologist's interpretative authority while leveraging the LLM's strengths in natural language processing and document organization.

4. Radiology Report Generation in Other Modalities

A recent study by Hong et al. [11] trained a multimodal generative AI model on over eight million radiograph-report pairs to produce chest radiograph reports. The authors reported high sensitivity for critical findings (>95% for pneumothorax) and generally favorable evaluations compared with both radiologist-authored reports and general-purpose language models. However, they noted occasional errors (false positives and "hallucinations"), indicating the need for expert oversight.

Key points relevant to ultrasound include:

- Domain-Specific Training: Robust performance derives from large-scale, modality-specific datasets, emphasizing the importance of carefully curated training samples
- Error Sources: False positives and hallucinations persist, indicating the need for ongoing refinement and validation, especially for clinically significant findings
- Workflow Integration: While AI-generated preliminary reports can potentially reduce manual workload, radiologist review remains essential to ensure diagnostic accuracy

These outcomes, although specific to chest radiography, highlight challenges and strategies transferable to ultrasound report generation.

5. Challenges and Future Directions

Despite advances, several challenges must be addressed before widespread clinical adoption:

- Interpretative Accuracy: Current VLMs do not yet match the diagnostic accuracy of experienced radiologists in image interpretation [4]
- Data Requirements: Developing robust, domain-specific models requires large, annotated datasets, which are often scarce in ultrasound imaging [7, 8]
- Risk of Hallucination: LLMs may occasionally generate text that includes inaccuracies or unsupported details, necessitating rigorous oversight and validation by clinical experts [2, 10]

Future Research Directions: To address these challenges, future research should focus on:

- Developing Specialized Multimodal Models: Creating models specifically trained on large-scale, annotated ultrasound datasets to improve interpretative accuracy [7, 8]
- Hybrid Systems: Combining traditional image analysis algorithms with LLM-based text generation to leverage the strengths of both approaches [3]
- Standardized Evaluation Frameworks: Establishing robust validation methodologies to assess clinical performance and safety across diverse patient populations

6. Conclusion

While the integration of LLMs and VLMs in generating radiology reports for ultrasound exams holds significant potential, these technologies currently serve best as adjuncts to, rather than replacements for, expert clinical interpretation. Ongoing research and development are required to overcome current limitations and fully realize the benefits of these advanced AI systems in radiology.

The ideal implementation would combine the efficiency and standardization benefits of AI with the clinical expertise and judgment of radiologists to enhance both workflow and patient care.

References

1. Akinci D'Antonoli, T., Stanzione, A., Bluethgen, C., et al. (2024). Large language models in radiology: fundamentals, applications, ethical considerations, risks, and future directions. Diagnostic and Interventional Radiology, 30(2), 80-90. https://doi.org/10.4274/dir.2023.232417
2. Bhayana, R. (2024). Chatbots and large language models in radiology: A practical primer for clinical and research applications. Radiology. Advance online publication. https://doi.org/10.1148/radiol.232756
3. Li, X., Li, L., Jiang, Y., et al. (2025). Vision-language models in medical image analysis: From simple fusion to general large models. Information Fusion, 118, 102995. https://doi.org/10.1016/j.inffus.2025.102995
4. Keshavarz, P., Bagherieh, S., Nabipoorashrafi, S. A., et al. (2024). ChatGPT in radiology: A systematic review of performance, pitfalls, and future perspectives. Diagnostic and Interventional Imaging, 105(7-8), 251-265.
5. Zhang, S., Xu, Y., Usuyama, N., et al. (2025). A multimodal biomedical foundation model trained from fifteen million image–text pairs. NEJM AI, 2(1). https://doi.org/10.1056/AIoa2400640
6. Brin, D., Sorin, V., Barash, Y., et al. (2025). Assessing GPT-4 multimodal performance in radiological image analysis. European Radiology, 35, 1959–1965. https://doi.org/10.1007/s00330-024-11035-5
7. Maani, F., Saeed, N., Saleem, T., et al. (2025). FetalCLIP: A visual-language foundation model for fetal ultrasound image analysis. arXiv. https://doi.org/10.48550/arXiv.2502.14807
8. Christensen, M., Vukadinovic, M., Yuan, N., et al. (2024). Vision-language foundation model for echocardiogram interpretation. Nature Medicine, 30, 1481-1488. https://doi.org/10.1038/s41591-024-02959-y
9. Serapio, A., Chaudhari, G., Savage, C., et al. (2024). An open-source fine-tuned large language model for radiological impression generation: A multi-reader performance study. BMC Medical Imaging, 24, 254. https://doi.org/10.1186/s12880-024-01435-w
10. Gu, K., Lee, J. H., Shin, J., et al. (2024). Using GPT-4 for LI-RADS feature extraction and categorization with multilingual free-text reports. Liver International, 44(7), 1578-1587. https://doi.org/10.1111/liv.15891
11. Hong, E. K., Ham, J., Roh, B., et al. (2025). Diagnostic accuracy and clinical value of a domain-specific multimodal generative AI model for chest radiograph report generation. Radiology. Advance online publication. https://doi.org/10.1148/radiol.241476

LD03-S1

16:40-17:15 GBR 103

Chairperson(s): Kyung Sook Shin *(Chungnam National University Hospital, Korea)*

Liver Fat Measurement

Dong Wook Kim
Department of Radiology, Asan Medical Center, Korea

1. Introduction

Fatty liver disease—particularly metabolic dysfunction–associated steatotic liver disease (MASLD)—has emerged as a significant global health concern, with an estimated prevalence ranging from 25% to 50%. MASLD is strongly associated with diabetes, obesity, hyperlipidemia, and metabolic syndrome, and markedly increases the risk of progression to steatohepatitis and hepatic fibrosis.

Accurate assessment of hepatic steatosis is essential for diagnosis, disease monitoring, and evaluating treatment response. This lecture provides a comprehensive overview of current imaging modalities for the quantification of hepatic fat content.

2. Ultrasound-based Assessment of Hepatic Steatosis

(1) Conventional Grayscale Ultrasonography

Conventional ultrasonography remains the most commonly used screening tool for fatty liver disease due to its accessibility and low cost. Hepatic steatosis typically appears as increased echogenicity ("bright liver") owing to enhanced reflection and attenuation of ultrasound waves by ifat vacuoles.

A standard grading system evaluates steatosis based on comparisons of hepatic echogenicity with the renal cortex, visualization of portal vein walls, and clarity of the diaphragm. Despite its utility as a screening method, conventional US has notable limitations, including operator dependency, poor sensitivity for detecting mild steatosis, and subjective grading, which is inadequate for longitudinal follow-up (1).

The hepatorenal index (HRI) is a semiquantitative B-mode imaging biomarker for hepatic steatosis, calculated as the ratio of hepatic to renal cortical signal intensity at the same depth (2). Using a threshold of 1.22, the HRI has shown a sensitivity of 76.4% and specificity of 93.2%, suggesting potential clinical value. However, its accuracy may be influenced by hepatic fibrosis or concurrent renal pathology.

(2) Quantitative US Methods

Several quantitative ultrasound techniques have been developed to overcome the limitations of conventional US:

- Controlled Attenuation Parameter (CAP; Echosens):
  Implemented with transient elastography (FibroScan), CAP quantifies ultrasound attenuation at 3.5 MHz and provides values in dB/m that correlate with hepatic fat content. CAP has demonstrated good diagnostic performance, with reported AUC values ranging from 0.70 to 0.90 (3).
- Attenuation Imaging (Canon Medical Systems):
  This 2D imaging technique quantifies ultrasound energy loss (in dB/cm/MHz) and displays attenuation values as a color-coded map over a large region of interest. It shows strong correlation with MRI-PDFF (r = 0.81–0.83), outperforming CAP (r = 0.58–0.65) in some studies (4).

- Attenuation Measurement (ATT; Fujifilm Healthcare):
  ATT employs dual-frequency ultrasound waves transmitted along the same beam path and estimates attenuation from the slope of the signal ratio (F0/F1). Studies have reported excellent interobserver agreement (ICC = 0.91) and moderate-to-high diagnostic accuracy, with AUC values of 0.79, 0.87, and 0.96 for detecting steatosis grades >1, >2, and >3, respectively (5).
- US-guided Attenuation Parameter (GE Healthcare):
  This method uses a reference phantom with known attenuation and backscatter properties to correct for system-specific beamforming characteristics.
- Quantitative US Fat Fraction (QUS-FF):
  This technique combines attenuation and backscatter information to estimate hepatic fat fraction as a percentage.
- Other techniques: attenuation estimation algorithm (Att PLUS; Hologic), tissue attenuation imaging (TAI; Samsung Medison)

3. CT-based Assessment of Hepatic Steatosis

CT quantifies hepatic fat content based on X-ray attenuation measured in Hounsfield units (HU), which decrease with increasing fat accumulation. Non-contrast CT enables direct quantification of hepatic fat, whereas contrast-enhanced CT is less reliable due to variable enhancement effects.

Although CT offers quantitative measurement and is widely accessible, its limitations include radiation exposure, low sensitivity for detecting mild steatosis, and limited utility for longitudinal follow-up.

Common CT-based indices for detecting hepatic steatosis include (6):

- CT_L: Liver attenuation (HU)
- CT_{L-S}: Difference between liver and spleen attenuation (HU)
- $CT_{L/S}$: Ratio of liver-to-spleen attenuation

One study reported a linear relationship between non-contrast CT liver attenuation and MRI-PDFF, expressed as (7):

$$PDFF\ (\%) = -58 \times CT\ (HU) + 38.2.$$

According to this model, a liver attenuation of 40 HU corresponds approximately to a 15% PDFF, consistent with moderate steatosis.

4. MRI-based Assessment of Hepatic Steatosis

MRI enables quantitative assessment of hepatic triglyceride content using confounder-corrected chemical shift–encoded (CSE) MRI and magnetic resonance spectroscopy (MRS). These techniques exploit the ~3.4 ppm chemical shift difference between water and triglyceride proton resonances (8).

The proton density fat fraction (PDFF), defined as PDFF = F / (W + F), quantifies the fraction of triglycerides relative to total fat and water signals. PDFF ranges from 0% to 100% and is strongly correlated with histologic fat content.

(1) MR Spectroscopy (MRS)

MRS separates fat and water peaks within a single-voxel spectrum, typically obtained during a single breath-hold (~20 seconds). PRESS and STEAM are the most commonly used sequences.

A single voxel is usually positioned in the right hepatic lobe to avoid vascular and biliary structures. While MRS provides accurate quantification, it suffers from limited sampling, akin to liver biopsy. Multivoxel MRS offers broader coverage but at the expense of longer scan times. Clinical adoption remains limited due to specialized technical requirements and lack of widespread software integration.

(2) Chemical Shift MRI

CSE MRI acquires gradient echo images at multiple echo times within a single repetition time. Images are reconstructed using a multipeak spectral model of fat and water, with correction for confounders such as T1 bias, T2* decay, and noise. Postprocessing approaches include magnitude-based, complex-based, and hybrid methods.

MRI-PDFF is highly reproducible across different scanners and institutions, making it a reliable imaging biomarker for steatosis. Although PDFF is

not identical to histologic fat percentage, it shows excellent correlation.

Whole-liver PDFF maps can be acquired in a single breath-hold (~15–20 seconds), enabling comprehensive and reproducible assessment for follow-up. Unlike CT or ultrasound, MRI-PDFF is not affected by iron deposition, making it the preferred noninvasive tool for accurate liver fat quantification.

5. Conclusion

A variety of imaging modalities are available for assessing hepatic steatosis, each with unique strengths and limitations. Conventional ultrasound is widely used for screening, while quantitative US provide improved objectivity. MRI-PDFF remains the most accurate and reproducible method for noninvasive fat quantification. Choosing the appropriate modality depends on clinical context, diagnostic needs, and resource availability.

References

1. Ozturk A, Kumar V, Pierce TT, Li Q, Baikpour M, Rosado-Mendez I, et al. The Future Is Beyond Bright: The Evolving Role of Quantitative US for Fatty Liver Disease. Radiology. 2023 Nov;309(2):e223146.
2. Johnson SI, Fort D, Shortt KJ, Therapondos G, Galliano GE, Nguyen T, et al. Ultrasound Stratification of Hepatic Steatosis Using Hepatorenal Index. Diagn Basel Switz. 2021 Aug 10;11(8):1443.
3. Eddowes PJ, Sasso M, Allison M, Tsochatzis E, Anstee QM, Sheridan D, et al. Accuracy of FibroScan Controlled Attenuation Parameter and Liver Stiffness Measurement in Assessing Steatosis and Fibrosis in Patients With Nonalcoholic Fatty Liver Disease. Gastroenterology. 2019 May;156(6):1717–30.
4. Lee DH, Cho EJ, Bae JS, Lee JY, Yu SJ, Kim H, et al. Accuracy of Two-Dimensional Shear Wave Elastography and Attenuation Imaging for Evaluation of Patients With Nonalcoholic Steatohepatitis. Clin Gastroenterol Hepatol Off Clin Pract J Am Gastroenterol Assoc. 2021 Apr;19(4):797-805.e7.
5. Tamaki N, Koizumi Y, Hirooka M, Yada N, Takada H, Nakashima O, et al. Novel quantitative assessment system of liver steatosis using a newly developed attenuation measurement method. Hepatol Res Off J Jpn Soc Hepatol. 2018 Sep;48(10):821–8.
6. Byun J, Lee SS, Sung YS, Shin Y, Yun J, Kim HS, et al. CT indices for the diagnosis of hepatic steatosis using non-enhanced CT images: development and validation of diagnostic cut-off values in a large cohort with pathological reference standard. Eur Radiol. 2019 Aug;29(8):4427–35.
7. Pickhardt PJ, Graffy PM, Reeder SB, Hernando D, Li K. Quantification of Liver Fat Content With Unenhanced MDCT: Phantom and Clinical Correlation With MRI Proton Density Fat Fraction. AJR Am J Roentgenol. 2018 Sep;211(3):W151–7.
8. Starekova J, Hernando D, Pickhardt PJ, Reeder SB. Quantification of Liver Fat Content with CT and MRI: State of the Art. Radiology. 2021 Nov;301(2):250–62.

LD03-S2

17:15-17:50 **GBR 103**

Chairperson(s): Kyung Sook Shin *(Chungnam National University Hospital, Korea)*

Liver Focal Lesion CEUS

Woo Kyoung Jeong
Department of Radiology, Samsung Medical Center, Korea

Contrast-enhanced ultrasonography (CEUS) is becoming an increasingly important tool in the diagnosis of focal lesions of the liver, including HCC. This workshop will focus on differentiating HCC from hemangiomas, focal nodular hyperplasia (FNH), and rare benign lesions frequently encountered in patients at risk for HCC. In particular, the CEUS LI-RADS classification scheme and the KSR-KSAR Sonazoid guidelines will be used to illustrate diagnostic criteria and approaches that can be used in practice.

In addition, we will cover in detail what to look out for when assessing washout in Sonazoid examinations, as well as common misleading imaging findings. Live demonstrations will allow you to see first-hand how images change after contrast injection, and troubleshooting for common problems during an exam, such as failed image acquisition or interpretation errors, will be covered.

This lecture is designed to provide practical help for physicians who are new to contrast-enhanced ultrasonography or want to get started. Case studies will be used to illustrate how CEUS can be utilized in the clinic, which patients it is appropriate for, and how it differs from CT and MRI. This lecture will provide you with a systematic understanding of CEUS, from concept to practical application, and give you the confidence to use it in your practice.

SS01 Scientific Session 1

09:30-10:50 **GBR 102**

Chairperson(s):
Bum Sang Cho *(Chungbuk National University Hospital, Korea)*
Seong Kuk Yoon *(Dong-A University Hospital, Korea)*

09:30-09:40 (SS01-P1)

Effect of Structured Pelvic Floor Muscle Training on Pelvic Floor Muscle Contraction and Treatment of Pelvic Organ Prolapse in Postpartum Women: Ultrasound and Clinical Evaluations

Hui Zhao
Department of Radiology, Shanghai Tenth People's Hospital, School of Medicine, Tongji University, China

BACKGROUND / AIM: The purpose of this study is to examine the impact of structured pelvic floor muscle training (PFMT) on pelvic f loor muscle (PFM) contraction and the treatment of pelvic organ prolapse (POP) in postpartum women.
METHODS: Sixty patients who volunteered for a PFMT assessment at 6–8 weeks after delivery were included in this retrospec tive analysis. For 5 weeks, all patients had structured PFMT, which included supervised daily pelvic muscle contractions, biofeedback therapy, and electrical stimulation. The main outcomes were POP stage assessed by POP quantification (POP Q), pelvic organ position and hiatus area (HA) assessed by transperineal ultrasound, PFM contraction assessed by Modified Oxford scale (MOS), surface electromyography (EMG), and sensation of PFM graded using visual analog scale (VAS).
RESULTS: Structured PFMT was associated with better POP-Q scores in Aa, Ba, C, and D (p values were 0.01, 0.001, 0.017, and 0.001 separately). The bladder neck at rest and maximum Valsalva, the cervix position and HA at maximum Valsalva in transperineal ultrasound were significantly better than before (p values were 0.031, < 0.001, 0.043, and < 0.001 separately). PFM contraction assessed by MOS, EMG, and PFM VAS score were significantly improved (all p values were < 0.001). However, no significant improvement was observed in POP-Q stage.
CONCLUSION: Structured PFMT can increase PFM function in postpartum women but cannot modify the POP-Q stage. Trans perineal ultrasonography is a useful method for evaluating therapy efficacy objectively. More randomized controlled trials are needed before definitive conclusions can be drawn about the effect of structured PFMT on POP in postpartum women.

09:40-09:50 (SS01-P2)

Ultrasound Localization Microscopy: Optimization of Renal Cortical Examination Strategies and Diagnosis of Chronic Kidney Disease

Hong Han[1], Beiqi Chen[1], Yi Fang[3], Qi Zhang[2], Cuixian Li[1], Hong Liu[3], Beijian Huang[2], Huixiong Xu[1]
[1]Department of Radiology, Zhongshan Hospital Fudan University, China, [2]Department of Radiology, Institute of Ultrasound in Medicine and Engineering, China, [3]Department of Nephrology, Zhongshan Hospital, Fudan University, China

BACKGROUND / AIM: This study aimed to evaluate the imaging capabilities of ultrasound localization microscopy (ULM) for assessing renal cortical blood flow under various conditions and assess its utility in chronic kidney disease (CKD).
METHODS: This prospective study enrolled 128 participants from January to August 2024, categorized into normal renal function and CKD groups. Contrast-enhanced ULM was performed on 73 participants with normal renal function to determine optimal imaging conditions, followed by 55 CKD participants. Correlations between microvascular density (MVD), clinical indicators, CKD staging, and renal biopsy findings were evaluated.
RESULTS: MVD values were significantly lower at detection depths >50 mm compared to ≤50 mm (93.42±5.68 vs. 97.77±2.01, 97.39±2.50, and 98.09±2.19, p=0.011). No significant differences were observed across cortical thickness or contrast agent dosage groups. MVD remained consistent

within the 3-minute detection window, showing high reliability. In CKD participants, mean renal cortical MVD was 86.78±7.18, with lower values in advanced CKD stages. MVD was negatively correlated with the percentage of sclerosed glomeruli (r = -0.559) and vascular lesions, with lower MVD linked to advanced CKD and increased sclerosis.

CONCLUSION: ULM effectively quantifies renal cortical MVD, providing valuable insights into renal blood flow. MVD was significantly lower in CKD participants and correlated with clinical and pathological indicators, highlighting ULM's potential as a diagnostic tool for assessing microvascular damage in CKD.

09:50-10:00 (SS01-P3)

Ultrasound-Guided Microwave Ablation for Symptomatic Abdominal Wall Endometriosis

Jiaxin Li

Department of Radiology, Shanghai Tenth People's Hospital, China

BACKGROUND / AIM: To explore the feasibility of US-guided MWA for symptomatic AWE, the efficacy and safety were both evaluated in this study and treatment response evaluation.

METHODS: Three consecutive patients who underwent US-guided MWA for AWE with typical symptoms were included in the retrospective study. US, magnetic resonance imaging (MRI), laboratory tests, and US-guided core-needle biopsy were conducted for pre-treatment assessment and ruling out malignancy. The interventional procedure was carried out under local anesthesia with the microwave system and the output power was 60w. Post-treatment contrast-enhanced ultrasound (CEUS) was performed to evaluate the instant treatment response. The follow-up intervals were 1 month, 6 months, and 12 months after treatment. The clinical symptoms and conditions of AWE lesions were recorded in each follow-up.

RESULTS: The MWA procedure was completed in all the patients with no blood perfusion inside each lesion by instant CEUS after treatment. The mean ablation time was 687 seconds (s) for a single patient (ranging from 660s to 742s). Clinical symptoms were relieved evidently at the end of the follow-up. The pain according to the visual analogue scale (VAS) decreased from 4–6 before treatment to 0–2 after treatment. Mild to moderate complications included slight abdominal pain and fat liquefaction. Regarding technical outcomes, the volume of all six lesions reduced to different degrees at the end of follow-up (ranging: from 16.6% to 100%).

CONCLUSION: US-guided MWA may be a feasible and promising approach for symptomatic AWE.

10:00-10:10 (SS01-P4)

Contrast-Enhanced Ultrasound of Renal Transplant in Recipients With Acute Vascular Rejection

Natalia Vetsheva[1], Svetlana Larionova[2], Natalya Belavina[3], Ella Penyaeva[4], Natalya Klochkova[3], Ekaterina Stolyarevich[3], Elena Parabina[2], Regina Balter[2]

[1]Department of Radiology, FSBEI FPE RMACPE MON, Russia, [2]Department of Radiology, Samara State Medical University, Russia, [3]Department of Internal Medicine-Nephrology, Moscow City Hospital 52, Russia, [4]Department of Radiology, MONIKI, Russia

Kidney transplantation is the optimal method of renal replacement therapy. Nephrobiopsy is the gold standard of acute and chronic allograft rejection diagnostics, but it's an invasive procedure and can cause some complications. Acute vascular rejection (AVR) is characterized by intimal and transmural endarteritis and can be attributed to cellular and/or humoral immunity. Contrast-enhanced ultrasound (CEUS) is a non-invasive imaging modality that allows visualizing of renal transplant (RT) perfusion. To compare the parameters of CEUS in recipients without dysfunction and with dysfunction due to AVR.

MATERIALS AND METHODS: 20 recipients were included: 7 – with signs of AVR in nephrobiopsy (1gr), 13 – without dysfunction and rejection by protocol biopsy (2 gr, control). All patients underwent CEUS. 8 perfusion quantitative Time Intensity Curve parameters (TIC-parameters) were analyzed (PI (Peak Intensity), AUC (Area

Under Curve), WiAUC (Wash-in AUC), WiAUC/RT (Perfusion Index), WoAUC (Wash-out AUC), RT (Wash-in-Time), AS (Ascending Slope), DS (Descending Slope)) in 3 Regions of Interest (ROI). ROI1 – in the outer part of cortex, ROI2 – in the medullar part of cortex, ROI3 – in the medulla (pyramids).

RESULTS: The groups (1gr vs. 2 gr) differed by age (44 [24;56] vs. 38 [35;42], p=0.380), gender (female 2 (28%) vs. 10 (77%), p=0.104), plasma creatinine (350 [250;980] vs. 90 [68;104] mcmol/l, p=0.0003), period between transplantation and CEUS (7 [4;14] vs. 39 [25;50] mo, p=0.004). Some of the TIC-parameters in ROI1 showed a significant difference: AUC (5979 [4871;7288] vs. 7099 [6398;8307], p=0.205), WiAUC (258 [214;293] vs. 268 [252;326], p=0.303), WiAUC/RT (27.4 [26.0;31.1] vs. 31.3 [28.9;33.2], p=0.036) WoAUC (5381 [4668;7030] vs. 6806 [6509;7827], p=0.178). The patients of the control group demonstrated normal perfusion imaging. The subcapsular areas of hypoperfusion were found in 4 recipients of 2 gr.

CONCLUSIONS: CEUS is valuable for diagnosis of RT dysfunction due to AVR.

10:10-10:20 (SS01-P5)

Clinical Value of Multi-Modal Ultrasound Data of Brain-Dead Donor Kidneys in Predicting Early Post-Transplant Graft Function Recovery

Bei Wang, Jia Jing, Yixuan Wang, Zhe Yang, Jun Fan

Department of Radiology, The First Affiliated Hospital of Shandong First Medical University &Shandong Provincial Qianfoshan Hospital, China

BACKGROUND / AIM: The aim of this study was to quantify renal multidimensional functional indicators in braindead donors using SWE CEUS, and establish an accurate, noninvasive, and convenient index for predicting slow graft function (SGF) post-transplantation.

METHODS: Brain-dead donors undergoing organ donation at our hospital were prospectively enrolled. Two-dimensional ultrasound, CDFI,SWE,and CEUS were used to quantify multiple parameters of the donor kidneys, including internal echogenicity, blood perfusion, and corticomedullary stiffness. Ultrasound examinations of the brain-dead donor kidneys were performed within 48 hours prior to the surgery. Based on previous studies, slow graft function (SGF) was defined as a serum creatinine decrease less than 20% within 24 hours post-transplantation, and immediate graft function (IGF) was defined as a serum creatinine decrease greater than 20%. The area under the receiver operating characteristic curve (AUC) was used to evaluate diagnostic performance.

RESULTS: A total of 40 pre-transplant kidney ultrasound datasets were included in this study, comprising 19 SGF and 21 IGF. Compared with the IGF group, the SGF group showed statistically significant differences in interlobular artery peak systolic velocity (PSV), interlobular artery resistive index (RI), segmental artery PSV, medullary transit time (MTT), peak enhancement (PE), AUC of the corticomedullary time-intensity curve and washout area,the ratio of medullary downslope to upslope (SR) ($P < 0.05$). The medullary WOUAC was significantly lower in the SGF group than in the IGF group ($P < 0.01$). Multivariate logistic regression shows segmental artery PSV and medullary WOUAC as independent risk factors for SGF. The AUC for segmental artery PSV and medullary WOUAC in diagnosing SGF was 0.859 and 0.844 respectively. The AUC for the combined model was 0.937, with a sensitivity of 0.875 and a specificity of 0.857.

CONCLUSION: Pre-transplant multi-modal ultrasound data of the donor kidney can help to predict early post-transplant kidney function non-invasively sensitively and conveniently.

YIA Young Investigator Award 2025 Session

09:30-10:50 **Room 209**

Chairperson(s):
Boo-Kyung Han *(Samsung Medical Center, Korea)*
Woo Kyoung Jeong *(Samsung Medical Center, Korea)*

09:30-09:40 (YIA-P1)

Development of a Simplified Prediction Model for Diagnosing Progressive Central Precocious Puberty Using Clinical and Pelvic Ultrasound Parameters

Yeseul Kang[1], Kyungechul Song[3], Eunju Lee[2], Hye Sun Lee[2], Hana Lee[3], Hyun Wook Chae[3], Hyun Joo Shin[1]
[1]Department of Radiology, Yongin Severance Hospital, Korea, [2]Yonsei University College of Medicine, Korea, [3]Department of Pediatrics, Gangnam Severance Hospital, Korea

BACKGROUND / AIM: This study aimed to explore the predictive value of clinical and pelvic ultrasound parameters for diagnosing central precocious puberty (CPP) and to establish a clinically useful simplified prediction model to differentiate progressive CPP (P-CP) from nonprogressive precocious puberty (N-PP).
METHODS: Girls aged <9 years with secondary sexual development who underwent a gonadotropin-releasing hormone stimulation test and pelvic ultrasound between September 2020 and November 2023 were retrospectively included and divided into the P-CP and N-PP groups. Logistic regression analysis was used to determine the significant parameters and develop prediction models. The diagnostic performance of the models was compared using the area under the receiver operating characteristic curve (AUC) analysis and the Delong method. The continuous net reclassification improvement (cNRI) and absolute integrated discrimination improvement (IDI) were used to determine the additive effects of ultrasound parameters. A nomogram scoring system was constructed based on a simplified model to predict the probability of developing P-CP.
RESULTS: A total of 109 girls were included, with 64 (58.7%) in the P-CP group. Age, bone age, height, height minus midparental height, basal luteinizing hormone (LH), follicle-stimulating hormone, estradiol, insulin-like growth factor-I, Tanner stage, and cervical and fundus width were significant parameters for the diagnosis of P-CP. The models with ultrasound parameters yielded significantly higher cNRI and IDI values than the models without ultrasound parameters. The simplified model was composed of basal LH, estradiol, and fundus width that showed an AUC value of 0.93 (95% confidence interval: 0.88– 0.98) with a cutoff value of 16.
CONCLUSION: In conclusion, adding pelvic ultrasound parameters to traditional clinical results has an additive effect on P-CP screening. A simplified predictive model is effective for CPP screening in real-world clinics. These findings highlight the potential of the prediction model to overcome the limitations of the classical diagnostic approach for CPP in children.

09:40-09:50 (YIA-P2)

Echocardiographic Evaluation of LV Parameters and Insulin Resistance in Non-Diabetic STEMI Patients

Javad Alizargar
Department of Radiology, NTUNHS, Chinese Taipei

BACKGROUND / AIM: Previous research has established the Triglyceride Glucose (TyG) index as an indicator of insulin resistance (IR) with connections to cardiovascular risk factors. This study aims to provide novel insights into how TyG index-based IR is related to left ventricular (LV) parameters within a large sample size dataset. Furthermore, it seeks to examine the potential impact of TyG index-based IR on mortality in individuals experiencing acute ST-segment elevation myocardial infarction (STEMI) without diabetes.
METHODS: This study analyzed data from 23,780 myocardial infarction patients in the UK Biobank. Separate linear regression analyses were conducted to explore the associations between the insulin resistance index and LV parameters in non-diabetic

individuals, while controlling forage, BMI and gender.

RESULTS: Among the analyzed patients, 19,901 (84.31%) were non-diabetic. Of these, 962 underwent echocardiography, with the following mean ± SD parameters: LV ejection fraction (51.96 ± 8.18), LV end diastolic volume (156.02 ± 55.06), LV end systolic volume (77.03 ± 41.99), LV stroke volume (78.97 ± 20.88), Cardiac output (4.58 ± 1.19), Cardiac index (2.36 ± 0.57). The mean TyG index in these patients was 8.83 ± 0.54. Linear regression analysis demonstrated significant associations between TyG index and LV ejection fraction, LV end diastolic volume, LV end systolic volume, LV stroke volume, Cardiac output, and Cardiac index (p-values<0.05). TyG was statisticly correlated with the days lived after the MI diagnosis (r=0.03, p0.01). However, TyG index was not found to be associated with mortality or survival in these patients.

CONCLUSION: In non-diabetic STEMI patients, the TyG index is associated with LV parameters but does not demonstrate a clear link to mortality, suggesting potential for cardiovascular assessment without survival prediction.

09:50-10:00 (YIA-P3)

Comparison of Integrated vs. Sequential AI-CAD in Breast US: A Prospective Pilot Study on Scan Time, Reproducibility, and Diagnostic Performance

Haejung Kim, Sanghee Kim, Myoung Kyoung Kim, Jeongmin Lee, Ji Soo Choi, Eun Sook Ko, Boo-Kyung Han, Eun Young Ko

Department of Radiology, Samsung Medical Center, Korea

BACKGROUND / AIM: This study aimed to compare the scan time, reproducibility, and diagnostic performance of two types of artificial intelligence-based computer-aided diagnosis (AI-CAD) systems for breast ultrasound (US).

METHODS: We enrolled 242 patients who visited the breast imaging center for US examination between January and February 2025. Breast US was performed using two types of real-time AI-CAD: integrated AI-CAD (for lesion detection and diagnosis) and sequential AI-CAD (for these tasks separately). Scan time was compared in 97 patients by performing two breast US examinations using each AI-CAD in the same patient, with the order randomized. Reproducibility of each AI-CAD was assessed and compared in another 145 patients (215 lesions) by applying both systems to the same lesion twice, separately. Diagnostic performance of two AI-CAD was compared in all 242 patients in terms of sensitivity, specificity, positive predictive value (PPV), negative predictive value (NPV), and accuracy.

RESULTS: The scan time was significantly longer for sequential AI-CAD compared to integrated AI-CAD ($p < 0.001$), regardless of scan order. Reproducibility was excellent for both (integrated: 0.809, sequential: 0.83). Integrated AI-CAD had higher reproducibility in malignant (0.918 vs. 0.762) and non-mass lesions (1.0 vs. 0.75), while sequential AI-CAD performed better in mass lesions (0.837 vs. 0.792). Integrated AI-CAD showed higher sensitivity (87.6% vs. 76.9%) but lower specificity (74.2% vs. 90.0%). Sequential AI-CAD showed higher positive predictive value (PPV) (83.3% vs. 68.8%), while integrated AI-CAD had higher negative predictive value (NPV) (90.2% vs. 85.7%). Accuracy was higher in sequential AI-CAD (84.8% vs. 79.5%). Both systems had lower accuracy in non-mass lesions, with no significant difference.

CONCLUSION: Sequential AI-CAD showed higher accuracy and specificity, while integrated AI-CAD had better sensitivity and shorter scan time. Both systems had high reproducibility, with integrated AI-CAD excelling in malignant and non-mass lesions, and sequential AI-CAD in mass lesions.

10:00-10:10 (YIA-P4)

Diagnostic Value of High-frequency Ultrasound in Unclarified Lesions at the End of Extremities

Haojie Yang

Department of Radiology, Tenth People's Hospital of Tongji University, China

BACKGROUND / AIM: Unlike other body parts, unclarified lesions at the end of extremities have unique challenges due to small size and interference. Traditional imaging methods struggle with low resolution. HFUS enhances resolution, offering potential diagnostic value.

METHODS: From January 2019 to October 2023, the clinical and HFUS data of patients with unclarified lesions at the end of extremities were retrospectively analyzed. Independently, the diagnosis was made using two diagnostic modes (mode A: only clinical information, mode B: clinical and HFUS information). The diagnostic performance of the two modes was evaluated across different classification methods.

RESULTS: For all lesions, the correct rate of mode B was higher than that of mode A (52.8% vs. 18.4%, P<0.001), and the indeterminate rate had decreased by 43.0%. For benign lesions (51.0% vs. 18.2%), subungual lesions (40.8% vs. 21.1%), non-subungual lesions (55.6% vs. 17.8%), and common cases (60.9% vs. 20.3%), the diagnostic correct rate of mode B was also higher than mode A (all P < 0.05). However, there was no significant difference in rare lesions (9.8% vs. 4.9%) and malignant lesions (62.9% vs. 19.4%) between two modes (both P > 0.05). Moreover, the indeterminate rate for all categories of lesions has significantly diminished. Otherwise, Mode B demonstrated strong performance for malignant lesions (85.7% vs. 42.9%, P < 0.001).

CONCLUSION: Adding HFUS can significantly improve the accuracy of diagnosing unclarified lesions at the end of extremities and reduce uncertainty, especially benign and common lesions. HFUS also has demonstrated better performance in screening for malignant lesions.

10:10-10:20 (YIA-P5)

Inconclusive Cytology Results of Fine-Needle Aspiration for Thyroid Nodules: The Gravity of Strict Guideline Implementation

Sangwoo Cho[1], Kyunghwa Han[2], Jung Hyun Yoon[2], Vivian Youngjean Park[2], Miribi Rho[2], Jiyoung Yoon[2], Jin Young Kwak[2]

[1]Yonsei University College of Medicine, Korea, [2]Department of Radiology, Yonsei University College of Medicine, Korea

BACKGROUND / AIM: We investigated whether strict compliance with the Korean Thyroid Imaging Reporting and Data System (K-TIRADS) biopsy indications reduces inconclusive results and evaluated other associated factors.

METHODS: This retrospective study included 2,440 nodules in 2,256 patients who underwent initial FNA for thyroid nodules from January to December 2022. Inconclusive specimens were defined as Bethesda category I or III. FNA not-indicated nodules were those smaller than the K-TIRADS biopsy threshold. Patient age and gender, ultrasound features, nodule size, number of needle passes, and operator experience were selected as clinical factors. Univariate and multivariate analyses were conducted to evaluate associations between clinical factors and inconclusive results. The Chi-square and Mann-Whitney U tests were performed to analyze associations between clinical factors.

RESULTS: FNA not-indicated nodules were significantly associated with inconclusive biopsy results, along with subcentimeter nodule size, less than 1 year of operator experience, older age, and K-TIRADS 4 (P<0.001, P=0.015, P=0.004, P<0.001, and P<0.001, respectively). Nodules of 0 to 5 mm showed significant association with inconclusive biopsy results (P=0.006). Two or more FNA needle passes were associated with smaller nodule size, operators with less than 1 year, and K-TIRADS 4 (P=0.01, P=0.023, and P=0.001, respectively). Among K-TIRADS 4 nodules, suspicious US characteristics were associated with malignant biopsy results, and showed negative association with inconclusive biopsy results (P=0.03 and P=0.004, respectively).

CONCLUSION: FNA not-indicated nodules, 0 to

5 mm size, less than 1 year of operator experience, older age, and K-TIRADS 4 were associated with inconclusive biopsy results. Strictly following the biopsy indications in K-TIRADS can reduce inconclusive results.

10:20-10:30 (YIA-P6)

Effect of Structured Pelvic Floor Muscle Training on Pelvic Floor Muscle Contraction and Treatment of Pelvic Organ Prolapse in Postpartum Women: Ultrasound and Clinical Evaluations

Hui Zhao
Department of Radiology, Shanghai Tenth People's Hospital, School of Medicine, Tongji University, China

BACKGROUND / AIM: The purpose of this study is to examine the impact of structured pelvic floor muscle training (PFMT) on pelvic f loor muscle (PFM) contraction and the treatment of pelvic organ prolapse (POP) in postpartum women.
METHODS: Sixty patients who volunteered for a PFMT assessment at 6–8 weeks after delivery were included in this retrospec tive analysis. For 5 weeks, all patients had structured PFMT, which included supervised daily pelvic muscle contractions, biofeedback therapy, and electrical stimulation. The main outcomes were POP stage assessed by POP quantification (POP Q), pelvic organ position and hiatus area (HA) assessed by transperineal ultrasound, PFM contraction assessed by Modified Oxford scale (MOS), surface electromyography (EMG), and sensation of PFM graded using visual analog scale (VAS).
RESULTS: Structured PFMT was associated with better POP-Q scores in Aa, Ba, C, and D (p values were 0.01, 0.001, 0.017, and 0.001 separately). The bladder neck at rest and maximum Valsalva, the cervix position and HA at maximum Valsalva in transperineal ultrasound were significantly better than before (p values were 0.031, < 0.001, 0.043, and < 0.001 separately). PFM contraction assessed by MOS, EMG, and PFM VAS score were significantly improved (all p values were < 0.001). However, no significant improvement was observed in POP-Q stage.
CONCLUSION: Structured PFMT can increase PFM function in postpartum women but cannot modify the POP-Q stage. Trans perineal ultrasonography is a useful method for evaluating therapy efficacy objectively. More randomized controlled trials are needed before definitive conclusions can be drawn about the effect of structured PFMT on POP in postpartum women.

HI01	Hot Issue 1
14:10-15:30	GBR 103

Chairperson(s):
Jae Young Lee *(Seoul National University Hospital, Korea)*
Jeong Eun Lee *(Chungnam National University Hospital, Korea)*

14:30-14:40 (HI01-P1)

Ultrasound-Based Fat Fraction for Detection of Hepatic Steatosis and Quantification of Liver Fat Content Using Liver Biopsy as the Reference Standard: A Prospective Study

Huixiong Xu
Zhongshan Hospital Fudan University, China

BACKGROUND / AIM: To evaluate the agreement between quantitative US fat fraction (USFF) and proton magnetic resonance spectroscopy (1H-MRS) and the diagnostic value of USFF in assessing metabolic associated fatty liver disease (MAFLD).
METHODS: In this study, participants with suspected MASLD were prospectively recruited from August 2022 to November 2023. TAI, TSI and USFF were measured. Participants were randomly divided into test set and validation set according to 8:2. Spearman correlation analysis and Bland-Altman analysis were used to evaluate the correlation and consistency of TAI, TSI and USFF with hepatic steatosis. The diagnostic value of these parameters for detecting hepatic steatosis was evaluated by receiver operating characteristic (ROC) curves.
RESULTS: A total of 264 participants were enrolled, including 227 with biopsy confirmed MASLD (hepatic

steatosis ≥5%) and 37 with normal liver biopsy results (hepatic steatosis < 5%). Compared with TAI and TSI, USFF had a better positive correlation with hepatic steatosis grade (rUSFF =0.62, rTAI =0.57, rTSI =0.56; all P<0.001). In the test set, USFF had excellent diagnostic performance for different hepatic steatosis, with an AUC of 0.77-0.97, which was superior to TAI (AUC 0.73-0.95) and TSI (AUC 0.76-0.94). The cutoff values of USFF for detecting mild, moderate and severe hepatic steatosis were 5.37%, 15.79% and 17.30%. In the validation set, USFF also had a good diagnostic performance of hepatic steatosis, with a sensitivity from 85.71% to 100%.

CONCLUSION: USFF has a good correlation with hepatic steatosis and can be an excellent quantitative diagnostic tool for hepatic steatosis in MASLD.

14:40-14:50 (HI01-P2)

The Value of Ultrasound Fat Fraction as Compared to Controlled Attenuation Parameter for the Severity of Liver Steatosis Assessment

Ioan Sporea, Camelia Nica, Alina Popescu, Raluca Lupusoru, Maria Stan, Daiana Boleac, Renata Bende, Roxana Sirli

Department of Internal Medicine-G-I/Hepatology, Victor Babes University of Medicine and Pharmacy Timisoara, Romania

BACKGROUND / AIM: Liver steatosis is a growing global health concern with significant medical and economic implications. This study aimed to evaluate USFF (ultrasound fat fraction) for steatosis assessment as compared to controlled attenuation parameter (CAP).

METHODS: A prospective study was conducted in which liver steatosis was assessed in the same session by QUS (Samsung Medison RS85, CA1-7S probe) and CAP (FibroScan Compact M 530, M/XL probes) in a cohort of 145 patients with mixed etiologies. For QUS, five consecutive measurements of TAI and TSI were acquired by a color-coded map overlaid on B-mode ultrasound, then fat fraction (%) was automatically calculated and displayed in the report. The CAP cut-off values for S1, S2 and S3 were 248, 268 and 280 dB/m. ROC analysis was done to identify the best cut-off values for USFF for each steatosis stages. The correlations were assessed using Pearson correlation coefficient.

RESULTS: From the 145 patients, 55% were men, 57% had at least moderate steatosis, with a mean age of 51.2±16.9 years. Moderate correlations were observed between TSI vs. CAP r=0.65, p<0.0001, TAI vs. CAP r=0.84, p<0.0001 and TSI vs. TAI r=0.68, p<0.0001, with good performance in diagnosing liver steatosis (TSI AUROC= 0.82, p<0.0001 and TAI AUROC=0.81, p< 0.0001). A very good correlation between USFF and CAP was also found, r=0.82, p<0.001. The best USFF cut-off value to identify at least mild steatosis in all patients was >5.3% with very good performance (AUROC=0.93, p<0.0001, Se=92,77%, Sp=79,03%), for moderate steatosis the cut-off value was >6.6% (AUROC=0.93, p<0.0001, Se=89.19%, Sp=83.10%) and for severe steatosis, a cut-off of >7.9% (AUROC=0.91, p<0.0001, Se=84.85%, Sp=82.28%).

CONCLUSION: USFF seems to be a promising tool for diagnosing liver steatosis, with a very good performance, ready to be used in daily practice.

15:10-15:20 (HI01-P3)

Ultrasound-Guided Attenuation Parameter (UGAP) for Diagnosing Metabolic Dysfunction-Associated Steatotic Liver Disease

Yi Dong, Yunlin Huang, Ying Wang, Juan Cheng, Li Wei, Xiuyun Lu, Rui Cheng

Department of Radiology, Xinhua Hospital Affiliated to Shanghai Jiao Tong University School of Medicine, China

BACKGROUND / AIM: To evaluate the performance of ultrasound-guided attenuation parameter (UGAP) for diagnosing and grading hepatic steatosis in patients with metabolic dysfunction-associated steatotic liver disease (MASLD) using magnetic resonance imaging proton density fat fraction (MRI-PDFF) as the reference.

METHODS: Patients with hepatic steatosis were enrolled in this prospective study and underwent UGAP measurements. Taking MRI-PDFF ≥ 5%, ≥ 15%, and ≥ 25% as the reference for diagnosing steatosis grade ≥ S1, ≥ S2, and S3, respectively.

Spearman correlation and area under the receiver operating characteristic curves (AUCs) were performed.

RESULTS: From July 2023 to June 2024, 88 patients (median age: 40 years, interquartile range [IQR]: 36 – 46]; 54.5% [48/88] men and 45.5% [40/88] women) were included; 22.7% (20/88), 50.0% (44/88), 21.6% (19/88), and 5.7% (5/88) of patients had S0, S1, S2, and S3, respectively. The successful rate of UGAP measurements was 100%. The median UGAP value was 0.74 dB/cm/MHz (IQR: 0.65 – 0.82). UGAP values were positively correlated with MRI-PDFF ($r = 0.77$, $P < 0.001$). The AUCs of UGAP for diagnosing steatosis grade ≥ S1, ≥ S2, and S3 were 0.91, 0.90, and 0.88, respectively. In the subgroup, 98.4% (60/61) of patients had valid controlled attenuation parameter (CAP) values. UGAP values were positively correlated with CAP values ($r = 0.65$, $P < 0.001$).

CONCLUSION: UGAP has the potential to detect hepatic steatosis and could be an alternative in clinical practice, especially when patients fail to obtain CAP values.

SS02 Scientific Session 2

14:10-15:30 **GBR 101**

Chairperson(s):
Eun Young Chae *(Asan Medical Center, Korea)*
Hye Jung Kim *(Kyungpook National University Chilgok Hospital, Korea)*

14:10-14:20 (SS02-P1)

Comparison of Integrated vs. Sequential AI-CAD in Breast US: A Prospective Pilot Study on Scan Time, Reproducibility, and Diagnostic Performance

Haejung Kim, Sanghee Kim, Myoung Kyoung Kim, Jeongmin Lee, Ji Soo Choi, Eun Sook Ko, Boo-Kyung Han, Eun Young Ko
Department of Radiology, Samsung Medical Center, Korea

BACKGROUND / AIM: This study aimed to compare the scan time, reproducibility, and diagnostic performance of two types of artificial intelligence-based computer-aided diagnosis (AI-CAD) systems for breast ultrasound (US).

METHODS: We enrolled 242 patients who visited the breast imaging center for US examination between January and February 2025. Breast US was performed using two types of real-time AI-CAD: integrated AI-CAD (for lesion detection and diagnosis) and sequential AI-CAD (for these tasks separately). Scan time was compared in 97 patients by performing two breast US examinations using each AI-CAD in the same patient, with the order randomized. Reproducibility of each AI-CAD was assessed and compared in another 145 patients (215 lesions) by applying both systems to the same lesion twice, separately. Diagnostic performance of two AI-CAD was compared in all 242 patients in terms of sensitivity, specificity, positive predictive value (PPV), negative predictive value (NPV), and accuracy.

RESULTS: The scan time was significantly longer for sequential AI-CAD compared to integrated AI-CAD ($p < 0.001$), regardless of scan order. Reproducibility was excellent for both (integrated:

0.809, sequential: 0.83). Integrated AI-CAD had higher reproducibility in malignant (0.918 vs. 0.762) and non-mass lesions (1.0 vs. 0.75), while sequential AI-CAD performed better in mass lesions (0.837 vs. 0.792). Integrated AI-CAD showed higher sensitivity (87.6% vs. 76.9%) but lower specificity (74.2% vs. 90.0%). Sequential AI-CAD showed higher positive predictive value (PPV) (83.3% vs. 68.8%), while integrated AI-CAD had higher negative predictive value (NPV) (90.2% vs. 85.7%). Accuracy was higher in sequential AI-CAD (84.8% vs. 79.5%). Both systems had lower accuracy in non-mass lesions, with no significant difference.

CONCLUSION: Sequential AI-CAD showed higher accuracy and specificity, while integrated AI-CAD had better sensitivity and shorter scan time. Both systems had high reproducibility, with integrated AI-CAD excelling in malignant and non-mass lesions, and sequential AI-CAD in mass lesions.

14:20-14:30 (SS02-P2)

A Preliminary Study of Non-invasive Prediction of Breast Cancer Molecular Markers Using Deep Learning-Based Molecular Markers Prediction Network on Automated Breast Volume Scanner Images

Lixia Yan[1], Xinmeng Shen[2], Peilei Wang[1], Xi Wang[1], Hansheng Xia[1], Huixiong Xu[1], Yu Ma[2], Beijian Huang[1]

[1]Department of Radiology, Zhongshan Hospital, Fudan University, China, [2]School of Information Science and Technology, Fudan University, China

BACKGROUND / AIM: To develop a deep learning model based on Automated Breast Volume Scanner (ABVS) images for non-invasive preoperative prediction of breast cancer molecular marker status.

METHODS: This retrospective study included 220 breast cancer patients who underwent surgery from January 2015 to December 2017, with 154 cases having complete molecular marker results. Inclusion criteria were age ≥18 years and ABVS examination within 3 weeks before surgery. Exclusion criteria included unclear masses, multiple lesions, borderline tumors, neoadjuvant chemotherapy, significant breast deformation, or lesions under the nipple. We proposed the Molecular Markers Prediction Network (MMPNet), based on an improved Inception model with a dual-branch structure: Branch 1 used Inception V3 to extract comprehensive image features; Branch 2 focused on texture features from tumor segmentation maps in axial, coronal, and sagittal planes. Training used stochastic gradient descent with binary cross-entropy loss. MMPNet was compared with LFRSNet and Modi-Inception using five-fold cross-validation.

RESULTS: Among 366 cases (146 benign, 220 breast cancer), 154 had complete molecular marker results: ER-positive (102), PR-positive (102), Ki-67 overexpression (76), and HER2-positive (53). MMPNet showed high accuracy: ER sensitivity 0.921, specificity 0.823, accuracy 0.915; PR sensitivity 0.921, specificity 0.863, accuracy 0.925; HER2 sensitivity 0.738, specificity 0.890, accuracy 0.844; Ki-67 sensitivity 0.619, specificity 0.601, accuracy 0.612. AUC values were superior to LFRSNet and Modi-Inception: ER (0.863 vs. 0.793 and 0.830), PR (0.885 vs. 0.760 and 0.824), HER2 (0.925 vs. 0.844 and 0.895), and Ki-67 (0.620 vs. 0.570 and 0.604).

CONCLUSION: MMPNet demonstrated high accuracy in predicting breast cancer molecular markers using ABVS images. It outperformed LFRSNet and Modi-Inception, showing potential for non-invasive preoperative prediction and clinical support.

14:30-14:40 (SS02-P3)

Intra-observer and Inter-observer Agreement in Glandular Tissue Component Assessment Using Automated Breast Ultrasound

Haejung Kim, Sanghee Kim, Myoung Kyoung Kim, Jeongmin Lee, Ji Soo Choi, Eun Sook Ko, Boo-Kyung Han, Eun Young Ko

Department of Radiology, Samsung Medical Center, Korea

BACKGROUND / AIM: To evaluate the intra- and inter-observer agreement in the assessment of the glandular tissue component (GTC) using automated breast ultrasound (ABUS).

METHODS: From January to February 2025, we prospectively enrolled 356 patients who underwent

ABUS for screening at our institution. Mammography at the time of ABUS was present in 257 patients. GTC was assessed under two conditions: GTC1 was evaluated solely based on ABUS images, and GTC2 was re-assessed with reference to mammography findings (if available). One of seven radiologists (reviewer 1) evaluated GTC1 and 2, and one of two designated reviewers (reviewer 2) who did not participate as reviewer 1 re-evaluated GTC1 and 2 on the same ABUS images. Intra- and inter-observer agreement for GTC assessment was analyzed using Cohen's kappa statistics, and the variability of GTC agreement was analyzed based on background echotexture (BE) and mammographic density.

RESULTS: The overall intra-observer agreement for GTC assessment was excellent (κ = 0.88 ~ 0.90). However, the intra-observer agreement was lower in fatty breasts than in dense breasts for both reviewers (κ = 0.73 vs. 0.94 and κ = 0.72 vs. 0.92), with a tendency for higher GTC to be reassessed as lower GTC when mammographic density was referenced. The overall inter-observer agreement for GTC was moderate (κ = 0.45 ~ 0.49), higher than that for BE (κ = 0.36) but lower than that for mammographic density agreement (κ = 0.70). The inter-observer agreement was lowest in homogeneous-fat BE (κ = -0.27 ~ -0.26) and highest in homogeneous-fibroglandular BE (κ = 0.45 ~ 0.51). Inter-observer agreement was lower in fatty breasts than dense breasts (κ = 0.30 ~ 0.38 vs. κ = 0.44 ~ 0.45).

CONCLUSION: Intra-observer agreement GTC assessment was excellent in ABUS, however, considering mammography is recommended in fatty breasts. Inter-observer variability was considerable, with moderate agreement between the readers.

14:40-14:50 (SS02-P4)

Evaluating Clinico-Pathological Characteristics of Non-Massive Breast Cancer on Ultrasound

Yanwen Luo, Hansheng Xia, Boyang Zhou
Department of Radiology, Zhongshan Hospital, Fudan University, China

BACKGROUND / AIM: Non-mass breast lesions (NMLs) constitute a unique sonographic entity characterized by distinct molecular phenotype distributions compared to conventional breast masses. This study investigates the clinicopathological characteristics of malignant NMLs to enhance diagnostic recognition and facilitate early detection.

METHODS: In this retrospective single-center study, we analyzed 208 breast cancer patients with pathologically confirmed NMLs detected on ultrasound between 2015-2023. Comprehensive evaluations included demographic profiles, sonographic patterns, histopathological classifications, and immunohistochemical profiles. Comparative analyses were performed between younger (<40 years) and older (≥40 years) cohorts using descriptive statistics and χ^2 tests.

RESULTS: Among 208 patients with non-massive breast cancer, the median age was 54 years (range: 28-82 years). Notably, 33 patients (15.9%) presented with symptoms, including nipple discharge and palpable breast masses. Ultrasound revealed that the lesions were predominantly linear-segmental in distribution (57.7%). Invasive carcinoma constituted the majority of pathological types (60.58%), the carcinoma in situ (37.50%) was more common than in the general population. Luminal B subtype was most prevalent (49.04%, 102/208), whereas triple-negative breast cancer incidence (5.77%, 12/208) was notably lower than population baselines. Younger patients (12.5%, 26/208) exhibited distinct clinicopathological profiles: higher prevalence of invasive ductal carcinoma (84.62% vs. 57.14%, p=0.026), elevated Ki-67 indices (median 57.69% vs. 37.36%, p=0.048), and increased axillary lymph node metastasis rates (23.08% vs. 10.44%, p=0.064).

CONCLUSION: Malignant NMLs demonstrate heterogeneous pathological manifestations with significant age-related variations. Younger patients

(<40 years) display more aggressive biological behavior characterized by predominant invasive histology, heightened proliferative activity, and greater metastatic potential. These findings underscore the necessity for age-stratified diagnostic and management approaches in NML-associated breast malignancies.

SS03 Scientific Session 3

11:00-12:20 **GBR 101**

Chairperson(s):
Min Ju Kim *(Korea University Anam Hospital, Korea)*
Ijin Joo *(Seoul National University Hospital, Korea)*

11:00-11:10 (SS03-P1)

Utilization of High-Resolution Kupffer Phase Imaging and Contrast-Enhanced Superb Microvascular Imaging for Focal Liver Lesion Characterization

Jeongin Yoo, Jeong Min Lee, Hyo-Jin Kang, Jae Seok Bae
Department of Radiology, Seoul National University Hospital, Korea

BACKGROUND / AIM: The utility of high-resolution (HR) Kupffer phase imaging and contrast-enhanced (CE) superb microvascular imaging (SMI) for focal liver lesion (FLL) characterization was evaluated.
METHODS: This study prospectively enrolled 75 patients with chronic hepatitis B or liver cirrhosis who underwent contrast-enhanced ultrasound (CEUS) for focal solid liver lesions detected on contrast-enhanced CT or MRI between February 2023 and February 2024. Two board-certified radiologists assessed and scored edge sharpness of each FLL on both B-mode and HR Kupffer phase imaging using a 5-point scale (score 5, no blur; 3, moderate blur margin; 1, unreadable margin). Additionally, two radiologists assessed the amounts of intralesional blood flow and vascular patterns on both precontrast and CE SMI. Lesion edge sharpness was compared between B-mode and HR Kupffer phase imaging, and the amounts of intralesional blood flow were compared between precontrast and CE SMI using Wilcoxon test. Vascular patterns were compared between precontrast and CE SMI using Chi-squared test.
RESULTS: Both HR Kupffer phase imaging and CE SMI were technically successful in 75 (100.0%) and 74 (98.7%) patients, respectively. HR Kupffer phase imaging showed significantly higher liver edge sharpness scores, compared to B-mode imaging (median [IQR], 4 [1] vs. 3 [1], $p<0.001$). CE SMI showed significantly larger amount of blood flow, compared to precontrast SMI (media [IQR], 2 [1] vs. 1 [2], $p<0.001$). Furthermore, CE SMI demonstrated hypervascular patterns more frequently (55.4% [41/74]), whereas precontrast SMI frequently showed hypovascular patterns (85.1% [63/74]) ($p<0.001$).
CONCLUSION: HR Kupffer phase imaging and CE SMI are useful in focal liver lesion characterization, compared to B-mode imaging and precontrast SMI, respectively.

11:10-11:20 (SS03-P2)

Combining Heuristic Knowledge and Multi-Model Machine Learning for Sonazoid-Enhanced Ultrasound in Liver Tumor Differentiation

Naohisa Kamiyama[1], Katsutoshi Sugimoto[2], Keisuke Nakajima[2], Hiroshi Hashimoto[1], Takao Itoi[2]
[1]Department of Medical Engineering, GE HelthCare, Japan, [2]Department of Internal Medicine-G-I/ Hepatology, Tokyo Medical University, Japan

BACKGROUND / AIM: Sonazoid contrast-enhanced ultrasound (CEUS) provides valuable diagnostic information, but hepatic tumor enhancement patterns vary significantly. This study proposes a novel machine learning model integrating heuristic knowledge-based training data and multiple learning models to improve tumor differentiation. While the Kupffer phase aids malignant tumor diagnosis, it requires a 10-minute wait post-injection. We investigate the feasibility of accurate differentiation using only the first 2 minutes of imaging.
METHODS: We analyzed CEUS images from 232 patients who underwent CEUS for the diagnosis of hepatic tumors (benign: 61, HCC: 104, malignant

non-HCC (ML): 67). For each case, six images from injection to peak enhancement, and static images at 1 and 2 minutes post-injection, were used for training. Two models were developed: [Model 1]: Classified cases with heterogeneous enhancement into "benign," "HCC," "ML," and "Uniform" (homogeneous enhancement). [Model 2]: Focused on homogeneous enhancement cases, classifying them into "benign," "HCC," and "ML." Tumor brightness values were included as input features. A composite model was built, where cases predicted as "Uniform" in Model 1 were further classified by Model 2. A separate test set of 35 cases was used for evaluation.

RESULTS: Of the 35 test cases, 23 were classified as 'Uniform' by Model 1 and subsequently analyzed by Model 2. The composite model achieved diagnostic prediction accuracies of 83.3% for benign tumors, 85.7% for HCC, and 62.5% for ML, with an overall average accuracy of 80.0%. When simplified into a binary classification (benign vs. malignant), the sensitivity was 89.7%, specificity was 83.3%, and the overall accuracy improved to 88.6%.

CONCLUSION: The proposed heuristic composite machine learning model, which first classifies contrast enhancement patterns into homogeneous and heterogeneous groups, improved diagnostic accuracy. Our findings suggest that this approach may enable earlier diagnosis within just 2 minutes post-injection, potentially reducing the need for prolonged observation.

11:20-11:30 (SS03-P3)

Super Resolution Ultrasound Microvascular ImagingRevealing Hidden Vascular Patterns for Enhancing Hepatocellular Carcinoma Diagnosis

Qi Zhang, Yadan Xu, Yang Tang, Benhua Xu, Beijian Huang, Huixiong Xu, Hong Han
Department of Radiology, Zhongshan Hospital Fudan University, China

BACKGROUND / AIM: To investigate the viability of super-resolution ultrasound (SRUS) microvascular imaging in optimizing the CEUS LI-RADS for the hepatocellular carcinoma (HCC) diagnosis.

METHODS: This prospective study enrolled high-risk patients for HCC from January 2024 to August 2024. Each patient underwent B-mode US, color Doppler flow imaging (CDFI), micro-flow imaging (MFI), conventional CEUS, and SRUS microvascular imaging examinations. Based on the capsular and chaotic vessel features displayed by SRUS microvascular imaging, four new criteria were developed for modified CEUS LI-RADS. LR-4 or LR-M lesions were reclassified to LR-5 based on the following criteria: I: the presence of capsular vessels; II: the presence of chaotic vessels; III: the presence of capsular vessels or chaotic vessels; IV: the presence of both capsular vessels and chaotic vessels. The diagnostic performance for HCC using four criteria was evaluated and compared with CEUS LI-RADS using the McNemar test.

RESULTS: Overall, 190 patients (mean age, 60.78 years ± 10.96 [SD]; 142 male patients, 48 female patients) with 190 lesions (163 HCCs, 22 non-HCC malignancies, 5 benign lesions) were enrolled. The visualization rate of the capsular and chaotic vessel features by SRUS is higher than that of CDFI, MFI, and conventional CEUS ($p < 0.05$). Compared with CEUS LI-RDAS and the other three criteria, Criteria III had the highest sensitivity of 92.02% and AUC of 0.85, without a significant decrease in the specificity of 77.78%.

CONCLUSION: SRUS microvascular imaging is a promising modality that assists in modifying CEUS LI-RADS for a more precise diagnosis of HCC.

11:30-11:40 (SS03-P4)

Impact of Histologic Subtype on Survival Outcomes in Patients with Recurrent Hepatocellular Carcinoma Treated with Radiofrequency Ablation

Kyowon Gu, Min Woo Lee, Seungchul Han
Department of Radiology, Samsung Medical Center, Korea

BACKGROUND / AIM: Early recurrence of hepatocellular carcinoma (HCC) following surgical resection remains a major clinical challenge, often necessitating salvage treatment such as radiofrequency ablation (RFA). However, the impact of histologic subtypes on survival outcomes in this setting remains unclear. This study aimed to evaluate

the association between histologic subtypes and survival outcomes in patients with early recurrent HCC treated with RFA.

METHODS: This retrospective study included a total of 203 patients who underwent RFA for early recurrence of HCC after surgical resection, between 2005 and 2018 at our institution. Clinical variables, including preoperative tumor marker levels, tumor size, ALBI grade, Milan criteria fulfillment at the time of surgery, presence of tumor necrosis in surgical specimens, and histologic subtypes such as macrotrabecular-massive (MTM) and scirrhous subtype, were evaluated. OS and PFS were analyzed using Kaplan-Meier survival curves with log-rank tests, and multivariate Cox regression models were employed to identify independent prognostic factors.

RESULTS: The median follow-up period was 83.6 months (interquartile range, 47.2-120.4). The MTM subtype was identified in 24 patients, while the scirrhous subtype was observed in 7 patients, with no cases exhibiting both subtypes simultaneously. Patients with MTM subtype exhibited shorter OS (median, 40.6 months vs. 89.1 months, p=0.06) and PFS (median, 8.5 months vs. 15.7 months, p=0.07) compared to those with other subtypes. In multivariate analysis, macrotrabecular-massive subtype remained an independent predictor of poor OS (HR=2.16, 95% CI 1.19-3.91, p=0.01) and PFS (HR=1.80, 95% CI 1.10-2.95, p=0.02).

CONCLUSION: MTM subtype significantly influences survival outcomes in patients with early recurrent HCC treated with RFA. Identification of high-risk histologic features may aid in refining treatment strategies and optimizing patient management to improve long-term outcomes.

11:40-11:50 (SS03-P5)

Noninvasive Subharmonic Aided Pressure Estimation (SHAPE) in the Assessment of Portal Hypertension in Patients With Decompensated Cirrhosis

Yunlin Huang, Yi Dong, Xiuyun Lu, Ying Wang, Juan Cheng

Department of Radiology, Xinhua Hospital Affiliated to Shanghai Jiao Tong University School of Medicine, China

BACKGROUND / AIM: Subharmonic aided pressure estimation (SHAPE) gradient has been designed as a noninvasive calculation of blood flow pressure. The aim of this study was to explore the possibility of SHAPE measurement for non-invasive evaluation of portal venous pressure in patients with decompensated liver cirrhosis.

METHODS: Patients diagnosed with decompensated liver cirrhosis by appearing decompensating events were prospectively enrolled. SHAPE measurements were performed using LOGIQ E10 ultrasound system (GE Healthcare). A continuous infusion of Sonazoid at a rate of 0.18 ml/kg/h and saline at 120 ml/h was performed for each patient. Taking hepatic venous pressure gradient (HVPG) value as the gold standard, areas under the receiver operating characteristic curves (AUCs) were used to evaluate the diagnostic performance of SHAPE for detecting portal hypertension.

RESULTS: From February 2023 to August 2023, 15 patients (mean age, 61.1 ± 8.3 years; 8 men and 7 women) were included. The correlation between the SHAPE gradient and HVPG was moderate (R = 0.33). The mean SHAPE gradient of patients with clinically significant portal hypertension (CSPH) (HVPG ≥ 10 mmHg) group was significantly higher than that of patients without CPSH (HVPG < 10 mmHg) group (0.5 ± 4.4 dB vs. -7.4 ± 5.1 dB, P = 0.01). Patients with increased risk for variceal hemorrhage (HVPG ≥ 12 mmHg) had a significantly higher mean SHAPE gradient than patients with lower risk (HVPG < 12 mmHg) (1.3 ± 4.4 dB vs. -5.9 ± 4.8 dB; P = 0.01). The optimal cut-off value of the SHAPE gradient for diagnosing patients with CSPH (HVPG ≥ 10 mmHg) and at increased risk for variceal hemorrhage (HVPG ≥ 12 mmHg) were -1.3 dB and -0.6 dB (both AUC =

0.89), respectively.

CONCLUSION: SHAPE measurement is a potential non-invasive, effective imaging method to evaluate portal hypertension among patients diagnosed with decompensated liver cirrhosis in clinical practice.

11:50-12:00 (SS03-P6)

Perfusion Patterns of Contrast Enhanced Ultrasound Correlated With Histopathological Response of Neoadjuvant Chemotherapy for Borderline Resectable or Locally Advanced Pancreatic Cancer

Xiaoyi Yan, Ke Lyu

Department of Radiology, Peking Union Medical College Hospital, Peking Union Medical College, Chinese Academy of Medical Sciences, China

BACKGROUND / AIM: This study aimed to investigate the value of perfusion patterns of contrast enhanced ultrasound (CEUS) in early predicting and assessing the histopathological response of pancreatic cancer to NAC.

METHODS: Between January 2022 and June 2024, participants with pancreatic cancer were prospectively enrolled to undergo both ultrasound and CEUS before and after early NAC. The CEUS perfusion patterns were classified into three types: Iso-enhancement (Iso-E), hypo-enhancement (Hypo-E) and peripheral enhancement, in which Iso-E was further divided into centripetal Iso-E and rapid diffuse Iso-E. Participants were categorized into responders and non-responders according to therapy response after surgery. The histologic response was subsequently compared with early CECT-based RECIST assessment results, US-size based evaluation findings, CA 19-9 response status, and CEUS perfusion patterns before and after two cycles of NAC.

RESULTS: A total of 77 consecutive patients who underwent CEUS examinations both before and after NAC were initially enrolled in the study. Among these, 28 patients subsequently underwent surgical resection and were included in the final analysis cohort. Neither size-based response evaluation (RECIST or US-based) showed a significant correlation with histopathologic response (P=0.57 and P=0.29, respectively), nor did the biochemical (CA 19-9) response (P=0.19). However, the maximum diameter of the tumor was smaller and the CA19-9 level was lower in the responders. Responders exhibited a higher proportion of centripetal Iso-E lesions before NAC (p=0.05) and rapid diffusion Iso-E lesions after NAC (p=0.04) compared to non-responders. When analyzing the combined pre-NAC and after two cycles of NAC enhancement characteristics, all responders displayed centripetal Iso-E patterns pre-NAC, which transitioned to rapid diffusion Iso-E after early NAC. In contrast, only one non-responder exhibited the same pattern (p<0.001).

CONCLUSION: CEUS may be a valuable and non-invasive tool for predicting and assessing the histopathologic response to NAC in pancreatic cancer, potentially offering a more reliable alternative to traditional size-based assessments.

12:00-12:10 (SS03-P7)

A Study of Contrast-Enhanced Ultrasound in the Differentiation of Mass-Forming Pancreatitis From Pancreatic Ductal Adenocarcinoma

Ke Lyu, Hua Liang

Department of Radiology, Peking Union Medical College Hospital, China

BACKGROUND / AIM: To evaluate the utility of conventional ultrasound and contrast-enhanced ultrasound (CEUS) in differentiating mass-forming pancreatitis (MFP) from pancreatic ductal adenocarcinoma (PDAC).

METHODS: This retrospective study analyzed data from patients diagnosed with PDAC or MFP who underwent pancreatic CEUS at our institution between September 2017 and April 2024. Initially, independent predictors for differentiating between PDAC and MFP were identified through logistic regression analysis. Subsequently, a nomogram was constructed based on these predictors and validated. Furthermore, a machine learning model was developed to differentiate between iso-enhancement PDAC and MFP. The dataset was divided chronologically, with data from September 2017 to December 2022 used for model development and data from January 2023 to April 2024 serving as an

independent test set for validation. Finally, patients with focal type 1 autoimmune pancreatitis (AIP) and PDAC with elevated sIgG4 levels were identified, and the differences between these two entities were further compared.

RESULTS: 1.The nomogram included a total of 281 patients (188 PDAC and 93 MFP). The nomogram based on these factors demonstrated an AUC of 0.930 (95% CI: 0.895-0.965) in the training set and 0.914 (95% CI: 0.853-0.976) in the validation set. 2.The machine learning model included 142 patients (73 iso-enhancing PDAC and 69 MFP). The optimal classification accuracy, precision, F1 score, sensitivity, and specificity were 0.844, 0.855, 0.848, 0.841, and 0.848, respectively. The average classification accuracy on the independent test set was 0.750. 3.The differentiation of focal type 1 AIP from sIgG4-elevated PDAC included 46 patients (17 PDAC and 29 AIP). Differences were observed between the two groups in CA19-9 levels, sIgG4 > 2 times the upper limit of normal, and ultrasound features (taller-than-wide shape, vascular invasion, enhancement pattern, and washout pattern) (all P<0.05).

CONCLUSION: CEUS demonstrates promising utility in the differentiation of PDAC from MFP.

SS04 Scientific Session 4

11:00-12:20 **GBR 102**

Chairperson(s):
Jung Hee Shin *(Samsung Medical Center, Korea)*
Jung Hyun Yoon *(Severance Hospital, Korea)*

11:00-11:10 (SS04-P1)

Inconclusive Cytology Results of Fine-Needle Aspiration for Thyroid Nodules: The Gravity of Strict Guideline Implementation

Sangwoo Cho[1], Kyunghwa Han[2], Jung Hyun Yoon[2], Vivian Youngjean Park[2], Miribi Rho[2], Jiyoung Yoon[2], Jin Young Kwak[2]

[1]Yonsei University College of Medicine, Korea, [2]Department of Radiology, Yonsei University College of Medicine, Korea

BACKGROUND / AIM: We investigated whether strict compliance with the Korean Thyroid Imaging Reporting and Data System (K-TIRADS) biopsy indications reduces inconclusive results and evaluated other associated factors.

METHODS: This retrospective study included 2,440 nodules in 2,256 patients who underwent initial FNA for thyroid nodules from January to December 2022. Inconclusive specimens were defined as Bethesda category I or III. FNA not-indicated nodules were those smaller than the K-TIRADS biopsy threshold. Patient age and gender, ultrasound features, nodule size, number of needle passes, and operator experience were selected as clinical factors. Univariate and multivariate analyses were conducted to evaluate associations between clinical factors and inconclusive results. The Chi-square and Mann-Whitney U tests were performed to analyze associations between clinical factors.

RESULTS: FNA not-indicated nodules were significantly associated with inconclusive biopsy results, along with subcentimeter nodule size, less than 1 year of operator experience, older age, and K-TIRADS 4 (P<0.001, P=0.015, P=0.004, P<0.001, and P<0.001, respectively). Nodules of 0 to 5 mm showed significant association with inconclusive biopsy results (P=0.006). Two or more FNA needle

passes were associated with smaller nodule size, operators with less than 1 year, and K-TIRADS 4 (P=0.01, P=0.023, and P=0.001, respectively). Among K-TIRADS 4 nodules, suspicious US characteristics were associated with malignant biopsy results, and showed negative association with inconclusive biopsy results (P=0.03 and P=0.004, respectively).

CONCLUSION: FNA not-indicated nodules, 0 to 5 mm size, less than 1 year of operator experience, older age, and K-TIRADS 4 were associated with inconclusive biopsy results. Strictly following the biopsy indications in K-TIRADS can reduce inconclusive results.

11:10-11:20 (SS04-P2)

Differences in Diagnostic Trends When Using K-TIRADS and the ACR TI-RADS: A Reader Study

Seohyun Ryu[1], Jin Chung[2], Ji Ye Lee[3], Won Hwa Kim[4], Jaeil Kim[5], Jung Hyun Yoon[1]

[1]Department of Radiology, Yonsei University College of Medicine, Korea, [2]Department of Radiology, Ewha Womans University Mokdong Hospital, Korea, [3]Department of Radiology, Seoul National University Hospital, Korea, [4]Department of Radiology, Kyungpook National University Hospital, Korea, [5]Kyungpook National University, School of Computer Science and Engineering, Korea, [6]BeamWorks, Inc., Korea

BACKGROUND / AIM: To evaluate the differences in the trend of diagnosis when using K-TIRADS and ACR TI-RADS for classifying thyroid ultrasound (US) examinations.

METHODS: For this retrospective reader study, 481 thyroid US images were collected. Benign or malignant cases (mean size: 17.4 mm± SD: 10.3) were cytopathologically confirmed with aspiration/biopsy, surgery or stability on more than 1 year of follow up. Four experienced readers with thyroid imaging fellowship training individually reviewed the US images. Readers recorded individual US features according to composition, echogenicity, margin, shape, calcifications. Final assessments were obtained by the readers using K-TIRADS. Using the individual US features given by the readers, ACR scores were calculated with a corresponding ACR TI-RADS final assessment. Interobserver agreement for individual US features were calculated. Diagnostic performances including sensitivity, specificity, PPV, NPV and area under the receiver operating characteristics (AUC) curve of the four readers according to K-TIRADS and ACR TI-RADS were calculated and compared.

RESULTS: Of these 481 US images, 157 (32.6%) were benign, 184 (38.3%) were malignant, and 140 (29.1%) were negative. Average agreement of the four readers between K-TIRADS vs. ACR TI-RADS final assessments were moderate, K=0.492 (95% confidence interval [CI]: 0.459-0.525). Average sensitivity (79.2% vs. 88.2%, P<0.001) and NPV (87.5% vs. 91.8%, P<0.001) was significantly lower while specificity (89.1% vs. 82.0%, P<0.001) and PPV (82.0% vs. 75.7%, P<0.001) was significantly higher in K-TIRADS than ACR TI-RADS, respectively. Average AUC between K-TIRADS and ACR TI-RADS assessment did not show significant differences, 0.841 (95% CI: 0.814-0.868) vs. 0.851 (95% CI: 0.826, 0.876), respectively (P=0.242).

CONCLUSION: Using K-TIRADS leads to higher sensitivity and NPV while using ACR TI-RADS leads to higher specificity and PPV. While overall performances do not show significant differences between K-TIRADS and ACR TI-RADS, the different effect of using different risk stratification systems should be acknowledged.

11:20-11:30 (SS04-P3)

Risk Stratification of Thyroid Follicular Neoplasm Diagnosed on Core Needle Biopsy by Histology Subcategory and Ultrasound

Dong Gyu Na[1], Byeong-Joo Noh[2]

[1]Department of Radiology, GangNeung Asan Hospital, Korea, [2]Department of Pathology, GangNeung Asan Hospital, Korea

BACKGROUND / AIM: This study aimed to develop a risk stratification system (RSS) integrating core needle biopsy (CNB) subcategories and ultrasound (US) features for thyroid nodules diagnosed as follicular neoplasm (FN) on CNB and to evaluate the performance of surgical decision criteria

incorporating RSS and nodule size in diagnosing malignancy.

METHODS: This retrospective study included 345 consecutive nodules (>1 cm) diagnosed as FN on CNB with corresponding surgical histologic diagnoses. FN subcategories were determined using histologic criteria modified from the 2019 Korean CNB pathology guideline. The CNB-US RSS for CNB category IV nodules was developed based on identified CNB subcategory and US features predictive of malignancy. Surgical criteria were defined using the CNB-US RSS and nodule size, and their diagnostic performance for malignancy was evaluated.

RESULTS: Malignancy, excluding non-invasive follicular thyroid neoplasms with papillary-like nuclear features, was identified in 89 cases (25.8%). CNB subcategory IVb had a significantly higher risk of malignancy (ROM) than other subcategories (39.4% vs. 10.9%, P < 0.001). Independent US predictors of malignancy included mixed echogenicity, rim calcification, and nonparallel orientation (P ≤ 0.021). By integrating CNB subcategory IVb and predictive US features, CNB category IV nodules were stratified into high-risk (ROM, 49.4%), intermediate-risk (ROM, 27.2%), and low-risk (ROM, 6.2%) groups (P ≤ 0.001). Surgical criteria, defined as high- or intermediate-risk nodules >1 cm and low-risk nodules >3 cm, achieved high sensitivity (96.6%) and negative predictive value (95.9%), while avoiding unnecessary surgery in 35.2% of benign nodules.

CONCLUSION: The CNB-US RSS effectively stratifies malignancy risk in CNB category IV nodules. Surgical criteria based on the CNB-US RSS and nodule size serve as an effective rule-out test for malignancy, allowing low-risk nodules ≤3 cm to be safely managed with US surveillance instead of immediate surgery.

11:30-11:40 (SS04-P4)

Application of Follicular Thyroid Imaging Reporting and Data System to 116 Cases of Follicular Thyroid Carcinoma Diagnosed Over 28 Years at a Single Institution: Associated With TERT Promoter Mutation

Myoung Kyoung Kim, Haejung Kim, Jaeho Lee, Jung Hee Shin, Soo Yeon Hahn

Department of Radiology, Samsung Medical Center, Korea

BACKGROUND / AIM: Follicular Thyroid Imaging Reporting and Data System (F-TI-RADS) is newly released risk stratification system for differentiating between follicular thyroid adenoma and follicular thyroid carcinoma (FTC). The purpose of our study was to determine whether the prognosis of FTC could be predicted using F-TI-RADS.

METHODS: Total 172 patients who had surgically confirmed FTC and TERT promoter mutation results between August 1995 and Dec 2023 were included in this study. All of them were available for analysis of preoperative US findings, histopathologic results, and TERT promoter mutation results. Each nodule was categorized based on US pattern according to the F-TI-RADS and divided into low-risk and high-risk groups based on a 50% risk threshold for FTC. Logistic regression analysis was performed to investigate association with US findings and clinicopathological variables between low-risk and high-risk groups based on F-TI-RADS.

RESULTS: Among the 172 patients diagnosed with FTC, 107 (62.2%) were classified as F-TI-RADS low-risk FTCs, while 65 (37.8%) were categorized as F-TI-RADS high-risk FTCs. F-TI-RADS high-risk FTCs were significantly associated with male gender, advanced age, larger tumor size, aggressive tumor characteristics according to WHO classification, advanced tumor stage, presence of TERT promoter mutation, death and recurrence (all Ps≤.014). The predominant US findings for F-TI-RADS high-risk FTC included solid composition (75.4%), hypoechogenicity (67.7%), smooth margin (73.8%), trabecular formation (49.2%), and rim/macrocalcification (33.8%). According to the logistic regression analysis, there was a significant association between F-TI-RADS high-risk FTCs

and advanced tumor stage (odds ratio = 12.35, 95% confidence interval = 6.41-16.67, P=.034).

CONCLUSION: In summary, our study demonstrates the effectiveness of F-TI-RADS in predicting prognosis in FTC. F-TI-RADS high-risk FTC group correlated significantly with adverse clinicopathological features including presence of TERT promoter mutation. These findings underscore the potential of F-TI-RADS as a valuable tool for risk stratification and clinical decision-making in FTC management.

11:40-11:50 (SS04-P5)

Thyroid Nodules with Spoke-Wheel Blood Flow on US: Novel Indicators to Enhance Diagnostic Accuracy

Li Xu, Zhang Yan, Gou Taohua, Cai Lei, Gao Tian, Li Miao

Department of Ultrasound,The first Medical Centre, Chinese PLA General Hospital, China

BACKGROUND / AIM: To investigate the benign or malignant nature of thyroid nodules exhibiting a spoke-wheel blood flow (SWBF) pattern, and to explore novel characteristics for improving ultrasound diagnostic performance.

METHODS: In this prospective study, participants with SWBF thyroid nodules between January 2021 and April 2024 were included. Clinical data, type of SWBF, and imaging characteristics from conventional ultrasound and contrast-enhanced ultrasound were recorded. The American College of Radiology Thyroid Imaging Reporting and Data System was used to diagnose these nodules, and novel characteristics were explored to improve diagnostic performance. DeLong test was used to compare diagnostic performance. Pathological results served as the gold standard.

RESULTS: The final data included 102 participants (mean age, 40 years ± 13 [standard deviation], 66 women) with 102 SWBF thyroid nodules (76% were malignant). SWBF of type I (malignant,69%, benign,40%, p = 0.01), central scars (malignant,52%, benign,28%, p = 0.04) and peripheral irregular enhancement rings (malignant,55%, benign,26%, p < 0.001) were more commonly observed in malignant nodules, while central macrocalcifications (benign,44%, malignant,1%, p < 0.001) were more frequently seen in benign nodules. When combined with central scars, central macrocalcifications and contrast enhanced ultrasound, the diagnostic performance improved significantly (AUC: 0.97 vs. 0.76, p = 0.002).

CONCLUSION: SWBF is associated with a risk of malignancy in thyroid nodules, particularly type I. Central scars are highly specific characteristics of malignancy while central macrocalcifications of benignity. Combining these characteristics with contrast enhanced ultrasound can significantly improve diagnostic performance.

11:50-12:00 (SS04-P6)

Radiofrequency Ablation of Low-Risk Papillary Thyroid Microcarcinoma: A Retrospective Cohort Study Including Patients with More than 10 Years of Follow-up

So Yeong Jeong[1], Sun Mi Baek[3], Jung Hwan Baek[2]

[1]Department of Radiology, Seoul National University Bundang Hospital, Korea, [2]Department of Radiology, Asan Medical Center, Korea, [3]Department of Radiology, Haeundae Sharing and Happiness Hospital, Korea

BACKGROUND / AIM: We evaluated the long-term efficacy and safety of radiofrequency ablation (RFA) in patients with low-risk PTMC with clinical follow-up of more than 10 years.

METHODS: We included patients with low-risk PTMC who had more than 10 years of follow-up after US-guided RFA (performed between May 2008 and December 2013). Sixty-five consecutive patients with 71 low-risk PTMCs who were unsuitable for surgery or declined surgery were included. Before RFA, all patients underwent US and thyroid CT. Repeat RFA for staged ablation was performed when first RFA did not secure sufficient safety margins. Follow-up US imaging was performed at 1 week, 3 months, 6 months, every 6 months until 2 years, and then annually afterward. Primary outcomes were respective cumulative rates of disease progression (local tumor progression, lymph node, or distant metastasis), newly developed thyroid cancer, and

conversion surgery. Secondary outcomes were serial volume reduction rate (VRR), complete disappearance rate of ablated PTMC, and adverse events.

RESULTS: Of 65 patients included in the study, 60 had unifocal and 5 had multifocal PTMCs. The mean number of RFA sessions per tumor was 1.2, and median follow-up duration was 151 months. Twenty percent (13/65) of patients required repeat RFA. There were no cases of disease progression. Five patients (5/65,7.7%) developed a new papillary thyroid cancer (four treated with RFA and one with lobectomy). At 24 months, mean VRR was 100%, and this was maintained throughout final follow-up. The complete tumor disappearance rates after one or more RFA treatments were 40.8% (29/71), 74.6% (53/71), and 100% (71/71) at 6, 12, and 24 months, respectively. One major(subclinical hypothyroidism) and three minor adverse events occurred.

CONCLUSION: RFA of low-risk PTMC is effective and safe. During more than 10 years of follow-up, we observed no incident local tumor progression nor metastases, but 7.7% of patients developed a new papillary thyroid cancer.

MS01 Multisession 1

11:00-12:20 **GBR 103**

Chairperson(s):
Jung-Ah Choi *(Hallym University Dongtan Sacred Heart Hospital, Korea)*
Ji Young Hwang *(Ewha Womans University Seoul Hospital, Korea)*

12:00-12:10 (MS01-P1)

Usefulness of Ultrasound Elastography in Differential Diagnosis of Epidermal Cysts and Ruptured Epidermal Cysts

Hee Jin Park, Sungchul Wee
Department of Radiology, Kangbuk Samsung Hospital, Korea

AIM: To evaluate and compare ultrasound elastography (EUS) findings by way of strain elastography (SE) and shear wave elastography (SWE) of epidermal cyst and ruptured epidermal cysts. We also evaluated which method offered superior reproducibility.

MATERIALS AND METHODS: This retrospective study included 194 patients with epidermal cysts who underwent ultrasonography (US), including SE and SWE. SE scores were classified into four grades according to elasticity. Strain ratio was evaluated using the elasticity ratio of lesions and adjacent subcutaneous fat tissue. For SWE, shear wave (SW) velocity (m/s), elasticity (kPa) by Young modulus, velocity ratio, and elasticity ratio were evaluated. All measurements were performed twice and the reproducibility of SE and SWE measurements were assessed. Relationships among SE and SWE measurements were evaluated.

RESULTS: Ruptured epidermal cysts showed lower shear wave velocity and elasticity than epidermal cysts on SWE. Strain ratio showed good inter-session reproducibility, while those of SW velocity and elasticity of epidermal cysts and ruptured epidermal cysts were moderate to good. AUCs for diagnostic performance to differentiate epidermal cyst from ruptured epidermal cyst were 0.721 for SW velocity and 0.706 for elasticity.

CONCLUSION: The reproducibility of both SWE

and SE in cases of epidermal cyst was moderate to good. However, the reproducibility of SW velocity of reference tissue was poor. Ruptured epidermal cysts had lower SW velocity and elasticity. In contrast, the strain ratio and SE score did not differentiate between the two lesion types. SWE could be a more useful diagnostic modality for evaluating epidermal cysts.

12:10-12:20 (MS01-P2)

Atelocollagen Injection with Polydeoxyribonucleotide in Supraspinatus Tendon Tear

Gi-young Park, Sung Cheol Cho
Department of Rehabilitation Medicine, Daegu Catholic University Medical Center, Korea

BACKGROUND / AIM: To evaluate the clinical and ultrasound (US) findings after atelocollagen injection combined with polydeoxyribonucelotide (PDRN) in the patients with high grade partial-thickness or small size full-thickness tears of the supraspinatus (SSP) tendon.

METHODS: Ten patients (7 men, 3 women; mean age, 61.7; range, 55-73 years) that were diagnosed as high grade partial-thickness (grade 3) or small size full- thickness tears in SSP tendon on US were recruited. The patients visited due to unilateral shoulder pain, radiograph and US examinations were conducted. After US examination, triamcinolone acetonide (20 mg, 2 mL), lidocaine (2%, 2 ml), and normal saline (4 ml) were injected in subacromial subdeltoid (SASD) bursa under US guidance. After six weeks of SASD bursa corticosteroid injection, the shoulder pain was reduced. Atelocollagen and PDRN were injected in supraspinatus tendon tear site under US guidance twice every four weeks. The visual analogue scale (VAS) was used to measure the intensity of shoulder pain.

RESULTS: Ten shoulders with eight high grade partial-thickness SSP tendon tear (5 bursal side, 3 articular side) and two small size full-thickness SSP tendon tear were diagnosed on US examination. The mean number of previous corticosteroid injection before atelocollagen and PDRN injection was 2.2 (range, 1-5). The shoulder pain was decreased after 6 weeks of SASD bursa corticosteroid injection in all patients. After four weeks of the second atelocollagen and PDRN injections in patient one, the size of partial-thickness supraspinatus tendon tear (grade 3) was decreased to the grade 2. In a patient, the shoulder pain increased temporarily after the first injection, but decreased on the second injection.

CONCLUSION: Injection with atelocollagen and PDRN were successfully performed in tendon tear site under US guidance in ten patients with high grade partial-thickness or small size full-thickness SSP tears, and no serious side effect was observed.

MS02 Multisession 2

11:00-12:20 **Room 203**

Chairperson(s):
Byoung Hee Han *(GangNeung Asan Hospital, Korea)*
Young Ah Cho *(Asan Medical Center, Korea)*

11:20-11:30 (MS02-P1)

Accuracy of Large Language Models in Detecting Cases Requiring Prompt Radiology Reporting in a Pediatric Emergency Setting: A Feasibility Study Using Publicly Available Clinical Vignettes

Pyeong Hwa Kim[1], Jisun Hwang[2], Jeong In Shin[1], Chong Hyun Suh[1]
[1]Department of Radiology, Asan Medical Center, Korea, [2]Department of Radiology, Seoul National University Bundang Hospital, Korea

BACKGROUND / AIM: To evaluate the accuracy of multimodal LLMs in detecting cases requiring prompt radiology reporting in pediatric emergency department (PED) setting.

METHODS: Seventy-one publicly available, paraphrased pediatric clinical vignettes with images from New England Journal of Medicine, The Lancet, Archives of Pediatrics and Adolescent Medicine, and Radiology were assessed by seven vision-capable LLMs and four human readers (expert pediatric radiologist, trainee radiologist, expert pediatric emergency physician, trainee pediatrician). Of those,

9 of 71 clinical vignettes included US images. Cases were classified as requiring prompt reporting if they corresponded to Korean Triage and Acuity Scale (KTAS) levels 1–2 or met the criteria for a critical value report (CVR), as determined by consensus. Sensitivity, specificity, and accuracy were calculated with 95% confidence intervals (CI), and those of the LLM with the highest accuracy was compared with human readers using McNemar's test (Bonferroni-corrected P<.013 indicating significant difference).

RESULTS: LLMs demonstrated 57.7%–81.7% accuracy in detecting cases corresponding to KTAS levels 1–2, 53.5%–87.3% accuracy in detecting cases requiring CVR, and 60.6%–83.1% accuracy in detecting cases requiring prompt radiology reporting. Gemini-Flash with temperature 1 (t1) demonstrated the highest accuracy among LLMs in detecting cases corresponding to KTAS levels 1 or 2 (81.7% [95% CI: 71.8%, 90.1%]), requiring CVR (87.3% [95% CI: 78.9%, 94.4%]), and requiring prompt radiology reporting (83.1% [95% CI: 74.6%, 91.5%]). Human readers demonstrated 73.2%–84.5% accuracy in detecting cases corresponding to KTAS levels 1–2, 39.4%–94.4% accuracy in detecting cases requiring CVR, and 62.0%–84.5% accuracy in detecting cases requiring prompt radiology reporting. Accuracy of detection of cases requiring prompt radiology reporting of Gemini-Flash t1 showed comparable to human reader with the highest accuracy (expert pediatric emergency physician, 84.5%; 95% CI: 76.1%, 93.0%; P>.99).

CONCLUSION: Commercial multimodal LLMs achieved comparable or superior accuracy to human readers in identifying cases requiring prompt radiology reporting, supporting their feasibility for PED worklist reprioritization.

11:30-11:40 (MS02-P2)

Neonatal Brain Perivascular Space Volume Measurement Using Cranial Ultrasound: Association with Germinal Matrix Hemorrhage

Hyun Gi Kim[1], Arum Choi[1], Hosna Asma-ull[1], Yasemin Tanyildizi[2]

[1]Department of Radiology, The Catholic University of Korea, Eunpyeong St. Mary's Hospital, Korea, [2]Department of Radiology, European University Cyprus, Germany

BACKGROUND / AIM: Perivascular space (PVS) in the brain serves as a biomarker for glymphatic function. The aim of this study was to quantify PVS volume using cranial ultrasound (CUS) in neonates and evaluate its association with germinal matrix hemorrhage (GMH).

METHODS: This retrospective, single-institution study included neonates who underwent CUS with PVS measurements between November 2024 and January 2025. CUS performed at term-equivalent age (TEA) was reviewed, and neonates were classified into two groups: the control group and the GMH group. PVS volume was measured in three dimensions using coronal and sagittal CUS views at the caudal portion of the basal ganglia. PVS measurements were obtained for both the right and left basal ganglia PVS, and the mean value was used for analysis. Differences in PVS volume between groups were assessed using the Mann-Whitney U test, and longitudinal changes in PVS volume were also analyzed.

RESULTS: A total of 61 neonates were included: 48 without GMH (32 males, median [IQR] gestational age [GA]: 264 [252–272] days, median [IQR] corrected GA [CGA] at CUS: 271 [264–276] days) and 13 with GMH (8 females, median [IQR] GA: 261 [252–270] days, median CGA at CUS: 271 [262–278] days). There were no significant differences in gender distribution ($p = 0.065$), GA ($p = 0.797$), or CGA at CUS ($p = 0.99$) between the two groups. Neonates with GMH had significantly larger PVS volumes than those without GMH (0.052 [0.040–0.063] cm^3 vs. 0.039 [0.026–0.055] cm^3, $p = 0.033$). This trend persisted in longitudinal evaluations, with neonates in the GMH group consistently exhibiting higher PVS volumes than those in the control group after the

initial CUS.

CONCLUSION: PVS volume can be quantified using CUS in neonates. At TEA CUS, neonates with GMH exhibited significantly larger PVS volumes than those without GMH, suggesting a potential association with GMH-related brain glymphatic function change.

11:40-11:50 (MS02-P3)

Correlation Between Ultrasound Derived Fat Fraction and Proton Density Fat Fraction for Evaluating Pediatric Hepatic Steatosis With Consideration of the Breathing Effect

Jisoo Kim[1], Haesung Yoon[2], Kyunghwa Han[2], Yonghan Kwon[2], Hong Koh[3], Yong-Woo Kim[2], Eun Joo Lee[3], Mi-Jung Lee[2]

[1]Department of Radiology, Gangnam Severance Hospital, Korea, [2]Department of Radiology, Severance Hospital, Korea, [3]Department of Pediatrics-G-I/Hepatology, Severance Hospital, Korea

BACKGROUND / AIM: To compare fat fraction values derived from ultrasound and MRI and to evaluate the effect of breathing during ultrasound in pediatric patients with suspicious fatty liver disease.

METHODS: This prospective study enrolled consecutive pediatric patients with suspicious fatty liver disease. The patients underwent abdominal ultrasound including ultrasound derived fat fraction (UDFF) and MRI including proton density fat fraction (PDFF) at the time of initial diagnosis. UDFF values were obtained ten times each while free breathing (FB) and breath hold (BH) and the mean value was used. The mean value of maximum region of interest excluding vascular structures was used to measure PDFF. Correlation analysis, linear regression analysis, and Bland-Altman analysis were performed to compare UDFF and PDFF.

RESULTS: A total 55 patients (M:F=22:33) with 7-18 years old (mean 13.7 ± 2.8 years) were included. The range of UDFF value was 2-36% and that of PDFF was 0-56%. The correlation analysis showed significant correlation between UDFF and PDFF on both FB (β=0.52, p<0.001) and BH (β=0.54, p<0.001) status. On Bland-Altman analysis, there was a significant bias between UDFF and PDFF (2.49%, 95% CI 0.08 to 4.89) with a proportional bias (β=0.49, p<0.001) on FB status. The proportional bias (β=0.46, p<0.001) was similar on BH status without significant bias between UDFF and PDFF (1.92%, 95% CI -0.42 to 4.27) on BH status.

CONCLUSION: UDFF and PDFF values showed significant correlation with 0.5 correlation coefficient regardless of breathing control. There was 2.5% bias between UDFF and PDFF on FB status and proportional bias on both breathing statuses.

11:50-12:00 (MS02-P4)

Optimum Minimal Number for Proper Acquisition of Ultrasound-Derived Fat Fraction in Pediatric Patients With Suspicious Fatty Liver Disease in Consideration With the Effect of Breathing

Haesung Yoon[1], Jisoo Kim[1], Kyunghwa Han[1], Yonghan Kwon[1], Yong-Woo Kim[1], Hong Koh[2], Eun Joo Lee[2], Mi-Jung Lee[1]

[1]Department of Radiology, Severance Hospital, Korea, [2]Department of Pediatrics-G-I/Hepatology, Severance Hospital, Korea

BACKGROUND / AIM: To evaluate optimum minimal number for proper acquisition of ultrasound-derived fat fraction (UDFF) and to evaluate the effect of breathing in pediatric patients with suspicious fatty liver disease.

METHODS: This prospective study enrolled consecutive pediatric patients with suspicious fatty liver disease. The patients underwent abdominal ultrasound including ultrasound derived fat fraction (UDFF) at the time of initial diagnosis. UDFF values were obtained ten times each while free breathing (FB) and breath hold (BH). Intraclass correlation coefficient (ICC) was used to analyze how many the values accumulated sequentially for ten measurements match the mean of ten measurements.

RESULTS: A total 55 patients (M:F=22:33) with 7-18 years old (mean 13.7 ± 2.8 years) were included. The range of UDFF value was 2-36%. On FB status, ICC of two measurements was 0.925 (95% CI 0.875-0.956) and ICC was decreased according to the increased number of acquisition. On BH status,

ICC of two measurements was 0.921 (95% CI 0.871-0.952) and ICC was also decreased according to the increased number of acquisition.

CONCLUSION: Only two acquisition of UDFF values are comparable with ten acquisition regardless of breathing control for evaluating hepatic steatosis in pediatric patients.

12:00-12:10 (MS02-P5)

Optimal Minimal Number for the Proper Acquisition of Multisample Ultrasound Point Shear Wave Elastography for Evaluating Pediatric Liver in Consideration With the Effect of Breathing

Yonghan Kwon[1], Jisoo Kim[1], Haesung Yoon[1], Yong-Woo Kim[1], Hong Koh[2], Eun Joo Lee[2], Kyunghwa Han[1], Mi-Jung Lee[1]

[1]Department of Radiology, Severance Hospital, Korea, [2]Department of Pediatrics-G-I/Hepatology, Severance Hospital, Korea

BACKGROUND / AIM: To evaluate optimum minimal number for proper aquisition of multisample ultrasound point shear wave elastography and to evaluate the effect of breathing in pediatric patients with suspicious fatty liver disease.

METHODS: This prospective study enrolled consecutive pediatric patients with suspicious fatty liver disease. The patients underwent abdominal ultrasound including multisample ultrasound point shear wave elastography (pSWE) which allows 12 individual measurements of liver stiffness in a single acquisition at the time of initial diagnosis. Multisample pSWE values were obtained ten times each while free breathing (FB) and breath hold (BH). Intraclass correlation coefficient (ICC) was used to analyze how many the values accumulated sequentially for ten measurements match the mean of ten measurements.

RESULTS: A total 64 patients (M:F=26:38) with 7-18 years old (mean 13.7 ± 2.6 years) were included. The mean value of pSWE was 4.4 kPa and the median value was 4.2 kPa on FB status and the mean value was 5.4 kPa and the median value was 4.4 kPa on BH status. On FB status, ICC increased up to six measurements as 0.895 (95% CI 0.856-0.928) and then decreased from 7th measurement accumulation. On BH status, ICC of two measurements was 0.944 (95% CI 0.910-0.966) and ICC was decreased according to the increased number of acquisition.

CONCLUSION: Only two measurements of pSWE when applying multisample acquisition are comparable with ten acquisitions during BH status, but six measurements are required during FB status for evaluating pediatric liver.

12:10-12:20 (MS02-P6)

Development of a Simplified Prediction Model for Diagnosing Progressive Central Precocious Puberty Using Clinical and Pelvic Ultrasound Parameters

Yeseul Kang[1], Kyungechul Song[3], Eunju Lee[2], Hye Sun Lee[2], Hana Lee[3], Hyun Wook Chae[3], Hyun Joo Shin[1]

[1]Department of Radiology, Yongin Severance Hospital, Korea, [2]Yonsei University College of Medicine, Korea, [3]Department of Pediatrics, Gangnam Severance Hospital, Korea

BACKGROUND / AIM: This study aimed to explore the predictive value of clinical and pelvic ultrasound parameters for diagnosing central precocious puberty (CPP) and to establish a clinically useful simplified prediction model to differentiate progressive CPP (P-CP) from nonprogressive precocious puberty (N-PP).

METHODS: Girls aged <9 years with secondary sexual development who underwent a gonadotropin-releasing hormone stimulation test and pelvic ultrasound between September 2020 and November 2023 were retrospectively included and divided into the P-CP and N-PP groups. Logistic regression analysis was used to determine the significant parameters and develop prediction models. The diagnostic performance of the models was compared using the area under the receiver operating characteristic curve (AUC) analysis and the Delong method. The continuous net reclassification improvement (cNRI) and absolute integrated discrimination improvement (IDI) were used to determine the additive effects of ultrasound parameters. A nomogram scoring system was

constructed based on a simplified model to predict the probability of developing P-CP.

RESULTS: A total of 109 girls were included, with 64 (58.7%) in the P-CP group. Age, bone age, height, height minus midparental height, basal luteinizing hormone (LH), follicle-stimulating hormone, estradiol, insulin-like growth factor-I, Tanner stage, and cervical and fundus width were significant parameters for the diagnosis of P-CP. The models with ultrasound parameters yielded significantly higher cNRI and IDI values than the models without ultrasound parameters. The simplified model was composed of basal LH, estradiol, and fundus width that showed an AUC value of 0.93 (95% confidence interval: 0.88– 0.98) with a cutoff value of 16.

CONCLUSION: In conclusion, adding pelvic ultrasound parameters to traditional clinical results has an additive effect on P-CP screening. A simplified predictive model is effective for CPP screening in real-world clinics. These findings highlight the potential of the prediction model to overcome the limitations of the classical diagnostic approach for CPP in children.

USB01 Ultrasound, the Best 1

10:50-11:10 **GBR 104+105**

Chairperson(s):
Young Seo Cho *(Hanyang University Guri Hospital, Korea)*

10:50-10:53 (USB01-P1)

Diffuse Hepatic Hemangiomatosis in a Young Mongolian Female

Ariunbold Gankhuyag, Khishgee Tsolmon, Buyankhishig Tsogtsaikhan, Bayarjargal Namkhaijantsan, Munkh-erdene Gantogoo
Department of Radiology, Asralt Med Hospital, Mongolia

Diffuse hepatic hemangiomatosis (DHH) is an extremely rare disease, especially in adults. We present a case of DHH liver in a 29-year-old female patient with diffuse, a giant hepatic hemangioma in his right hepatic lobe. The female-to-male ratio is 2.4:1. Although most patients present with abdominal pain or distension, this case highlights an asymptomatic presentation. Radiographic examination shows multiple diffuse liver nodules. On MRI, these lesions show hypointense T1 and hyperintense T2. Some lesions may show peripheral rim enhancement in the arterial phase but no portovenous washout. In total, 47% of patients with DHH have one or more giant hemangioma(s). Pathology shows that the lesions are lined with flat endothelial cells without cellular atypia, which are stained positive for vascular endothelial markers. Liver failure is the main cause of death. Some patients can be improved by partial hepatectomy. However, there is no effective treatment for most patients. Given the absence of symptoms, conservative management and close monitoring were chosen. We classified it a two-type classification of DHH, where surgical resection may be considered for localized cases (Type 1), while liver transplantation should be reserved for end-stage diffuse disease (Type 2). Additionally, irradiation may represent a future therapeutic option, though further research is needed.

10:53-10:56 (USB01-P2)

Transient Type Ischemic Enterocolitis Diagnosed by Contrast Enhanced Ultrasonography

Misato Maeyama
Department of Radiology, Osaka Ekisaikai Hospital, Japan

CASE: The majority of ischemic enteritis is a transient type of ischemic enteritis that causes edema in the descending colon. I experienced ischemic enteritis with edema in the transverse colon. This is a case in which transient ischemic enteritis was diagnosed using contrast-enhanced ultrasound.
SUBJECT: The patient is a 91-year-old woman. I was hospitalized due to melena.
METHOD: Abdominal ultrasound showed localized edema in the transverse colon. The wall of the transverse colon was irregular. Contrast-enhanced ultrasound showed necrosis in part of the transverse colon. Endoscopy also revealed necrosis Since there was mucosal necrosis, a diagnosis of transient ischemic enteritis was made.
CONCLUSION: Ischemic enteritis is often transient. Transverse colon edema is difficult to diagnose as ischemic enteritis. Contrast enhanced ultrasonography examination can distinguish between necrosis and disease classification.

USB02 Ultrasound, the Best 2

15:30-16:00 **GBR 104+105**

Chairperson(s):
Myoung Seok Lee *(Seoul National University Boramae Medical Center, Korea)*

15:30-15:33 (USB02-P1)

Tracing the Tardus Parvus: Unmasking Common Iliac Artery Stenosis as a Cause of Renal Allograft-Mediated Hypertension

Ahnee Mae Ahyong, Ferdinand Morabe
Department of Radiology, National Kidney and Transplant Institute, Philippines

BACKGROUND: Renal allograft-mediated hypertension is a well-recognized indicator of transplant renal artery stenosis (TRAS). However, not all cases are due to TRAS, as stenosis of the native aortoiliac vasculature can also present similarly. This highlights the crucial role of accurate Doppler imaging in establishing a definitive diagnosis.
CASE REPORT: A 46 year-old male patient underwent renal allograft transplantation in 2009. The patient had a recent rising trend in blood pressure and slightly elevated creatinine levels, prompting a renal allograft biopsy to rule out causes of graft dysfunction, such as rejection. However, a preliminary Doppler ultrasound prior to the biopsy revealed tardus parvus waveforms in the segmental arteries, raising suspicion for TRAS. Further Doppler evaluation of the main renal artery and right external iliac artery above the anastomosis, consistently demonstrated tardus parvus waveforms, suggesting a more proximal arterial pathology. In contrast, Doppler interrogation of the distal abdominal aorta and the left external iliac artery revealed normal triphasic, high-resistance waveforms. This pattern raised suspicion for a hemodynamically significant stenosis at a more proximal iliac artery segment, rather than isolated TRAS. Subsequent MR angiography confirmed a short-segment stenosis in the right common iliac artery. Digital subtraction angiography verified the lesion, and successful

balloon angioplasty with stenting was performed. Post-intervention Doppler ultrasound demonstrated normal waveforms of the renal allograft vessels, confirming resolution of the vascular compromise.

CONCLUSION: Transplant rejection is often the primary concern in patients presenting with hypertension and rising creatinine levels, prompting the need for a biopsy. However, a comprehensive Doppler ultrasound is essential beforehand to rule out vascular causes. This case highlights the importance of evaluating the proximal vasculature, as iliac artery stenosis can mimic TRAS. Early detection and intervention can prevent unnecessary procedures and help preserve graft function.

15:33-15:36 (USB02-P2)

The Value of Color Doppler Ultrasound in the Diagnosis and Management of Symptomatic Enhanced Myometrial Vascularity (EMV)

Inshirah Momin[1], Mittali Shah Patani[1], Asif Momin[3], Shenaz Momin[4]

[1]Department of Radiology, Bhatia General Hospital, India, [2]Department of Radiology, Bhatia General Hospital, India, [3]Department of Radiology, Head of Imaging Bhatia Hospital, India, [4]Department of Radiology, BYL NAIR HOSPITAL and TN Medical College Mumbai, India

The use of color doppler is an important tool to evaluate patients with abnormal bleeding after induced or spontaneous abortion. Color doppler is diagnostic of the presence of intense and turbulent focal myometrial vascularity known as enhanced myometrial vascularity (EMV), which appears to be an acquired AV malformation. The presence of this sign suggests a trophoblastic type of flow in patients with positive beta hcg value. These were treated with intramuscular methotrexate injection with follow-up US showing complete resolution of this EMV as well as sympotomatic relief from abnormal bleeding. As documented in some reported cases of EMV, spontaneous remission is known, but after many weeks, hence, elective treatment in our cases allowed patients to be symptom-free earlier rather than anticipating delayed spontaneous remission. Angiographic embolization and ultrasound-guided D&C are also available but more invasive and expensive options. Thus, color doppler US (transabdominal or transvaginal) proves to be the best available modality in the diagnosis and management of these cases. It helped relieve these patients from the anxiety and stress by documenting absent EMV in the follow-up scans.

15:36-15:39 (USB02-P3)

The Role of Ultrasound in the Detection of Urothelial Carcinoma in Low-Resource Settings

Karen Tehani San Pedro, Maria Regina Cruz-tuble

Department of Radiology, National Kidney and Transplant Institute, Philippines

Urothelial carcinoma, the most common type of urinary bladder cancer, is a significant cause of morbidity and mortality worldwide. While the diagnosis of urothelial carcinoma is confirmed through cystoscopy with biopsy, ultrasound plays a significant role in the initial work-up for hematuria, particularly in low-resource settings. This is a case of a 36-year old Filipino male with a three-month history of intermittent hematuria. Ultrasound of the kidneys and urinary bladder was done, which revealed an adequately distended urinary bladder with thickened and irregular walls. Of note was an irregular, heterogeneous, predominantly echogenic mass with polypoid, papillary, and frond-like extensions arising from the posterior and left posterolateral wall of the urinary bladder, measuring approximately 5.6 x 7.3 x 5.3 cm. This mass demonstrated extensions to the right posterolateral urinary bladder wall. Color Doppler interrogation likewise showed marked internal vascularity. Floating medium-level echoes were also seen within the urinary bladder lumen. Kidneys with normal in size and echogenicity, with mild dilatation of the bilateral collecting systems. The main impression was an irregular urinary bladder mass which was likely neoplastic in etiology. A triphasic whole abdominal CT scan was then carried out for further evaluation of extent, confirming involvement of the bilateral ureterovesical junctions with resultant ureteropelvocaliectasia. Cystoscopy with transurethral resection of the tumor was

done, which was proven to be high-grade invasive urothelial carcinoma on histopathology. Patient was eventually discharged improved. This case highlights the role that ultrasound may play in the diagnosis of urothelial carcinoma, offering an accessible, low-cost, and non-invasive alternative for the initial detection of suspicious lesions. For this young patient, detection via ultrasound facilitated timely intervention and vastly improved clinical outcome.

15:39-15:42 (USB02-P4)

The Great Escape With Good Steal: A Case Report of an Arteriovenous Fistula of the Arm With Thrombi, Collaterals and Steal Phenomenon in a Chronic Kidney Disease Patient

Ma Katrina Villanueva
Department of Radiology, National Kidney and Transplant Institute, Philippines

INTRODUCTION: Chronic kidney disease (CKD) is a worldwide health crisis. In the Philippines alone, approximately one Filipino is affected every hour. For these patients, dialysis is a treatment option. Arteriovenous fistula (AVF) is the vascular access of choice for patients undergoing hemodialysis because compared with central venous catheters and grafts, AVFs last longer and are associated with fewer complications.

CASE: A CKD patient since 2017, and on hemodialysis via right arm AVF since 2020, presented with mild right arm swelling for two weeks. On Doppler ultrasound, it showed a patent distal brachial artery to cephalic vein AVF with adequate blood flow, but with partial steal at the distal brachial artery outflow. Multilevel segmental dilatation of the cephalic vein, with multiple thrombi and reverse flow in the forearm cephalic vein, with collateral formations are likewise noted.

DISCUSSION: Steal phenomenon is reversal of blood flow through the arterial segment distal to the vascular access, which can lead to ischemia. Thrombus in an AVF can cause impaired dialysis access, pain, swelling, and distal ischemia. However, this patient only had mild arm swelling with no signs of ischemia and had unremarkable hemodialysis sessions. This may be due to several collateral vessels, reversal of flow in the forearm cephalic vein and presence of partial steal that the blood flow is being redirected and does not cause severe pressure to the distal extremity.

CONCLUSION: Doppler ultrasound is a non-invasive imaging modality that can be used to examine the morphologic and functional status of vascular accesses. It could assess flow volume measurement and detect complications for appropriate management.

15:42-15:45 (USB02-P5)

A Case Report of Ductal Carcinoma of the Breast Metastasizing to the Ipsilateral Axillary Lymph Node

Khishgee Tsolmon
Department of Radiology, Mongolian National University of Medical Sciences, Mongolia

Invasive ductal carcinoma starts in cells that line the milk ducts in your breast. It can spread from your milk duct to surrounding breast tissue. accounts for about 80% of all breast cancer cases in women. From there, the cancer can get into your bloodstream or lymphatic system and spread to other areas of your body. Axillary lymph node metastases (ALN) are important predictors of future prognosis in breast cancer patients. We report a case of ductal carcinoma metastasizing o the Ipsilateral axillary lymph node. On ultrasound imaging, it has suspected l.nodes in left axillae, left side perivascular area in neck. On contrast chest computed tomography, it has impression well defined, slightly hyperdensive, soft tissue density mass like lesion in left axillary region, multiple lymphadenopathies in left neck regions, well defined, soft tissue density nodular like lesion in left breast. Pathological examination revealed metastatic carcinoma in axillary lymph node, left breast mass, invasive ductal carcinoma ER (-), PR (+) <10%, HER2 (-); cervical lymph node left V, Positive for malignancy, adenogenic tumor.

15:45-15:48 (USB02-P6)

Cesarean Scar Endometriosis: A Case Report with Ultrasound and CT Imaging Features

Munkh-Uyanga Boldbaatar[1], Otgonchimeg Ishdorj[1], Enkhmaa Altantsog[1], Sumiyabazar Boldoo[1], Aisulu Byekbolat[2], Ankhzaya Batmunkh[1]
[1]*Department of Radiology, Rehamed Hospital, Mongolia,* [2]*Department of Radiology, MNUMS MDI, Mongolia*

BACKGROUND: Cesarean scar endometriosis (CSE) is a rare but significant cause of anterior abdominal wall masses in women with a history of Cesarean sections. It typically presents as a painful swelling near the surgical scar, with symptoms exacerbating cyclically during menstruation. Due to its nonspecific presentation, imaging plays a crucial role in differentiating CSE from other post-surgical masses.

CASE PRESENTATION: We report the case of a 40-year-old woman, gravida 3, para 3, who presented with a gradually enlarging, painful mass at the left edge of her Cesarean section scar. The pain had progressively worsened over two years, with noticeable cyclic exacerbation. On physical examination, a tender, firm, and well-defined mass approximately 1.5 cm in diameter was palpated near the lower abdominal wall at the left edge of the surgical scar. Grayscale ultrasound confirmed the presence of a well-circumscribed, hypoechoic lesion within the subcutaneous tissue. Color Doppler showed increased vascularity, suggestive of active endometrial tissue. Computed tomography (CT) demonstrated a hyperdense, soft-tissue lesion adjacent to the rectus abdominis muscle with mild post-contrast enhancement without evidence of deep tissue invasion or involvement of surrounding structures. The patient underwent total surgical resection of the lesion, and histopathological analysis confirmed the diagnosis of CSE. Hormonal therapy options were discussed for symptom management, and the patient was informed about the risk of recurrence. At her six-month follow-up, she remained symptom-free, with no evidence of recurrence.

CONCLUSION: CSE should be considered in women presenting with an anterior abdominal wall mass following Cesarean delivery, mainly if symptoms are cyclical. Ultrasound is the first-line imaging modality, while CT provides valuable information for further lesion characterization. Early recognition, accurate imaging, and timely intervention are essential for optimal patient outcomes.

15:48-15:51 (USB02-P7)

The Role of Ultrasound in First Episode of Urinary Tract Infection in Females – A Case Report

Xanicia Long[1], Kanak Naidu[2]
[1]*Department of Family Medicine, National Healthcare Group, Singapore,* [2]*Department of Emergency Medicine, Khoo Teck Puat Hospital, Singapore*

It is reported that 1 in 3 women have their first episode of UTI by their mid-20s. UTI can be suspected from history and physical examination, and urine studies can be used to confirm diagnosis. No imaging studies are indicated in uncomplicated cystitis. We report a case of a 48 year-old lady with no past medical history presenting to the emergency department with fever, chills and dysuria. Her temperature was 39°C but the rest of her vitals were stable. Physical examination revealed a soft abdomen with no palpable masses, renal punch was equivocal. Urine analysis showed pyuria and microscopic hematuria, urine culture showed mixed bacterial growth. She had no history of UTI. Ultrasound scan showed a 4.6 cm×5.2 cm×4.7 cm echogenic mass with internal vascularity in the upper pole of her right kidney. CT kidneys showed hyper vascular soft tissue and macroscopic fat of -1024 Hounsfield suggestive of angiomyolipoma (AML). There was surrounding peri-renal fat stranding without features of rupture or haemorrhage. Her symptoms resolved after a course of cephalosporin and she was given an outpatient specialist follow-up. Swapnil N. et al. reported a case of superimposed pyelonephritis and cystitis in a patient with renal AML. Monge Mirallas JM et al. reported a case of renal AML in a young female presenting with fever, chills, and flank pain with positive renal punch; histology of excised lesion showed granulomatous changes suggestive of chronic inflammation. M. Bide et al. reported a case of renal AML presenting as isolated high-grade fever which resolved post-excision of the lesion, suggesting

a possible correlation. Hence while imaging is not routinely performed in uncomplicated first-episode UTIs, we propose that a bedside ultrasound (moreover being a time-saving and cost-efficient scan) would be a simple yet helpful preliminary imaging in all UTI cases to prevent missing genitourinary lesions which might present atypically.

USB03 Ultrasound, the Best 3

10:30-11:00 **GBR 104+105**

Chairperson(s):
Seungchul Han *(Samsung Medical Center, Korea)*

10:30-10:33 (USB03-P1)

Ultrasound and Computed Tomography in the Diagnosis of Hepatocellular Carcinoma Complicated by Hepatogastric Fistula

Bat-Erdene Battseren[1], Badamsed Tserendorj[1], Delgertsetseg Davaa[1], Davaasuren Baasandorj[2], Telmen Munkhjargal[2], Uugantuya Purevdorj[3]
[1]Department of Radiology, Third State Central Hospital of Mongolia, Mongolia, [2]Department of Radiology, Third State Central Hospital of Mongolia - residency, Mongolia, [3]Department of Radiology, Mongolian National Unerversity of Medical Sciences - residency, Mongolia

CLINICAL CASE: Patient D.S., an 82-year-old female, presented with complaints of fatigue and weakness, poor appetite, and limited food intake (barely consuming meat). She reported unintentional weight loss, mild chills, and general body discomfort in the evening, which improved after taking ibuprofen. Physical examination revealed slight tenderness in the upper abdomen and occasional heartburn. Anamnesis morbi: In 2023, the patient was diagnosed with liver cancer and underwent two sessions of transarterial chemoembolization in June and July 2023. In November 2024, due to persistent symptoms, the patient was hospitalized for one week at Bayanzurkh District Hospital; however, the symptoms did not improve. On February 7, 2025, the patient presented to the Emergency Department of the Third State Central Hospital of Mongolia and underwent the following tests. Lab Analysis (2025.02.07): alb-27.8 g/l (↓) Total protein-49.6 g/l (↓) C-reactive protein (CRP)-58.28 mg/L (↑) Urea-8.8 mmol/L (↑) WBC-15.96 10*9/L (↑) Neut%-84.7% (↑) Sedimentation rate-47 mm/hour (↑) B-R-A-H-M-S PCT-0.31 ng/mL (↑) Abdominal ultrasound (2025.02.07): A 91 × 80 mm heterogeneous mass with vascularization on color Doppler was detected, protruding outward from liver segment S4. CECT (2025.02.07): The diagnosis of a liver-gastric fistula caused by hepatocellular carcinoma has been confirmed by Computed Tomography after oral administration of contrast media: The contrast agent appears to have migrated from the stomach's antrum into the cavity of the liver mass, suggesting the formation of a hepato-gastric fistula The patient is elderly, and the risk of surgical treatment is high. Currently, palliative care is being provided at the National Cancer Center.

CONCLUSION: Hepatogastrointestinal fistulas resulting from the spread of hepatocellular carcinoma are rare but should be closely monitored in patients with large tumors near the gastrointestinal tract or those with tumors that have grown outward.

10:33-10:36 (USB03-P2)

Decreasing Mortality Risk in Hepatic Abscesses – The Value of Ultrasound in Early Recognition and Percutaneous Drainage

Karen Tehani San Pedro, Maria Regina Cruz-tuble
Department of Radiology, National Kidney and Transplant Institute, Philippines

While considered rare worldwide, hepatic abscesses are more common in low-resource settings and developing countries. As a liver abscess carries significant mortality risk in untreated patients, prompt recognition of this pathology via sonography will lead to earlier intervention and better clinical outcomes. This is a case of a 74-year old Filipino male who came in with a 6-day history of high-grade fever, associated with loss of appetite and episodes of decreased sensorium. Prior to going to the emergency room, patient had chills and generalized body weakness. Emergency whole abdomen ultrasound was done, which revealed a large, heterogeneous, septated, predominantly hypoechoic focus with anechoic components in the left liver lobe, measuring approximately 6.0 x 6.2 x 3.4 cm. No internal vascularity was seen on color Doppler study. The primary consideration was a hepatic abscess. A triphasic CT scan was done which showed a complex, multiloculated, multiseptated focus with thick, enhancing walls occupying segments 2, 3, and 4A. Ultrasound-guided pigtail catheter insertion was done, which yielded purulent output. Final culture studies showed broth positive results for Staphylococcus epidermidis. The patient underwent antibiotic medication and serial follow-up on ultrasound, which revealed decreasing size of the hepatic abscess at 2.8 x 2.8 x 2.8 cm on Day 6 post-pigtail insertion. A follow-up ultrasound done one month post-pigtail insertion showed complete resolution of the abscess collection. The value of sonography in quickly and accurately identifying intraabdominal solid organ pathologies which may have otherwise been clinically enigmatic cannot be discounted. In this case, the quick identification of the liver abscess allowed for timely medical and surgical intervention for this elderly patient. Ultrasound likewise played a major role in gaining access for percutaneous drainage and in its follow-up and eventual resolution.

10:36-10:39 (USB03-P3)

Peroneal Brevis Tendon Passes Under the Peroneal Trochlea at the Lateral Hindfoot: A Case Report

Kwang Jae Lee, Yong-Soon Yoon, Hanna Kim
Department of Rehabilitation Medicine, Presbyterian Medical Center (Jesus Hospital), Korea

INTRODUCTION: Paroneus brevis (PB) is a short muscle that lies in the lateral part of the lower leg deep to the Peroneus longus (PL) around the ankle joint. When tendons of the PB and PL pass the hind foot, they are divided at the peroneal trochlea so PB tendon passes over it and PL tendon passes under it. Present case shows different pathway of PB tendon and there was no informed articles about it, so we report this anomalous tendon running.

CASE: This 29-year-old female patient was suffering from foot pain in the right side about 2 months during walking without definite trauma. Pain was evoked during active ankle eversion and there was focal tenderness around the peroneal trochlea and numeric rating scale (NRS) was 5 during walking. There were no abnomal findings in weight bearing AP and Lateral foot plain radiographs. US images showed thickened PB tendon passing underneath the peroneal trochlea attaching to the styloid process of the 5th metatarsal base. it passed over the peroneal trochlea in the left side. She felt pain during the probe traced over the peroneal trochlea which is the usual size and location in the calcaneal bone. We injected steroid peritendon area around the trochlea and pain was subsided (NRS 1 during walking) checking in 2 weeks of injection. But we warned her that pain woud be elicited even with your daily activities due to anatomic variant of the PB tendon. This kind of anatomic variant should make PB tendon be more susceptible to the friction injury about the peroneal trochlea.

CONCLUSION: This present case shows anatomic variant of the PB tendon which passes under the peroneal trochlea and it could be the pain source due to PB tendinopathy during walking. We report a rare anatomic variant of PB tendon pathway.

10:39-10:42 (USB03-P4)

Acute Acalculous Cholecystitis

Saindelger Batbaatar
Department of Radiology, Allergy Med Hospital, Mongolia

BACKGROUND: Acute Acalculous cholecystitis is an acute inflammation of the gallbladder that occurs without gallstones. It usually occurs in critically ill patients, but it has also been implicated as a cause of cholecystitis in previously healthy individuals. It accounts for about 5-10% of acute cholecystitis cases.
A CASE OF REPORT: A 69-year-old male presented with abdominal pain in the upper right quadrant, fever, and nausea that started 3 days ago. He has a history of heart disease and high blood pressure and has been hospitalized for extended periods in recent years for treatment. Ultrasonography- gallbladder wall thickening 5.6 cm, wall edema, gallbladder distention-5.9 cm, sludge in the lumen.
CONCLUSION: 1. Ultrasound imaging is the first choice due to its availability, lack of radiation, high resolution for diagnosis, differential diagnosis, staging, establishment of a role in interventional management, follow-up, and screening to assess the prevalence of abdominal. 2. Acute Acalculous cholecystitis occurs without gallstones, so ultrasound is crucial in confirming the absence of stones and distinguishing it from calculous cholecystitis, which is caused by gallstones. 3. Detecting Complications - Ultrasound helps in identifying complications like gangrene, perforation, or abscess formation, enabling timely intervention to prevent severe outcomes. 4. Guiding Further Diagnostics - Ultrasound results are unclear, the decision to perform other imaging tests like CT scan or HIDA scan for more detailed information.

10:42-10:45 (USB03-P5)

From Start to Finish: The Role of Ultrasound in the Diagnosis and Management of Portal Vein Thrombosis

Tanya Katherine Cinco, Maria Regina Cruz-Tuble
Department of Radiology, NKTI, Philippines

Portal vein thrombosis is defined as partial or complete obstruction of blood flow in the portal vein, due to the presence of a thrombus in the vasal lumen. It is a common consequence of a variety of diseases that alter coagulation status. Chronic portal vein thrombosis can eventually lead to cavernous transformation of the portal vein, portal hypertension, and the development of varices, which can potentially be life-threatening. Ultrasound may be used as first-line imaging for the diagnosis of portal vein thrombosis, with a specificity reaching up to 95%. Due to its low-cost and safety, subsequent follow-ups for cases of portal vein thrombosis may utilize ultrasound to monitor extent and treatment response. A 55 year-old male, diagnosed case of myeloproliferative neoplasm, consulted for increasing abdominal pain. Abdominal Doppler ultrasound was done, demonstrating a normal-sized liver and a non-dilated main portal vein. Color Doppler study of the portal vein, however, showed absent flow in the main portal vein. The left and right portal veins were not delineated. Multiple tortuous vessels were noted along the course of the portal vein, highly suggestive of cavernous transformation. Increased peak systolic velocities were noted in the hepatic arteries, consistent with hepatic artery buffer response. There was also note of an enlarged spleen with multiple splenic varices, likely secondary to portal hypertensive changes. Abdominal ultrasound color Doppler imaging has a 98% negative predictive value, and is considered the imaging modality of choice in diagnosing portal vein thrombosis. Anti-coagulation therapy may commence once the diagnosis has been made, and subsequent follow-ups may utilize ultrasound in monitoring treatment response.

USB04 Ultrasound, the Best 4

15:00-15:20 **GBR 104+105**

Chairperson(s):
Hee Mang Yoon *(Asan Medical Center, Korea)*

15:00-15:03 (USB04-P1)

Postoperative Recurrence of a Yolk Sac Tumor in a Pediatric Patient With Immature Testicular Teratoma

Huiyong Hu, Haorong Zhang, Hairong Wang
Department of Radiology, Shanghai Children's Hospital, Shanghai Jiao Tong University, School of medicine, China

BACKGROUND: Pediatric testicular tumors are an uncommon solid entity. This case report describes the ultrasound diagnosis and management of a rare instance of recurrent yolk sac tumor following surgical intervention for an immature testicular teratoma in a child, highlighting the distinctive features of recurrence and the pivotal role of ultrasound surveillance in such scenarios.
CASE PRESENTATION: A 3-month-old boy presented with a 5-day history of cough and hoarseness, accompanied by 2 days of wheezing. Physical examination inadvertently revealed a left scrotal mass. Scrotal ultrasound imaging revealed a heterogeneous mass within the left testis, measuring 14×13×12 mm, with well-defined margins, a partial anechoic area, and internal hyperechoic foci. Color Doppler imaging indicated hypovascularity within the mass. Preoperative alpha-fetoprotein (AFP) levels were elevated at 65.58 ng/ml. Testis-sparing surgery was performed, and pathology confirmed an immature teratoma containing neural tube structures within a 40x field of vision. Fourteen months postoperatively, the left scrotum began to enlarge progressively. Ultrasound examination identified an oval hypoechoic mass measuring 20×13×15 mm, devoid of calcification and liquefaction, with abundant blood flow signals on Doppler imaging. Spectral Doppler confirmed hypervascularity, suggestive of a malignant tumor, likely a yolk sac tumor. Preoperative AFP levels were 16.17 ng/ml. The patient underwent a radical orchidectomy, and pathology confirmed the diagnosis of yolk sac tumor. The child's postoperative vital signs were stable, with a favorable outcome during follow-up.
CONCLUSION: Recurrence of pediatric testicular tumors is a rare occurrence. Compared to patients with mature teratomas, those with immature teratomas are at a higher risk of recurrence. This necessitates a more meticulous management approach, including tumor marker monitoring and regular ultrasound follow-up to ensure timely detection and appropriate treatment of recurrence.

15:03-15:06 (USB04-P2)

Microvascular Imaging (Advanced Dynamic Flow) for Detection, RFA Planning, Post-RFA Evaluation of Recurrent Thyroid Cancer

Jae Ho Shin
Department of Radiology, Korea University Anam Hospital, Korea

For effective radiofrequency ablation (RFA) of recurrent thyroid cancer, (1) accurate detection, (2) RFA planning, and (3) Post-RFA evaluation with microvascular imaging such as advanced dynamic flow (ADF) are crucial. In terms of accurate detection, ADF sensitively identifies abnormal vascular signals of the recurrent thyroid cancer, differentiating from reactive lymph nodes, and increasing conspicuity of the tumor borders. In terms of RFA planning, ADF provides tumor's overall vascularity, adjacent vascularity, and feeder information for proper voltage settings, thereby improving technical success. In terms of post-RFA evaluation, ADF evaluates technical efficacy by assessing the ablated vessels and neovascularization. In the following presentation, three cases of recurrent thyroid cancer (papillary thyroid cancer [PTC], medullary thyroid cancer [MTC]) are discussed and the importance of ADF in each case. First case was a 70s-male patient with recurrent PTC, in which grey scale had limitations in delineating clear demarcations of the recurrent PTC within muscle echotexture. However, ADF improved visualization and correct targeting of the recurrent PTC. Second case was a 40s-male patient with recurrent PTC at right neck level III, in which

ADF provided feeder information and abnormal vascularity information of the recurrent PTC for RFA planning. Immediate post-RFA demonstrated complete ablation of the feeders and abnormal vascularity on ADF. The last case was a 40s-male patient with recurrent MTC at left supraclavicular region. 18F-DOPA (18F-dihydroxyphenylalanine) PET/CT and ADF correctly localized the recurrent MTC (arrows), and ADF provided useful vascularity information. Hydrodissection-assisted RFA was successfully and safely performed utilizing the 3 mm active electrode. After 1 month, ADF demonstrated approximate volume reduction of 80% and complete obliteration of the abnormal vascularity.

15:06-15:09 (USB04-P3)

Ultrasound Detection and Aspiration of Milk of Calcium in Juvenile Dermatomyositis: A Case Report

Jae-Yeon Hwang, Jung-Eun Cheon,
Young Hun Choi, Seunghyun Lee, Yeon Jin Cho,
Jae Won Choi, Seok Young Koh
Department of Radiology, Seoul National University Hospital, Korea

Juvenile dermatomyositis (JDM) is an autoimmune inflammatory myopathy that may lead to soft tissue calcinosis, a debilitating complication characterized by dystrophic calcium deposition. Milk of calcium, a rare form of calcinosis, may mimic cystic soft tissue lesions, making imaging-based differentiation essential for accurate diagnosis and treatment. This case demonstrates ultrasound's role in precise lesion characterization and procedural guidance, facilitating successful intervention in a patient with JDM-associated refractory calcinosis. A 15-year-old male with JDM and progressive soft tissue calcifications presented with right upper arm swelling, pain, and restricted movement. MRI revealed multiple T2 hyperintense, T1 hypointense lesions with peripheral rim enhancement, primarily along the anterior biceps and triceps muscles, suggesting calcinosis with possible milk of calcium collection. CT further delineated multiple soft tissue and fascial calcifications with associated fluid-containing structures. Ultrasound provided definitive lesion characterization, demonstrating a heterogeneous fluid collection with internal echogenic foci, floating debris, and sedimentation, confirming the presence of milk of calcium. Posterior acoustic shadowing confirmed calcific material, while surrounding soft tissue thickening suggested an inflammatory response. Given the patient's persistent symptoms, ultrasound-guided aspiration was performed, yielding thick, yellowish fluid with calcium sediment, leading to symptom resolution. This case demonstrates the essential role of ultrasound in both diagnosis and intervention. Unlike MRI and CT, ultrasound enabled real-time, high-resolution assessment of the fluid component, allowing for accurate differentiation from solid calcinosis and guiding a targeted procedure. Early ultrasound evaluation can enhance diagnostic confidence, procedural success, and overall management of soft tissue calcinosis in JDM.

15:09-15:12 (USB04-P4)

Common Carotid Artery–Internal Jugular Vein Fistula – A Rare Complication of Central Venous Catheterization

Karen Tehani San Pedro, Maria Regina Cruz-tuble
Department of Radiology, National Kidney and Transplant Institute, Philippines

Central venous catheterization is a mainstay of management for quick hemodialysis access in renal failure patients, aside from other clinical uses such as rapid fluid and medication infusion, monitoring, and interventional access. This procedure, however, comes with risks of complications of vascular, cardiac, or pulmonary nature. One rare complication is the inadvertent creation of a fistulous connection between two large vessels, which may require surgical intervention if not promptly recognized and if growth is left unchecked. This is a case of a 56 year old Filipino male, known Chronic Kidney Disease secondary to Diabetes Mellitus, who underwent emergency right internal jugular vein catheterization one month prior for initiation of emergency hemodialysis. A few days prior to consult, blood was noted leaking on the catheter site while ongoing hemodialysis. Physical examination

revealed a palpable thrill at the right cervical region near the puncture site. Neck Doppler ultrasound was requested which revealed a 0.4 cm-wide tract connecting the proximal right common carotid artery and the proximal right internal jugular vein. Heterogeneous, iso-to-hypoechoic foci partly line the tract and slightly extend into the common carotid artery and internal jugular vein lumens, likely representing partial thrombosis. Alongside these thrombi, Doppler imaging revealed a patent anechoic tract approximately 0.1-0.2 cm-wide with color bruit artifact and high-velocity flow, connecting the two vessels. The diagnosis of a patent common carotid artery-internal jugular vein arteriovenous fistula with partial thrombosis was made. Neck CT angiography was done which confirmed these findings. Follow-up CT angiography after two weeks showed decrease in the size of the fistula, and patient was discharged improved. While a common clinical practice, one must be aware and wary of the complications of central venous catheterization. Ultrasound provides quick, safe, and effective evaluation of possible complications, and monitoring to determine the need for further intervention.

Abdomen

SE-001

A Case of Diaphragmatic Lipoma Initially Misdiagnosed as a Hepatic Tumor

Yasushi Seki
Department of Radiology, IKEDA City Hospital, Japan

While lipoma is a common soft-tissue tumor which can develop in any area of the body, lipomas of diaphragmatic origin are not commonly encountered in routine clinical practice. Herein, we report a case of diaphragmatic lipoma initially suspected to be a hepatic tumor in a screening ultrasound examination. A 57-year-old male who had undergone abdominal ultrasound as an ordinary health check-up was referred to our hospital for further evaluation of a tumor which appeared to reside in the left hepatic lobe. The patient had no symptoms or complaints. Blood tests showed no elevation of relevant tumor markers. Our ultrasound examination revealed that a 72×75-mm tumorous lesion was observed outside but adjacent to the left hepatic lobe. The tumor showed heterogeneously high internal echogenicity, with no blood flow signals as observed by color Doppler sonography. Furthermore, the tumor slided with respiration over neighboring structures such as the liver and the anterior wall of the stomach; while it firmly attached to the diaphragm. Based on these ultrasonographic findings, the tumor was speculated to be a lipoma originating from the diaphragm. Likewise, plain and contrast-enhanced (CE-) CT images showed a decreased CT value (-111 HU) and hypovascular nature of the tumor, which were consistent with the features generally observed in lipoma. CE-CT also demonstrated a branch of inferior diaphragmatic artery passing thorough the tumor margin, suggesting the diaphragmatic origin of the tumor. The patient underwent laparotomy with tumor removal, which led to the pathological diagnosis of diaphragmatic lipoma. In the current case, real-time ultrasound observation of positional shift with respiration between the tumor and its surrounding structures enabled an accurate determination of the tumor location. In addition,

surgical removal of the tumor allowed to exclude morphologically similar malignant neoplasms including liposarcoma, which led the definitive diagnosis.

SE-002

A Rare Case of Liposarcoma in Retroperitoneal Space

Dorjkhand Ichinkhorloo
Department of Radiology, Mongolian National University of Medical Sciences, Mongolia

INTRODUCTION: The incidence of retroperitoneal liposarcoma is 2.5 per million people, making it an uncommon tumor. It is challenging to make an early diagnosis because there are no particular clinical symptoms. They typically require long-term and frequently indefinite follow-up because they are linked to a high rate of recurrence even after anatomically complete resection.This case study describes a patient who underwent total surgical resection as treatment for retroperitoneal liposarcoma.

CASE REPORT: A 34-year-old male has no symptoms and checked routine abdominal ultrasound, there was a mass in posterior to the right kidney. The texture was heterogeneous, 6.5 x 3.5 x 6.0 cm, with mildly irregular contour with few vascularities. In abdominal CT with contrast, PET-CT and MRI there were three lesions located in the lower to right lobe of the liver and para/supramesocolic and right paracolic spaces with heterogeneous texture and adipose tissue that supplied vascularity from surrounding muscle tissue. The surgical intervention is performed to resect the right retroperitoneal tumor, and histologically, the tumor is confirmed to be liposarcoma.

DISCUSSION: Fat, loose connective tissue, fascia, muscles, lymphatic tissue, or leftover embryonic tissue are the main sources of retroperitoneal tumors, of which 80% are malignant. Due to the extra-abdominal space's vast capacity, liposarcoma can grow without squeezing important organs, leading to an uncommonly early diagnosis. When the retroperitoneal liposarcoma does show clinical symptoms, it has typically spread to engulf adjacent organs and become massive. Most retroperitoneal liposarcomas (>75%) present "late," with substantial size. Fortunately, the patient's tumor in this case report was less than 10 cm and was found incidentally, meaning it wasn't large enough to compress other organs. As a result, it's critical to concentrate on the surrounding tissues of essential organs when doing a routine abdominal ultrasound examination.

SE-003

Acute Cholangitis Caused by Choledocholithiasis and Common Bile Duct Ascariasis: A Case Report

Saranchimeg Boldbaatar, Erdenesuren Dashzeveg, Munkh-Orgil Rentsensambuu, Erdenebulgan Batmunkh
Department of Radiology, The Second State Central Hospital, Mongolia

Ascaris lumbricoides infecting the is CBD relatively rare. However, in some cases, after the infection is acquired, the Ascaris can migrate from the small intestine into the bloodstream and then enter the biliary system. This may lead to the formation of stones in the bile ducts, obstruction, or even cause acute cholangitis. A 22-years-old man was presented at our emergency department with complaints of abdominal pain, vomiting with yellow-green color, and nausea. The symptoms started 4 days ago. This male herder. Physical examination revealed a pulse rate of 73 beats/min, respiratory rate of 17 breaths/min, and blood pressure of 147/82 mmHg. Laboratory tests were leukocytosis, biochemical tests ALP, BILD, GGT and ALT were elevated.

ULTRASOUND EXAMINATION: The bile ducts inside and outside the liver are dilated up to 0.8 cm in size. In the gallbladder, there is a stone of 0.8 cm in size in the body portion. The CBD is dilated to 1.0 cm.

MRCP: The gallbladder measures 9.2x2.7 cm, with a wall thickness of 0.4 cm. The bottom part of the gallbladder contains a stone with a diameter of 0.3 cm, with reduced T2 signal intensity. The bile is thick and contains sediment. The CBD is dilated up to 1.3 cm, with a stone measuring up to 0.9 cm and

multiple stones with reduced T2 signal intensity. MRCP and ultrasound are more sensitive to acute cholangitis caused by choledocholithiasis and CBD ascariasis. Although ultrasound is highly sensitive for acute cholangitis detection and follow-up and can be used as an initial screening, its further use is limited. Therefore, MRCP is the most suitable diagnostic tool for acute cholangitis. Timely diagnosis of acute biliary stasis is crucial for the patient's prognosis. We present a case where we promptly diagnosed and removed Ascaris lumbricoides and a stone from the common bile duct using the ERCP method.

SE-004

AI-Guided Ultrasound and Epigenetic Analysis of Hepatic Fibrosis: A Multi-Omics Deep Learning Model for Predicting Fibroblast Plasticity and Cirrhotic Progression in Non-Alcoholic Steatohepatitis

Sahnaz Vivinda Putri[1], Rini Winarti[2], Prihantini Prihantini[3], Rifaldy Fajar[3]
[1]Health Management Laboratory, International University Semen Indonesia, Indonesia, [2]Department of Biology, Yogyakarta State University, Indonesia, [3]Mathematical and Computational BioMedicine Research Group, The Integrated Mathematical, Computational, and Data Science for BioMedicine Research Community Foundation, Indonesia

BACKGROUND / AIM: Non-Alcoholic Steatohepatitis (NASH) is a major cause of progressive liver fibrosis, but current diagnostic tools fail to capture fibroblast plasticity, a key driver of antifibrotic treatment resistance. This study applies an AI-based multi-omics fibrosis model integrating ultrasound shear wave elastography (SWE), single-cell transcriptomics, and epigenomics to estimate fibroblast reprogramming and cirrhotic transition risk non-invasively.
METHODS: This study utilized datasets from the UK Biobank Liver Imaging Study (N ≈ 1,800) and the National Institute of Diabetes and Digestive and Kidney Diseases (NIDDK) Liver Tissue Cell Distribution System (LTCDS) (N ≈ 1,900) for SWE and MRI-based liver stiffness assessment, Human Liver Single-Cell Atlas (GSE136103) and NASH scRNA-seq datasets (GSE162694) for fibroblast state profiling, and NIH Roadmap Epigenomics Project and Blueprint Epigenome Project for chromatin accessibility and enhancer modifications. Deep contrastive learning (Vision Transformer + ResNet50) extracted SWE-derived stiffness maps, while graph-based modeling predicted fibrosis progression. AI-assisted single-cell trajectory inference identified fibroblast-to-myofibroblast transitions, and enhancer-target analysis mapped epigenetic fibrosis markers. A deep learning fusion model integrating stiffness, transcriptomic, and epigenomic features was trained and validated using 5-fold cross-validation.
RESULTS: The model achieved AUROC = 0.86 (95% CI: 0.83–0.89), sensitivity 87.4%, specificity 83.1%, and predicted fibroblast reprogramming 3.9 years before clinical fibrosis onset ($p < 0.0001$). Fibrotic transition probability >5.4% per year correlated with epigenetic fibroblast markers (Pearson $r = 0.76$, $p < 0.0001$), while TGFβ1 enhancer methylation predicted cirrhosis with 84.6% accuracy. Liver stiffness progression from 5.8 kPa to 8.4 kPa predicted cirrhosis with 82.7% accuracy, while enhancer H3K27ac loss correlated with fibrosis severity. Decision-curve analysis showed a +31.4% clinical benefit over standard fibrosis models.
CONCLUSIONS: This study supports AI-based ultrasound and epigenetic integration for early fibrosis prediction and treatment monitoring, offering a non-invasive approach to risk stratification and therapy guidance.

SE-005

Bibliometric Analysis of Machine Learning-Driven Ultrasound in Liver Cancer Diagnosis: Trends and Insights (2020-2025)

Rian Ka Praja, Reny Rosalina
Universitas Palangka Raya, Indonesia

Liver cancer, particularly hepatocellular carcinoma (HCC), remains a leading cause of cancer-related mortality worldwide. Ultrasound imaging, a widely used modality for liver cancer diagnosis, has witnessed transformative advancements through machine learning (ML) and artificial intelligence

(AI). This study conducts a bibliometric analysis of recent literature (2020-2025) to map research trends, key topics, and emerging themes in ML-powered ultrasound for liver cancer diagnosis. A bibliometric analysis was performed using Scopus, retrieving 134 relevant articles published between 2020 and 2025. VOSviewer 1.6.19 was employed for network visualization of key research themes, co-occurrence of terms, and collaboration networks. The analysis identified major research clusters centered on "deep learning," "machine learning," and "artificial intelligence" in ultrasound-based liver cancer diagnosis. "Contrast-enhanced ultrasound" and "convolutional neural networks" emerged as significant subfields. The integration of ML techniques in ultrasound images demonstrated advancements in feature extraction, classification, and computer-aided diagnosis. Recurrence prediction and prognosis assessment were notable research directions. Additionally, convolutional neural networks (CNNs) and ensemble learning models showed increased adoption for improving liver cancer detection and classification accuracy. The bibliometric insights reveal a growing research focus on ML-enhanced ultrasound for liver cancer diagnosis, emphasizing AI-driven feature extraction, classification, and prognosis prediction. Future research should address standardization, clinical validation, and real-world deployment of ML-based ultrasound applications for HCC detection. These findings contribute to understanding the evolving landscape of AI-powered ultrasound in liver cancer diagnostics and highlight key research gaps for further exploration.

SE-007

Cystic Echinococcosis of the Liver

Saindelger Batbaatar

Department of Radiology, Allergy Med Hospital, Mongolia

BACKGROUND: Hydatid cyst is a common name for the larval stage of a tapeworm species of Echinococcus granulosus which is transmitted from animals to humans via the fecal–oral route. Hydatid cysts of the liver are often asymptomatic and often represent an incidental finding on medical imaging. Mongolia is considered a high-endemic country for echinococcosis, with significant disease prevalence among both humans and livestock.

A CASE REPORTS: a 51-year-old male. who had Laparoscopic cholecystectomy 4 years ago. Six months after the surgery, an ultrasound revealed a liver cyst in the segment VII of the liver measuring 0.9x1.1 cm. The regularly with ultrasound every six months, but for the past two years, the patient did not undergo follow-up ultrasound exams. Over the past month, the patient experienced intermittent right-sided abdominal pain. Two days ago, he developed a more severe pain in the right upper abdomen along with a fever of 38°C. Ultrasonography- liver simple Cyst in the S-VII, VIII of the liver 9.0*7.2 cm size, anechoic, oval in shape, with regular margins. Simple Cyst /stage III/.

ABDOMINAL COMPUTED TOMOGRAPHY: The lesion is located in segments VII and VIII of the right lobe of the liver, measuring 9.5 x 7.3 cm, with a uniformly thick wall (wall thickness is 0.2 cm) and a fluid density content (7.0-8.7 HU). A right lobe resection of the liver has been performed.

CONCLUSION: - It is important to define the shape, size, and location of the cyst for diagnostic purposes. This helps to differentiate it from other conditions such as liver tumors, abcess Imaging studies (ultrasound, CT) typically used for this purpose. - As the cyst enlarges, it may rupture. If it ruptures, the fluid inside, which may contain blood, can cause anaphylactic shock (a severe allergic reaction).

SE-009

Endoscopic Ultrasonography (EUS) Compared with Magnetic Resonance Cholangiopancreatography (MRCP) in Diagnosing Patients with Malignancy Causing Obstructive Jaundice: A Systematic Review and Meta-analysis

Divo Helmizar[1], Roland H[2]
[1]*STAN, Indonesia,* [2]*Department of Internal Medicine, Siti Rahmah Islamic Hospital, Indonesia*

BACKGROUND: Malignant biliary obstruction leading to obstructive jaundice poses a significant diagnostic challenge in clinical practice. Endoscopic ultrasonography (EUS) and magnetic resonance cholangiopancreatography (MRCP) are widely used non-invasive imaging techniques for evaluating these cases. However, the relative accuracy of EUS compared to MRCP in diagnosing malignancy remains a subject of debate. This systematic review and meta-analysis aimed to compare the diagnostic performance of EUS and MRCP in detecting malignant causes of obstructive jaundice, focusing on their sensitivity, specificity, and overall efficacy.
METHODS: A comprehensive literature search was conducted in PubMed, Embase, Scopus, and Cochrane Library databases for studies published up to December 2024. Studies comparing the diagnostic accuracy of EUS and MRCP in patients with suspected malignant biliary obstruction were included. Pooled sensitivity, specificity, positive likelihood ratio (PLR), and negative likelihood ratio (NLR) were calculated. Heterogeneity was assessed using I^2 statistics. Data were analyzed using Review Manager 5.4.1.
RESULTS: A total of eight studies met the inclusion criteria. The pooled sensitivity and specificity of EUS were 93.1% (95% CI: 89.6%–95.3%) and 88.4% (95% CI: 85.5%–93.2%), respectively, while MRCP demonstrated a sensitivity of 83.5% (95% CI: 80.3%–89.7%) and specificity of 83.4% (95% CI: 78.8%–87.0%). The PLR was 8.87 (95% CI: 6.48–12.34) for EUS and 5.06 (95% CI: 3.88–6.78) for MRCP. Similarly, the NLR was lower for EUS (0.07, 95% CI: 0.03–0.12) compared to MRCP (0.16, 95% CI: 0.12–0.22). Moderate heterogeneity was observed across studies (I^2 = 42.8%).
CONCLUSION: EUS demonstrates superior diagnostic accuracy over MRCP for detecting malignant obstructive jaundice. It should be the preferred modality, especially when MRCP results are inconclusive. However, selection should consider patient factors, hospital facilities, and operator expertise. Further studies are needed to confirm these findings.

SE-011

Machine Learning-Driven Ultrasound Multi-Omics Profiling for Real-Time Prediction of Hepatic Stellate Cell Activation and Fibrotic Progression

Elfiany Syafruddin[1], Sahnaz Vivinda Putri[2], Rini Winarti[3], Prihantini Prihantini[4], Rifaldy Fajar[4]
[1]*Computational Science Research Laboratory, Bulukumba Muhammadiyah University, Indonesia,* [2]*Health Management Laboratory, International University Semen Indonesia, Indonesia,* [3]*Department of Biology, Yogyakarta State University, Indonesia,* [4]*Mathematical and Computational BioMedicine Research Group, The Integrated Mathematical, Computational, and Data Science for BioMedicine Research Community Foundation, Indonesia*

BACKGROUND / AIM: Liver fibrosis is a progressive condition leading to cirrhosis and hepatocellular carcinoma, yet early detection remains a challenge. Hepatic stellate cell (HSC) activation plays a central role in fibrosis, but existing clinical tools lack the ability to identify pre-clinical fibrotic transitions non-invasively. Shear wave elastography (SWE) assesses liver stiffness, while single-cell transcriptomics uncovers key molecular drivers of fibrosis. This study applies machine learning to integrate imaging, transcriptomics, and deep learning for early fibrosis risk stratification.
METHODS: SWE-based liver stiffness data were obtained from NHANES (N=1,100, FibroScan measurements). Single-cell RNA sequencing (scRNA-seq) data profiling HSC activation were sourced from GEO datasets (GSE158723, GSE132662, N=3,000 cells), while bulk liver transcriptomic data for fibrosis progression were retrieved from GTEx and Expression Atlas (N=1,200 samples). AI modeling included self-supervised deep learning

(Swin Transformer + ResNet50) for fibrosis-specific radiomic feature extraction and multi-modal transformers for integrating scRNA-seq data with liver stiffness measurements. Longitudinal fibrosis progression was modeled using recurrent neural networks (RNNs) and reinforcement learning. The model was trained on 960 patients (80%) and validated on 240 patients (20%), with performance evaluated using AUROC, sensitivity, specificity, and decision-curve analysis (DCA).

RESULTS: The model achieved AUROC = 0.84 (95% CI: 0.826–0.854), sensitivity = 78.6%, specificity = 79.1%, PPV = 74.2%, NPV = 82.9%. HSC gene expression patterns (COL1A1, ACTA2, TGFβ1) predicted fibrotic transition 2.6 years before clinical onset ($p<0.0001$). Liver stiffness threshold >6.8 kPa was predictive of cirrhotic progression (HR = 3.29, $p<0.0001$). Liver stiffness dynamics strongly correlated with fibrosis stage progression, confirming reproducibility across independent validation cohorts ($p<0.0001$). DCA indicated a +24.7% net clinical benefit over conventional fibrosis staging tools.

CONCLUSIONS: This analysis integrates ultrasound elastography, single-cell transcriptomics, and bulk RNA-seq to develop a real-time, non-invasive fibrosis prediction model, improving early risk assessment and guiding preventive antifibrotic interventions.

SE-012

The Impact of Ultrasound Quality Control on Liver Cancer Screening Outcomes: The Importance of Intercostal Scan Quality

Woo Kyoung Jeong, Yeun-Yoon Kim
Department of Radiology, Samsung Medical Center, Korea

BACKGROUND AND OBJECTIVES: Liver cancer ultrasound is an established surveillance method for high-risk populations, but diagnostic accuracy varies. To enhance the efficiency of surveillance tests, quality assessments of cancer screening imaging are regularly conducted in Korea. This study aims to identify factors influencing screening outcomes through analysis of recent evaluation data.

MATERIALS AND METHODS: This study analyzed imaging quality scores (total score, subcostal scan score, and intercostal scan score) from liver cancer screening institutions evaluated in 2024. Correlations between imaging quality scores and key screening outcome indicators, including cancer detection rate, interval cancer rate, and false-positive rate, were assessed.

RESULTS: A total of 2,378 medical institutions were analyzed. The median total score was 89 out of 100 (1Q=78; 3Q=97), the subcostal scan score was 40 out of 40 (1Q=32; 3Q=40), and the intercostal scan score was 20 out of 24 (1Q=14; 3Q=24). Cancer detection rates showed significant positive correlations with total and intercostal scan scores ($P=0.039$ and $P=0.016$, respectively). Interval cancer rates were negatively correlated with intercostal scan scores ($P=0.010$). However, false-positive rates exhibited positive correlations with the total and intercostal scan scores ($P=0.005$ and $P=0.013$, respectively).

CONCLUSION: Among the imaging quality parameters of liver cancer screening ultrasound, intercostal scan quality is significantly associated with key screening outcome indicators

SE-013

Ultrasound Liver Imaging Reporting and Data System Version 2017: A Systematic Review and Meta-Analysis

Sunyoung Lee[1], Ja Kyung Yoon[1], Jaeseung Shin[2], Anum Aslam[3], Aya Kamaya[4], Shuchi K Rodgers[5], Claude B. Sirlin[6], Victoria Chernyak[7]

[1]Department of Radiology, Severance Hospital, Korea, [2]Department of Radiology, Samsung Medical Center, Korea, [3]Department of Radiology, University of Michigan Medicine, United States, [4]Department of Radiology, Stanford University, United States, [5]Department of Radiology, Thomas Jefferson University, United States, [6]Department of Radiology, University of California San Diego, United States, [7]Department of Radiology, Columbia University Irving Medical Center, United States

BACKGROUND: The US Liver Imaging Reporting and Data System (LI-RADS) includes an assessment category (US-1, Negative; US-2, Subthreshold; and US-3, Positive) and a visualization score reflecting image quality (VIS-A, No or minimal limitations; VIS-B, Moderate limitations; and VIS-C, Severe limitations). The US-3 and VIS-C impact patient management.

PURPOSE: To establish the distributions of categories and visualization scores, estimate the proportions of HCC and overall malignancy in the US-3, and identify variables associated with the VIS-C by conducting a meta-analysis.

METHODS: A systematic search of articles published between January 1, 2017 and September 17, 2023 identified studies reporting distributions of US LI-RADS v2017 categories or visualization scores. Characteristics of the study design, patient cohorts, and outcomes of interest (distributions for US categories and visualization scores, percentages of probable or definite HCC and malignancy for US-3, and variables associated with VIS-C) were extracted. For the meta-analysis, estimates were established with random effects models.

RESULTS: Fifteen studies comprising 39,166 US examinations were included. Of all examinations, 89.7% (95% CI: 86.8, 91.8) were categorized US-1, 4.4% (95% CI: 2.8, 6.2) US-2, and 5.9% (95% CI: 4.1, 8.0) US-3. Of the US-3 examinations, 25.9% (95% CI: 17.1, 34.7) had probable or definite HCC and 26.4% (95% CI: 18.4, 34.5) had overall malignancy. Of all examinations, 59.7% (95% CI: 46.9, 67.8) were assigned VIS-A, 32.5% (95% CI: 21.9, 41.6) VIS-B, and 7.8% (95% CI: 2.8, 14.3) VIS-C. Obesity (OR, 2.37; 95% CI: 1.57, 3.59), nonalcoholic fatty liver disease (NAFLD) (OR, 2.24; 95% CI: 1.64, 3.06), and Child-Pugh B or C (OR, 2.41; 95% CI: 1.43, 4.06) were associated with VIS-C.

CONCLUSION: Overall, 90% of surveillance US results were negative (US-1), and 92% were of adequate quality (VIS-A or VIS-B); 26% of patients with US-3 results had HCC. VIS-C was associated with obesity, NAFLD, and cirrhosis.

SE-014

Utilizing Machine Learning-Integrated Endoscopic Ultrasound for Optimized Prediction of Biliary Drainage Success in Patients with Malignant Biliary Obstruction: Insights from a Retrospective Analysis

Aryofri Afan[1], Divo H[2]

[1]Institut Asia Malang, Indonesia, [2]STAN, Indonesia

BACKGROUND: Hepatopancreatobiliary cancers frequently cause malignant biliary obstruction (MBO), often necessitating biliary drainage to relieve symptoms. Endoscopic ultrasound (EUS) plays a vital role in both diagnosing MBO and performing therapeutic drainage. Integrating machine learning (ML) with EUS may enhance clinical decision-making by improving predictions of biliary drainage success. This study aims to evaluate the predictive capability of ML models in determining drainage outcomes in MBO patients.

METHOD: This retrospective study analyzed 90 patients with MBO who underwent EUS-guided biliary drainage between 2021 and 2023. Data on clinical, imaging, and procedural factors were collected. Three ML models—logistic regression, random forest, and neural networks—were trained on 70% of the dataset, with the remaining 30% used for validation. Successful drainage was defined as a bilirubin reduction of over 50% within 7 days. Model performance was assessed using area under the curve (AUC), and key clinical predictors were identified

using statistical analysis.

RESULT: Among the 90 patients, 63 (70%) were used for ML training and 27 (30%) for validation. The random forest model achieved the highest predictive accuracy (AUC = 0.89, 95% CI: 0.82–0.95, $p < 0.001$), surpassing logistic regression (AUC = 0.79, $p = 0.002$) and neural networks (AUC = 0.84, $p < 0.001$). Successful drainage occurred in 72 patients (80%), with significant predictors including tumor size (OR: 1.45, $p = 0.004$), stent placement (OR: 2.12, $p < 0.001$), and baseline bilirubin (OR: 1.28, $p = 0.01$). Patients with successful drainage had fewer complications (15% vs. 32%, $p = 0.03$), and the random forest model reduced complications by 20% compared to conventional methods.

CONCLUSION: ML models, particularly random forest, improve prediction of biliary drainage success in MBO patients. These findings support the integration of ML into clinical practice to optimize treatment strategies and enhance patient outcomes.

Breast

SE-015

Comparative Diagnostic Accuracy of Ultrasound, Mammography, and Magnetic Resonance Imaging in Detecting Breast Cancer Lesions in Patients with Breast Implants: A Comprehensive Systematic Review

Roland Helmizar[1], Vina Tri Septiana[2], Nana Liana[3]
[1]Department of Internal Medicine, Baiturrahmah University, Indonesia, [2]Department of Radiology, Baiturrahmah University, Indonesia, [3]Department of Pathology, Baiturrahmah University, Indonesia

BACKGROUND: Detecting breast cancer lesions in patients with breast implants presents significant challenges due to implant-related artifacts and reduced visibility of breast tissue. Imaging techniques such as ultrasound (US), mammography (MG), and magnetic resonance imaging (MRI) are commonly used for cancer detection, but their effectiveness in this specific population remains uncertain. This systematic review aims to evaluate and compare the diagnostic accuracy of US, MG, and MRI in identifying breast cancer lesions in patients with implants.

METHODS: A systematic search was conducted in PubMed, Embase, EBSCO, and Cochrane Library for studies published up to December 2025 evaluating the diagnostic performance of US, MG, and MRI in patients with suspected breast cancer and breast implants. Sensitivity, specificity, positive predictive value (PPV), negative predictive value (NPV).

RESULTS: A total of eight studies were included. MRI demonstrated the highest sensitivity (91.3%, 95% CI: 87.0–94.1%), outperforming US (80.6%, 95% CI: 74.4–87.8%) and MG (73.2%, 95% CI: 66.1–79.3%, $p < 0.001$). Specificity was highest for MG (88.4%, 95% CI: 82.3–92.6%), followed by MRI (85.1%, 95% CI: 78.2–90.0%) and US (77.8%, 95% CI: 71.0–83.2%). MRI also showed the highest PPV (87.2%) and NPV (90.5%), while US had a lower PPV (78.3%) but a relatively high NPV (84.1%).

CONCLUSION: MRI demonstrates the highest sensitivity, PPV, and NPV, making it the most reliable imaging modality for detecting breast cancer in patients with implants, while MG offers the highest specificity. These findings support MRI's role in improving diagnostic accuracy, especially in high-risk or inconclusive cases.

SE-016

Initial Experience of Ultrasound-Guided Intralesional Steroid Injection in Treating Idiopathic Granulomatous Mastitis – Still an Uphill Task or There Is Light at the End of the Tunnel?

Asif Momin[1], Shenaz Momin[2], Manthan Parikh[1]
[1]Department of Radiology, Head & Neck Cancer Institute of India, India, [2]Department of Radiology, BYL NAIR HOSPITAL and TN Medical College Mumbai, India

Idiopathic granulomatous mastitis (IGM) is a benign condition which, however at times, is difficult to diagnose and treat due to its refractory nature and uncertain treatment options. Ultrasound guided localised abscess aspiration was done, followed by periductal local triamcinolone acetamide injection

along with injectable lignocaine as an alternate treatment option. We used this therapeutic option recently in three cases avoiding surgical methods with the hope to improve patients' quality of life in otherwise affected by recurrence and prolonged treatment. This is based on the published article on the framework and guidelines for intra lesional steroid injection. This was done after excluding malignancy by FNAC or biopsy and treating localised abscess with bacteriological and microbiological testing for corynebacterium and mycobacterium. Also, accurate graphical documentation of the extent and severity disease by targeted ultrasound was used as a roadmap. This was a useful step for judging the exact response to local steroid injection compared to the pretreatment clinical drawing. This presentation highlights further scope in developing consensus regarding non-surgical treatment option of otherwise intractable idiopathic granulomatous mastitis reducing the cost and improving the patient's acceptance to this new line of treatment. Using these guidelines we have documented clinical as well as sonographic improvement during the follow up scans while addressing the residual disease. Depending on the depth and degree of involvement, additional steroid dosage using maximum permissible limits followed by local corticosteroid ointment application through the multi-disciplinary team(MDT) approach seems to be an effective method. Patient education about the potential delay in steroid action for persistent palpable lesions or recurrence is crucial.

SE-017

The Correlation Between Ultrasound Features and Histologic Findings of BI-RADS 3 Breast Nodular Lesions

Tsendsaikhan Batkhuu
Department of Radiology, Radiologist, Mongolia

PURPOSE: The purpose is determine of the BI-RADS system in ultrasound findings assigned to BI-RADS 3 category,using cytologic and histologic results.

MATERIALS AND METHOD: The study was carried out at Khan-Uul District Health Center (Ulaanbaatar,Mongolia). The study was retrospective study design. 82 women of breast lesions classified as probably benign at ultrasound(BI-RADS 3 category) were included in the study according and breast ultrasound was performed.

RESULTS: Our study included 82 nodular lesions, classified as BI-RADS 3, in patients. The medium transverse diameter of all lesions was 11.6 mm(range: 4-37 mm). The cytologic results were 13(15.6%)C1, 1(1.6%)C2, 62(75.4%)C3 and 6(7.4%) C4. The subsequent percutaneous biopsy revealed benign results (B1,B2) in 56 cases(68.3%), uncertain potential malignancy results (B3) in 22 cases (26.8%) and malignancy results(B4,B5) in 4 cases(4.9%). The 56 lesions classified benign after 6 month of follow-up, the 22 lesions classified as B3 were subjected to surgical biopsy confirmation and the 4 cases classified as B4 or B5 underwent definitive surgery. Only two patients had a family history of breast cancer (2.4%), but only one of the one had a malignant lesion.All 56 cases(68.3%) that underwent 6 month of follow-up for a benign lesion were stable.

CONCLUSIONS: BI-RADS category 3 is specifically applied in case of hypoechoic circumscribed, oval solid masses, parallel to the skin as well as in case of isolated, non-homo geneous echoes within the solid nodular lesions, complicated cysts with uniform low-level echoes and clustered microcysts in the form of microlobulated or oval masses, especially in lesions with large dimensions, which should be estimated by setting a dimensional cut-off. Risk for this reason clinical and anamnestic data like age, hormone therapy, and family history and personal history of breast cancer should be evaluated with a multidisciplinary approach, to select cases that require histologic verification instead of the usual short-term follow-up.

Cardiovascular

SE-018

Deep Learning-Driven Nanobubble Ultrasound Imaging for Subcellular Endothelial Dysfunction Assessment in Atherosclerosis: A Multi-Scale Computational Approach

Rini Winarti[1], Sahnaz Vivinda Putri[2], Elfiany Syafruddin[3], Prihantini Prihantini[4], Andi Nursanti[5], Rifaldy Fajar[4]

[1]Department of Biology, Yogyakarta State University, Indonesia, [2]Health Management Laboratory, International University Semen Indonesia, Indonesia, [3]Computational Science Research Laboratory, Bulukumba Muhammadiyah University, Indonesia, [4]Mathematical and Computational BioMedicine Research Group, The Integrated Mathematical, Computational, and Data Science for BioMedicine Research Community Foundation, Indonesia, [5]Department of Pharmacology, Wallacea University, Indonesia

BACKGROUND / AIM: Atherosclerosis is a leading cause of cardiovascular disease, with endothelial dysfunction (ED) as its earliest indicator. However, current imaging techniques lack the resolution to assess subcellular endothelial integrity in vivo. This study develops a deep learning-based nanobubble ultrasound imaging model to analyze endothelial glycocalyx degradation, lipid nano-vesicle retention, and nitric oxide bioavailability, enabling non-invasive, real-time detection of early atherosclerotic changes before arterial plaque formation.

METHODS: A self-supervised deep learning framework was implemented for nanobubble contrast quantification and vascular elasticity mapping. Physics-informed endothelial glycocalyx mapping (PI-EGM) was applied using Manchester Corneal Confocal Microscopy (MCCM) dataset, while dual-phase frequency harmonics imaging (70-100 MHz) from Vascular Ultrasound Imaging Dataset (Kaggle) enhanced endothelial resolution. Contrastive nanobubble tracking (CNT-Net) was trained on STARE and DRIVE datasets for vascular segmentation and lipid nano-vesicle retention analysis. Training used 475,200 frames from 610 subjects, validated against 198 endothelial biopsy samples (Heidelberg Retinal Tomograph III). Prospective validation was performed on 412 individuals (ages 40-72) at cardiovascular risk.

RESULTS: The model detected subcellular endothelial dysfunction with 85.6% accuracy (95% CI: 83.2–88.1), outperforming flow-mediated dilation (AUC = 0.64), optical coherence tomography (AUC = 0.76), and lipidomic biomarkers (AUC = 0.87, $p < 0.01$). Early-stage endothelial glycocalyx deterioration correlated with increased vascular permeability, impaired nitric oxide diffusion, and lipid nano-vesicle retention, accelerating inflammatory adhesion molecule upregulation. Glycocalyx thinning (<300 nm) was detected with 79.2% sensitivity (95% CI: 76.1–82.3), correlating with carotid intima-media thickening ($R^2 = 0.77$, $p < 0.01$). One-year MACE risk prediction achieved HR = 2.89 (95% CI: 2.31–3.52, $p < 0.01$), surpassing conventional imaging.

CONCLUSIONS: This study presents an AI-driven nanobubble ultrasound imaging framework for subcellular endothelial dysfunction assessment, providing a novel, non-invasive biomarker for preclinical atherosclerosis risk stratification. Further validation is required for clinical translation.

SE-019

Evaluation of Access Routes Using Ultrasound Before Cardiac Catheterization

Masayuki Fujioka[1], Koichi Yabunaka[3], Tomohiro Nakashouji[2]

[1]Department of Laboratory Medicine, Katsuragi Hospital, Japan, [2]Department of Internal Medicine-Cardiology, Katsuragi Hospital, Japan, [3]Department of Radiology, Ono Memorial Hospital, Japan

INTRODUCTION: Although the radial artery is the main access route for cardiac catheterization, it is necessary to choose an appropriate access route to avoid complications such as occlusion and dissection. We report our experience of preoperative evaluation of access routes using ultrasound (US).

SUBJECTS AND METHODS: Participants were 119 patients (60 males, 59 females, age 78.1 ± 9.5

years) with a total of 338 limbs who underwent US evaluation of the upper limb arteries as the access route before cardiac catheterization or treatment at our hospital between January and December 2024. In all cases, US was performed during the pre-catheterization medical examination. The intraluminal diameter of the radial artery around the puncture site and brachial artery was measured using B-mode. The presence or absence of bending or meandering was assessed. In addition, the presence or absence of stenosis or occlusive lesions was determined using color Doppler and pulsed Doppler.

RESULTS: The diameters of the radial artery and brachial artery were 2.2 mm ± 0.5 mm and 4.0 mm ± 0.7 mm, respectively. Abnormal findings were observed in 119 cases, 32 (26.9%) cases (44 limbs). These included occlusion in 16 radial arteries, severe stenosis in 11 radial arteries and 1 subclavian artery, and bending or meandering in 10 radial arteries and 7 brachial arteries.

CONCLUSION: We experienced no complications in cases where the vessel diameter was smaller than the sheath or where there were abnormal findings in the access route by selecting the radial artery on the healthy side or femoral artery as the access route. Preoperative evaluation of the access route using US, which is noninvasive and easy to perform, enables the procedure to be performed with greater safety and efficiency.

SE-020

Implementing Vascular Scientist-Led Contrast-Enhanced Ultrasound (CEUS) Endovascular Aneurysm Repair (EVAR) Scans to Enhance the Patient Pathway in the United Kingdom

Ming Yeung

Department of Surgery, Manchester University NHS Foundation Trust, United Kingdom

OBJECTIVE: To evaluate the effectiveness of implementing Vascular Scientist-led CEUS service for the detection of endoleaks following EVAR. This project aimed to enhance workflow efficiency by reducing dependency on Radiologists, thus optimising resource utilisation and reducing patient waiting times.

METHOD: Previously, patients' CEUS scan appointments were scheduled based on Radiologist's availability, as a Radiologist was required to prepare and administer the contrast agent. Through intensive collaboration with Pharmacy, Learning and Development, Radiology and Vascular Surgery teams this service improvement model was developed which enabled Vascular Scientists to achieve competency to administer contrast agents. Waiting times for scan appointments and length of scan of this new Vascular Scientist-led pathway was compared to the Radiologist-led pathway to assess its effectiveness using existing performance data.

RESULTS: Since the implementation of this pathway in November 2023, this implementation has led to a reduction in the average waiting time for an appointment from 13 days (Radiologist-led) to 7 days (Vascular Scientist-led). Additionally, scan duration was reduced streamlining the overall patient experience. Importantly, the new pathway also allowed for a more efficient allocation of Radiologist and Vascular Scientist time, as Radiologists could focus on other critical diagnostic and interventional tasks, while Vascular Scientists fully managed the CEUS process.

CONCLUSION: The introduction of Vascular Scientist-led CEUS EVAR service has proven to be a feasible and effective approach. This service improvement model not only enhances the efficiency of patient care, reducing appointment waiting times and scan duration, but optimises the use of Radiologists and Vascular Scientists time and consequently results in a financial saving to the National Health Service(NHS). The service will undergo re-audit and quality assurance to ensure quality and safety is maintained. This initiative represents a significant step forward in improving the delivery of vascular ultrasound services and developing the role and expertise of Vascular Scientists.

SE-021

Molecular Imaging Agents in Cardiovascular Ultrasound: Bridging Diagnostics and Targeted Therapy

Reny Rosalina[1], Rian Ka Praja[2]
[1]*Department of Biochemistry & Molecular Biology, Universitas Palangka Raya, Indonesia,* [2]*Department of Microbiology, Universitas Palangka Raya, Indonesia*

Cardiovascular ultrasound has advanced with molecular imaging agents, improving diagnostic accuracy, targeted therapy, and specificity for detecting inflammation, fibrosis, and ischemia. These innovations enable early disease detection and theranostic applications. This study uses a bibliometric approach to explore recent trends in molecular imaging agents, focusing on their development, clinical applications, and potential to enhance precision medicine in cardiovascular care. The publications were retrieved from the Scopus database with search terms related to molecular imaging agents for ultrasound and cardiovascular ultrasound, ranging from 2015 to 2025. The exported bibliometric data were analysed using the VOSviewer 1.6.20 program to examine and visualize the publication pattern throughout time. A total of 1,742 publications were analyzed, highlighting research on cardiovascular ultrasound imaging. "Echocardiography" is central and closely linked to "contrast agents," reflecting a strong interest in enhanced imaging techniques. The prominence of "microbubble" and "Doppler ultrasound" suggests a focus on microbubble-based agents for improved myocardial perfusion and real-time visualization. "Nanoparticles" are linked to "cardiac fibrosis," "inflammation," and "oxidative stress," highlighting emerging molecular imaging, especially nanoparticles and molecular probes for early disease detection. This shift toward targeted imaging aids in identifying conditions like atherosclerosis and heart failure. The link between "contrast agents" and "stress echocardiography" reflects advancements in ischemic heart disease assessment. The presence of "gadobutrol" and "cardiac imaging" suggests cross-disciplinary research with MRI to enhance diagnostics. The link between "contrast agents" and "safety" highlights ongoing studies on biocompatibility and regulation. Trends indicate a shift toward theranostics, where molecular probes and nanoparticles enable both imaging and therapy, advancing precision cardiovascular medicine. This study reflects a dynamic research landscape where contrast agents, nanoparticles, and molecular probes are evolving to enhance cardiovascular ultrasound imaging. The integration of targeted imaging approaches and nanoparticle-based diagnostics will likely shape the future of non-invasive cardiovascular disease assessment and treatment.

Genitourinary

SE-022

Bilateral Duplex Collecting Systems With Bilateral Ectopic Vaginal Implantation Causing Recurrent Urinary Tract Infection and Incontinence in a Pediatric Patient

Raenald Julian, Maria Regina Cruz-Tuble, June Danica Dumago
Department of Radiology, National Kidney and Transplant Institute, Philippines

INTRODUCTION: Duplicated collecting systems are a congenital anomaly involving the urinary tract. Most cases are unilateral, with incomplete duplication and orthotopic insertion of the ureter. This report describes a rare case of bilateral complete double collecting systems with bilateral ectopic ureter insertions into the vagina. The patient's ultrasound, computed tomography (CT), voiding cystourethrography (VCUG), renal scintigraphy, and intraoperative findings are discussed.

CASE: The patient is a pediatric female who presented with recurrent urinary tract infections and incontinence. Ultrasound and computed tomography (CT) showed bilateral complete duplicated collecting systems with ectopic insertion of both superior moieties into the vagina. Hydronephrosis were seen in both superior moieties (severe in the right and mild in the left). Renal scintigraphy showed markedly decreased uptake in the right superior

moiety, whereas the left superior moiety showed normal uptake.

DISCUSSION: Consistent with the Weigert-Meyer rule, the superior moiety ureters of the patient inserted ectopically while the inferior moieties inserted normally into the urinary bladder. The superior moiety collecting systems were hydronephrotic, which were likely due to stenosis. Renal scintigraphy showed a non-functional right superior moiety in contrast to a functional left superior moiety. The patient was eventually treated with open pelvoureterostomy of the left kidney to protect and preserve its superior moiety.

CONCLUSION: This case describes a rare scenario of bilateral duplicated collecting system with ectopic insertion of both superior moieties into the vagina. This case also highlights the complementary role of utilizing multiple imaging modalities in not only diagnosing double collecting systems, but also in identifying any possible associations (ectopic ureteric insertion, obstruction, ureteroceles, reflux, and renal dysplasia) which could affect management.

SE-024

Interdisciplinary Expansion of Ultrasound in Ovarian Cancer: Insights from a Bibliometric Analysis of Screening, Biomarkers, and Computational Advancements

Reny Rosalina[1], Rian Ka Praja[2]

[1]Department of Biochemistry & Molecular Biology, Universitas Palangka Raya, Indonesia, [2]Department of Microbiology, Universitas Palangka Raya, Indonesia

Ovarian cancer is a leading cause of mortality among women, emphasizing the need for effective early screening. Ultrasound, as a non-invasive tool, shows promise in detecting ovarian abnormalities. This bibliometric analysis examines research on ultrasound-based screening to assess the current state of the field. The Scopus database was used to extract papers published between 2005 and 2025 with the search terms “ultrasound” and “ovarian cancer.” The exported record of the search results and the references were analyzed using VOSviewer 1.6.20 to visualize publication patterns. The literature has grown over the past 20 years but has slowed after 2020. The United States was the largest contributor, with 748 publications included. A total of 748 publications were included in the results. Ultrasound remains central to ovarian cancer research, strongly linked to screening, diagnosis, and adnexal mass detection. Emerging research areas include metastasis, microbubbles, and chemotherapy, indicating its evolving role in monitoring disease progression and treatment response. Established research focuses on integrating ultrasound with biomarkers like CA-125 and MRI. The presence of terms like “breast cancer” and “pregnancy” suggests interdisciplinary expansion in gynecologic and oncologic imaging. Microbubbles, as ultrasound contrast agents, are gaining interest for enhancing tumor visualization and assessment. The role of ultrasound is expanding beyond diagnosis to treatment monitoring and disease evaluation. Strong connections between ultrasound, CA-125, and MRI suggest advancements in computational imaging, particularly with machine learning applications. In conclusion, ultrasound remains a crucial tool for ovarian cancer research. While publication trends have slowed, key areas like screening, diagnosis, and biomarker integration remain active. The expansion into treatment monitoring, interdisciplinary imaging, and computational advancements highlights its growing role. Future research may leverage artificial intelligence and multi-modal imaging to improve diagnostic accuracy and patient outcomes.

SE-025

Modifying Sleeping Posture May Be An Effective Management Plan In Patients With Nutcracker Syndrome

Seung Hyup Kim[1], Joongyub Lee[1], Eungtaek Kang[2], Suhnggwon Kim[2], Hyo Jeong Lee[3], Myung Kim[4], Dong Hyun Lee[4], Sang Eun Lee[4]

[1]Department of Radiology, Seoul National University Hospital, Korea, [2]Department of Internal Medicine-Nephrology, Seoul K Clinic, Korea, [3]Department of Radiology, Ewha Womans University Mokdong Hospital, Korea, [4]Department of Urology, SNU Healthy Prostate Clinic, Korea

The nutcracker phenomenon (NCP) refers to the compression of the left renal vein (LRV) between the abdominal aorta and the superior mesenteric artery. When NCP is associated with symptoms such as hematuria, proteinuria, or left flank pain, it is termed nutcracker syndrome (NCS). NCP is a dynamic condition that varies with changes in the patient's posture. Doppler ultrasound (US) is a valuable diagnostic tool to evaluate NCP, as it provides insights into how the degree of compression changes with different postures. This dynamic assessment is particularly useful in educating NCS patients about the importance of avoiding the supine sleeping posture. The purpose of this study was to evaluate the varying degrees of NCP with postural changes. In 325 patients with NCP, identified via Doppler US in the supine position using a criterion of peak flow velocity (PFV) of the aortomesenteric LRV exceeding 100 cm/sec, Doppler US measurements were repeated in the left lateral decubitus (LLD) and right lateral decubitus (RLD) positions. The PFV measurements (mean ± standard deviation) of the aortomesenteric LRV were as follows: 174 ± 41.9 cm/sec in the supine position, 80.1 ± 40.8 cm/sec in the LLD position, and 131 ± 54.6 cm/sec in the RLD position. These findings highlight the variations in LRV compression and corresponding PFVs across different postures, emphasizing that the supine posture is the most detrimental and the LLD posture the most favorable for NCS patients. This study underscores the importance of posture-based strategies in managing NCS symptoms. Encouraging patients to adopt the LLD sleeping posture can significantly relieve symptoms and improve their quality of life. This exhibition will present representative cases of NCS patients whose symptoms improved solely through this simple modification of sleeping posture, without the need for additional treatment modalities.

SE-026

Study on Changes in Blood Flow Through Uterine Arteries, Umbilical Artery and Cerebral Media Artery During Preeclampsia by Doppler Ultrasound

Zambaga Ganzorigt

Department of Radiology, Khuree Maternity Hospital, Mongolia

INTRODUCTION: 16% of maternal mortality is related to hypertensive discorders during pregnancy as stated at who survey. Preeclampsia can lead to several complications such as fetal growth retardation, preterm delivery, placental abruption, HELP syndrome, eclampsia, and desorders of hepatic, renal, brain, cardiac and ocular activities, introducing Doppler ultrasound of blood flow through uterine arteries, umbilical artery, cerebral media artery made it possible to study the placental insufficiency related to preeclampsia.

GOAL: To reveal changes in blood flow through uterine arteries, umbilical artery and cerebral media artery during preeclampsia by Doppler ultrasound and evaluate fetal wellbeing.

OBJECTIVES: 1. To determine risk factors of pregnant woman whose pregnancy is complicated by preeclampsia 2. To reveal changes in blood flow through uterine arteries, umbilical artery and cerebral media artery during preeclampsia by Doppler ultrasound 3. Evaluate fetal wellbeing.

METHODOLOGY: Hospital based Cohort model of analytical method was used in the study. 280 clients who had service First Maternity Hospital, Ulaanbaatar, from 10 Jan to 28 Feb 2021 and whose gestational age was above 24 weeks were involved in the study.

RESULTS: 1. Pl of right uterine artery was icreased for 27.5% mild preeclampsia and for 6.8% of severe preeclampsia (P=0.18). Increase in Ri of right uterine artery for 68.9% of mild preeclampsia and 10.3%

of severe preeclampsia had statistical significance. Increase in Ri of left uterine artery for 75.8% of mild preeclampsia and 13.7% of severe preeclampsia had statistical significance (P=0.00). Increase in Pi of left uterine artery for 31% of mild preeclampsia and 3.4% of severe preeclampsia had statistical significance (P=0.047). 2. In 24.19 preeclampsia cases RI of umbilical artery was increased and had statistical significance (P=0.046%) but increase in Pl of umbilical artery for 44.8% of cases did not have statistical significance (P=0.072%).

SE-027

The Role of Ultrasound in Diagnosis of Renal Lymphangiectasia, an Uncommon Cause of Perirenal Collections

Xanicia Long[1], Kok Kit Ng[2]
[1]Department of Family Medicine, National Healthcare Group, Singapore, [2]Department of Urology, Changi General Hospital, Singapore

Renal lymphangiectasia (RLM) is a rare condition characterized by dilatation of perirenal, parapelvic or intrarenal lymphatics, hypothesized to result from malformation of lymphatic tissues. For years, computer tomography intravenous pyelography (CT IVP) has been regarded the first line imaging tool as it can check for obstruction and characterize perirenal collections based on Hounsfield unit and contrast excretion. We discuss the role of ultrasound as a potential alternative diagnostic tool with a review of literature. A PubMed search using the keywords “renal lymphangiectasia”, “perirenal collections”, “ultrasound”, “imaging” was performed to review relevant articles dating from 2015 to present. A 2011-2016 single-center study by Vaidehi K. Pandya et al. suggested that CT IVP was the gold standard imaging modality based on characteristic findings of non-enhancing perirenal collections with HU<10, coupled with normal contrast excretion. However, a 2020 case report by Simone Guadagni et al. described the first ever case of RLM successfully diagnosed on contrast-enhanced US, in a 27 year-old female with vague abdominal discomfort and no past medical history. In a 2022 case series by Yanyu Li et al., out of 4 patients diagnosed with RLM, 1 solely underwent contrast-enhanced US, 2 underwent contrast-enhanced US followed by CT IVP, and the last patient was screened with simple US. This case series also discusses potential advantages of US over CT: (1)US can be used in renal impairment patients as the contrast used is not nephrotoxic unlike CT; (2)US has less radiation compared to CT; (3)US is time-saving and more cost-effective. While contrast-enhanced US proves to be a promising alternative to CT for diagnosis of RLM, it is key to individualize workup on a case-by-case basis to ensure timely diagnosis and intervention. The paradigm shift towards relying on radiological imaging has obliterated the need for invasive biopsy/aspiration, allowing patients to be conservatively managed.

SE-028

Young Female Perivascular Epithelioid Cell Tumor of Uterus: A Case Report

Garamjav Khishigdavaa[1], Uyan-Egshig Dorjnamjim[1], Nergui Olzvoi[2]
[1]Department of Radiology, DCDR Hospital of Mongolia, Mongolia, [2]Department of Radiology, Grandmed Hospital, Mongolia

Perivascular epithelioid cell tumors (PEComas) are a rare group of mesenchymal neoplasms composed of distinctive cells that show a focal association with blood vessel walls and usually express melanocytic and smooth-muscle markers. Malignant PEComa is an uncommon disease, due to its relative rarity, little is known about the histogenesis and prognostic factors of this tumor. We describe a case of unusual PEComa in a 22-year-old female patient with regional lymph node involvement. PEComas have been found in various organs and have a tendency to affect women, with approximately 40% of tumors originating from the uterus.

OBJECTIVE: We present here a rare case of epithelioid cell tumor that was accidentally detected during routine ultrasound at GrandMed Hospital.

METHOD: We examined a 22-year-old female patient who was referred to our outpatient clinic with mild pain in her lower abdomen for a few days. For diagnostic purposes, we performed abdominal US, and revealed a suspected lesion of uterine and large

lymph nodes in the pelvic cavity. So, subsequently performed pelvic contrast MRI was performed, pelvic CECT, and biopsy was done after surgery removed.

RESULTS: A color doppler US showed a hyper-vascularized lesion in the posterior wall of the uterine. CECT and pelvic MRI detected a 32*38*25 mm-sized, focal lesion in the uterine, also enlarged hypervascularization lymph nodes in the pelvic cavity. The diagnosis is confirmed by biopsy after removed surgery and immunohistochemical markers.

CONCLUSION: PEComa is rare and although pelvic MRI is usually the gold standard for diagnosis, it can be diagnosed in the US

Head & Neck

SE-029

Small but Significant Carotid Space – Pictorial Essay of Common and Rare Pathologies

Shenaz Momin[1], Asif Momin[2], Inshirah Momin[3]

[1]Department of Radiology, BYL NAIR HOSPITAL and TN Medical College Mumbai, India, [2]Department of Radiology, Head and Neck Cancer Institute of India and Bhatia Hospital, India, [3]Department of Radiology, Bhatia General Hospital, India

The carotid space is a small, distinct area composed of a major artery, vein, and critical nerve; hence, most of the pathologies are mostly related to these three inherent structures. However, there are some small percentages of other pathologies rarely seen and can be diagnosed by ultrasound with additional confirmation using cross-sectional modalities. Due to its distinct anatomy, small compact size, and vertical extent from skull base to thorax, the diagnostic determinants are location of the lesion, typical tissue signature, or specific color doppler features. Besides the typical vein, artery, and nerve-related lesions, rare abnormalities can be explained based on embryological origin or diffuse inflammatory or infective involvement. The typical lesions are paragangliomas involving carotid body tumors, vagus nerve and jugular veins. Neurogenic lesions like schwannomas and neurofibromas are commonly encountered. Rare lesions would include tumor thrombus of the jugular vein in the primary thyroid cancers or head and neck SCCs. Ectopic parathyroid adenomas, minor salivary gland neoplasms, and metastatic lymph nodes. Infiltrative lesions seen with either lymphomatous or infective etiology, like tuberculosis, have distinct appearances. Some specific vascular pathologies known in this region are jugular ectasia, carotid pseudoaneurysms, dissections, as well as diffuse arteritis. Ultrasound evaluation of these lesions is crucial in the accurate management of pathologies. An initial correct diagnosis of these small but significant specific lesions opens further avenues in the management procedures like preoperative embolization as well as real-time guidance for interventional procedures and post-treatment evaluation of infective and oncological lesions.

Musculoskeletal

SE-030

A Case of Extensor Carpi Radialis Brevis Tear Following Internal Fixation of Distal Radius Fracture

Dong Hwee Kim, Ki Hoon Kim, Hong Bum Park
Department of Rehabilitation Medicine, Korea University Ansan Hospital, Korea

INTRODUCTION: Distal radius fractures are common injuries treated with open reduction and internal fixation (ORIF) using volar plates and screws. While effective, complications such as extensor tendon injuries, including extensor carpi radialis brevis (ECRB) tears, can impair hand function. This case highlights an ECRB tear diagnosed via ultrasonography in a patient initially suspected of radial neuropathy.
CASE REPORT: A 78-year-old man presented with persistent tingling in his right hand for six months following ORIF for a distal radius fracture. Neurological examination revealed hypoesthesia in the fingers, weakness in wrist and finger movements, and atrophy of the abductor pollicis brevis and first dorsal interosseous muscles. Electrodiagnostic studies confirmed right ulnar neuropathy at the elbow and incomplete right median sensory neuropathy at the wrist. Ultrasonography revealed ulnar nerve compression 1 cm distal to the medial humeral epicondyle, and sonography-guided perineural injections provided partial symptom relief. However, wrist pain and restricted extension persisted. Follow-up ultrasonography identified an ECRB tear 4.5 cm proximal to the right ulnar styloid process. Implant removal and trigger point injections into the extensor carpi radialis muscles resulted in significant pain relief and improved wrist mobility.
CONCLUSION: ECRB tears can occur due to screw fixation following distal radius fractures. Ultrasonography is essential for diagnosing such injuries and guiding treatment. This case emphasizes considering extensor muscle injuries in patients with persistent wrist pain post-fixation and highlights the diagnostic value of ultrasonography.

SE-033

Diagnostic Shoulder Ultrasound: A Case-Based Review of Its Clinical Impact

Jee Won Chai, Dong Hyun Kim, Hyo Jin Kim, Jiwoon Seo
Department of Radiology, Seoul National University Boramae Medical Center, Korea

Shoulder ultrasound is a valuable tool for the prompt and accurate diagnosis of various shoulder pathologies, guiding treatment decisions. This case-based review highlights its role in evaluating rotator cuff tendinopathy, calcific tendinitis, rotator cuff tears, adhesive capsulitis, humerus greater tubercle fracture, acromioclavicular joint injury, spinoglenoid notch ganglion cysts with nerve compression, and subacromial and subcoracoid impingement. Ultrasound enables real-time assessment of tendon integrity, dynamic impingement testing, and early identification of adhesive capsulitis and nerve compression syndromes. By providing immediate, cost-effective, and accurate diagnoses, shoulder ultrasound influences treatment plans, optimizing patient outcomes and reducing the need for advanced imaging.

SE-035

High Resolution Ultrasound Finding of Big Toe Lesion: MR Correlation

Dalsu Park
Department of Radiology, OSBONE HOSPITAL, Korea

PURPOSE: Big toe lesion ultrasound is not usually use by clinical field and I would want to present useful ultrasound findings.
METHOD: I make film by everyday routine practice. I used 15 to 18 Mhz hockey stick probe
RESULT: High resolution ultrasound is very useful modality in big toe lesion.
CONCLUSION: High resolution ultrasound is essential front line modality for gout, abductor hallucis tendon injury with medial wall fx,mallet toe,focal abscess and bone growing lesion. high resolution ultrasound is also useful for big toe lesion. sometimes more useful than MRI.

SE-036

Median Neuropathy as a Complication of Radial Forearm Free Flap Surgery: A Case Report

Nackhwan Kim
Department of Rehabilitation Medicine, Incheon Sejong Hospital, Korea

BACKGROUND: Surgical resection of primary intraoral malignancies is a widely utilized therapeutic approach in otolaryngology. Following tumor excision, radial forearm free flap reconstruction (RFFR) is often performed to restore postoperative swallowing function, speech ability, and aesthetic integrity. However, median neuropathy as a postoperative complication of RFFR has not been previously reported.

CASE PRESENTATION: A 61-year-old female was diagnosed with squamous cell carcinoma of the right tongue (clinical stage T2N0M0, pathological stage T2N1M0). She underwent hemiglossectomy and RFFR performed by an otolaryngologist. Postoperatively, the patient reported paresthesia, including tingling sensations in the palm and fingers of the donor limb. Nerve conduction studies (NCS) and needle electromyography (EMG) were conducted. The NCS revealed uninterpretable findings, prompting further evaluation with ultrasonography, which identified an altered anatomical course of the nerves. A repeated electromyographic assessment, considering the aberrant nerve trajectory, confirmed a diagnosis of complete left median neuropathy at the mid-forearm level and complete left superficial radial neuropathy at the same level. Ultrasonographic imaging further demonstrated an altered course of the left median nerve and a focal reduction in cross-sectional area at the mid-forearm.

CONCLUSION: Radial forearm free flap reconstruction is commonly employed to manage soft tissue defects following head and neck cancer resection. While surgeons anticipate favorable postoperative outcomes, donor-site complications remain a concern, including partial skin graft loss, tendon exposure, diminished superficial radial nerve sensation, cold intolerance, aesthetic concerns, and functional impairment of the donor arm. In this case, the patient underwent RFFR following tumor excision, and median neuropathy with anatomical deviation of the median nerve was detected two months postoperatively via EMG and ultrasonography. This complication has not been previously documented in the literature. Given the altered anatomical structures following surgery, ultrasonography-guided EMG serves as a valuable diagnostic tool for identifying postoperative nerve complications.

SE-037

Phlegmasia Alba Dolens in May-Thurner Syndrome: A Rare Syndrome of Acute Deep Vein Thrombosis and Literature Review

Seul Ki Lee
Department of Radiology, The Catholic University of Korea, St. Vincent's Hospital, Korea

Phlegmasia alba dolens is a rare but serious complication of acute deep vein thrombosis that is characterized by extensive venous obstruction and impaired venous return, resultaing in significant limb swelling. This condition is often associated with underlying anatomical or pathological factors, such as May-Thurner Syndrome, which arises from the compression of the left common iliac vein by the overlying right common iliac artery. This case, accompanied by a literature review, discusses the clinical presentation of a 47-year-old male patient diagnosed with acute DVT in the setting of May-Thurner Syndrome. It provides the review of pathophysiology and diagnostic challenges associated with this condition, highlighting the critical need for early recognition and timely intervention of phlegmasia alba dolens to prevent progression to more severe complications, including phlegmasia cerulea dolens or venous gangrene, which carry a higher risk of morbidity and mortality.

SE-038

Reproducibility of Shear Wave and Strain Elastography Depending on the Size of the Region of Interest: A Study Using Epidermal Cysts

Hee Jin Park, Sungchul Wee
Department of Radiology, Kangbuk Samsung Hospital, Korea

PURPOSE: We sought to evaluate the reproducibility of measurement on ultrasound elastography (EUS) according to the size of the region of interest (ROI) using cases of surgically confirmed epidermal cysts.
METHODS: This retrospective study included 201 cases with surgically confirmed epidermal cysts who underwent strain elastography (SE) and shear wave elastography (SWE) twice each. To assess the strain ratio on SE, the SW velocity, and the SW elasticity of the epidermal cyst, a circular ROI was drawn manually atop of the lesion and adjacent subcutaneous fat tissue. The inter-session reproducibility of EUS values was assessed, and the absolute difference values of EUS between the first and second sessions were compared to the ROI size and ROI ratio.
RESULTS: The intra-class correlation coefficient values of strain ratio, SW velocity, and SW elasticity in cases with ROI diameters of ≥2 mm were greater than those in cases with ROI diameters of <2 mm. The difference in inter-session variability of the strain ratio was positively correlated with the ROI ratio. The inter-session differences in SW velocity and elasticity were significantly negatively correlated with both ROI diameter and ROI ratio. An ROI diameter of ≥2 mm significantly correlated with lower inter-session differences in SW velocity compared to an ROI diameter of <2 mm.
CONCLUSION: It was preferable to select a larger ROI (≥2 mm in diameter) to reduce inter-session variability in SWE for assessing epidermal cysts. The inter-session variability in strain ratio increased with an increasing ROI ratio relative to the lesion size.

SE-040

Sonographic Mulder Sign: Does It Always Indicate Morton's Neuroma?

Hyejung Choo
Department of Radiology, Inje University Busan Paik Hospital, Korea

Morton's neuroma, a perineural fibrosis of the common plantar nerve, is a common cause of forefoot pain, particularly in middle-aged women. On ultrasonography, it typically appears as a non-compressible, round-to-oval or ginkgo leaf-like hypoechoic mass in the intermetatarsal space. The sonographic Mulder sign—characterized by the hypoechoic mass popping toward the plantar surface when the metatarsal heads are squeezed—is often considered a specific indicator of Morton's neuroma on ultrasonography. However, based on my experience, this sign is not exclusive to Morton's neuroma. Here, I present a case of intermetatarsal bursitis demonstrating a sonographic Mulder sign, highlighting the need for careful differential diagnosis.

SE-041

State of Musculoskeletal Ultrasound in Kazakhstan: Teaching Resources and Literature Availability

Yerlan Yemeshev
Department of Radiology, TMC Qonrad, Kazakhstan

Musculoskeletal ultrasound (MSK US) is gaining recognition as a valuable diagnostic tool in Kazakhstan, particularly in rheumatology, sports medicine, and orthopedic practice. However, the development of MSK US education and training remains in its early stages. This study aims to assess the current state of MSK US teaching resources available in Kazakhstan, focusing on textbooks and educational materials in Kazakh and Russian languages. Despite the increasing demand for MSK US, the availability of dedicated learning resources remains limited. There is no exact number of MSK ultrasound specialists in Kazakhstan due to the absence of a national MSK ultrasound society. Training opportunities are scarce, with only two

short-term courses conducted in 2024 by Russian radiologists. Most training relies on international courses and materials, often in English, which poses a language barrier for many local specialists. While some Russian-language textbooks on general ultrasound diagnostics include sections on musculoskeletal applications, only two dedicated textbooks on MSK ultrasound are available in Russian, and comprehensive Kazakh-language resources are nonexistent. Additionally, only one medical institution in Kazakhstan currently offers structured MSK ultrasound training, highlighting the need for greater educational integration. To advance MSK US education in Kazakhstan, there is a need for structured training programs, the development of textbooks in Kazakh and Russian, and the adaptation of international guidelines to the local context. Collaboration between medical universities, professional societies, and healthcare institutions can enhance accessibility to high-quality educational resources and improve MSK US proficiency among medical professionals.

Pediatric

SE-042

A Systematic Review and Meta-Analysis of Diagnostic Performance of Ultrasound for Differentiating Malignant From Benign Cervical Lymphadenopathy in Children

Jayoung Moon[1], Jisun Hwang[2], Pyeong Hwa Kim[3]
[1]Department of Radiology, Ajou University Hospital, Korea, [2]Department of Radiology, Seoul National University Bundang Hospital, Korea, [3]Department of Radiology, Asan Medical Center, Korea

OBJECTIVES: To evaluate the diagnostic performance of ultrasound (US) features used to differentiate malignant from benign cervical lymphadenopathy in children.

METHODS: PubMed and EMBASE were searched for articles reporting the diagnostic performance of US features to differentiate benign and malignant cervical lymphadenopathy in children. Article quality was evaluated using the QUADAS-2 tool. Sensitivity and specificity were pooled using a bivariate random-effects model. Further sensitivity analyses and meta-regression were performed to determine the potential source of heterogeneity. The area under the receiver operating characteristic curve was calculated using the hierarchical summary receiver operating characteristic model.

RESULTS: Ten articles (1,077 children) were included. Among the retrieved US features, abnormal vascularity, heterogeneous echogenicity, abnormal hilum echogenicity, and long-axis/short-axis (L/S) ratio were significantly associated with malignant lymphadenopathy, with pooled diagnostic odds ratios of 36 (95% confidence interval [CI]: 14–92), 17 (3–91), 16 (5–54), and 7 (5–9), respectively. The most sensitive US features were abnormal hilum echogenicity (0.86, 95% CI: 0.66–0.95) and heterogeneous echogenicity (0.84, 95% CI: 0.25–0.99). Abnormal vascularity (0.91, 95% CI: 0.82–0.97) was the most specific. Substantial heterogeneity was found in both sensitivity and specificity ($I2 > 50\%$; $p < 0.01$), although the source was not revealed.

CONCLUSION: Among US features, abnormal

vascularity, heterogeneous echogenicity, abnormal hilum echogenicity, and L/S ratio are useful for differentiating malignant from benign cervical lymphadenopathy in children, showing good diagnostic performance. These findings should be carefully interpreted due to unexplained heterogeneity, which may lower the validity of the pooled estimates.

SE-043

Challenging Pilomatricoma in Children: Sonographic Clues and Seiral Change

So-Young Yoo, Ji Hye Kim, Tae Yeon Jeon, Ji Eun Park
Department of Radiology, Samsung Medical Center, Korea

Pilomatricoma is a benign superficial tumor of the hair follicle, most commonly occurring in the first and second decade. Clinical diagnosis is frequently made based on its typical presentation as a superficial, firm, painless subcutaneous nodule mainly located in the head and neck or extremities. Although pilomatricoma show typical sonographic features including superfical subcutaneous location and presence of calcification, it may simulate other benign or malignant soft tissue tumors with atypical features, making a preoperative diagnosis challenging. We will present three pediatric cases of head and neck pilomatricoma of which imaging diagnosis was challenging and review sonographic diagnostic clues including serial changes.

SE-044

Pediatric Hernias Reviews

Ji Eun Park, Ji Hye Kim, So-Young Yoo, Tae Yeon Jeon
Department of Radiology, Samsung Medical Center, Korea

Pediatric hernias are a common clinical problem. Ultrasound is an excellent modality for the initial assessment of hernias in the pediatric population. It is quick, non-invasive, with no radiation dose or requirement for general anesthetic. The purpose of this pictorial essay is to raise awareness of the wide spectrum of hernias encountered in children. Inguinal hernia : Inguinal hernia is the most prevalent type of abdominal wall hernia. Incarcerated Hernia: The blood supply is still intact but compromised due to the trapping of tissue. Strangulated Hernia: The blood supply is completely cut off, which can lead to tissue necrosis (death). Direct Hernia : Protrusion of the intra-abdominal contents through a weak abdominal wall Indirect Hernia : Protrusion toward the inguinal canal Umbilical hernia : Umbilical hernias are the most common ventral abdominal wall hernia and occur in the midline through the umbilicus. Epigastric hernia : Epigastric hernias occur ventrally through a defect in the linea alba, superior to the umbilicus. Diaphragmatic hernia : Diaphragmatic hernias are defined as either congenital or acquired defects in the diaphragm Incisional hernia : Incisional hernias are the most common type of anterior abdominal wall hernia, owing to the frequency with which abdominal surgical procedures are performed.performed. Hiatal hernia : Hiatus hernias occur when there is herniation of abdominal contents through the esophageal hiatus of the diaphragm into the thoracic cavity. Hoff's fat pad hernia : Hoffa fat pad herniation is defined as herniation of infrapatellar fat through a defect in the lateral retinaculum. The present pictorial review presents an overview on the use of ultrasonography in the evaluation of pediatric hernia. Ultrasonography has emerged as the most convenient imaging tool for diagnosing inguinal hernia due to its advantages, such as portability and absence of radiation.

SE-045

Sonographic Findings of Renal Cystic Lesions in Pediatric Patients: Key Features and Differential Diagnoses

Minjee Cho[1], Haesung Yoon[1], Jisoo Kim[2], Yong-woo Kim[1], Mi-Jung Lee[1]
[1]Department of Radiology, Severance Hospital, Korea, [2]Department of Radiology, Gangnam Severance Hospital, Korea

Renal cysts can be the first sign of underlying cystic pathologies in children, requiring thorough examination. Ultrasonography is the primary imaging modality due to its accessibility and absence of ionizing radiation. Understanding the sonographic features of pediatric renal cystic lesions can be helpful in diagnosing different kinds of diseases compared with adults. From the standpoint of unilateral versus bilateral involvement, a calyceal diverticulum appears as a cyst-like lesion involving a single kidney, complicated by intra-diverticular lithiasis in 30-50% of cases. It should be differentiated from a simple renal cyst and close observation may be needed. Localized cystic kidney disease (LCKD) is a rare non-familiar disease characterized by a cluster of small, simple cysts and intervening normal renal parenchyma. Compared to LCKD, multicystic dysplastic kidney (MCDK) shows randomly distributed non-communicating cysts with absent or dysplastic renal parenchyma. The disease typically affects an entire kidney, with the contralateral kidney often showing compensated hypertrophy or other urinary tract abnormalities. When there are bilateral renal cystic lesions, autosomal dominant polycystic kidney disease (ADPKD) and renal cysts from tuberous sclerosis complex (TSC) can be considered. In ADPKD, kidneys are generally normal at birth and the number and size of cysts increase with age. TSC commonly manifests not only renal cysts but also renal angiomyolipomas, which are visualized as hyperechoic lesions. A family history in ADPKD and clinical symptoms including cutaneous findings in TSC are critical for exact diagnosis. Simple renal cysts are rare in the pediatric age group, with an incidence below 1%. Therefore, the risk of cystic kidney disease should be evaluated in any child presenting with renal cysts. For accurate diagnosis and proper patient care, ultrasonography can serve as an excellent tool for assessing the number, size, location and laterality of lesions.

SE-046

Ultrasonographic Measurement of Anterior Fontanelle Size in Infants with Deformational Plagiocephaly: Correlation with Severity and Developmental Delay

Dong Rak Kwon
Department of Rehabilitation Medicine, Daegu Catholic University Medical Center, Korea

OBJECTIVES: We aimed to investigate the relationship between the severity of deformational plagiocephaly (DP) and anterior fontanelle size and to explore the connection between fontanelle size and developmental delay.

MATERIALS AND METHODS: We enrolled 189 infants (122 boys and 67 girls; mean corrected age: 119.79 days) out of the 256 who visited our clinic for plagiocephaly between March 2022 and June 2023. This study analyzed the correlation between cranial vault asymmetry (CVA) and anterior fontanelle size as measured using anteroposterior (AP) skull radiography and ultrasonography. The severity of DP was graded from minimal to severe based on the Argenta classification. Infants were grouped according to CVA severity as follows: Group 1 (CVA ≤ 5 mm), Group 2 (5 mm < CVA < 10 mm), and Group 3 (CVA ≥ 10 mm). Additionally, 40 infants underwent the Denver Developmental Screening Test II (DDST-II) for neurodevelopmental delays and were divided into groups based on the presence or absence of developmental delays for fontanelle size comparison.

RESULTS: Age showed a significant negative correlation with fontanelle size (correlation coefficient: −0.234, $p < 0.05$), indicating that fontanelle size decreases as infants age. No significant differences in fontanelle size were observed among the three CVA groups ($p = 0.074$) or between the developmentally delayed and non-delayed groups ($p = 0.09$). This study found no correlation between CVA and fontanelle size or between fontanelle size and developmental delay.

CONCLUSIONS: The findings show that, while anterior fontanelle size decreased with age, there was no significant correlation between fontanelle size and the severity of deformational plagiocephaly or developmental delays.

SE-047

Ultrasound Diagnosis of Inflammatory Processes in Soft Tissues of the Gluteal Region: A Case of a Benign Neoplasm with Calcification Signs

Zhanar Kozhakhmetova, Inabat Sary, Yurana Albaeva
Department of Radiology, University Medical Centre, Kazakhstan

OBJECTIVE: To evaluate the ultrasound findings of soft tissue lesions in the gluteal region of a patient suspected of having a benign adipose tissue neoplasm.

MATERIALS AND METHODS: Patient M., a 6-year-old boy, was admitted to the National Research Center for Maternal and Child Health in Astana with a tumor-like mass in the left gluteal-perineal area..History of the disease: According to the grandmother, the family visited an oncologist at the Scientific Center of Pediatrics and Pediatric Surgery on January 13, 2025, due to a benign adipose tissue neoplasm in the left gluteal-perineal area. A planned hospitalization was recommended for surgical operation.

RESULT: Ultrasound examination of soft tissues: Scanning the soft tissues of the gluteal region revealed multiple large hyperechoic formations with diameters of 4-8-17-24 mm with a tendency to merge, predominantly along the medial surface on the right side. These masses had a heterogeneous structure due to hyperechoic inclusions producing distinct acoustic shadows (calcifications) without signs of blood flow in the Doppler mode (Color Doppler). No pathological lesions were found in the presacral region.

CONCLUSION: Ultrasound findings of large soft tissue masses in the right gluteal region with signs of calcification (possible focal panniculitis?).

Histopathological Conclusion: Fibrous-adipose tissue with foci of chronic inflammation and petrification.

CONCLUSIONS: The ultrasound examination revealed multiple large hyperechoic formations in the soft tissues of the gluteal region with signs of calcification, indicating an inflammatory process possibly related to focal panniculitis. The absence of blood flow in the Doppler mode confirmed the chronic nature of the tissue changes. These findings were confirmed by histopathological analysis, which showed fibrous-adipose tissue with foci of chronic inflammation and petrification. Thus, ultrasound proves to be an important and effective tool for detecting inflammatory processes in soft tissues, playing a crucial role in differential diagnosis and treatment planning.

SE-048

Ultrasound Diagnosis of Patau Syndrome

Baigalmaa Ulaankhuu
Department of Radiology, Gurvan Gal General Hospital, Mongolia

INTRODUCTION: Trisomy 13 or Patau syndrome in 1960, was described as one genetic disorder in which an extra copy of chromosome 13 in a person's cells. Trisomy13, or Patau syndrome, has a prevalence of 1 per 12000-20000 birth etc. However, it's important to note that many affected pregnancies end in miscarriage or stillbirth, so the incidence of Patau syndrome in pregnancies may be higher than the live birth prevalence. Trisomy 13 fetuses may show various anomalies including all or not with midfacial hypoplasia (cyclopia and proboscis), ventriculomegaly, enlarged cistern magna, microcephaly, cleft lip and palate, microphthalmia, omphalocele, cardiac defects, polydactyly.

CASE PRESENTATION: O, 37 years old, a VIII gravida with 5 children alive and previous pregnancies with intrauterine death. her LMP was on April 17, 2019. She didn't take a first-trimester combined test. A prenatal ultrasound examination performed at 33 weeks of pregnancy revealed multiple structural abnormalities with a middle-frontal proboscis (a snout-like protrusion from the forehead with absent nasal bone) and Cyclopia (only one eye is recognizable between the mouth and proboscis), Hydrocephaly, ventricular septal defect,

and polyhydramnios /AFI-32.4/. The parents opted for a termination of this pregnancy.

DISCUSSION: Trisomy 13 is a chromosomal aneuploidy that has a low survival rate. The first-trimester ultrasound examination can detect chromosomal abnormalities, including Trisomy 13, and the prenatal US examination should be done carefully to avoid misdiagnosis of fetal congenital anomalies in its early stage. To provide the assessment on prenatal 3/4D dimensional ultrasound examination for detection of fetal anomalies. All pregnant women must be evaluated by mid-trimester USS for fetal structural anomalies. If needed cytogenetic study should be done as soon as possible.

SE-049

Ultrasound Diagnosis of Soft Tissue Lesions of the Anterior Chest Wall: A Clinical Case of Tuberculosis

Zhanar Kozhakhmetova, Nurgul Orynbassar, Yurana Albaeva
Department of Radiology, University Medical Centre, Kazakhstan

OBJECTIVE: To demonstrate a clinical case of tuberculosis affecting the soft tissues of the chest wall, emphasizing the role of ultrasound diagnosis and histopathological confirmation for the early detection of this rare form of extrapulmonary tuberculosis.

MATERIALS AND METHODS: Patient M., a 9-year-old boy, was admitted to the National Research Center for Maternal and Child Health in Astana with a tumor-like mass in the left parasternal region at the level of the fifth rib along the parasternal and mid-clavicular lines. The lesion was first noticed at the age of 2, with no history of trauma. The growth of the neoplasm has been in parallel to the child's growth.On 12.02.2025, the CT scan revealed a focal lesion in the soft tissues parasternally to the left. consistent with disease progression. The admission was planned for a surgical management purpose.

RESULTS: Ultrasound Diagnosis of Soft Tissues: On scanning the soft tissues of the anterior surface of the upper third of the chest, both centrally and leftward, the masses were visualized measuring 50x 24x58 mm and 40x11x40 mm. The structure was heterogeneous due to fluid collections with suspended echogenic debris and small solid hyperechogenic inclusions, without clear acoustic shadowing (clots). No blood flow was detected in color Doppler mode. Axillary and subclavian lymph nodes were not enlarged.

CONCLUSION: The echographic image suggests soft tissue masses on the anterior chest wall, possibly a lymphangioma with signs of abscess formation. However,a specific process, such as tuberculosis,cannot be excluded.

Histopathological Conclusion: The hyalinized fibrotic tissue with adipose tissue, granulomatous inflammation and giant multinucleated cells of the Pirogov-Langhans type.

CONCLUSIONS: Tuberculosis of the soft tissues is a rare but significant form of extrapulmonary tuberculosis, which often goes unnoticed due to its localized nature and the absence of pronounced lymphadenopathy.

SE-050

Ultrasound Imaging of Inguinal Lesions in Infancy: Differential Diagnoses and Key Features

Jeongil Son, Haesung Yoon, Jisoo Kim, Yongwoo Kim, Mijung Lee
Department of Radiology, Severance Hospital, Korea

The diagnostic approach to infant patients presents various challenges, as clinical symptoms can easily overlap due to the relatively small body size compared to the organs. X-ray and CT are the preferred modalities for obtaining a wide field of view and ensuring high sensitivity in the initial evaluation. However, in many cases, particularly with inguinal lesions, the limited view can lead to false negatives due to resolution limitations. Ultrasound (US) offers higher resolution and sensitivity than other imaging modalities, making it particularly valuable for assessing superficial and narrow areas, thus aiding in differential diagnosis in such cases. For cystic lesions in the inguinal area, such as hydrocele and lymphangioma, key

features on US can be distinguished by structural characteristics like loculation and septation. However, chronic or inflammatory hydrocele can resemble lymphangioma, and vice versa. Therefore, clinical correlation with inflammatory signs is crucial for accurate diagnosis. Differentials for solid inguinal lesions in infants include inguinal hernia, undescended testis, and fibrous hamartoma of infancy (FHI). In the case of inguinal hernias, differentiation between bowel and ovarian herniation can be achieved by identifying peristalsis and air artifacts in the bowel loops, as well as a hypoechoic, ovoid, solid mass with follicles in the ovarian tissue. Bowel wall thickening (>3 mm) and reduced or absent Doppler flow may suggest incarcerated hernias. Similarly, undescended testis presents as an oval-shaped hypoechoic mass in the inguinal canal or pelvic cavity. It is important to localize the testis and examine the contralateral side when abnormal features are detected. FHI, a rare benign tumor composed of fibrous, adipose, and myxoid tissue, typically appears as a well-defined, heterogeneous hyperechogenic mass on US. In conclusion, understanding the key features of inguinal lesions and correlating them with clinical findings is essential for accurate differential diagnosis and appropriate management.

Physics

SE-051

A High-Frequency Real-Time Doppler System for Monitoring Hemodynamics of the Microcirculation in Small Animal Brains

Wontae Son, Seoyun Chang, Changyang Lee, Jinhyoung Park
Sungkyunkwan University, Korea

OBJECTIVES: A real-time Doppler system was developed to measure blood flow for the investigation of microcirculatory hemodynamics in deep brain regions.
METHODS: High-frequency (24MHz) real-time Doppler system was implemented by using a high speed (250MHz) analog-to-digital converter (ADC) and a field-programmable gate array (FPGA) embedded board having operational frequency of 100 MHz. A programmable high-frequency ultrasound platform was also developed to enhance the flow visualization. Echo data of 3 mm in depth was saved in the internal buffer of FPGA, and the Doppler processing was performed at specific locations within this depth. Doppler signals from hippocampus were acquired using a 24 MHz single element transducer.
RESULTS: Flow signal was acquired from a string phantom with a moving string of 1.0 mm in diameter, simulating blood flow. The peak flow velocity in was 3 mm/s, and this value could be displayed in real-time. From an in vivo study, a single-element ultrasound transducer operating at a frequency of 24 MHz. Doppler signals at 24 MHz from deep brain region revealed a flow velocity of 1.5 mm/s in the hippocampus.
CONCLUSIONS: A high-frequency real-time Doppler system was successfully implemented. Using this system, the flow signal from a regions in a small animal brain along the stimulated pathway was acquired with enhanced spatial resolution. Integrating systems capable of monitoring microvessels and continuously tracking various vital signs with therapeutic ultrasound could significantly enhance treatment efficacy.

SE-052

AI-Driven Ultrasound Chromatin Profiling for Non-Invasive, Real-Time Detection of 3D Genome Architecture Disruptions in Early Cancer and Aging

Rifaldy Fajar[1], Prihantini Prihantini[1], Sahnaz Vivinda Putri[2], Rini Winarti[3], Andi Nursanti[4]
[1]Mathematical and Computational BioMedicine Research Group, The Integrated Mathematical, Computational, and Data Science for BioMedicine Research Community Foundation, Indonesia, [2]Health Management Laboratory, International University Semen Indonesia, Indonesia, [3]Department of Biology, Yogyakarta State University, Indonesia, [4]Department of Pharmacology, Wallacea University, Indonesia

BACKGROUN/AIM: The 3D genome architecture regulates gene expression, and its disruption is a defining feature of oncogenesis and aging-related diseases. However, existing methods such as high-throughput chromosome conformation capture (Hi-C), assay for transposase-accessible chromatin using sequencing (ATAC-seq), and single-cell Hi-C (scHi-C) are invasive and lack real-time monitoring. This study explores a novel deep learning-assisted ultrasound-based biospectroscopy approach for non-invasive, real-time chromatin topology mapping in living tissues, providing an alternative to sequencing-based assays.

METHODS: This study applies AI-enhanced ultrasound wavefront analysis to measure chromatin stiffness variations associated with heterochromatin/euchromatin transitions, enhancer miswiring, and epigenetic remodeling. A self-supervised deep learning model was trained on data from the Encyclopedia of DNA Elements (ENCODE) consortium (n≈2,190), the National Institutes of Health (NIH) Roadmap Epigenomics Project (n≈6,800), and The Cancer Genome Atlas (TCGA) (n≈1,237 cancer patients), reconstructing chromatin conformation at 12-nm resolution. Additionally, an AI-driven 3D Chromatin Reorganization Atlas mapped disease-associated genome remodeling using data from the Genotype-Tissue Expression (GTEx) project (n≈4,691 tissue samples) and the Medical Information Mart for Intensive Care (MIMIC-IV) database (n≈16,400 ICU stays) for clinical validation.

RESULTS: The ultrasound-based chromatin profiling approach achieved 87.8% accuracy (95% CI: 86.3–89.2) in detecting chromatin compaction compared to Hi-C and ATAC-seq. AI-predicted chromatin topology disruptions were identified 8.9 years (95% CI: 8.2–9.7) before tumor formation ($p<0.0001$). Longitudinal tracking confirmed persistent chromatin accessibility alterations in pre-malignant tissues, correlating with oncogene transcription. Regional chromatin condensation patterns were tissue-specific, with reproducible elasticity signatures across cancer types and aging tissues. Real-time monitoring achieved a 24.3× speedup over conformation assays ($p<0.0001$), and enhancer rewiring correlated with oncogene activation ($R=0.91$, $p<0.0001$). Chromatin stiffness differentials predicted tumor progression rates, offering a biomarker for clinical risk stratification.

CONCLUSIONS: This study presents a transformative ultrasound-based approach for real-time, non-invasive chromatin monitoring, integrating AI with large-scale genomic datasets to improve early cancer and aging diagnostics.

SE-053

AI-Driven Ultrasound-Based Intracellular Trafficking Profiling for Real-Time, Non-Invasive Detection of Organelle Transport Dysregulation in Neurodegeneration and Cancer Metastasis

Prihantini Prihantini[1], Sahnaz Vivinda Putri[2], Rini Winarti[3], Andi Nursanti[4], Rifaldy Fajar[1]
[1]Mathematical and Computational BioMedicine Research Group, The Integrated Mathematical, Computational, and Data Science for BioMedicine Research Community Foundation, Indonesia, [2]Health Management Laboratory, International University Semen Indonesia, Indonesia, [3]Department of Biology, Yogyakarta State University, Indonesia, [4]Department of Pharmacology, Wallacea University, Indonesia

BACKGROUND / AIM: Intracellular trafficking governs organelle transport, essential for neuronal function and cancer cell invasion. Dysregulation in organelle transport is an early marker of

neurodegeneration and metastasis, yet current methods rely on ex vivo fluorescence microscopy, preventing real-time assessment in humans. This study develops an AI-driven ultrasound framework for non-invasive intracellular transport tracking, enabling early detection of neurodegenerative and metastatic processes by analyzing real-time sub-micron organelle motion in living tissues.

METHODS: High-frequency ultrasound elastography was used to track real-time intracellular organelle motion, particularly mitochondria and vesicles, by analyzing sub-micron motion signatures. A deep learning framework was trained on 6,400 ultrasound-derived intracellular transport waveforms, using a self-supervised learning approach to reconstruct spatiotemporal organelle motion patterns. A graph-based trajectory model was developed to quantify intracellular motility, detecting abnormalities associated with neurodegeneration and metastasis. Disease-specific intracellular transport disruptions were identified by comparing AI-generated motility indices with neuronal atrophy markers and metastatic signatures. Validation utilized datasets from: the UK Biobank Neuroimaging Subset (n=3,920) for neurodegeneration-associated transport patterns, the MIMIC-IV Neurodegeneration Cohort (n=1,860) for clinical progression correlations, and the Allen Brain Atlas Histopathology Dataset (n=890) for axonal transport validation.

RESULTS: Intracellular organelle transport mapping accuracy was 86.4% (95% CI: 85.2–87.6). Neurodegeneration prediction achieved 82.7% accuracy ($p<0.0001$), detecting disease onset 6.9 years (95% CI: 6.3–7.5) before clinical symptoms. Real-time intracellular transport tracking was 22.8× faster than fluorescence-based imaging ($p<0.0001$). AI-extracted axonal transport disruption metrics strongly correlated with neuronal atrophy and metastasis ($R = 0.84$, $p<0.0001$). Mitochondrial motility reduction was observed in Alzheimer's patients, correlating with tau protein accumulation, while metastatic cells showed enhanced lysosomal transport speeds.

CONCLUSIONS: This study establishes AI-driven ultrasound intracellular trafficking profiling as a non-invasive, real-time diagnostic tool, offering earlier neurodegeneration and metastasis detection than current imaging methods.

SE-054

Developing a Dual-Frequency Needle Ultrasonic Transducer for Cortical Network Study in Small Animal Brains with Low-Frequency

Daegan Kee, Taewon Choi, Seunghoo Kim, Yeji Seo, Jinhyoung Park
Sungkyunkwan University, Korea

INTRODUCTION: A dual-frequency ultrasonic needle transducer was developed to investigate cortical networks in small animal brains by simultaneously delivering low-frequency stimulations while performing optical imaging.

MATERIALS & METHODS: The operational frequency of a needle ultrasonic transducer with a diameter of less than 2 mm was lowered using a PMN-PT piezoelectric single crystal with a high dielectric constant and a poling technique employing alternating current. A needle transducer with dual resonance peaks at 6 MHz and 1 MHz was developed, where longitudinal and spurious modes were respectively generated. A glass capillary puller was used to fabricate a beam guide, which was subsequently attached to the transducer to enhance the precision of acoustic delivery. Focalized ultrasonic stimulations were applied to the primary somatosensory cortex (S1) to investigate cortical networks and motor responses.

RESULTS: The beam guide enabled localized delivery, and the pressure measured at the tip of the guide reached 0.15 MPa. Additionally, the guide narrowed the beam width, improving stimulation precision. Due to the small size of the transducer, the visible field of view was maximized to observe brain activity using wide-field cerebral blood volume (CBV) imaging. CBV increases were detected in response to ultrasonic stimulation at S1. Notably, stimulation at S1 also induced CBV elevation in the primary motor cortex (M1), a region which is known to be functionally connected to S1.

CONCLUSION: The low-frequency (1 MHz) needle ultrasonic transducer capable of delivering focalized cortical stimulations was successfully developed.

The transducer effectively stimulated S1, and the linked activation was measured in M1. These results confirm the transducer's utility for studying cortical connectivity. Further investigations will optimize stimulation parameters and assess broader neurophysiological effects. Acknowledgements This work was supported by the National Research Foundation of Korea(NRF) grant funded by the Korea government(MSIT) (RS-2023-00265524, RS-2024-00348848).

SE-055

Dual-Frequency Implantable Transparent Ultrasonic Transducers for Integrated Brain Stimulation and Monitoring

Minseok Koo, Changyang Lee, Jinhyoung Park
Sungkyunkwan University, Korea

INTRODUCTION: High-voltage alternating current (AC)-poling of PMN-PT single crystal has been reported to increase the transparency of the element and enhance nonlinear vibrations. Utilizing these properties of PMN-PT, we propose a novel dual-frequency transparent transducer capable of both low-frequency stimulation and hemodynamic response monitoring via high-frequency Doppler imaging and wide-field optical imaging.

MATERIALS & METHODS: Transducer was fabricated by applying Indium-Tin-Oxide (ITO) electrodes to PMN-PT crystal and loading transparent epoxy-backing layer. High-voltage AC-poling was performed to increase transparency and acoustic output at 1-MHz. Performance evaluation was done using impedance analyzer, hydrophone system and phantom imaging. Transparency of the transducer was examined via UV-Vis spectrometer. For in-vivo assessment, transducer was implanted to the mouse skull, and low-frequency stimulation-evoked hemodynamic responses at the cortex and deep-brain region were measured through wide-field optical imaging and 7-MHz Doppler imaging after applying 1-MHz stimulation pulses.

RESULTS: The optical transmittance in the AC-poled PMN-PT was increased by 11.2% compared to that of DC-poled PMN-PT. Additionally, impedance peak was observed at both 7-MHz and 1-MHz for the high-voltage AC-poled transducer. Especially, the impedance at 1-MHz was 762-Ω and 112-Ω at DC-poled and AC-poled transducer, respectively, showing significant impedance drop at AC-poled transducer. 7-MHz Doppler imaging was successfully acquired using string phantom and mouse in-vivo experiment, while hydrophone measurement at 1-MHz showed sufficient acoustic pressure (up to 0.4-MPa) for ultrasound neuromodulation. Hemodynamic responses were observed in both cortex region (wide-field optical imaging) and deep-brain region (Doppler imaging) after 1-MHz ultrasound stimulation.

CONCLUSION: With a single transducer, we could not only deliver 1-MHz stimulation pulses but also simultaneously monitor the post-stimulus hemodynamic responses through 7-MHz Doppler imaging and wide-field optical imaging due to its transparent and dual-frequency characteristics, respectively. Acknowledgements This work was supported by the National Research Foundation of Korea(NRF) grant funded by the Korea government(MSIT) (RS-2023-00265524, RS-2024-00348848).

Therapeutic Ultrasound

SE-056

Cryo-Shocked Tumor-Reprogrammed Sonosensitive Antigen-Presenting Cells Improving Sonoimmunotherapy via T Cells and NK Cells Immunity

Xindi Qian
Department of Medical Ultrasound and Center of Minimally Invasive Treatment for Tumor, Shanghai Tenth People's Hospital, Tongji University, China

Ultrasound has demonstrated versatility in cancer immunotherapy, yet insufficient co-stimulating molecules and loss of peptide-major histocompatibility complex I (MHC-I) expression on tumor cells lead to poor therapeutic effect, and the concurrent enhancement of both T cells and Natural killer (NK) cells through an ultrasound strategy has not to be fully exploited. We used reprogrammed

antigen-presenting cells (APC)-like tumor cells to construct a sonosensitive system, named dead APC-4T1-N3-LipoH (DPNL). Upon ultrasound irradiation, DPNL cells could co-stimulate the antigen-presenting program and strikingly elicit antigen-specific T cell-mediated adaptive immunity in tumor draining lymph nodes (TDLNs) as well as MHC-I unrestricted NK cell-mediated innate immunity within tumors for comprehensive sonoimmunotherapy for solid tumors. The constructed sonosensitive, cryo-shocked, reprogrammed tumor cells exhibit dual homologous targeting features of both APC and tumor cells as well as co-stimulating molecules (CD80, CD86), serving as a spatiotemporal sonosensitizer delivery cargo and initiator for amplifying NK cell-based innate immunity and T cell-based adaptive immunity. This study utilized and elucidated the role of ultrasound and co-stimulating molecules in antigen-presenting process: triggering MHC-I unrestricted NKG2D-NKG2DL pathway in TIME and binding to co-stimulating receptors on T cells in TDLNs. Reprogramming cancer cells into APC-like subsets and conjugating them with clinically approved sonosensitizer HMME via click chemistry represents a clinically accessible and efficient sonosensitizer delivery strategy, which provides a new insight into spatiotemporal modulation of immune response and potentially advance cancer sonoimmunotherapy. The above research has been published in Advanced Materials (https://doi.org/10.1002/adma.202413289).

SE-057

Dual Receptor Targeting, Treatment, and Imaging With a Chitosan Nanoplatform That Simultaneous Administration of Gallic Acid and Ultra-Small Magneses Nanoaggregates

D Singh
MPGI, India

INTRODUCTION: The use of theranostic nanoparticles in cancer detection and treatment has recently attracted a lot of interest. This research aimed to create theranostic chitosan nanoparticles for imaging and treatment of breast cancer that were functionalized gallic acid and ultra-small magneses nano aggregates with and folic acid (GC-MNNPs-FA).
METHOD: The nanoparticles (NPs) were studied and evaluated for their potential anti-cancer effects.
RESULT: The developed nontargeted theranostic NPs, and GC-MNNPs-FAand dual targeted theranostic NPs have small particle sizes and good surface charge, respectively. Research on the cytotoxicity of folate receptor (FR) expressing breast cancer cells found that GC-MNNPs-FA, a dual-targeted theranostic NP, inhibited cell proliferation in MCF-7 and T-47D cells by 54.17 and 42.23 times, respectively, compared to free PB. Also, unlike free PB, the created NPs could effectively block MCF-7 cells' ability to advance from the G1 to the S phase of the cell cycle. Compared to free PB, GC-MNNPs-FA and dual-targeted theranostic NPs were able to dramatically decrease tumour vascularity and reduce hypoxic tumour volume, according to ultrasound and photoacoustic (USG/PA) imaging. In addition, optical imaging in vivo showed that the dual-targeted theranostic NPs accumulated specifically in tumours. The biocompatibility of the created nanoformulations was further validated by histopathological and in vitro hemocompatibility investigations.
CONCLUSION: Based on our findings, theranostic chitosan nanoparticles functionalised with GC-MNNPs-FA were not effective in imaging or treating breast cancer.

SE-058

RCP vs. EUS-FNA in the Diagnosis of Presumed Malignant Biliary Obstruction: A Systematic Review and Meta-analysis

Derizal Derizal[1], Roland Helmizar[2]
[1]IP Trisakti, Indonesia, [2]Department of Internal Medicine, Baiturrahmah University, Indonesia

The common etiologies of obstructive jaundice were biliary stone and biliary neoplasms. The gold standard to diagnose malignancy causing obstructive jaundice is endoscopic retrograde cholangiopancreatograph y (ERCP). Other modalities include endoscopic ultrasonography guided fine needle aspiration (EUS-FNA). Thus, we aim to compare the sensitivity of EUS-FNA and ERCP in the diagnosis of patients with presumed

malignancy causing obstructive jaundice. We performed a systematic search study from PUBMED, EMBASE, EBSCO, PROQUEST, snowballing, global index medicus, GARUDA, SINTA, and several digital libraries of universities in Indonesia until January 31, 2024. There were 5 studies that met the eligibility criteria. The main outcome measurement were sensitivity. Data were analyzed using Review Manager 5.4.1. The overall pooled sensitivity of ERCP for diagnosis of malignant biliary obstruction were 62.2% [95% CI 57.7– 74.7%] and the overall pooled sensitivity of EUS- FNA for diagnosis of malignant biliary obstruction were 86.7% [95% CI 72.5–89.4%]. EUS-FNA was more superior to ERCP in the diagnosis of malignancy causing obstructive jaundice.

Thyroid

SE-060

A Study Compared the Thyroid Ultrasound Measurements of Citizens and Those of Workers Who Were Exposed to X-Rays

Amgalanbayar Tumendelger
Department of Otorhinolaryngology, ENT DOCTORS SOCIETY IN MONGOLIA, Mongolia

PURPOSE: To evaluate the impact of abnormal working conditions on the thyroid gland

MATERIALS AND METHODS: Group 1, A total of 501 participants (147 males and 344 females; mean age, 55.1 ± 9.46 years) who underwent thyroid ultrasound examination at Erdenet Medical Hospital in 2022. Group 2, A total of 42 employees (15 women, 27 men; mean age, 42.4 ± 8.98) who have been working with X-ray for 2-10 years. All of 543 people were included in this cross-sectional study, and statistical data processing was done using SPSS 25. The length (L), antero-posterior depth (D), and transversal width (W) of each lobe of the thyroid gland were measured. A formula was used to calculate the volume of the thyroid gland. Volume = 0.47 x (L x D x W). Thyroid nodules were classified according to TIRADS.

RESULTS: For group 1, the mean thyroid volume was 8.62 ± 5.38 ml while the that of group 2 was 8.88 ± 3.54 ml. Group 1 had a 55.7 percent prevalence of thyroid nodules, while group 2 had a 30.9 percent prevalence. In the TIRADS category, Groups 1 and 2 had TIRADS-2 at 52.3 %, TIRADS-3 at 2.8 %, TIRADS-2 at 30.9 %, and TIRADS-3 at 2.3 %. TIRADS-4 was 0.6% in group 1.

CONCLUSION: There was no difference in thyroid nodule distribution, thyroid volume, or TIRADS classification between the two groups. However, there was a difference in age between the two groups (<0.005).

SE-061

Efficacy and Determinants of Single-Session Ethanol Ablation in Thyroid Cysts 10 mL and Larger

Kai-Lun Cheng
Department of Radiology, Chung Shan Medical University Hospital, Chinese Taipei

BACKGROUND: Ethanol ablation (EA) is widely recognized as a first-line therapy for recurrent symptomatic cystic thyroid nodules after initial aspiration. However, its effectiveness may be diminished when the cyst's initial volume exceeds 10 mL. This study aimed to evaluate the outcomes of single-session EA in patients with thyroid cysts measuring ≥10 mL in volume.

METHODS: This retrospective analysis included 70 patients categorized into three groups based on initial cyst volume: Group 1 (≥10, <20 mL), Group 2 (≥20, <40 mL), and Group 3 (≥40 mL). The primary endpoints were the volume reduction ratio (VRR) and therapeutic success (VRR >50%) at the 6-month follow-up. Secondary measures included symptom relief, cosmetic improvements, and factors associated with VRR.

RESULTS: At six months, the median VRR was 94.8% (interquartile range: 88.3–98.1%), with a therapeutic success rate of 90%. Significant reductions in nodule size, along with improved symptom scores and cosmetic outcomes, were observed (all p < 0.001). Nodules ≥40 mL exhibited worse symptom and cosmetic scores compared to

those in the 10–20 mL range ($p < 0.05$), though VRR differences were not statistically significant ($p = 0.944$). A higher solid component and increased vascularity were negatively correlated with VRR ($p = 0.001$ and $p = 0.002$, respectively).

CONCLUSION: Single-session EA is an effective treatment for thyroid cysts ≥10 mL, achieving substantial volume reduction and symptomatic improvement. However, nodules with a larger size, greater solid content, or increased vascularity may require individualized treatment approaches to optimize outcomes.

SE-062

Efficacy and Safety of Thermal Ablation for Indeterminate Thyroid Nodules: A Systematic Review and Meta-Analysis

Hunjong Lim[1], Se Jin Cho[1], Younbeom Jeong[1], So Yeong Jeong[1], Jung Hwan Baek[2]

[1]Department of Radiology, Seoul National University Bundang Hospital, Korea, [2]Department of Radiology, Asan Medical Center, Korea

BACKGROUND / AIM: The management of indeterminate thyroid nodules, classified as Bethesda III and IV, remains challenging because of the limitations of biopsy methods such as fine-needle aspiration and core needle biopsy for differentiating benign from malignant nodules. While diagnostic lobectomy is the standard approach for management of indeterminate thyroid nodules, thermal ablation (TA) is increasingly being considered for patients who are unable or unwilling to undergo surgery. This systematic review and meta-analysis therefore evaluates the efficacy and safety of TA for indeterminate thyroid nodules.

METHODS: A comprehensive search of MEDLINE, EMBASE, and COCHRANE databases was performed up to June 11, 2024, to identify studies that used TA on patients with indeterminate thyroid nodules. Data extraction and quality assessment were independently performed by two radiologists according to PRISMA guidelines. The analysis yielded the serial volume reduction ratios (VRRs) of ablated nodules, regrowth rates, delayed surgeries, malignancy detection post-ablation, and procedure-related complications.

RESULTS: Our analysis included nine studies with 293 nodules and revealed a progressive increase in VRR, reaching a plateau at 12 months. The pooled VRR at 12 months was 78.4%. Complications were minimal, with major complications occurring in only 1.4% of cases and no metastasis being reported. Regrowth and delayed surgery were observed in 2.4% and 0.7% of cases, respectively, with two cases showing malignancy upon delayed surgery.

CONCLUSION: TA shows promise as a safe and effective treatment for indeterminate thyroid nodules. Despite low post-ablation malignancy rates, the residual risk warrants close follow-up, especially in larger nodules. Advanced TA techniques such as hydrodissection may enhance outcomes by increasing the likelihood of complete ablation.

SE-063

Efficacy of Radiofrequency Ablation for Solid Thyroid Nodules

Javzmaa Divaa[1], Otgonbayar Setevdorj[2]

[1]Department of Radiology, The Mongolian Society of Radiology, [2]Department of Surgery, First Central Hospital of Mongolia, Mongolia

OBJECTIVES: Thyroid nodules (TNs) are a common clinical issue, and their prevalence has been increasing over the last 2 decades 3 due to the widespread use of ultrasound (US) imaging. Nodular goiter is the most common cause of thyroid disease in Mongolia, as in other countries. We have introduced a new method of RFA treatment (2019) in our country.

PURPOSE: To assess the effectiveness of radiofrequency ablation (RFA) for solid thyroid nodules.

MATERIALS AND METHODS: This retrospective study was approved by the Research Ethics Committee of the Mongolian National University of Medical Sciences and informed consent was obtained from all patients before RFA. The study was conducted from 9th Jan 2019 to 15th Oct 2021, 485 nodules from 183 patients (M:F=5:145; mean age±SD=49.4±10.5 years) who met the eligibility criteria and provided written informed consent were

enrolled at the First Central Hospital of Mongolia. Nodules were assessed pre-treatment and at 1, 3, 6, 12, and 24 months post-treatment. Nodule volume were recorded at each time point.

RESULTS: For the primary outcome of nodule volume reduction, the absolute volume reduction at the 24-month follow-up was 266 (81.8%). Completely destroyed 39 (12%), volume increased by 20 (5.5%). The median volume reductions at the 1, 3, 6, 12, and 24-months follow-ups were 33.4%, 56.8%, 70.6%, 73.7% and 74.9% respectively. Median volume statistically decreased by a significant p=0.0001. At 12 months follow up after RFA, the nodules decreased most. All study subjects recovered without sequelae. Therefore, no patient experienced a life-threatening or delayed complication during the follow-up.

CONCLUSION: Our study demonstrates that RFA is a safe and effective treatment for solid thyroid nodules. Advantages of RFA include no surgical scars or general anesthesia, low complication rates, and avoiding lifelong thyroid hormone replacement.

SE-064

Longterm Clinical Outcomes of Thermal Ablation for Benign Thyroid Nodules and Unresolved Issues: A Comprehensive Systematic Review

So Yeong Jeong[1], Jung Hwan Baek[2]

[1]Department of Radiology, Seoul National University Bundang Hospital, Korea, [2]Department of Radiology, Asan Medical Center, Korea

Thermal ablation is widely accepted as an efective and safe method for treating benign thyroid nodules. Many studies reporting short-term results have consistently demonstrated the efcacy and safety of thermal ablation. However, as the clinical application of thermal ablation grows and follow-up periods extend, long-term clinical outcomes of thermal ablation have revealed several issues, including regrowth and diagnosis of malignancy in ablated lesions. In this systematic review, we analyze the long-term clinical outcomes of thyroid thermal ablation, focusing on regrowth, delayed surgery, and the potential for malignancy after thermal ablation and propose solutions to address these unresolved issues and enhance the management of benign thyroid nodules through thermal ablation.

SE-065

Prognostic Significance of Clinicopathological and Ultrasonographic Features in Anaplastic Thyroid Carcinoma Beyond TERT Promoter Mutation

Haejung Kim[1], Goeun Park[2], Myoung Kyoung Kim[1], Jae Ho Lee[1], Young Lyun Oh[3], Tae Hyuk Kim[4], Jung Hee Shin[1], Soo Yeon Hahn[1]

[1]Department of Radiology, Samsung Medical Center, Korea, [2]Samsung Medical Center, Korea, [3]Department of Pathology, Samsung Medical Center, Korea, [4]Department of Internal Medicine-Endocrine, Samsung Medical Center, Korea

BACKGROUND / AIM: TERT promoter mutation is associated with poor prognosis in differentiated thyroid carcinoma, with US features varying by mutation status. However, this correlation in anaplastic thyroid carcinoma (ATC) is understudied. We investigated the association between clinicopathological characteristics and US features of ATC with TERT mutation status and prognosis.

METHODS: From November 1994 and May 2022, 58 consecutive ATC nodules from 58 patients were analyzed. Two radiologists retrospectively reviewed US features based on the revised Korean Thyroid Imaging Reporting and Data System (K-TIRADS) and American College of Radiology Thyroid Imaging Reporting and Data System (ACR-TIRADS). The association of clinicopathological variables and US features of ATC with the TERT promoter mutation status and survival period was analyzed.

RESULTS: Of all 58 ATC nodules (mean age ± standard deviation (SD), 66.74 ± 12.44 years), 32 nodules were tested for TERT promoter mutation and detected in 11 nodules. TERT promoter-mutated ATC was larger than TERT wild-type ATC (mean size ± SD, 5.47 ± 1.12 cm vs. 4.14 ± 1.77 cm, p = 0.032); however, no other significant differences in characteristics were observed. ATC with a survival period of less than 12 months were more likely to have lymph node metastasis (82.86% vs. 52.17%, p = 0.012) or distant metastasis at diagnosis (74.29%

vs. 17.39%, p < 0.001), larger size on US (mean size ± SD, 5.17 ± 1.49 cm vs. 3.95 ± 1.63 cm, p = 0.005), and suspicion for gross extrathyroidal extension on US (91.43% vs. 69.57%, p = 0.04) compared to ATC with a survival period of 12 months or more.

CONCLUSION: Advanced disease at diagnosis was a critical factor associated with one-year survival in patients with ATC, whereas the TERT promoter mutation status was not.

SE-066

Radiofrequency Ablation for Patients with Primary Hyperparathyroidism: A Multicenter, Non-Randomized, Open-Label, Single-Arm Prospective Clinical Trial

Eun Ju Ha[1], Jihoon Kim[2], Jung Hwan Baek[3]
[1]Department of Radiology, Ajou University Hospital, Korea, [2]Department of Radiology, Seoul National University Hospital, Korea, [3]Department of Radiology, Asan Medical Center, Korea

BACKGROUND / AIM: To evaluate the efficacy, safety and factors influencing the response of radiofrequency ablation (RFA) in patients with primary hyperparathyroidism (PHPT) using a prospective multicenter design.

METHODS: Between September 2022 and June 2024, 34 patients with 35 parathyroid lesions who either refused surgery or were ineligible for it underwent RFA for the treatment of PHPT across three hospitals. Nodule size, volume, and biochemical data including parathyroid hormone (PTH) and calcium levels, were compared before and after treatment (at 2 hours, 1 week, and 1, 3, 6, 12 months). Complications were assessed during and after treatment. Factors influencing the treatment response to RFA for PHPT were analyzed.

RESULTS: Significant reductions in nodule size and volume, as well as improvements in serum PTH, total calcium, ionized calcium, phosphorus, and 25-OH vitamin D3, were noted at the 3-, 6-, and 12-month follow-ups after RFA (all P < 0.05). Out of the 34 patients, 17 experienced a complete response with normalized serum PTH and calcium levels (50.0%), while 17 showed a partial response (50.0%) after a mean treatment session of 1.0. The initial serum PTH level was a key factor associated with the treatment response to RFA for PHPT, with an area under the receiver operating characteristic curve of 0.853 using a cutoff value of PTH ≥ 118 pg/mL. Transient voice change (n=1) and transient hypocalcemia (n=1) were reported after the procedure.

CONCLUSION: RFA is a safe and effective treatment option for patients with PHPT in selected cases. The initial PTH level is crucial for achieving biochemical cure after a single treatment.

SE-067

Reevaluating the Malignancy Risk of K-TIRADS 2 Benign Thyroid Nodules: An Intracystic Small Echogenic Focus With a Comet-Tail Artifact Is Not Highly Specific for Benignity

Jaeyong Min[1], Dong Gyu Na[1], Byeong-Joo Noh[2]
[1]Department of Radiology, GangNeung Asan Hospital, Korea, [2]Department of Pathology, GangNeung Asan Hospital, Korea

BACKGROUND / AIM: This study aimed to evaluate the malignancy risk of benign thyroid nodules classified as Korean Thyroid Imaging Reporting and Data System (K-TIRADS) 2, characterized by cystic composition, iso-/hyperechoic spongiform appearance, and intracystic echogenic foci with comet tail artifacts, in a large clinical cohort.

METHODS: This retrospective study included 3,773 consecutive thyroid nodules with final diagnoses among 4,412 nodules (>1 cm) that underwent biopsy. The ultrasound (US) features of the nodules were evaluated and documented during real-time US examinations. The malignancy risk of the three US patterns of K-TIRADS 2 benign nodules was estimated, and the malignancy risk of nodules with intracystic echogenic foci with comet tail artifacts was further analyzed based on the size of the echogenic foci's head and tail (small < 2 mm; large ≥ 2 mm).

RESULTS: The overall malignancy risk of K-TIRADS 2 nodules was 1.9% (3/155) [cystic, 0% (0/29); iso-/hyperechoic spongiform, 0% (0/29); intracystic echogenic foci with comet tail artifacts, 3.1% (3/97)], which was not significantly lower than

the malignancy risk of K-TIRADS 3 nodules (4.6%, 77/1,660; P=0.117). The three malignant tumors (one invasive encapsulated follicular variant papillary carcinoma and two follicular thyroid carcinomas) were found exclusively in partially cystic K-TIRADS 2 nodules with intracystic small echogenic foci with comet tail artifacts. No malignancies were detected in K-TIRADS 2 nodules with intracystic large echogenic foci with comet tail artifacts. The malignancy risk (5.6%, 3/54) of partially cystic nodules with small echogenic foci with comet tail artifacts was comparable to that of K-TIRADS 3 nodules (P=0.738).

CONCLUSION: The malignancy risk of partially cystic K-TIRADS 2 nodules with intracystic small echogenic foci with comet tail artifacts was similar to that of K-TIRADS 3 nodules. These nodules may need to be reclassified as low-suspicion K-TIRADS 3 nodules.

SE-068

Role of Radiofrequency Ablation in the Treatment of Symptomatic Distant Metastasis of Thyroid Cancer

Jae Ho Lee[1], Sae Rom Chung[1], Jung Hwan Baek[1], Dong Eun Song[2], Won Gu Kim[3], Tae Yong Kim[3], TaeYon Sung[4], Jeong Hyun Lee[1]

[1]Department of Radiology, Asan Medical Center, Korea, [2]Department of Pathology, Asan Medical Center, Korea, [3]Department of Internal Medicine, Asan Medical Center, Korea, [4]Department of Surgery, Asan Medical Center, Korea

BACKGROUND / AIM: To evaluate the efectiveness and safety of radiofrequency ablation (RFA) for the treatment of symptomatic distant metastasis of diferentiated thyroid carcinoma.

METHODS: The medical records of 12 patients who underwent RFA for the palliative treatment of 18 symptomatic distant metastases from thyroid cancer between January 2008 and December 2020 were analyzed. All patients were assessed for their degree of discomfort and underwent periodical evaluations as outpatients, including clinical examination, imaging, and serologic markers.

RESULTS: Among the 18 tumors treated, nine were soft tissue, and nine were bone metastases. The mean size of the treated tumors was 5.3 cm (range, 1.7–10.7 cm). All patients complained of pain, discomfort and/or bulging of the metastatic mass before RFA. After RFA, 11 out of the 18 patients with metastatic tumors (61.1%) reported a subjective improvement in symptoms. Nine out of 18 tumors decreased in size, with a mean size reduction ratio of 43%±22%. Although symptom improvement was achieved in 61.1% of the tumors, after a mean follow-up duration of 37.4 months, fve patients experienced progression of the tumor, four patients had a stable tumor status, and three patients died from pneumonia. There were no major adverse events related to RFA during the treatment or follow-up period.

CONCLUSION: RFA can be used as palliative therapy to relieve the symptoms caused by metastatic tumors; however, it has a limited role in improving the overall prognosis in patients with distant metastasis from thyroid cancer.

SE-069

Temporal Involutional Change on Ultrasonography After RFA for PTMC

Taehyuk Ham, Ji-hoon Kim, Ji Ye Lee, Meesun Lee

Department of Radiology, Seoul National University Hospital, Korea

BACKGROUND / AIM: Radiofrequency ablation (RFA) has been proposed as a promising alternative to surgery or active surveillance for papillary thyroid microcarcinoma (PTMC). However, ultrasonographic changes following RFA beyond mere “disappearance” are not well established. This study aims to investigate the temporal ultrasonographic features after RFA in patients with low-risk PTMC.

METHODS: This prospective cohort study included 98 patients with low-risk PTMC who underwent ultrasound-guided RFA between November 2018 and November 2021. Follow-up ultrasound assessments were conducted immediately post-RFA and at 2, 6, 12, 18, 24, 30, 36, 48, and 60 months to analyze ultrasonographic features and volume changes. In addition, a detailed analysis of characteristic ultrasonographic features was conducted by two radiologists independently to assess the temporal

evolution of these changes. Statistical analyses, including chi-square and t-tests, were performed to identify factors associated with 1-year residual nodularity.

RESULTS: A peripheral hypoechoic halo was observed in 91.84% of cases at 2 months post-RFA and completely resolved by 30 months. Ill-defined hypoechoic parenchymal changes were noted in 66.33% of nodules at 12 months, while capsular retraction was present in 61.86% of cases by 18 months. Linear ablation tracks were identified in 71.13% of cases at the same interval. The ablation zone volume initially expanded to 2.08 mL immediately after RFA. At 12 months, 29 of 97 cases (29.9%) still exhibited residual nodularity, with a mean volume of 0.02 mL. However, the volume progressively decreased, reaching 0 mL by 60 months, achieving a 100% volume reduction ratio (VRR). Statistical analysis revealed that larger initial and immediate post-RFA volumes were significantly associated with 1-year residual nodularity.

CONCLUSION: RFA induces characteristic and predictable ultrasonographic changes in PTMC, including hypoechoic halos, ill-defined parenchymal changes, capsular retraction, and progressive volume reduction. Recognizing these patterns may enhance the accuracy of long-term monitoring and improve management strategies for PTMC patients treated with RFA.

SE-070

The Intersection of Machine Learning and Ultrasound in Thyroid Cancer Diagnosis: A Bibliometric Study

Rian Ka Praja, Reny Rosalina
Universitas Palangka Raya, Indonesia

Thyroid cancer is a frequently occurring malignancy, and its early and accurate detection is vital for effective patient care. In recent years, research has increasingly focused on integrating machine learning with ultrasound imaging to improve diagnostic accuracy. This bibliometric study systematically examined the existing literature on the use of machine learning techniques for ultrasound-based thyroid cancer diagnosis. Advanced bibliometric methods were employed to evaluate and synthesize research findings in this field. Using the Scopus database, studies published between 2017 and 2024 were analyzed, and co-authorship as well as co-occurrence patterns were assessed using VOSviewer software (version 1.6.19). The search strategy identified 50 relevant publications, revealing a rising trend in research at the intersection of machine learning and thyroid cancer diagnosis. Co-occurrence analysis highlighted the use of various machine learning algorithms—including convolutional neural networks, support vector machines, and K-nearest neighbors—to enhance diagnostic precision in ultrasound imaging. Key research themes identified in the literature include feature extraction, classification models, and performance evaluation metrics. Among the algorithms studied, the support vector machine demonstrated a remarkable accuracy of 96%, positioning it as a promising tool for thyroid cancer diagnosis. This bibliometric analysis offers valuable insights into the current research landscape and potential future directions, emphasizing the growing role of machine learning in improving diagnostic outcomes for thyroid cancer.

SE-071

Thyroid Volume and Morphologic Change After Radiofrequency Ablation for Papillary Thyroid Microcarcinoma: CT-Based Analysis

Meesun Lee, Taehyuk Ham, Inpyeong Hwang, Ji Ye Lee, Ji-hoon Kim
Department of Radiology, Seoul National University Hospital, Korea

BACKGROUND / AIM: Radiofrequency ablation (RFA) is an emerging technique for treating papillary thyroid microcarcinoma (PTMC), but how it affects normal thyroid parenchyma remains unclear. We aimed to assess the impact of RFA on thyroid volume and morphology in patients with PTMC.

METHODS: In this single-center, prospective cohort study, we included 92 patients with PTMC (<1 cm) who underwent RFA and had pre- and 1-year post-ablation CT scans. Volumetric CT segmentations were performed to calculate volume loss of the ipsilateral, contralateral, and whole thyroid gland. Morphologic changes after RFA were evaluated at post-ablation CTs in comparison with pre-ablation CTs. The paired Wilcoxon signed-rank test was used to compare volumes between pre- and post-ablation CT scans. Multivariate linear regression analysis was conducted to identify the factors related to volume loss of the ipsilateral thyroid parenchyma.

RESULTS: After RFA, there was a 13.6% reduction of ipsilateral thyroid volume (95% CI: 11.5–15.7%, $p < .001$) resulting in a 6.1% loss of the total thyroid (95% CI: 4.0–8.2%, $p < .001$). There was no significant change in the contralateral parenchyma (mean: -1.3%, 95% CI: -3.7–1.1%, $p = .18$). Ipsilateral volume loss at 1 year remained stable at 5 years ($p = .09$). Radiofrequency ablation energy ($\beta = -10.66$, $p < .001$) was a significant predictor of ipsilateral thyroid volume loss, although there were no significant associations with pre-ablation tumor size, immediate ablation zone volume, and tumor volume loss. While PTMC was detectable in 69 (75.0%) pre-ablation CT scans, RFA led to loss of nodularity (91.3% [63/69]) accompanied by morphologic changes on post-ablation CTs, including linear ablation tracks (68.5% [63/92]), loss of calcification (62.5% [5/8]), thyroid capsular retraction (38.0% [35/92]), and intraparenchymal defects (5.4% [5/92]).

CONCLUSION: CT-based evaluation confirms minimal thyroid volume loss with characteristic morphological changes following RFA for PTMC.

SE-072

Ultrasound Characteristics of High-Grade Follicular-derived Carcinomas: Insights into Poorly Differentiated and Differentiated High-Grade Thyroid Carcinoma

Myoung Kyoung Kim, Jaeho Lee, Haejung Kim, Soo Yeon Hahn, Jung Hee Shin
Department of Radiology, Samsung Medical Center, Korea

BACKGROUND / AIM: The 2022 WHO classification has introduced two new categories of nonanaplastic high-grade follicular-derived carcinomas, which included differentiated high-grade thyroid carcinoma (DHGTC) and poorly differentiated thyroid carcinoma (PDTC). This study aims to identify the ultrasound features of high-grade follicular-derived thyroid carcinomas and differentiate between DHGTC and PDTC.

METHODS: Total 55 patients who had surgically confirmed DHGTC and PDTC between May 2022 and Dec 2024 were included in this study. All of them were available for analysis of preoperative US findings and histopathologic results. We investigated the ultrasound and clinicopathologic features of thyroid nodules and compared DHGTC with PDTC.

RESULTS: Case cohort included 47 cases of DHGTC and 8 cases of PDTC, with an average age of 42.1 years (Range 12-87). The median nodule size was 4 cm (IQR 2.5–5.2 cm). DHGTC predominantly exhibited a solid composition (75%), whereas PDTC showed a partial cystic composition in 75% of cases. Regarding growth patterns, DHGTC demonstrated a similar distribution of papillary and follicular patterns, whereas PDTC predominantly exhibited a follicular pattern (87.5%), which was significantly more frequent. In terms of risk classification, 70.2% of DHGTC cases were categorized as K-TIRADS 4 or 5, compared to 62.5% of PDTC cases. Among the 23 DHGTC cases that underwent fine needle aspiration (FNA), three were diagnosed as atypia of undetermined significance (AUS), and three as

benign; all exhibited a follicular growth pattern. Similarly, among the three PDTC cases that underwent FNA, all were diagnosed as AUS and demonstrated a follicular growth pattern.

CONCLUSION: DHGTC and PDTC exhibit similar suspicious ultrasonographic findings, with DHGTC favoring a solid composition, while PDTC more often presents with a partial cystic composition. Notably, in cases with a follicular growth pattern, FNA frequently results in an AUS diagnosis, highlighting the need for core needle biopsy.

Author Index

A

Afan, Aryofri: SE-014 (p200)
Ahn, Dongbin: CC03-S3 (p65)
Ahn, Hye Shin: CC06-S2 (p100)
Ahn, Kyung-Sik: MS01-S1 (p116)
Ahyong, Ahnee Mae: USB02-P1 (p185)
Albaeva, Yurana: SE-047 (p216), SE-049 (p217)
Alizargar, Javad: YIA-P2 (p163)
Altantsog, Enkhmaa: USB02-P6 (p188)
An, Jin Kyung: HI03-S3 (p130)
Aslam, Anum: SE-013 (p200)
Asma-ull, Hosna: MS02-P2 (p181)

B

Baasandorj, Davaasuren: USB03-P1 (p189)
Bae, Jae Seok: SS03-P1 (p171)
Bae, Soong June: SF05-S2 (p142)
Bae, Sua: IS01-S3 (p85)
Bae, Sung Hwan: CC02-S3 (p58)
Baek, Jung Hwan: HI02-S2 (p78), SS04-P6 (p178), SE-062 (p224), SE-064 (p225), SE-066 (p226), SE-068 (p227)
Baek, Sun Mi: SS04-P6 (p178)
Balter, Regina: SS01-P4 (p161)
Batbaatar, Saindelger: USB03-P4 (p191), SE-007 (p197)
Batkhuu, Tsendsaikhan: SE-017 (p202)
Batmunkh, Ankhzaya: USB02-P6 (p188)
Batmunkh, Erdenebulgan: SE-003 (p195)
Battseren, Bat-Erdene: USB03-P1 (p189)
Belavina, Natalya: SS01-P4 (p161)
Bende, Renata: HI01-P2 (p167)
Boldbaatar, Munkh-Uyanga: USB02-P6 (p188)
Boldbaatar, Saranchimeg: SE-003 (p195)
Boldoo, Sumiyabazar: USB02-P6 (p188)
Boleac, Daiana: HI01-P2 (p167)
Byekbolat, Aisulu: USB02-P6 (p188)

C

Cha, Dong Ik: HS01-S1 (p122)
Chae, Hyun Wook: YIA-P1 (p163), MS02-P6 (p183)
Chai, Jee Won: SE-033 (p210)
Chang, Jin Ho: CC09-S3 (p136)
Chang, Jung Min: HI03-S1 (p128)
Chang, Seoyun: SE-051 (p218)
Chang, Won Seok: SF06-S2 (p149)
Chen, Beiqi: SS01-P2 (p160)
Cheng, Juan: HI01-P3 (p167), SS03-P5 (p173)
Cheng, Kai-Lun: SE-061 (p223)
Cheng, Rui: HI01-P3 (p167)
Cheon, Jung-Eun: USB04-P3 (p193)
Chernyak, Victoria: SE-013 (p200)
Chiu, Ka-Fung Peter: MP02-S1 (p48), SF03-S1 (p125)
Cho, Minjee: SE-045 (p215)
Cho, Sangwoo: YIA-P5 (p165), SS04-P1 (p175)
Cho, Se Jin: SE-062 (p224)
Cho, Sung Cheol: MS01-P2 (p180)
Cho, Yeon Jin: USB04-P3 (p193)
Choi, Arum: MS02-P2 (p181)
Choi, Gayoung: CC08-S1 (p106)
Choi, Jae Won: USB04-P3 (p193)
Choi, Ji Soo: YIA-P3 (p164), SS02-P1 (p168), SS02-P3 (p169)
Choi, Taewon: SE-054 (p220)
Choi, Young Hun: USB04-P3 (p193)
Choo, Hyejung: SE-040 (p212)
Choo, Ki Seok: HS01-S2 (p123)
Chu, A Jung: CC01-S1 (p52)
Chung, Sae Rom: SE-068 (p227)
Cinco, Tanya Katherine: USB03-P5 (p191)
Cruz-tuble, Maria Regina: USB02-P3 (p186), USB03-P2 (p190), USB04-P4 (p193)
Cruz-Tuble, Maria Regina: USB03-P5 (p191), SE-022 (p205)

D

Dashzeveg, Erdenesuren: SE-003 (p195)
Davaa, Delgertsetseg: USB03-P1 (p189)
Derizal, Derizal: SE-058 (p222)
Destounis, Stamatia: MP01-S1 (p47)
Divaa, Javzmaa: SE-063 (p224)
Dong, Yi: HI01-P3 (p167), SS03-P5 (p173)
Dorjnamjim, Uyan-Egshig: SE-028 (p208)
Dumago, June Danica: SE-022 (p205)

E

Eom, Hye-Joung: CC01-S2 (p53)

F

Fajar, Rifaldy: SE-004 (p196), SE-011 (p198), SE-018 (p203), SE-052 (p219), SE-053 (p219)
Fan, Jun: SS01-P5 (p162)
Fang, Yi: SS01-P2 (p160)
Fujioka, Masayuki: SE-019 (p203)

G

Gankhuyag, Ariunbold: USB01-P1 (p184)
Gantogoo, Munkh-erdene: USB01-P1 (p184)
Ganzorigt, Zambaga: SE-026 (p207)
Gu, Kyowon: SS03-P4 (p172)

H

H, Divo: SE-014 (p200)
H, Roland: SE-009 (p198)
Ha, Eun Ju: SE-066 (p226)
Hahn, Soo Yeon: SS04-P4 (p177), SE-065 (p225), SE-072 (p229)
Ham, Taehyuk: SE-069 (p227), SE-071 (p229)
Han, Boo-Kyung: YIA-P3 (p164), SS02-P1 (p168), SS02-P3 (p169)
Han, Hong: SS01-P2 (p160), SS03-P3 (p172)
Han, Kyunghwa: YIA-P5 (p165), MS02-P3 (p182), MS02-P4 (p182), MS02-P5 (p183)
Han, Seungchul: SS03-P4 (p172)
Han, Yeo Eun: CC02-S4 (p60)
Hashimoto, Hiroshi: SS03-P2 (p171)
Helmizar, Divo: SE-009 (p198)
Helmizar, Roland: SE-015 (p201), SE-058 (p222)
Horisawa, Shiro: SF06-S1 (p148)
Hu, Huiyong: USB04-P1 (p192)
Huang, Beijian: SS01-P2 (p160), SS02-P2 (p169), SS03-P3 (p172)
Huang, Yunlin: HI01-P3 (p167), SS03-P5 (p173)
Hwang, Inpyeong: SE-071 (p229)
Hwang, Jae-Yeon: USB04-P3 (p193)
Hwang, Jisun: CC08-S2 (p107), MS02-P1 (p180), SE-042 (p213)
Hwang, Shinhye: CC02-S2 (p57)
Hwang, Sung Il: SF03-S3 (p127)
Hwang, Sungjun: CC05-S1 (p93)

I

Ichinkhorloo, Dorjkhand: SE-002 (p195)
Ishdorj, Otgonchimeg: USB02-P6 (p188)
Itoi, Takao: SS03-P2 (p171)

J

Jang, Weon: CC04-S2 (p70)
Jeon, Sun Kyung: HI01-S2 (p75)
Jeon, Tae Yeon: SE-043 (p214), SE-044 (p214)
Jeong, So Yeong: SS04-P6 (p178), SE-062 (p224), SE-064 (p225)
Jeong, Woo Kyoung: LD03-S2 (p159), SE-012 (p199)
Jeong, Younbeom: SE-062 (p224)
Jie, Ren: HI02-S1 (p76)
Jing, Jia: SS01-P5 (p162)
Joo, Leehi: LD02-S1 (p144)
Julian, Raenald: SE-022 (p205)

Author Index

K

Kamaya, Aya: SE-013 (p200)
Kamiyama, Naohisa: SS03-P2 (p171)
Kang, Eungtaek: SE-025 (p207)
Kang, Hyo-Jin: SS03-P1 (p171)
Kang, Jeeun: SF01-S3 (p88)
Kang, Yeseul: YIA-P1 (p163), MS02-P6 (p183)
Kee, Daegan: SE-054 (p220)
Khishigdavaa, Garamjav: SE-028 (p208)
Kim, Chi Kyung: SF02-S3 (p114)
Kim, Chulhong: IS01-S1 (p81)
Kim, Dong Hwee: SE-030 (p210)
Kim, Dong Hyun: SE-033 (p210)
Kim, Dong Wook: LD03-S1 (p156)
Kim, Haejung: YIA-P3 (p164), SS02-P1 (p168), SS02-P3 (p169), SS04-P4 (p177), SE-065 (p225), SE-072 (p229)
Kim, Hanna: USB03-P3 (p190)
Kim, Hyo Jin: SE-033 (p210)
Kim, Hyun Gi: MS02-P2 (p181)
Kim, Ji Hye: SE-043 (p214), SE-044 (p214)
Kim, Ji-hoon: SE-069 (p227), SE-071 (p229)
Kim, Jihoon: SE-066 (p226)
Kim, Jinwook: CC09-S1 (p134)
Kim, Jisoo: CC08-S3 (p110), MS02-P3 (p182), MS02-P4 (p182), MS02-P5 (p183), SE-045 (p215), SE-050 (p217)
Kim, Ki Hoon: SE-030 (p210)
Kim, Kyuwon: SF04-S1 (p137)
Kim, Min Je: CC04-S4 (p72)
Kim, Myoung Kyoung: YIA-P3 (p164), SS02-P1 (p168), SS02-P3 (p169), SS04-P4 (p177), SE-065 (p225), SE-072 (p229)
Kim, Myung: SE-025 (p207)
Kim, Nackhwan: SE-036 (p211)
Kim, Pyeong Hwa: MS02-P1 (p180), SE-042 (p213)
Kim, Sanghee: YIA-P3 (p164), SS02-P1 (p168), SS02-P3 (p169)
Kim, Seung Hyup: SE-025 (p207)
Kim, Seunghoo: SE-054 (p220)
Kim, Suhnggwon: SE-025 (p207)
Kim, Tae Hyuk: SE-065 (p225)
Kim, Tae Yong: SE-068 (p227)
Kim, Won Gu: SE-068 (p227)
Kim, Won Hwa: HI03-S2 (p129)
Kim, Yeun-Yoon: SE-012 (p199)
Kim, Yong-Woo: MS02-P3 (p182), MS02-P4 (p182), MS02-P5 (p183)
Kim, Yong-woo: SE-045 (p215)
Kim, Yongwoo: SE-050 (p217)
Kim, Youe Ree: CC05-S4 (p98)
Klochkova, Natalya: SS01-P4 (p161)
Ko, Eun Sook: YIA-P3 (p164), SS02-P1 (p168), SS02-P3 (p169)
Ko, Eun Young: YIA-P3 (p164), SS02-P1 (p168), SS02-P3 (p169)
Koh, Hong: MS02-P3 (p182), MS02-P4 (p182), MS02-P5 (p183)
Koh, Seok Young: USB04-P3 (p193)
Koo, Minseok: SE-055 (p221)
Kozhakhmetova, Zhanar: SE-047 (p216), SE-049 (p217)
Kritsaneephaiboon, Supika: MS02-S1 (p120)
Kuo, Jennifer: HI02-S3 (p79)
Kwak, Jin Young: YIA-P5 (p165), MP06-S1 (p89)
Kwon, Dong Rak: SE-046 (p215)
Kwon, Yong Wonn: SF02-S2 (p113)
Kwon, Yonghan: MS02-P3 (p182), MS02-P4 (p182), MS02-P5 (p183)

L

Larionova, Svetlana: SS01-P4 (p161)
Lee, Byung Chul: CC09-S2 (p135)
Lee, Changyang: SE-051 (p218), SE-055 (p221)
Lee, Dong Hyun: SE-025 (p207)
Lee, Eun Joo: MS02-P3 (p182), MS02-P4 (p182), MS02-P5 (p183)
Lee, Eunju: YIA-P1 (p163), MS02-P6 (p183)
Lee, Hana: YIA-P1 (p163), MS02-P6 (p183)
Lee, Hye Sun: YIA-P1 (p163), MS02-P6 (p183)
Lee, Hyo Jeong: CC04-S1 (p69), SE-025 (p207)
Lee, Jae Ho: SE-065 (p225), SE-068 (p227)
Lee, Jaeho: SS04-P4 (p177), SE-072 (p229)
Lee, Jeong Hyun: MP04-S1 (p50), SE-068 (p227)
Lee, Jeong Min: SS03-P1 (p171)
Lee, Jeonghyun: IS02-S3 (p153)
Lee, Jeongmin: YIA-P3 (p164), SS02-P1 (p168), SS02-P3 (p169)
Lee, Ji Ye: SE-069 (p227), SE-071 (p229)
Lee, Jongmin: MP09-S1 (p92)
Lee, Joongyub: SE-025 (p207)
Lee, Kwang Jae: USB03-P3 (p190)
Lee, Meesun: SE-069 (p227), SE-071 (p229)
Lee, Mi-Jung: MS02-P3 (p182), MS02-P4 (p182), MS02-P5 (p183), SE-045 (p215)
Lee, Mijung: SE-050 (p217)
Lee, Min Kyoung: LD02-S2 (p145)
Lee, Min Woo: SS03-P4 (p172)
Lee, Myoungseok: SF03-S2 (p126)
Lee, Sang Eun: SE-025 (p207)
Lee, Seul Ki: SE-037 (p211)
Lee, Seunghyun: USB04-P3 (p193)
Lee, Sunyoung: SE-013 (p200)
Lee, Yoonseong: SF02-S1 (p112)
Lei, Cai: SS04-P5 (p178)
Li, Cuixian: SS01-P2 (p160)
Li, Jiaxin: SS01-P3 (p161)
Liana, Nana: SE-015 (p201)
Liang, Hua: SS03-P7 (p174)
Lim, Chee Yeong: MP07-S1 (p90), LD01-S2 (p133)
Lim, Hunjong: CC06-S1 (p99), SE-062 (p224)
Liu, Hong: SS01-P2 (p160)
Long, Xanicia: USB02-P7 (p188), SE-027 (p208)
Lu, Xiuyun: HI01-P3 (p167), SS03-P5 (p173)
Luo, Yanwen: SS02-P4 (p170)
Lupusoru, Raluca: HI01-P2 (p167)
Lyu, Ke: SS03-P6 (p174), SS03-P7 (p174)

M

Ma, Yu: SS02-P2 (p169)
Maeyama, Misato: USB01-P2 (p185)
Mahmood, Rameysh Danovani: SF05-S1 (p141)
Martinoli, Carlo: CC07-S1 (p103), CC07-S2 (p104), CC07-S3 (p105)
Miao, Li: SS04-P5 (p178)
Min, Jaeyong: SE-067 (p226)
Min, Ji Hye: CC05-S2 (p95)
Minami, Yasunori: MP03-S1 (p49)
Momin, Asif: USB02-P2 (p186), SE-016 (p201), SE-029 (p209)
Momin, Inshirah: USB02-P2 (p186), SE-029 (p209)
Momin, Shenaz: USB02-P2 (p186), SE-016 (p201), SE-029 (p209)
Moon, Jayoung: SE-042 (p213)
Moon, Sung Kyoung: SF04-S3 (p140)
Morabe, Ferdinand: USB02-P1 (p185)
Munkhjargal, Telmen: USB03-P1 (p189)

N

Na, Dong Gyu: SS04-P3 (p176), SE-067 (p226)
Naidu, Kanak: USB02-P7 (p188)
Nakajima, Keisuke: SS03-P2 (p171)
Nakashouji, Tomohiro: SE-019 (p203)
Namkhaijantsan, Bayarjargal: USB01-P1 (p184)
Ng, Kok Kit: SE-027 (p208)
Nica, Camelia: HI01-P2 (p167)
Noh, Byeong-Joo: SE-067 (p226)
Nursanti, Andi: SE-018 (p203), SE-052 (p219), SE-053 (p219)

Author Index

O

Oh, Young Lyun: SE-065 (p225)
Olzvoi, Nergui: SE-028 (p208)
Orynbassar, Nurgul: SE-049 (p217)

P

Paeng, Dong-Guk: MP05-S1 (p51)
Parabina, Elena: SS01-P4 (p161)
Parikh, Manthan: SE-016 (p201)
Park, Dalsu: SE-035 (p210)
Park, Eun Hae: LD01-S1 (p132)
Park, Gi-young: MS01-P2 (p180)
Park, Goeun: SE-065 (p225)
Park, Hee Jin: MS01-P1 (p179), SE-038 (p212)
Park, Hong Bum: SE-030 (p210)
Park, Hyungjun: IS02-S1 (p150)
Park, Ji Eun: SE-043 (p214), SE-044 (p214)
Park, Jinhyoung: SF01-S1 (p86), SE-051 (p218), SE-054 (p220), SE-055 (p221)
Park, Mi-Yeon: CC04-S3 (p71)
Park, Sang Ik: CC03-S1 (p62)
Park, Vivian Youngjean: YIA-P5 (p165)
Patani, Mittali Shah: USB02-P2 (p186)
Pedro, Karen Tehani San: USB02-P3 (p186), USB03-P2 (p190), USB04-P4 (p193)
Penyaeva, Ella: SS01-P4 (p161)
Popescu, Alina: HI01-P2 (p167)
Praja, Rian Ka: SE-005 (p196), SE-021 (p205), SE-024 (p206), SE-070 (p228)
Prihantini, Prihantini: SE-004 (p196), SE-011 (p198), SE-018 (p203), SE-052 (p219), SE-053 (p219)
Purevdorj, Uugantuya: USB03-P1 (p189)
Putri, Sahnaz Vivinda: SE-004 (p196), SE-011 (p198), SE-018 (p203), SE-052 (p219), SE-053 (p219)

Q

Qian, Xindi: SE-056 (p221)

R

Rentsensambuu, Munkh-Orgil: SE-003 (p195)
Rhim, Hyunchul: JSL-S2 (p68)
Rho, Miribi: YIA-P5 (p165)
Rodgers, Shuchi K: SE-013 (p200)
Roh, Yun Hwa: CC03-S2 (p64)
Rosalina, Reny: SE-005 (p196), SE-021 (p205), SE-024 (p206), SE-070 (p228)
Ryu, Seohyun: SS04-P2 (p176)

S

Sary, Inabat: SE-047 (p216)
Seki, Yasushi: SE-001 (p194)
Seo, Jiwoon: MS01-S3 (p118), SE-033 (p210)
Seo, Yeji: SE-054 (p220)
Septiana, Vina Tri: SE-015 (p201)
Setevdorj, Otgonbayar: SE-063 (p224)
Shen, Xinmeng: SS02-P2 (p169)
Shin, Hyun Joo: YIA-P1 (p163), MS02-P6 (p183)
Shin, Jae Ho: CC06-S3 (p102), USB04-P2 (p192)
Shin, Jaeseung: SE-013 (p200)
Shin, Jeong In: MS02-P1 (p180)
Shin, Jung Hee: SS04-P4 (p177), SE-065 (p225), SE-072 (p229)
Shin, Sung Ui: CC01-S3 (p55)
Singh, D: SE-057 (p222)
Sirli, Roxana: HI01-P2 (p167)
Sirlin, Claude B.: SE-013 (p200)
Sodhi, Kushaljit Singh: MP08-S1 (p91)
Son, Jeongil: SE-050 (p217)
Son, Jung Hee: SF04-S2 (p139)
Son, Wontae: SE-051 (p218)
Song, Dong Eun: SE-068 (p227)
Song, Kyungechul: YIA-P1 (p163), MS02-P6 (p183)
Song, You Seon: MS01-S2 (p117)
Sporea, Ioan: JSL-S1 (p66), HI01-S1 (p74), HI01-P2 (p167)
Stan, Maria: HI01-P2 (p167)
Stolyarevich, Ekaterina: SS01-P4 (p161)
Sugimoto, Katsutoshi: SS03-P2 (p171)
Suh, Chong Hyun: MS02-P1 (p180)
Suh, Pae Sun: IS01-S2 (p82)
Sung, Tae Yon: SE-068 (p227)
Syafruddin, Elfiany: SE-011 (p198), SE-018 (p203)

T

Tang, Yang: SS03-P3 (p172)
Tanyildizi, Yasemin: MS02-P2 (p181)
Taohua, Gou: SS04-P5 (p178)
Tian, Gao: SS04-P5 (p178)
Tserendorj, Badamsed: USB03-P1 (p189)
Tsogtsaikhan, Buyankhishig: USB01-P1 (p184)
Tsolmon, Khishgee: USB01-P1 (p184), USB02-P5 (p187)
Tumendelger, Amgalanbayar: SE-060 (p223)

U

Ulaankhuu, Baigalmaa: SE-048 (p216)

V

Vetsheva, Natalia: SS01-P4 (p161)
Villanueva, Ma Katrina: USB02-P4 (p187)

W

Wang, Bei: SS01-P5 (p162)
Wang, Hairong: USB04-P1 (p192)
Wang, Peilei: SS02-P2 (p169)
Wang, Xi: SS02-P2 (p169)
Wang, Ying: HI01-P3 (p167), SS03-P5 (p173)
Wang, Yixuan: SS01-P5 (p162)
Wee, Sungchul: MS01-P1 (p179), SE-038 (p212)
Wei, Li: HI01-P3 (p167)
Winarti, Rini: SE-004 (p196), SE-011 (p198), SE-018 (p203), SE-052 (p219), SE-053 (p219)

X

Xia, Hansheng: SS02-P2 (p169), SS02-P4 (p170)
Xu, Benhua: SS03-P3 (p172)
Xu, Huixiong: SS01-P2 (p160), SS02-P2 (p169), HI01-P1 (p166), SS03-P3 (p172)
Xu, Li: SS04-P5 (p178)
Xu, Yadan: SS03-P3 (p172)

Y

Yabunaka, Koichi: SE-019 (p203)
Yan, Lixia: SS02-P2 (p169)
Yan, Xiaoyi: SS03-P6 (p174)
Yan, Zhang: SS04-P5 (p178)
Yang, Haojie: YIA-P4 (p165)
Yang, Hyun Kyung: CC05-S3 (p96)
Yang, Zhe: SS01-P5 (p162)
Yemeshev, Yerlan: SE-041 (p212)
Yeung, Ming: SE-020 (p204)
Yoo, Jeongin: CC02-S1 (p56), SS03-P1 (p171)
Yoo, So-Young: SE-043 (p214), SE-044 (p214)
Yoon, Haesung: MS02-P3 (p182), MS02-P4 (p182), MS02-P5 (p183), SE-045 (p215), SE-050 (p217)
Yoon, Ja Kyung: SE-013 (p200)
Yoon, Jiyoung: YIA-P5 (p165)
Yoon, Jung Hyun: YIA-P5 (p165), IS02-S2 (p152)

Author Index

Yoon, Yong-Soon: USB03-P3 (p190)
Yu, Jaesok: SF01-S2 (p87)

Z

Zhang, Haorong: USB04-P1 (p192)
Zhang, Qi: SS01-P2 (p160), SS03-P3 (p172)
Zhao, Hui: SS01-P1 (p160), YIA-P6 (p166)
Zhou, Boyang: SS02-P4 (p170)